



National Library  
of Canada

Acquisitions and  
Bibliographic Services Branch

395 Wellington Street  
Ottawa, Ontario  
K1A 0N4

Bibliothèque nationale  
du Canada

Direction des acquisitions et  
des services bibliographiques

395, rue Wellington  
Ottawa (Ontario)  
K1A 0N4

*Your file    Votre référence*

*Our file    Notre référence*

## NOTICE

The quality of this microform is heavily dependent upon the quality of the original thesis submitted for microfilming. Every effort has been made to ensure the highest quality of reproduction possible.

If pages are missing, contact the university which granted the degree.

Some pages may have indistinct print especially if the original pages were typed with a poor typewriter ribbon or if the university sent us an inferior photocopy.

Reproduction in full or in part of this microform is governed by the Canadian Copyright Act, R.S.C. 1970, c. C-30, and subsequent amendments.

## AVIS

La qualité de cette microforme dépend grandement de la qualité de la thèse soumise au microfilmage. Nous avons tout fait pour assurer une qualité supérieure de reproduction.

S'il manque des pages, veuillez communiquer avec l'université qui a conféré le grade.

La qualité d'impression de certaines pages peut laisser à désirer, surtout si les pages originales ont été dactylographiées à l'aide d'un ruban usé ou si l'université nous a fait parvenir une photocopie de qualité inférieure.

La reproduction, même partielle, de cette microforme est soumise à la Loi canadienne sur le droit d'auteur, SRC 1970, c. C-30, et ses amendements subséquents.

UNIVERSITY OF ALBERTA

**DSP IMPLEMENTATION OF DECISION-AIDED ERROR  
CORRECTION ALGORITHM FOR DIGITAL CELLULAR  
RADIO**

By

**Seema Madan**



A thesis submitted to the Faculty of Graduate Studies and Research in  
partial fulfillment of the requirements for the degree of  
**Master of Science.**

DEPARTMENT OF ELECTRICAL ENGINEERING

Edmonton, Alberta

Spring 1996



National Library  
of Canada

Acquisitions and  
Bibliographic Services Branch

395 Wellington Street  
Ottawa, Ontario  
K1A 0N4

Bibliothèque nationale  
du Canada

Direction des acquisitions et  
des services bibliographiques

395, rue Wellington  
Ottawa (Ontario)  
K1A 0N4

*Your file    Votre référence*

*Our file    Notre référence*

**The author has granted an irrevocable non-exclusive licence allowing the National Library of Canada to reproduce, loan, distribute or sell copies of his/her thesis by any means and in any form or format, making this thesis available to interested persons.**

**L'auteur a accordé une licence irrévocable et non exclusive permettant à la Bibliothèque nationale du Canada de reproduire, prêter, distribuer ou vendre des copies de sa thèse de quelque manière et sous quelque forme que ce soit pour mettre des exemplaires de cette thèse à la disposition des personnes intéressées.**

**The author retains ownership of the copyright in his/her thesis. Neither the thesis nor substantial extracts from it may be printed or otherwise reproduced without his/her permission.**

**L'auteur conserve la propriété du droit d'auteur qui protège sa thèse. Ni la thèse ni des extraits substantiels de celle-ci ne doivent être imprimés ou autrement reproduits sans son autorisation.**

ISBN 0-612-10732-9

**Canada**

UNIVERSITY OF ALBERTA  
LIBRARY RELEASE FORM

NAME OF AUTHOR: **SEEMA MADAN**  
TITLE OF THESIS: **DSP Implementation of Decision-Aided  
Error Correction Algorithm for Digital  
Cellular Radio**  
DEGREE: **MASTER OF SCIENCE**  
YEAR THIS DEGREE GRANTED: **1996**

Permission is hereby granted to the University of Alberta Library to reproduce single copies of this thesis and to lend or sell such copies for private, scholarly, or scientific research purposes only.

The author reserves all other publication and other rights in association with the copyright in the thesis, and except as hereinbefore provided, neither the thesis nor any substantial portion thereof may be printed or otherwise reproduced in any material form whatever without the author's prior written permission.



Seema Madan

C4H / 22, Janakpuri

New Delhi, India 110058

Date: 25<sup>th</sup> January 1996.

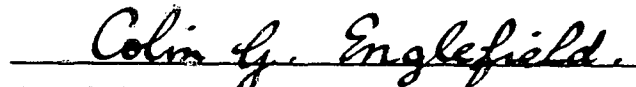
UNIVERSITY OF ALBERTA

FACULTY OF GRADUATE STUDIES AND RESEARCH

The undersigned certify that they have read, and recommend to the Faculty of Graduate Studies and Research for acceptance, a thesis entitled **DSP IMPLEMENTATION OF DECISION-AIDED ERROR CORRECTION ALGORITHM FOR DIGITAL CELLULAR RADIO** submitted by Seema Madan in partial fulfillment of the requirements for the degree of Master of Science.



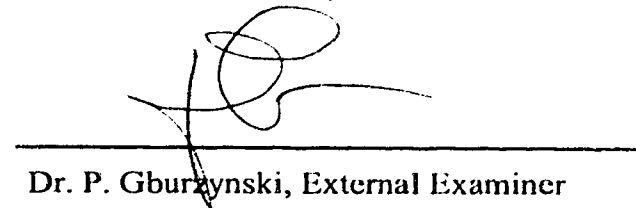
Dr. Paul A. Goud, Supervisor



Dr. Colin G. Englefield, Co-Supervisor



Dr. K. A. Stromsmoe, Internal Examiner



Dr. P. Gburzynski, External Examiner

Date: 22<sup>nd</sup> January 1996.

*Dedicated to my dear parents, sisters, and husband  
for their love, support and encouragement.*

## ABSTRACT

In mobile radio communication, the major cause of performance degradation for a traditional receiver based on differential detection is the multipath fading phenomenon associated with the channel. Amplitude and phase variations of the received signal due to fading result in severe and unpredictable random phase shifts superimposed onto the phase modulated transmitted signal. This leads to closure of the received signal eye-diagram, resulting in demodulation errors that exhibit an irreducible error floor. Decision-aided detection has been shown to be an effective error correcting method for BPSK modulation. Its performance for  $\pi/4$ DQPSK modulation as per the IS54 standard is evaluated in this research.

The decision-aided algorithm is used for tracking the phase variations due to the fading channel. The channel estimation is based on the fact that, in a typical case, only one out of one hundred first decisions is detected incorrectly. The reverse modulator recovers the phase change due to the channel, by subtracting the phase changes corresponding to the transmitted data from the total received phase change. The effect of any incorrect first decisions is reduced by a channel estimation filter, using samples before and after each decision sample. Once the phase change due to the fading channel is known, its effect on the differential detector output is removed so that the detected signal error rate is significantly reduced.

In this research, the transmitter and the flat fading channel model have been implemented using the Texas Instruments DSP TMS320C50, using equivalent complex base-band signals for the  $\pi/4$ DQPSK modulation. The modulated signal, distorted by the channel, is fed digitally to a TMS320C30 DSP where the decision-aided error correction algorithm is implemented. The test results show that the algorithm lowers the error floor, obtained at the output of a conventional differential detector, by a factor of more than 200. The performance is also evaluated for various values of signal to noise ratio (SNR). Under adequate SNR conditions, this method of error correction is quite attractive as compared to other techniques such as coding, insertion of pilot symbols, or the diversity method, because it requires no overhead bits. The implementation of the algorithm requires  $\approx 167$  instruction cycles/symbol; thus, for the TMS320C30 DSP @60ns instruction cycle, only 10 $\mu$ s/symbol are needed. This would allow the error correction method to be implemented for symbol rates up to 100ks/s. Also, since the algorithm does not require any modification to the frame structure of the signal, it may be preferred if the transmitting signal format has already been standardized. A second method of detection, which attempts to obtain the true channel characteristic from the incoming signal is also proposed, so as to obtain better results for the lower range of SNR values. This method has been shown to be useful for locating the errors, to remove the errors however, a complex correction algorithm may be required.



## **ACKNOWLEDGEMENTS**

I would like to express my sincere thanks to my supervisors, Dr. Paul A. Goud and Dr. Colin G. Englefield, for their interest, advice and support throughout my graduate program. I would also like to thank Dr. Ray E. Rink and Dr. Wayne D. Grover along with my supervisors for introducing me to the field of Digital Signal Processing, Telecommunications and Wireless Communications.

My sincere thanks to Telecommunications Research Laboratories and its sponsors, for the award of a Telecommunication Research Scholarship, and the unique and stimulating research environment. Also, I extend my thanks to the research staff and colleagues at TR Labs for many helpful discussions, particularly David Clegg and Jason Lamont for their help in PCB fabrication. Thanks are also due to Albert Lau for his help in setting up the initialization routine for the DSP platform.

Finally, I thank my family and friends for their encouragement and support, throughout the completion of this project.

# TABLE OF CONTENTS

<b>1. INTRODUCTION.....</b>	<b>1</b>
1.1. Mobile radio communications.....	1
1.2. Digital cellular system (IS54).....	4
1.3. Propagation channel.....	7
1.3.1. Path loss.....	7
1.3.2. Fading.....	9
1.3.3. Doppler effect.....	10
1.3.4. Delay spread.....	10
1.3.5. Noise.....	11
1.4. Decision-aided detection.....	12
1.5. Thesis overview.....	13
<b>2. TRANSCEIVER STRUCTURE AND ERROR FLOOR</b>	
<b>REDUCTION TECHNIQUES.....</b>	<b>15</b>
2.1. Structure of $\pi/4$ DQPSK transmitter.....	15
2.1.1. Data source.....	15
2.1.2. Data compressor and frame organizer.....	16
2.1.3. $\pi/4$ DQPSK Encoder.....	16
2.1.4. Pulse shaping filter.....	18
2.1.5. Radio frequency section.....	19
2.2. Radio propagation channel.....	20
2.2.1. Scattering model.....	20
2.2.2. Channel characteristics.....	23
2.2.2.1. Power spectra.....	23
2.2.2.2. Statistics of received signal envelope and phase.....	23
2.2.2.3. Level crossing rate and average fade duration.....	25
2.2.2.4. Envelope correlation.....	25
2.2.3. Channel model.....	26

2.3. Structure of $\pi/4$ DQPSK receiver.....	27
2.3.1. Demodulator section.....	27
2.3.2. Detector.....	27
2.3.2.1. Baseband differential detector.....	28
2.3.3. Performance measurement.....	30
2.4. Fading effect: Irreducible error floor.....	30
2.5 Error floor reduction techniques.....	31
2.5.1. Pilot symbol insertion.....	31
2.5.2. Reference tone approach.....	33
2.5.3. Coding and interleaving.....	35
2.5.4. Diversity.....	37
2.6. Summary.....	40
<b>3. DECISION-AIDED CHANNEL ESTIMATION AND</b>	
<b>ERROR CORRECTION.....</b>	<b>41</b>
3.1. Decision-aided detection.....	41
3.1.1. Block diagram.....	42
3.2. Channel estimation.....	44
3.2.1. Reverse modulation.....	44
3.2.2. Estimation filter.....	46
3.2.3. Channel phase finder.....	51
3.3. Error correction.....	52
3.4. Scheme II for decision-aided detection.....	55
3.4.1. Block diagram.....	56
3.4.2. Channel estimation.....	58
3.5. Summary.....	59
<b>4. DSP IMPLEMENTATION OF DECISION-AIDED DETECTOR.....</b>	<b>60</b>
4.1. Transmitter.....	60
4.1.1. Data source.....	61

4.1.2. Encoder and modulator.....	63
4.1.3. Pulse shaping filter.....	66
4.2. Flat fading channel.....	72
4.2.1. Gaussian sources.....	73
4.2.2. Doppler shift filter.....	76
4.2.3. Interpolating filter.....	78
4.3. Channel superposition on transmitted signal.....	80
4.3.1. Complex multiplication.....	80
4.3.2. Interface.....	80
4.4. Receiver.....	82
4.4.1. Additive white Gaussian noise source.....	83
4.4.2. Receiver bandpass filter.....	85
4.4.3. Decision-aided detector.....	86
4.4.3.1. Differential detector.....	87
4.4.3.2. Reverse modulator.....	89
4.4.3.3. Channel estimator and error corector.....	93
4.5. Error measurement.....	102
4.5.1. Duplicate data source with delay and storage.....	103
4.5.2. Comparators.....	103
4.6. Summary.....	103
<b>5. RESULTS.....</b>	<b>104</b>
5.1. Sampling rate, Doppler shift and related parameters.....	104
5.2. Performance of decision-aided detector.....	108
5.2.1. AWGN channel.....	108
5.2.2. Fading channel and AWGN, $f_d=40\text{Hz}$ .....	110
5.2.3. Fading channel and AWGN, $f_d=20\text{Hz}$ .....	111
5.3. Scheme II.....	112
5.4. Summary.....	118

**6. SUMMARY AND CONCLUSIONS.....119**

**REFERENCES.....124**

**APPENDIX A      PCB for interface between Texas Instruments  
                         TMS320C50 and TMS320C30 DSPs.....128**

**APPENDIX B      DSP program lists for real time transceiver  
                         implementation.....135**

## LIST OF FIGURES

Fig. 1.1.	Cellular mobile radio system.....	2
Fig. 1.2.	Slot and frame structure for IS54.....	6
Fig. 1.3.	Mobile radio environment.....	8
Fig. 1.4.	Fading phenomenon.....	9
Fig. 1.5.	Typical received signal strength variation.....	10
Fig. 1.6.	Delay spread phenomenon.....	11
Fig. 2.1.	(a) Basic communication system model. (b) Transmitter structure.....	15
Fig. 2.2.	Gray coding for $\pi/4$ DQPSK.....	16
Fig. 2.3.	Constellation for $\pi/4$ DQPSK modulation.....	17
Fig. 2.4.	Frequency response of pulse shaping filter.....	18
Fig. 2.5.	Quadrature modulator.....	19
Fig. 2.6.	Scattering model.....	21
Fig. 2.7.	Radio channel model.....	26
Fig. 2.8.	Block diagram of the baseband differential detector.....	28
Fig. 2.9.	Transmitter for pilot symbol insertion method.....	32
Fig. 2.10.	(a) Receiver for pilot symbol insertion method. (b) Fading estimation and compensation for pilot symbol insertion method.....	33
Fig. 2.11.	(a) System based on pilot tone insertion. (b) Pilot tone insertion using spectral manipulation.....	34
Fig. 2.12.	(a) Convolutional encoder. (b) Block encoder.....	36
Fig. 2.13.	Diversity combiners. (a) Selective combining. (b) Switched combining. (c) Maximal-ratio combining. (d) Equal gain combining.....	39
Fig. 3.1.	Block diagram of receiver.....	41
Fig. 3.2.	Block diagram for decision-aided detector.....	42
Fig. 3.3.	Vector diagram for reverse modulation process.....	45

Fig. 3.4.	Channel estimation.....	47
Fig. 3.5.	(a) Typical channel. (b) Error correction.....	52
Fig. 3.6.	Gray code to shift first decision.....	53
Fig. 3.7.	Decision range for different shift values.....	54
Fig. 3.8.	Block diagram for scheme II (Decision-aided error detection).....	57
Fig. 3.9.	Recovered channel.....	58
Fig. 4.1.	M-sequence generator.....	63
Fig. 4.2.	(a) Constellation state diagram. (b) Phase change state diagram.....	64
Fig. 4.3.	Frequency domain response of the raised cosine filter.....	67
Fig. 4.4.	Time domain and frequency domain response of SRRC filter.....	69
Fig. 4.5.	FIR filter structure.....	70
Fig. 4.6.	Multirate interpolation filter structure (M=4).....	70
Fig. 4.7.	Transmitted signal. (a) Eye-diagram. (b) Constellation diagram.....	72
Fig. 4.8.	Block diagram of fading channel model.....	73
Fig. 4.9.	Seed value generator for random generator.....	75
Fig. 4.10.	Circular buffer implementation of random 16-bit word generator.....	75
Fig. 4.11.	Time domain and frequency response of Doppler shift filter.....	77
Fig. 4.12.	Software architecture for fading channel.....	78
Fig. 4.13.	Fading channel simulator output. ....	79
Fig. 4.14.	Received signal waveform.....	81
Fig. 4.15.	Block diagram of interface circuit between DSP C50 and C30.....	81
Fig. 4.16.	Zero ISI waveform.....	85
Fig. 4.17.	Receiver bandpass filter output.....	86
Fig. 4.18.	Differential detector output ( $U+jV$ ).....	88
Fig. 4.19.	Extracted channel using angles.....	90
Fig. 4.20.	Extracted channel using $U_p$ and $V_p$ .....	90
Fig. 4.21.	Estimation filter design based on raised cosine filter.	
	(a) Filter response with $h(0) \neq 0$ and $h(0) = 0$ .....	95

	(b) Filter response with $h(0)=0$ .....	96
Fig. 4.22.	Estimation filter design based on least square fit.	
	(a) Filter response with $h(0)\neq 0$ .....	97
	(b) Filter response with $h(0)=0$ .....	97
Fig. 4.23.	Estimation filter design based on polynomial fit.	
	(a) Filter response with $h(0)\neq 0$ and $h(0)=0$ .....	99
	(b) Filter response with $h(0)=0$ .....	99
Fig. 4.24.	Estimation filter design based on Remez exchange algorithm.....	100
Fig. 4.25.	Estimated channel ( $U_{pf}$ and $V_{pf}$ ).....	102
Fig. 5.1.	Test setup for decision-aided detector.....	105
Fig. 5.2.	PDF of envelope of the fading channel (from theory and simulation).....	106
Fig. 5.3.	Relative power spectrum of fading signal (Doppler frequency=40Hz).....	107
Fig. 5.4.	Relative power spectrum of fading signal (Doppler frequency=20Hz).....	108
Fig. 5.5.	SER performance for $\pi/4$ DQPSK signal in an AWGN channel.....	109
Fig. 5.6.	SER performance of decision-aided detector for flat fading channel. ( $f_d=40$ Hz).....	111
Fig. 5.7.	SER performance of decision-aided detector for flat fading channel. ( $f_d=20$ Hz).....	112
Fig. 5.8.	Scheme II channel smoothing. (a) Recovered channel. (b) Actual channel possibilities.....	113
Fig. 5.9.	Error zone detection using $a_f$ , $a_r$ .....	115
Fig. 5.10.	Error zone detection using $a_I$ , $a_Q$ .....	115
Fig. 5.11.	Error zone detection using $Err\_ch$ .....	116
Fig. 5.12.	Smooth channel using derivatives.....	117
Fig. 5.13.	Scheme II smooth channel peak detection.....	118



## LIST OF TABLES

Table 2.1.	Relation between serial input data and differential phase angle.....	17
Table 2.2.	IS54 specifications for carrier frequency.....	19
Table 3.1.	Relation between $\text{ang}(C+jD)$ and data shift.....	54
Table 3.2.	Relation of $(U_p, V_p)$ and data shift with $(U_{p_{\text{new}}}, V_{p_{\text{new}}})$ .....	55
Table 4.1.	Features of DSP TMS320C50.....	60
Table 4.2.	Relation between data bits and state generator function.....	65
Table 4.3.	Look-up table for in-phase and quadrature part of modulator output.....	66
Table 4.4.	Features of DSP TMS320C30.....	83
Table 4.5.	Look-up table for first decision.....	89
Table 4.6.	Reverse modulator output.....	92
Table 4.7.	Logic for reverse modulator output.....	92
Table 4.8.	Test results based on raised cosine estimation design.....	95
Table 4.9.	Test results based on least square error fit.....	98
Table 4.10.	Test results based on polynomial fit.....	98
Table 4.11.	Test results based on Remez exchange algorithm.....	101
Table 4.12.	Test results based on Remez exchange algorithm, (with $U_{p_{\text{new}}}$ and $V_{p_{\text{new}}}$ ).....	101

## **LIST OF ABBREVIATIONS**

$\pi/4$ DQPSK	$\pi/4$ Shifted Differential Quadrature Phase Shift Keying
AFD	Average Fade Duration
AMPS	Advanced Mobile Phone Service
ARQ	Automatic Request for Retransmission
AWGN	Additive White Gaussian Noise
BER	Bit Error Rate
BPSK	Binary Phase Shift Keying
b/s/Hz	bits per second per Hertz
CDMA	Code Division Multiple Access
CDF	Cumulative Distribution Function
CT2	Cordless Telephone 2
DCS 1800	Digital Cellular System 1800
DECT	Digital European Cordless Telecommunications
DSP	Digital Signal Processor
EIA/TIA	Electronic Industries Association/Telecommunication Industry Association
FDMA	Frequency Division Multiple Access
FEC	Forward Error Control
FIR	Finite Impulse Response
FM	Frequency Modulation
GSM	Global System for Mobile Communications
IIR	Infinite Impulse Response
IS54	Interim Standard 54
IS95	Interim Standard 95
IS136	Interim Standard 136
ISI	Inter-Symbol Interference
kb/s	kilo-bit per second

<b>kbaud</b>	<b>kilo-baud</b>
<b>LCR</b>	<b>Level Crossing Rate</b>
<b>LO</b>	<b>Local Oscillator</b>
<b>MAHO</b>	<b>Mobile Station Assisted Handover</b>
<b>MSC</b>	<b>Mobile Service Switching Center</b>
<b>NADMCS</b>	<b>North American Dual Mode Cellular System</b>
<b>NMT</b>	<b>Nordic Mobile Telephone</b>
<b>NTT</b>	<b>Nippon Telephone and Telegraph Company</b>
<b>OK-QPSK</b>	<b>Offset Keying - Quadrature Phase Shift Keying</b>
<b>PBPF</b>	<b>Pilot Band-Pass Filter</b>
<b>PCB</b>	<b>Printed Circuit Board</b>
<b>PDC</b>	<b>Personal Digital Cellular</b>
<b>PDF</b>	<b>Probability Density Function</b>
<b>QPSK</b>	<b>Quadrature Phase Shift Keying</b>
<b>RF</b>	<b>Radio Frequency</b>
<b>SER</b>	<b>Symbol Error Rate</b>
<b>SNR</b>	<b>Signal to Noise Ratio</b>
<b>SRRC</b>	<b>Square Root Raised Cosine</b>
<b>TACS</b>	<b>Total Access Communication System</b>
<b>TCT</b>	<b>Tone Calibrated Technique</b>
<b>TDMA</b>	<b>Time Division Multiple Access</b>
<b>VSELP</b>	<b>Vector Sum Excited Linear Predictive Coding</b>
<b>WLAN</b>	<b>Wireless Local Area Network</b>

## LIST OF SYMBOLS

$C, D$	Vector measurement for phase difference between estimated and extracted channel
$CH_I, CH_Q$	Vector measurement for fading channel
$D_0$	Transmitted data symbol
$D_1$	First decision: decision made about the transmitted symbol at the output of differential detector
$D_2$	Second decision: decision made about the transmitted symbol at the output of decision-aided detector
$f_d$	Doppler frequency
$I_k, Q_k$	Received signal vector at the output of the sampler
$IF$	Improvement factor
$SI, SQ$	Vector measurement for received signal
$U, V$	Vector measurement for received differential phase angle
$U_p, V_p$	Vector measurement for extracted channel
$U_{pf}, V_{pf}$	Vector measurement for filtered channel estimate
$U_{pnew}, V_{pnew}$	Vector measurement for extracted channel after error correction

# **1. INTRODUCTION**

## **General Background**

The introduction of radio telephony in the world of conventional public telephone services was motivated by the need to communicate from remote locations or while on the move, as from a car or other vehicle. To decouple the telephone from its wires to the local exchange, thereby allowing mobility for the user, radio communication with the fixed wireline network needs to be used. This presents several challenges, such as: the efficient use of the limited frequency spectrum, the lossy and dispersive nature of the transmission medium, extreme random fading of the received signals, and the variable location of the mobile terminal. Over the past decade, wireless communications has advanced to the point where a different scale of mobility is provided to users for different applications. However, the quality and capacity of communication over radio channels is yet to meet the growing demand.

### **1.1 Mobile Radio Communications**

The driving forces behind the evolution and development of mobile radio communication from the first generation onward are: system capacity, extent of coverage or mobility (cellular, cordless, paging, satellite-based wireless, etc.), various transmission services for different applications (voice, data, messaging, video) and cost.

Experiments on radio communication were first conducted by Hertz in 1880. In 1897 Marconi demonstrated successful transmission of a radio signal over an 18 mile path. In 1921, the first land mobile radio telephone was installed by the Detroit Police Department, in the USA. As technology and demands increased, the trend in 1938 was to use higher frequencies (30MHz range).

Further developments led to the growth from simplex (push to talk) to full duplex operation at 150MHz in 1964. Subsequently (1970), frequency channel splitting was used, but which was soon found to be of limited in use in meeting the demand for service. In 1974, the Bell telephone system introduced the system *Advanced Mobile Phone Service (AMPS)* which was designed for use in a cellular planned network. The number of customers that could be served increased tremendously due to the division of the coverage area into cells, and the reuse of frequencies in non-adjacent cells; these features are shown in Fig. 1.1. To provide for seamless transfer of a call from one cell to another, it was proposed to execute a *handoff* operation as the mobile unit crosses cell boundaries.

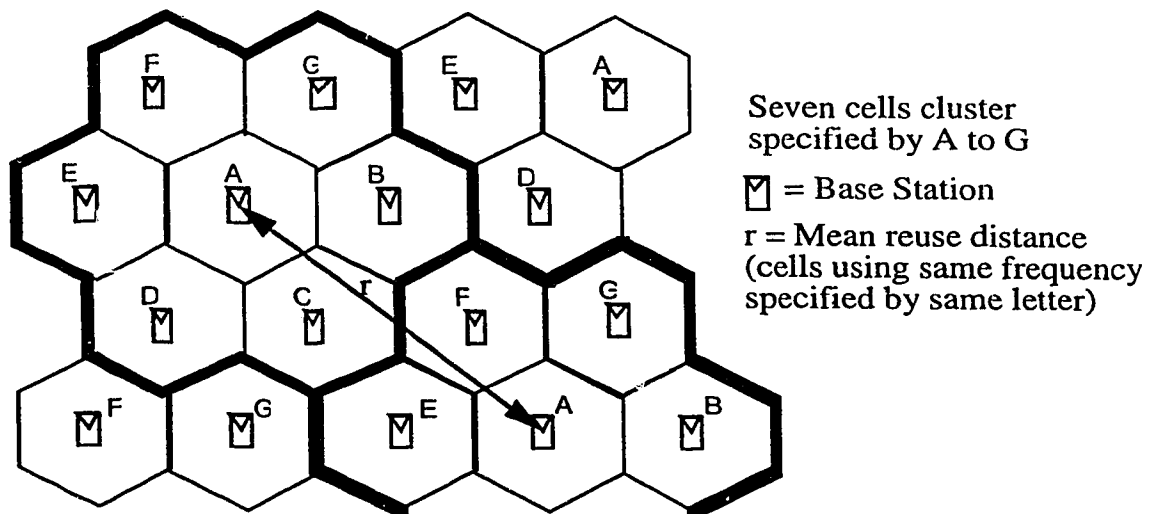


Fig. 1.1. Cellular mobile radio system.

Other first generation cellular systems, such as TACS, NMT, NTT and many others similar to AMPS were introduced in different parts of the world [1]. All these system use *frequency division multiple access (FDMA)*, and *analog frequency modulation* for speech transmission and *frequency shift keying* for signaling. Systems based on this technology are currently being used by more than 30 million subscribers worldwide. Additionally, first generation cordless

telephones using analog radio technologies were developed, but they provide low mobility (both in range and user's speed) and have low power compared to cellular.

A potential for further increase in capacity was made possible in early 1990, with the deployment of the second generation cellular systems using digital technology. These systems use *time division multiple access (TDMA)* or *code division multiple access (CDMA)*, low rate digital speech coding and bandwidth efficient modulation for more efficient use of the limited frequency spectrum. In addition to voice transmission, they offer such capabilities as point-to-point short messaging, broadcast messaging, and group addressing, etc.. The major standards are [2] the *Pan-European Global System for Mobile communications (GSM)* and *DCS1800; IS54* based on TDMA and *IS95* based on CDMA in North America; and *Personal Digital Cellular (PDC)* in Japan. Also, to provide increased user capacity in a quasi-static environment, digital cordless technology standards *CT-2 (second generation cordless telephone)* and *DECT (Digital European Cordless Telephone)* in Europe, and several different Industrial Scientific Medical band Technologies in the United States have evolved. These systems are, however, not compatible.

At the present time, work is in progress to evolve a third generation of cellular systems which will be capable of offering better voice quality (comparable to the fixed network), a suitable range of video and data services, comparable performance in vehicular, portable, rural, urban and indoor environments, and provision for wider mobility. Several wireless technologies currently provide wireless personal communications, but they need to overcome significant existing limitations. For example, digital cordless has a limited range;

digital cellular needs better voice encoding, has marginal circuit quality, limited data capabilities, holes in coverage and poor in-building coverage; wide area data needs to overcome a limited data rate, no voice capability and high cost; Wireless Local Area Networks (WLANs) have limited coverage and have no standards; paging and messaging systems are leading towards two way messaging and/or voice [3]. This implies that a lot of work is still required.

## **1.2 Digital Cellular System (IS54)**

Amidst the continuous evolution of new wireless communication technologies, efforts are also being made to improve the performance of existing cellular systems. The proposed second generation digital cellular communication system for North America (IS54) is currently being introduced into the market. The performance of this system is degraded significantly by the radio propagation channel [4]. This makes it essential to investigate and incorporate a suitable technique to combat the adverse effects of the propagation channel. This section presents the IS54 standard. The effects of the radio propagation channel on transmitted information signal are discussed in the next section. This is followed by a proposed technique to counteract the channel impairment. Finally, a thesis overview is presented.

The introduction of IS54 in the market is being driven by the need to serve the increasing number of subscribers. Instead of increasing system capacity by reducing the cell size and erecting more base-stations, which is a difficult and expensive solution, the use of digital technology was proposed by the EIA/TIA (Electronic Industry Association/Telecommunication Industry Association) subcommittee TR45.3 in the form of Interim Standard IS54. This is also known as the *North-American Dual Mode Cellular System (NADMCS)* because of the dual



nature of the mobile stations that ensures compatibility with the previously adopted AMPS analog system specifications. In less densely populated areas, where conversion from analog to digital can be slower (because the increased capacity offered by the digital system may not be required immediately), there exist a mix of analog and digital terminals as well as different types of base station equipment. Systems using the IS54 standard thus allow a smooth transition from the analog to the digitally implemented services to roaming subscribers.

The access scheme for IS54 is TDMA, and not FDMA as used in AMPS, because it allows easy transition to the new system enabling no change in the frequency plan of the old system. Also, with TDMA, the *mobile station assisted handover* (MAHO) procedure becomes faster and more accurate. In this process, the mobile unit measures the signal strength on channels from near-by base stations and reports them to its current base station. This reduces the signaling load between the base stations and the mobile services switching center (MSC). The time division multiple access scheme also facilitates the use of a flexible data rate by assigning the amount of time required (i.e. half the number of time slots for half rate channels) by each user.

The bit rate of a speech codec determines the capacity of a cellular system. The lower the bit rate, the lower the amount of spectrum consumed for one connection, permitting more simultaneous connections within the system bandwidth. The current implementation of the speech coding algorithm is *vector sum excited linear prediction coding* (VSELP) which uses 7.95kb/s for speech coding alone and 13kb/s with error protection [5].

The IS-54 system retains the 30kHz channel bandwidth of AMPS with a transmitter frequency in the 824-894MHz band. Each frequency channel provides a raw RF bit rate of 48.6kb/s. The modulation scheme has a spectral efficiency of 1.62b/s/Hz. This is achieved using a linear modulation method, called  $\pi/4$  shifted differential quadrature phase shift keying ( $\pi/4$  DQPSK), at a 24.3 kbaud channel rate. This has various advantages over other linear modulation schemes such as QPSK, OK-QPSK [6]. Since the encoding is differential, loss of data due to phase slips is reduced, enabling the use of simple non-coherent receivers. A *square root raised cosine* pulse shaping filter with *roll-off factor* equal to 0.35 is used to limit the bandwidth of the transmitted signal at the transmitter.

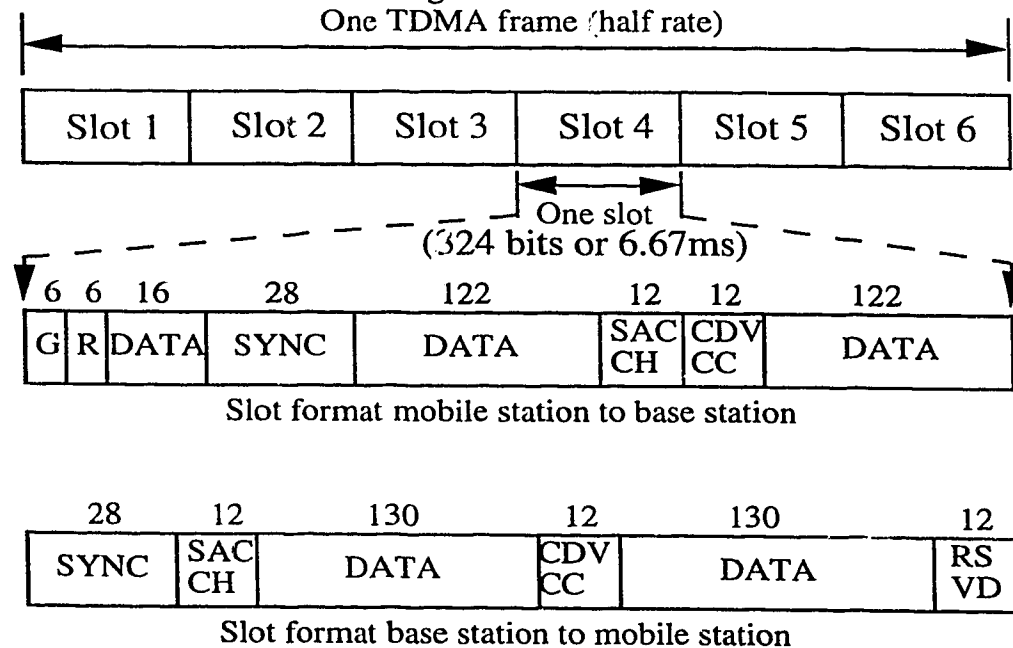


Fig. 1.2. Slot and frame structure for IS54.

The frame and time slot structure for each traffic channel in IS54 is shown in Fig. 1.2. The TDMA frame has a duration of 40ms for half rate channels, and the time slot duration is 40/6 ms for both full rate and half rate channels. The time slot formats for traffic to and from the base station are different. Each time frame

has a length of 1944 bits (972 symbols) and is divided into 6 slots of exactly 324 bits (162 symbols) in length. Each full rate traffic channel uses two equally spaced time slots of the frame, while each half rate channel uses one time slot of the frame. At a bit rate of 48.6 kbits/sec, 25 frames per second are transmitted.

For the purpose of this research, most of the parameters are taken from this standard. Because of the limited capacity of the available hardware and ease of implementation, some changes are made. The details of the relevant parameters that are selected are covered in later chapters.

### **1.3 Propagation Channel**

The radio signal transmitted from a mobile radio base station reaches a mobile terminal receiver after passing through a very harsh propagation channel. Because of terrain features and man-made structures, a line-of sight between the transmitting and receiving antennas seldom exists. Multipath propagation caused by reflection, diffraction and scattering is the principal mode of propagation for the information signal. The time-varying multiple paths formed by irregular terrain cause the signal energy to reach the receiver with different time delays, attenuations and phases. This gives rise to severe distortion of the information carried by the channel and results in many problems and limitations for mobile radio systems. To design an optimum method of mitigating the impairments caused by the complex time-varying multipath transmission channel, it is necessary to understand the impairments and to determine under what conditions their effects are most prominent.

#### **1.3.1 Path Loss**

The spatial separation between the transmitters and the receivers causes path-loss effects. This is primarily due to terrain effects and the presence of *radio*

*wave scatterers* along the path within the mobile radio environment. Antenna height, topography of the coverage area (hills, valleys), reflective properties of the surrounding structures (walls, buildings), and path obstructing features of intervening structures (building penetration), are some of many factors that affect path loss. Based on path loss measurement models, a tradeoff is made between coverage area and link power for a particular antenna design and radio frequency.

Fig. 1.3 shows the path loss region.

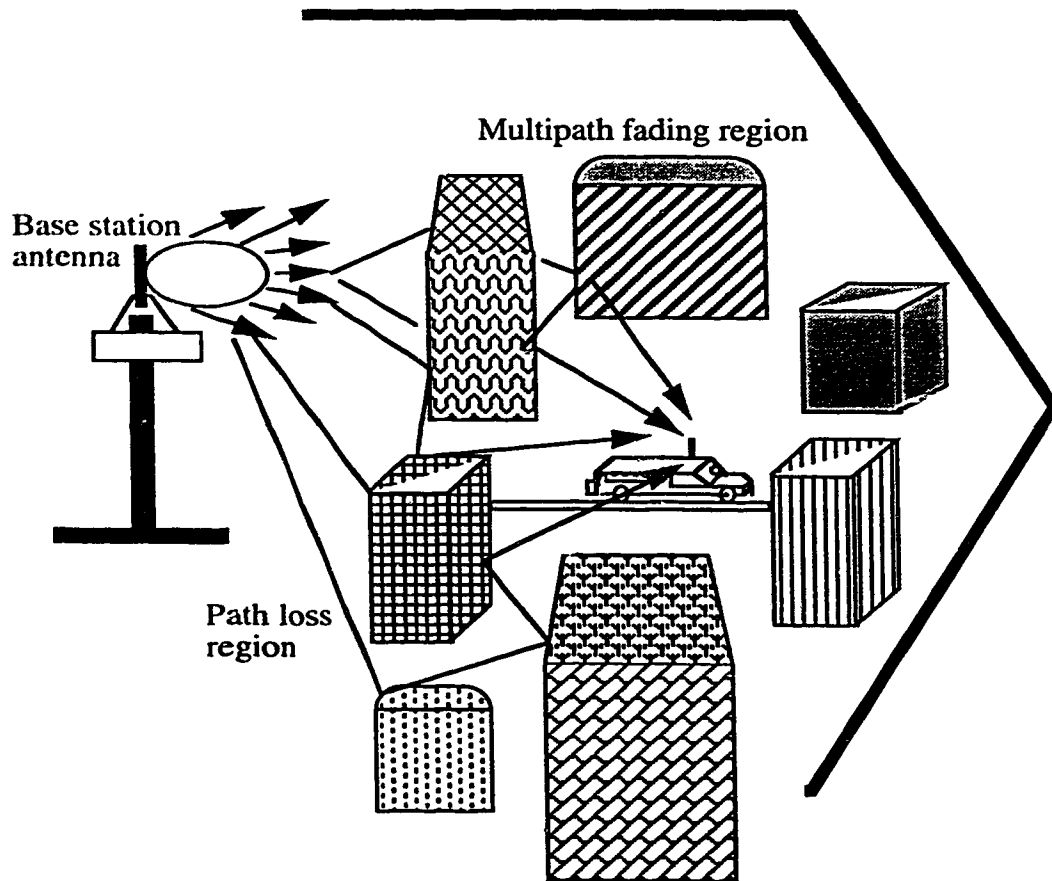


Fig. 1.3. Mobile radio environment.

### 1.3.2 Fading

The signal received by the mobile station consists of large number of plane waves whose amplitudes, phases and angles of arrival, relative to the direction of vehicle motion, are random. Their interference can be constructive or destructive. Fig. 1.4 illustrates this phenomenon.

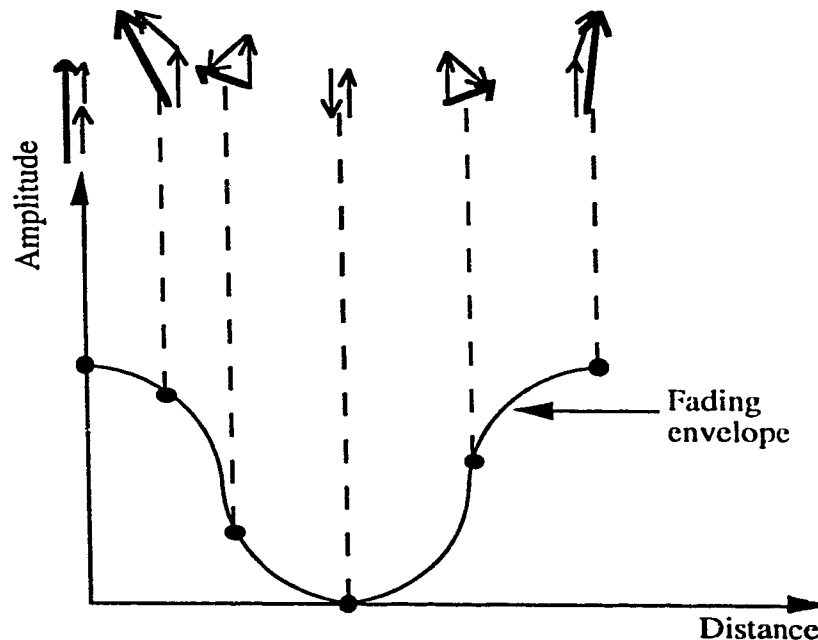


Fig. 1.4. Fading phenomenon.

Plane waves interfere and produce a varying field strength pattern with maxima and minima spaced about a quarter wavelength apart. With the short wavelengths of mobile radio frequencies, the received signal fades rapidly and deeply as the mobile moves around. Some fades are as low as 40dB below the mean signal strength. By reciprocity, the base station receiver experiences the same rapid fading. Signal fluctuation due to multipath effects caused by man-made structures in a local area is called *short term fading*. It is rapid and short lived as the mobile moves around. *Long term fading*, on the other hand, is a slow

variation mainly due to topology. *Shadowing*, where the mobile unit is located in the shadow region of mountains, hills etc. is also a cause of long term fading. The severity of multipath fading is shown in Fig. 1.5, which presents a typical segment of a fading signal received at a mobile unit. This is a cause of signal degradation and poor quality at receiver. The statistical characteristics of fading must be studied in order to find suitable methods for counteracting fading effects.

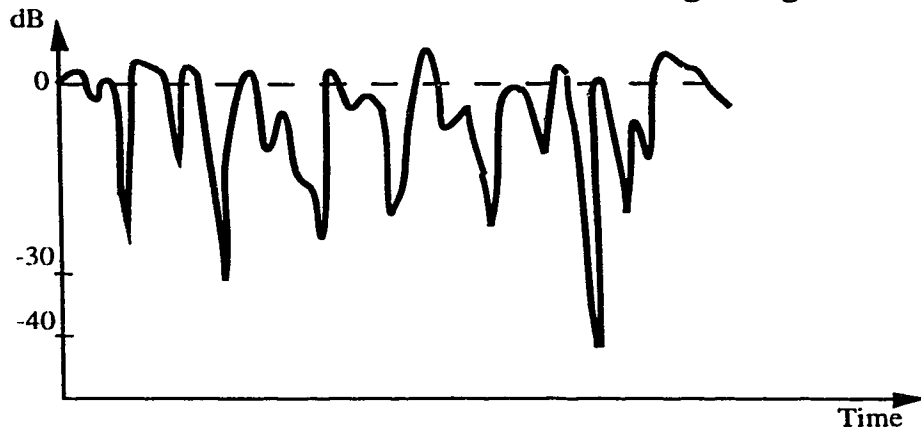


Fig. 1.5. Typical received signal strength variation.

### 1.3.3 Doppler effect

Vehicle motion relative to the base station transmitter causes a Doppler shift in the carrier frequency of the received signal. The amount of Doppler shift depends on the speed and direction of travel of the mobile unit with respect to the received signal and carrier frequency. Its value is very much less than the carrier frequency and determines the rate of short term fading, i.e., fades/sec. This creates a random frequency modulation of the transmitted carrier.

### 1.3.4 Delay spread

Random reflections and scattering that result in multipath cause replicas of the transmitted signal to reach the receiver with different propagation delays. As

shown in Fig. 1.6, a single sharp transmitted pulse would be received as a smeared and spread out form of the transmitted signal. This time dispersion, together with the symbol duration, determines if the time spreading is large enough for each symbol to overlap with its adjacent symbol to produce intersymbol interference (ISI).

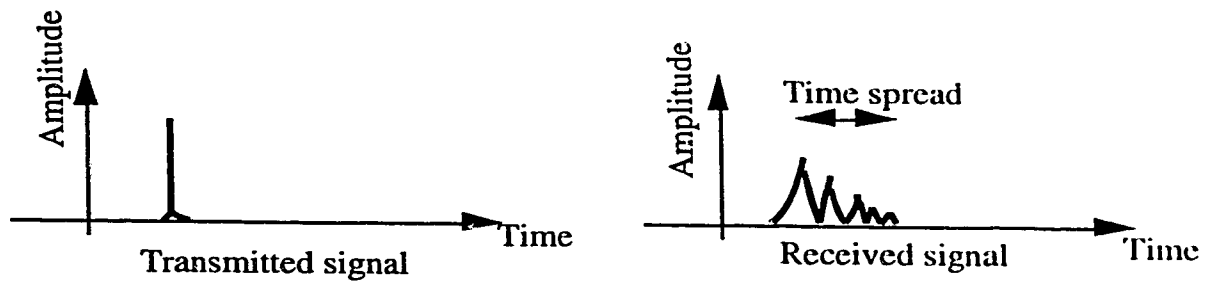


Fig. 1.6. Delay spread phenomenon.

The average rms or worst case value of the delay spread is dependent upon the geometric relationships between the transmitter, the receiver and the surrounding physical environment. Typically, the rms delay for an indoor environment is between 20ns to 300ns [7]. For an outdoor environment it is less than  $8\mu\text{s}$  for urban areas and between  $10\mu\text{s}$  to  $30\mu\text{s}$  for hilly and mountainous areas. For a delay spread  $\delta$ , symbol time  $T$ , and signal bandwidth  $W$ , the channel is dispersive in time or selective in frequency when  $\delta \gg T$  and  $\delta \gg 1/W$ . The channel is frequency selective because, at the same time, a signal fades different amounts for different frequencies within the bandwidth.

### 1.3.5 Noise

On a radio link electrical noise generated by external sources enters the receiver through the antenna. Internal noise, such as thermal noise, in the receiver, also contributes to the total noise in the system. Sources of man-made noise at the base station are automotive noise, power generating facilities, industrial

equipment, consumer products like lighting systems, medical equipment, electrical trains and buses. When selecting the base station site and antenna height, its surroundings are considered for noise level. All the noise sources combined together are generally characterized as additive white Gaussian noise (AWGN) [8].

#### **1.4 Decision-Aided Detection**

A receiver based on the conventional differential detector exhibits significant performance degradation due to the detrimental effects of the radio propagation channel. Considerable efforts have been made in the past to reduce the undesired effects of the multipath phenomenon. Techniques such as pilot symbol insertion, error correction coding and diversity can be used for performance improvement [9]. Some other signal processing schemes have also been proposed in the literature that are based on channel prediction, using the transmitted symbols alone [10, 11].

In this work, a receiver based on a decision-aided channel estimation and error correction algorithm has been investigated for  $\pi/4$ DQPSK modulation. Decision-aided feedback is used to estimate the phase variations due to a flat fading channel. Since, channel phase variations directly contribute to demodulation errors, estimation and removal of the channel phase variations can greatly improve the quality of the received signal. The channel estimation relies on the fact that typically, 99 out of 100 received symbols are detected correctly by the differential detector. Thus, the differential detector decisions (first decisions) may be used by a *reverse modulator* to remove the modulation from the received signal and recover the channel phase information. This extracted phase information is also typically correct 99 out of 100 times. To reduce the effect of



incorrect first decisions on the extracted channel, a low pass *channel estimation filter* is used. The smoothed channel characteristic, along with the differential detector decisions are then used for making a new decision for the data, thereby correcting many of the errors made in the first decision. The reverse modulation is done by complex conjugate multiplication of the baseband received signal vector and the first decision signal vector, and the channel estimation filter is a simple FIR filter. This technique can be implemented in real time using a *digital signal processor (DSP)*. Decision aided detection has been shown to be an effective error correcting method for binary phase shift keying (BPSK) [12, 13]. Its performance for  $\pi/4$ DQPSK modulation as per the IS54 standard is studied in this project, in order to achieve improved error performance for the North American digital cellular standard.

## **1.5 Thesis Overview**

This chapter has presented the various deleterious effects of the radio propagation channel on the signal transmitted as per digital cellular standards. The objective of this research is to improve the performance of IS54 based systems through the use of a decision-aided channel estimation and error correction algorithm.

Chapter 2 describes the basic structure of a digital transceiver and details of the channel model. The effect of a flat fading single path channel on the bit error rate, causing an irreducible error floor, is described next. An overview of channel compensation techniques which can be employed to improve system performance are presented.

Chapter 3 explains the structure of the decision-aided detector which is investigated in this thesis. The functional characteristics of each component in the channel estimator and error corrector module are described.

Chapter 4 presents the experimental implementation of the digital transceiver with the decision-aided detection, using two *Texas Instruments* DSPs. The test results obtained from the implemented detector are presented and discussed in chapter 5.

Chapter 6 summarizes and discusses the research results, and outlines areas for possible future research work.

## 2. TRANSCEIVER STRUCTURE AND ERROR FLOOR REDUCTION TECHNIQUES

In this chapter, the basic structure of a  $\pi/4$ DQPSK transmitter and model of the fading channel used, are described. The structure of the demodulator and differential detector used to recover the transmitted data are presented next. The effect of the channel on the bit error rate and the occurrence of an irreducible error floor is then discussed. This is followed by background information on various methods for lowering the irreducible error floor, including a brief discussion on their performance and limitations in combating fading effects.

### 2.1 Structure of $\pi/4$ DQPSK Transmitter

The basic structure of the communication system and a simplified model of the transmitter based on the IS-54 standard are shown in Fig. 2.1a and b. Each module of the transmitter is described briefly in the following sections:

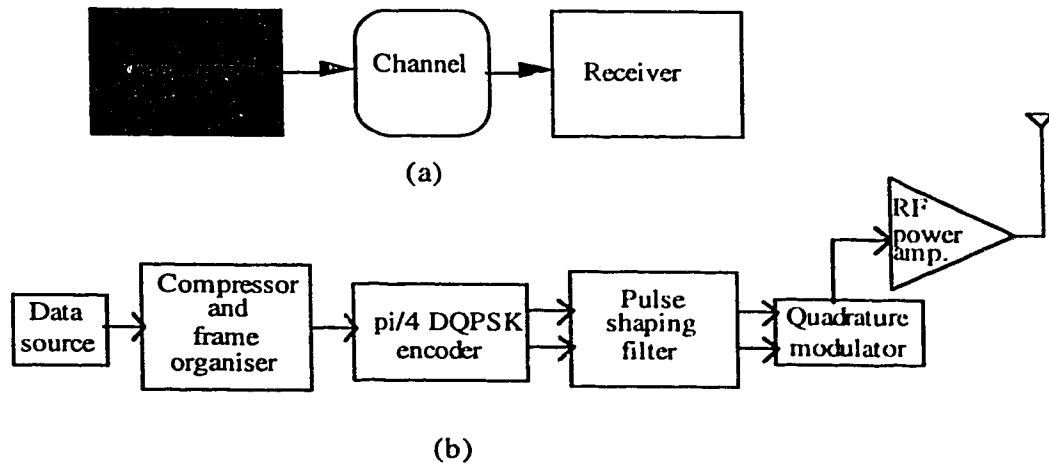


Fig. 2.1. (a) Basic communication system model. (b) Transmitter structure.

#### 2.1.1 Data Source

The data source is a binary digital information source such as digitized speech (64kb/s) or digital data, which is to be transmitted.

### 2.1.2 Data Compressor and Frame Organizer

The data compressor is used to eliminate redundancy in the speech signal, so as to reduce its bit rate. According to the IS54 standard, the *vector sum excited linear predictive (VSELP)* coding technique is used to compress the digitized voice signal from 64kb/s to 7.95kb/s [5]. This information payload, along with overhead bits and signaling bits, is then mapped onto a standard frame format, to produce a 48.6kb/s serial bit stream.

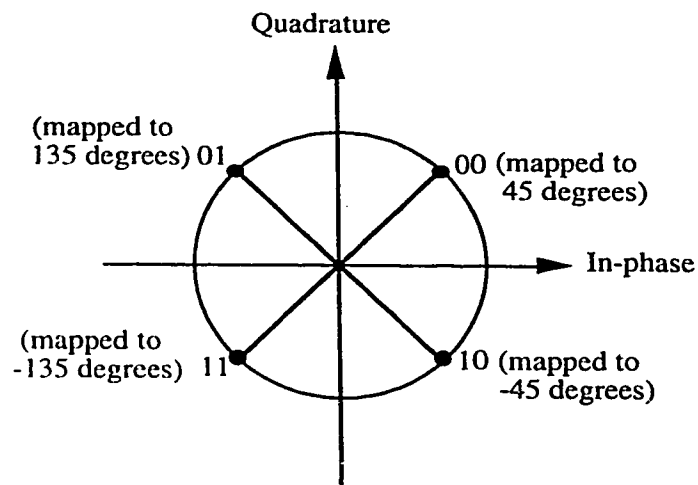


Fig. 2.2. Gray coding for  $\pi/4$ DQPSK.

### 2.1.3 $\pi/4$ DQPSK Encoder

The serial data stream is encoded into 2-level symbols using a Gray code format, as shown in Fig. 2.2, to reduce the probability of bit error. Each symbol is encoded differentially onto the in-phase and quadrature components (SI and SQ) of the equivalent complex baseband signal. The differentially encoded signal is obtained in accordance with the  $\pi/4$ DQPSK modulation format of Table 2.1.

TABLE 2.1  
RELATION BETWEEN SERIAL INPUT DATA AND DIFFERENTIAL  
PHASE ANGLE.

Input Data ( $b_1, b_0$ )	Differential Phase Angle ( $\Delta\phi$ )
0,0	$+\pi/4=+45^\circ$
0,1	$+3\pi/4=+135^\circ$
1,0	$-\pi/4=-45^\circ$
1,1	$-3\pi/4=-135^\circ$

Fig. 2.3 shows the signal constellation of  $\pi/4$ DQPSK modulation. The eight phase points can be considered to be formed by superimposing two quadrature phase shift keying (QPSK) signal constellations offset by  $45^\circ$  relative to each other. During each symbol period, a phase angle from one of the two QPSK constellations is transmitted. The two constellations are used alternately, so that each successive symbol is mapped into the phase changes given in Table 2.1.

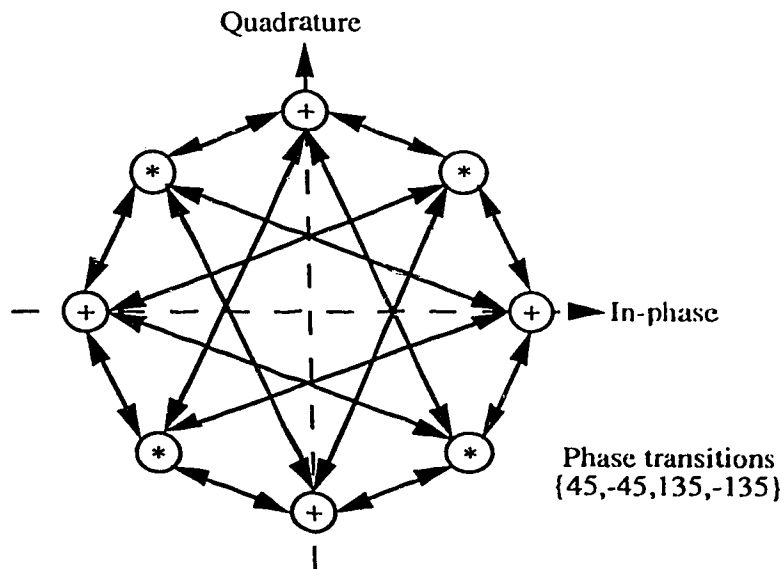


Fig. 2.3. Constellation for  $\pi/4$ DQPSK modulation.

### 2.1.4 Pulse Shaping Filter

The differentially encoded signals SI and SQ are passed through a baseband filter to limit the bandwidth of the transmitted signal. According to the IS54 standard, a *square root raised cosine (SRRC) filter* with a roll-off factor ( $\alpha$ ) of 0.35 should be used. The frequency response of this type of filter is defined as [14]

$$|H(f)| \equiv \begin{cases} 1 & 0 \leq |f| \leq \frac{1-\alpha}{2T} \\ \sqrt{\frac{1}{2} \left\{ 1 - \sin \left[ \frac{\pi(2fT-1)}{2\alpha} \right] \right\}} & \frac{1-\alpha}{2T} \leq |f| \leq \frac{1+\alpha}{2T} \\ 0 & |f| \geq \frac{1+\alpha}{2T} \end{cases} \quad (2-1)$$

where  $\alpha$  is the roll-off factor and  $T$  is the symbol duration. Fig. 2.4 shows the frequency response for a symbol rate of 1.2ks/s with  $\alpha = 0.35$ .

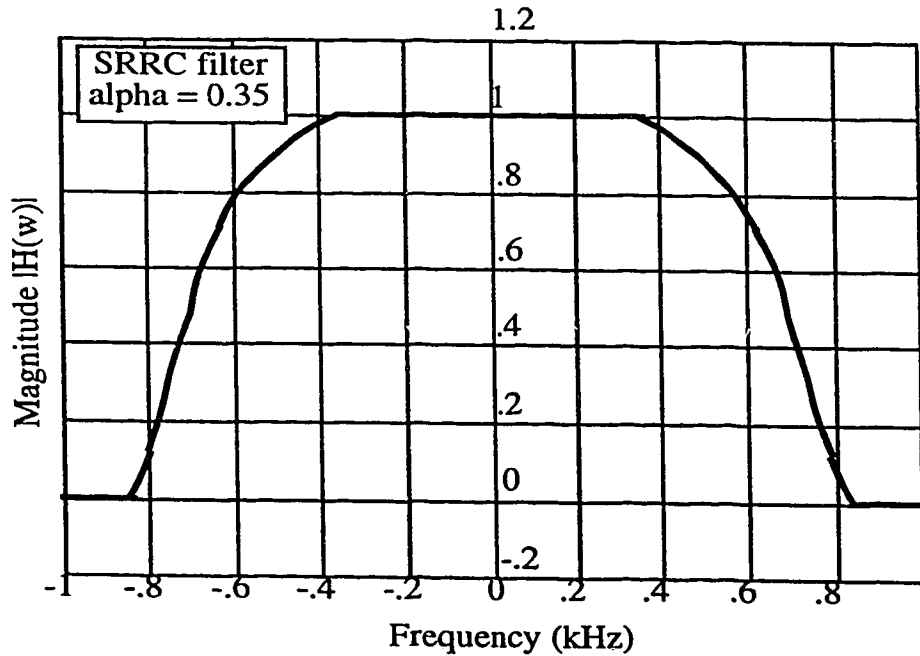


Fig. 2.4. Frequency response of pulse shaping filter.

### 2.1.5 Radio Frequency (RF) Section

The RF section in the transmitter has a quadrature modulator, a power amplifier and an antenna. The main components of the quadrature modulator are the oscillator which generates the carrier frequency, and the phase splitter, mixers and in-phase combiner which constitute the modulator. The carrier frequency is specified in the IS54 standards [5], as shown in Table 2.2.

TABLE 2.2  
IS54 SPECIFICATIONS FOR CARRIER FREQUENCY.

Transmitter	Channel Number	Center Frequency (MHz)
Mobile	$1 \leq N \leq 799$	$0.030N + 825.000$
	$990 \leq N \leq 1023$	$0.030(N - 1023) + 825.000$
Base	$1 \leq N \leq 799$	$0.030N + 870.000$
	$990 \leq N \leq 1023$	$0.030(N - 1023) + 870.000$

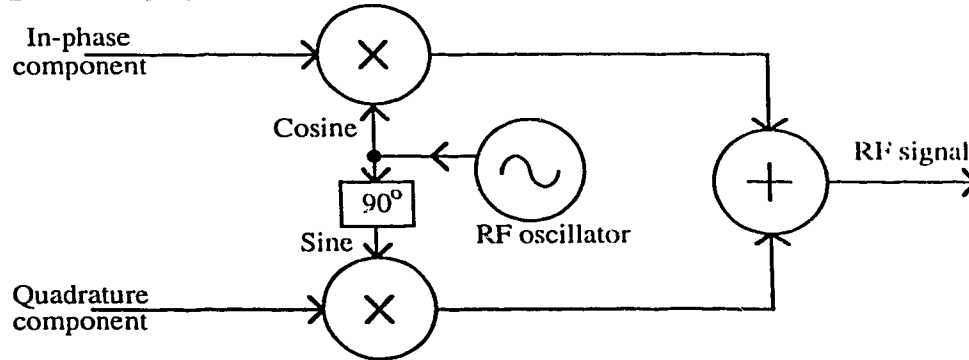


Fig. 2.5. Quadrature modulator.

The output of the oscillator is split into two components with a  $90^\circ$  phase shift, producing carriers that may be represented by  $\sin(\omega_c t)$  and  $\cos(\omega_c t)$ . The mixers multiply these phase-shifted signals by the in-phase and quadrature filtered baseband signals, as shown in Fig. 2.5. The output of the mixers are then added together by the combiner, resulting in the modulated RF signal. Finally, the signal is amplified and fed to the antenna. If  $h(t)$  is the time domain response of the

square root raised cosine filter, then the resultant phase modulated transmitted signal is given by

$$s(t) = \sum_n h(t - nT) \cos(\omega_c t + \phi_n) \quad (2-2)$$

where  $\omega_c$  is the carrier frequency of transmission and  $\phi_n$  is the absolute phase angle for the  $n^{\text{th}}$  symbol period (i.e.  $[n+1]T \geq t \geq nT$ ).

## 2.2 Radio Propagation Channel

Multipath propagation has already been mentioned as a principal feature of mobile radio channels. The characterization of multipath phenomena is presented in this section. Since the transmitted signal in the case of IS54 is narrow-band, and the delay spread in urban areas is less than 8  $\mu\text{sec}$ , all the signal frequency components are affected by the channel in a similar way. The fading is therefore called *flat fading*, implying that there is no frequency-selective behavior. Several multipath models have been proposed to explain the observed statistical characteristics of the radiated electromagnetic fields, and the associated signal envelope and phase [15]. However, they all lead to comparable statistical properties of the field for large numbers of constituent waves. A model based on scattered waves, describing the characteristics of the signal received by an antenna mounted on a mobile unit, is considered here.

### 2.2.1 Scattering Model

If the transmitted signal is vertically polarized, the field components seen at the receiver would normally be horizontally traveling waves. In general, due to scattering and diffraction the waves travel in other directions as well [16]. Since the wavelength of the signal is relatively small, each reflection may be considered as a ray. The signal at the receiving point is thus the resultant of  $N$  plane waves caused by multipath reflections of the transmitted wave. Each plane wave has a



random amplitude and angle of arrival at different locations. A typical component wave is shown in Fig. 2.6 with a spatial frame of reference.

The  $n^{\text{th}}$  incoming wave has an amplitude  $C_n$  and phase  $\phi_n$  with respect to an arbitrary reference, and spatial angle of arrival  $\alpha_n$  and  $\beta_n$ . The parameters  $C_n$ ,  $\phi_n$ ,  $\alpha_n$  and  $\beta_n$  are all random and statistically independent. The phase angles are assumed to be uniformly distributed from 0 to  $2\pi$ . The amplitude  $C$  has a mean square value of

$$E\{C_n^2\} = \frac{E_0}{N} \quad (2-3)$$

where  $E_0$  is a positive constant.

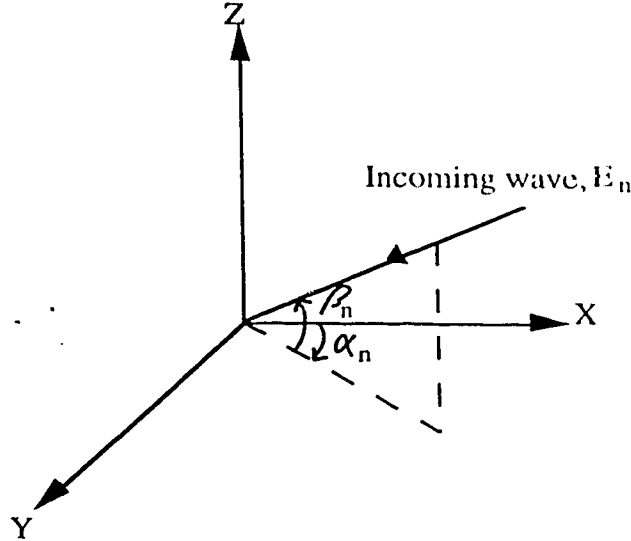


Fig. 2.6. Scattering model.

For  $N$  such waves, the resultant field at any receiving point  $(x_o, y_o, z_o)$  is

$$E(t) = \sum_{n=1}^N E_n(t). \quad (2-4)$$

If the transmitted signal is an unmodulated carrier, then

$$E_n(t) = C_n \cos(\omega_o t - \frac{2\pi}{\lambda} [x_o \cos \alpha_n \cos \beta_n + y_o \sin \alpha_n \cos \beta_n + z_o \sin \beta_n] + \phi_n). \quad (2-5)$$

The mobile receiving point is assumed to be moving with a velocity  $v$  in the x-y plane in a direction making an angle  $\gamma$  to the x-axis. The co-ordinates of the receiving point after a unit time are  $(v \cos \gamma, v \sin \gamma, z_0)$  and the received field is now given by

$$E(t) = CI(t)\cos w_c t - CQ(t)\sin w_c t \quad (2-6)$$

where  $CI(t)$  and  $CQ(t)$  are the in-phase and quadrature component that would be detected by receiver,  $w_c$  is the carrier frequency, and  $\lambda$  is the wavelength of the transmitted carrier frequency. Here,

$$CI(t) = \sum_{n=1}^N C_n \cos(w_n t + \theta_n) \quad (2-7)$$

$$CQ(t) = \sum_{n=1}^N C_n \sin(w_n t + \theta_n) \quad (2-8)$$

$$w_n = \frac{2\pi v}{\lambda} \cos(\gamma - \alpha_n) \cos \beta_n \quad (2-9)$$

$$\theta_n = \frac{2z_0\pi}{\lambda} \sin \beta_n + \phi_n. \quad (2-10)$$

Due to the motion of the receiver, each wave experiences a Doppler frequency shift. The Doppler frequency will have a maximum value of  $f_m = \pm \frac{v}{\lambda}$ , a value

which is very much less than the carrier frequency (typically  $f_m$  is less than 100Hz). If the value of  $N$  is sufficiently large ( $> 6$ ), then, by the central limit theorem, the quadrature components  $CI(t)$  and  $CQ(t)$  will be independent Gaussian processes which are completely characterized by their mean value and autocorrelation function. The mean of  $E(t)$  is zero, since the mean values of both  $CI(t)$  and  $CQ(t)$  are zero. Also,  $CI(t)$  and  $CQ(t)$  have an equal variance,  $\sigma^2$ , equal to the mean square value or the mean power.

The probability distribution function of CI and CQ is thus [17]

$$p_x(x) = \frac{1}{\sigma\sqrt{2\pi}} \exp\left(-\frac{x^2}{2\sigma^2}\right), \quad (2-11)$$

where  $x=CI(t)$  or  $CQ(t)$  and  $\sigma^2 = E\{C_n^2\} = \frac{E_o}{N}$ .

### 2.2.2 Channel Characteristics

The Gaussian model described above may be used to predict the field-measured statistics of the signal. These statistical properties can be used to duplicate multipath characteristics in an experimental laboratory study or for the purpose of simulation. These characteristics of the channel are important parameters for the design and evaluation of different radio systems.

#### 2.2.2.1 Power Spectra

The spectrum of the received signal is strictly bandlimited to the range  $\pm f_m$  around the carrier frequency, and is given by [18]

$$A_o(f) = \begin{cases} \frac{E_o}{4\pi f_m \sqrt{1 - \left(\frac{f}{f_m}\right)^2}} & \text{for } |f| \leq f_m \\ 0 & \text{elsewhere} \end{cases} \quad (2-12)$$

where  $f_m$  is the maximum Doppler shift. It may be noted that, the power spectral density becomes infinite at  $f_c + f_m$  and  $f_c - f_m$  but is immediately zero outside these limits. For a typical mobile radio system the value of the maximum Doppler shift  $f_m$  will be in the range 10 to 100Hz; although this frequency shift is small, it may cause deterioration of the message information.

#### 2.2.2.2 Statistics of Received Signal Envelope and Phase

The envelope  $r(t)$  of the complex baseband signal  $E(t)$ , received at a radio receiver is given by

$$E(t) = CI(t) + jCQ(t) \quad (2-13)$$

$$r(t) = \sqrt{CI^2(t) + CQ^2(t)} . \quad (2-14)$$

Since CI and CQ are both Gaussian distributed with equal variances  $\sigma^2$ , then  $r(t)$  has a Rayleigh probability density function (pdf) [19]

$$p_r(r) = \frac{r}{\sigma^2} \exp\left(-\frac{r^2}{2\sigma^2}\right) \quad (2-15)$$

where the mean power for the Rayleigh pdf is  $2\sigma^2$ . The probability that the envelope does not exceed a specified value  $R$  is given by the cumulative distribution function

$$\text{prob}(r \leq R) = P_r(R) = \int_0^R p_r(r) dr = 1 - \exp\left(-\frac{R^2}{2\sigma^2}\right) . \quad (2-16)$$

The received signal phase is a uniformly distributed random process, given in terms of CI(t) and CQ(t) by

$$\theta(t) = \tan^{-1}\left(\frac{CQ(t)}{CI(t)}\right) \quad (2-17)$$

$$\text{with} \quad p_\theta(\theta) = \frac{1}{2\pi} , \quad 0 \leq \theta \leq 2\pi . \quad (2-18)$$

Since the signal is composed of a number of components of random phase, the resultant phase is random and takes on all values in the range  $(0, 2\pi)$  with equal probability. The probability distribution function gives information such as the overall percentage of time, or the overall percentage of locations, for which the envelope lies below a specified value. However, it does not provide information about how this time is distributed. The level crossing rate (LCR) and average fade duration (AFD) are used to provide a quantitative measure of this property.

### 2.2.2.3 Level Crossing Rate and Average Fade Duration

The level crossing rate at any specified signal level is the expected rate at which the envelope crosses a specified level in the positive-going (or negative-going) direction. Mathematically, the level crossing rate is

$$n(r = A) = \frac{N}{T} \quad (2-19)$$

where N=total number of crossings over T second length of data. It can be shown that the theoretical LCR is given by [15]

$$n(r = A) = \sqrt{\frac{\pi}{\sigma^2}} A f_m \exp\left(-\frac{r^2}{2\sigma^2}\right) \quad (2-20)$$

where A is a specified level,  $f_m$  is the maximum Doppler shift and  $\sigma^2$  is the mean power of the envelope. The average fade duration ( $\bar{\tau}$ ), is used to quantitatively measure the average period of a fade below a specified level A. Mathematically, AFD is given by the total duration of N fades below level A, divided by N,

$$\bar{\tau}(r = A) = \frac{\sum_{i=1}^N t_i}{N} \quad (2-21)$$

where  $t_i$  is the duration of the  $i^{\text{th}}$  individual fade. Theoretically, [15]

$$\bar{\tau} = \sqrt{\frac{\sigma^2}{\pi}} \frac{\exp\left(\frac{A^2}{2\sigma^2}\right) - 1}{A f_m} \quad (2-22)$$

### 2.2.2.4 Envelope Correlation

The envelope correlation characteristic, based on time and space separation, has its importance in *diversity* and other applications. The correlation coefficient based on time separation is given by [20]

$$\zeta_r(\tau) = J_0^2(\beta v \tau) \quad (2-23)$$

where  $J_0$  is the Bessel function of the first kind of order zero and  $\tau$  is the time separation between envelopes. The correlation coefficient will be zero whenever  $J_0(\beta v \tau)$  is equal to zero, implying that for certain values of  $\tau$ , the probability that

two envelopes of the same signal, separated by  $\tau$ , fade simultaneously is zero. The first zero occurs when  $v\tau/\lambda = 0.38$ , which happens when the time separation is equal to  $\tau = 0.38\lambda/v$ . Spatial correlation is related to time correlation by  $d = v\tau$ , which therefore implies that two antennas separated by  $d = 0.38\lambda$  will receive uncorrelated envelopes.

### 2.2.3 Channel Model

The simulation model for fast flat fading that characterizes the statistical properties described above is shown in Fig. 2.7. Its implementation and performance is described in Chapter 4 and 5. Two Gaussian random generators are used to create an equivalent complex baseband signal with a Rayleigh distributed envelope. The Gaussian processes are fed into two lowpass filters with cutoff frequency equal to the maximum Doppler frequency in order to produce the correct amplitude versus frequency characteristic for the fading channel. The outputs of these shaping filters are the in-phase component,  $CI(t)$ , and the quadrature phase component,  $CQ(t)$ , of the channel. Their combined effect on the transmitted signal is to produce a uniformly distributed phase, a Rayleigh envelope and the required Doppler power spectrum.

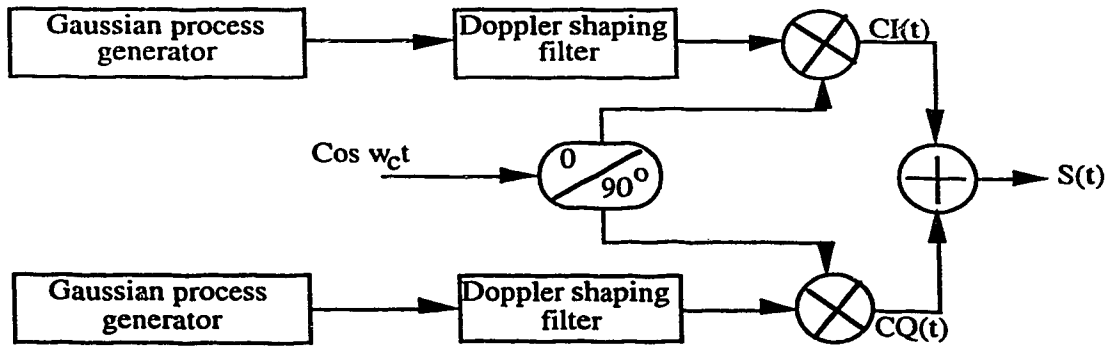


Fig. 2.7. Radio channel model.

## **2.3 Structure of $\pi/4$ DQPSK Receiver**

### **2.3.1 Demodulator Section**

This is very similar to the transmitter RF section in terms of components, but the sequence of operation and the signal flow are in the opposite direction. The demodulator recovers the base-band signal and clock from the modulated carrier. Base-band recovery is accomplished by multiplying the incoming signal with the local oscillator signal, and then low-pass filtering.

The receiver filter used is exactly the same as that used in the transmitter. The cascade of the two square root raised cosine filters gives an over all raised cosine filter which, as per Nyquist's second theorem, is a zero ISI filter. That is, the impulse response of this filter passes through zero at all sampling intervals except the desired symbol instant. The zero ISI condition holds true only for the ideal condition of no fading and distortion. The other purpose of the receiver lowpass filter is to limit the noise and remove unwanted frequency products resulting from the frequency down-conversion process.

The next stage is the sampler, which converts the signal to a discrete time signal at a sample rate equal to the symbol rate; the sampling frequency and timing are determined by the timing recovery circuitry. The clock recovery circuit is used to maintain the optimum decision point for the data, so that the ISI effect from neighboring symbols is minimized.

### **2.3.2 Detector**

$\pi/4$  shifted, differentially encoded quadrature phase shift keying is amenable to a number of different detection techniques. According to IS54, any detection scheme can be chosen so long as it meets the specified minimum performance. In general, the various proposed detection methods are classified as

coherent, differential and discrimination. A coherent detector is more complex to implement than the other methods due to the required additional circuitry for the carrier recovery. However, the performance of a coherent detector is 2-3dB better than that of a non-coherent detector in Gaussian and slowly fading channels. In a fast fading channel however, coherent detection results in a higher irreducible error floor than either differential or discriminator detection. The three non-coherent detection realizations, namely baseband differential detection, IF band differential detection and FM discriminator detection, have an equivalent BER performance [21]. Each method has its own design challenges. In the first method, the design of the local oscillator is quite intricate. If the local oscillator has a frequency difference of  $\Delta f$  relative to the unmodulated carrier, the phase drifts by  $2\pi\Delta fT$  during one symbol duration ( $T$ ). This phase drift causes a performance degradation. In the last two methods, the challenge lies in the design of the bandpass filter, which requires a specified amplitude and phase response [21]. Also, this filter needs to minimize the effect of noise and ISI. The baseband differential detection scheme has been selected for this research project from an implementation simplicity view-point.

### 2.3.2.1 Baseband Differential Detector

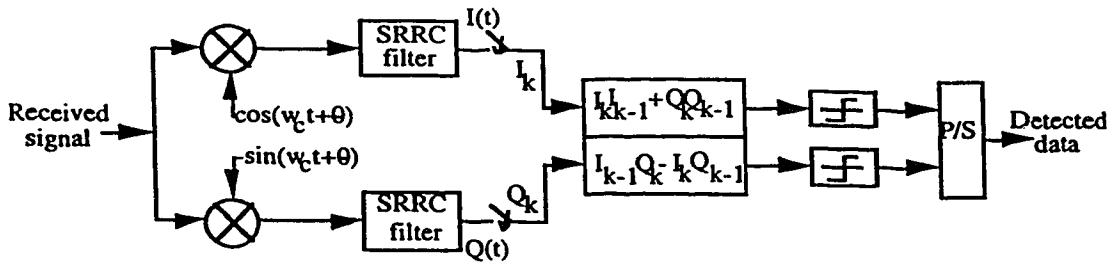


Fig. 2.8. Block diagram of the baseband differential detector.



The block diagram of the baseband differential detector is shown in Fig. 2.8. The local oscillator (LO) is assumed to have the same frequency as the transmitter, and with no phase difference. The effect of a different receiver LO frequency from the transmitter LO is described in [22]. Here, it is assumed that the receiver sampling clock is jitter free and synchronous with the transmitter frequency, and with the full eye opening occurring at  $t=nT$ , for the ideal channel. The two branches of the receiver recover the in-phase  $I(t)$  and quadrature  $Q(t)$  components of the received signal. The detected phase angle of the received signal is given by  $\phi = \tan^{-1}[Q(t)/I(t)]$ .

At the sampling instant  $t=kT$ , assuming that the channel is an ideal Nyquist channel and that the sampler output is  $I_k$  and  $Q_k$ , then

$$I_k = \cos(\phi_k) \quad (2-24)$$

$$Q_k = \sin(\phi_k) \quad (2-25)$$

where  $\phi_k$  is the signal phase at  $t=kT$ , which is preserved through the Nyquist channel. The change of phase angle over one symbol period contains the transmitted information. The data is detected by determining

$$U_k = \cos(\phi_k - \phi_{k-1}) = I_k I_{k-1} + Q_k Q_{k-1} \quad (2-26)$$

$$V_k = \sin(\phi_k - \phi_{k-1}) = I_{k-1} Q_k - I_k Q_{k-1} \quad (2-27)$$

The  $U_k$  and  $V_k$  values determine the quadrant of the transmitted signal. The decision for the data is then made based on the Gray code encoder used in the transmitter.

The detected data is determined according to the following conditions:

$$\begin{aligned} D1_i &= 1, \text{ if } U_k > 0; \\ D1_q &= 1, \text{ if } V_k > 0; \\ D1_i &= 0, \text{ if } U_k < 0; \\ D1_q &= 0, \text{ if } V_k < 0; \end{aligned} \tag{2-28}$$

where  $D1_i$  and  $D1_q$  are the two consecutive bits encoded by each symbol.

### 2.3.3 Performance Measurement

Whenever a signal is detected based on a noisy observation, there is a possibility of making an error. The error probability is defined by,

$$P_e = Pr(DI \neq D) \tag{2-29}$$

where  $D1$  is the detected data and  $D$  is the transmitted data.

The performance of a receiver is measured by sending a known sequence of data from the transmitter. The detected sequence at the receiver is then compared to the transmitted data sequence and the number of symbols or bits in error are measured. The signal and noise powers are measured at the detector input in order to calculate the signal to noise ratio (SNR). A good receiver design is one that minimizes the probability of error for a given signal to noise ratio.

## 2.4 Fading Effect: Irreducible Error Floor

When the received signal is corrupted by the multiplicative fading process that gives rise to the Rayleigh fading phenomenon, the bit error rate is higher than it would be in a Gaussian noise environment. The bit error rate (BER) is a function of the average signal level and the coherence bandwidth based on the delay spread. The BER is, in general, high for a low SNR, but decreases as the average signal level increases. At a certain signal level, however, the BER curve flattens out and the BER becomes constant even though the signal level

continues to increase. This bit error rate, called an *irreducible error* or *error floor*, that persists even for high SNR values, is due to *random FM*, as explained below.

Random FM is the direct result of the phase noise introduced by the fading channel. Because the received signal phase,  $\theta$ , varies with location, movement of the mobile produces a random change of  $\theta$  with time, equivalent to random phase modulation. This is normally called random FM, because the time derivative of  $\theta$  causes frequency modulation which will be detected by any phase sensitive detector; e.g. a differential detector or FM discriminator. The detected phase shifts due to the channel appear as noise to the receiver; in terms of the in-phase and quadrature signal components, the FM noise is given by

$$\dot{\theta} = \frac{d\theta}{dt} = \frac{d}{dt} \left[ \tan^{-1} \frac{CQ(t)}{CI(t)} \right] \quad (2-30)$$

The characteristics[18] of the pdf and power spectrum, of  $\dot{\theta}$  are functions of the vehicle speed  $v$  or, alternatively, of the Doppler frequency  $v/\lambda$ . Although, the highest probabilities occur for small values of  $\dot{\theta}$ , large excursions due to deep fades can also occur. The random FM spectrum [15, 18] shows that the energy is mainly confined to the frequency range  $0 \leq f \leq 2f_m$ , from where it falls off as  $1/f$ ; it is insignificant beyond  $5f_m$ .

Various methods, described in the literature, to improve the performance of the receiver in a fading environment are discussed in the following section.

## **2.5 Error Floor Reduction Techniques**

### **2.5.1 Pilot Symbol Insertion**

The pilot symbol insertion method has the potential to estimate the random phase in a Rayleigh fading system. The block diagram of such a transmitter is depicted in Fig. 2.9. In the transmitter, a known symbol, called a pilot symbol, is inserted in each frame containing  $N$  symbols (including the pilot

symbol). This is achieved using N-1:1 multiplexers that sample one pilot symbol followed by N-1 data symbols. The block diagram of the corresponding coherent demodulator is depicted in Fig. 2.10a. Assuming perfect frame synchronization, the receiver identifies the pilot symbols through a duplicate generator at its end. The fading distortion is measured using these known pilot symbol as

$$W(kNT) = \cos(\theta_{kn}) U(kNT) + \sin(\theta_{kn}) V(kNT) \quad (2-31)$$

$$Z(kNT) = \cos(\theta_{kn}) V(kNT) - \sin(\theta_{kn}) U(kNT) \quad (2-32)$$

where,  $U(t)$  and  $V(t)$  are the in-phase and quadrature components of the received signals and  $W(t)$  and  $Z(t)$  are the estimation of fading channel.  $\theta_{kn}$  is the phase of carrier at  $t=kNT$ . It is assumed here that a jitter free synchronous clock is generated in the receiver, and that the data is ISI free at  $t=nT$ .

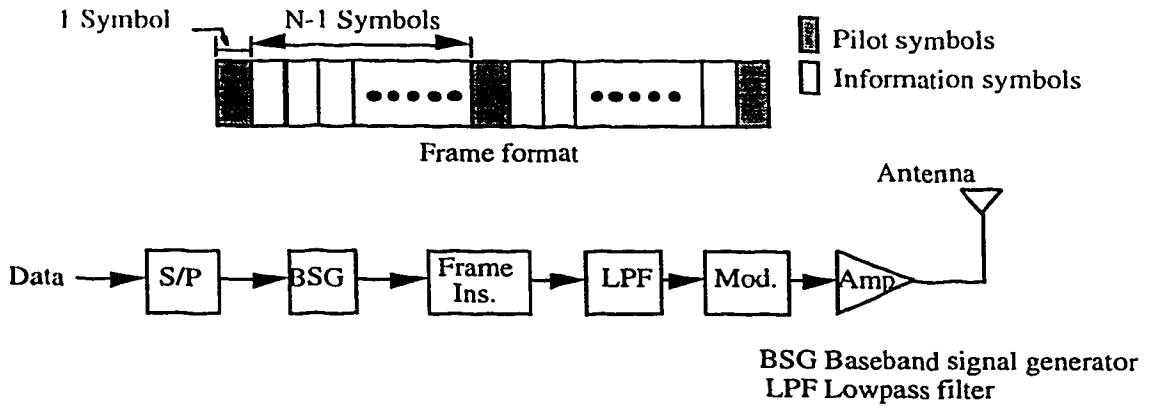


Fig. 2.9. Transmitter for pilot symbol insertion method.

The distortion in the other unknown symbols is compensated by interpolating the sequence of the measured information. Fig. 2.10b shows a more detailed configuration of the fading estimation and compensation section. The fade characteristics are used to recover the phase of the transmitted carrier which contains the information to be detected. A detailed mathematical model, and the analytical and numerical performance of this method have been given by [23,24].

This approach significantly reduces the error floor caused by the Doppler spread in a fast fading channel. However, because the pilot signals do not carry any message information, they represent a waste of power and frequency spectrum.

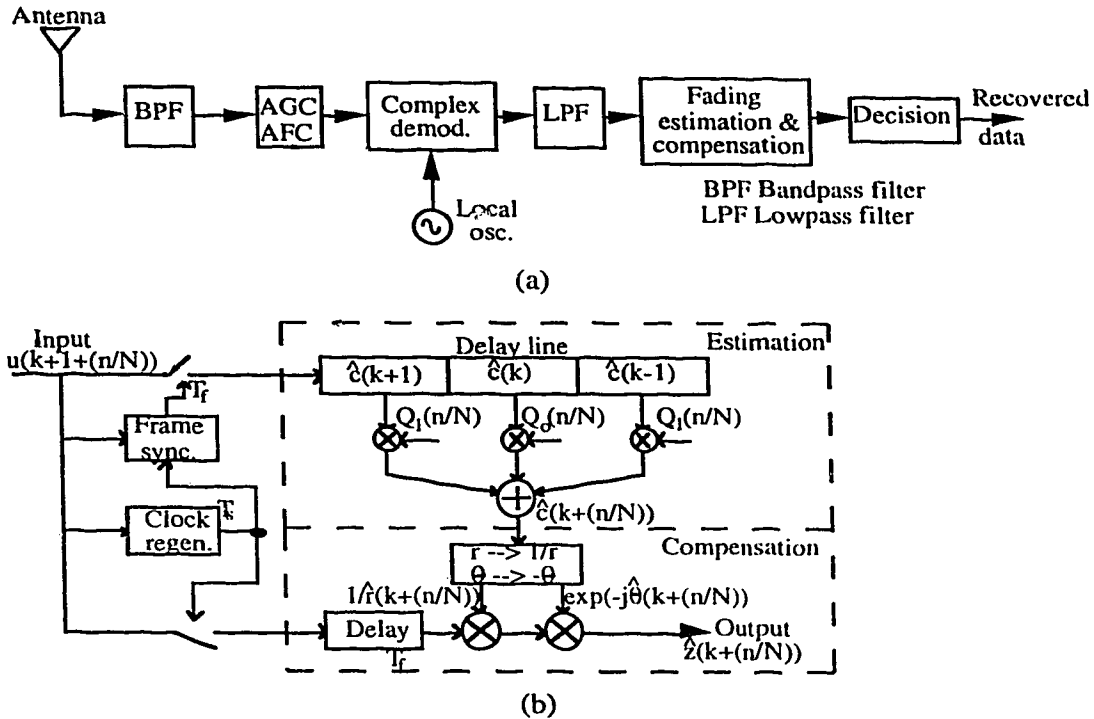


Fig. 2.10. (a) Receiver for pilot symbol insertion method.

(b) Fading estimation and compensation for pilot symbol insertion method.

### 2.5.2 Reference Tone Approach

Pilot-tone aided coherent demodulation is another efficient method to improve the performance of coherent demodulation in a fast Rayleigh fading environment. Fig. 2.11a is a block diagram of the complex baseband representation of the tone calibrated technique (TCT) system [25]. The transmitted power is split between the data bearing signal and low level pilot tone in such a manner that they do not interfere with each other, for example by separating them in frequency, Fig. 2.11b. Transparent tone in band (TTIB) [26],

creates an artificial null for the pilot tone by splitting and separating positive and negative frequency components. The total transmitted power is [25]

$$P_T = \frac{A^2 R_s (1+r)}{2} \quad (2-33)$$

$$r = \frac{a_p^2}{A^2 R_s} \quad (2-34)$$

where  $R_s$  is the symbol rate,  $r$  is the ratio of pilot tone power to data signal power,  $A$  is data signal level, and  $a_p$  is the pilot dc level.

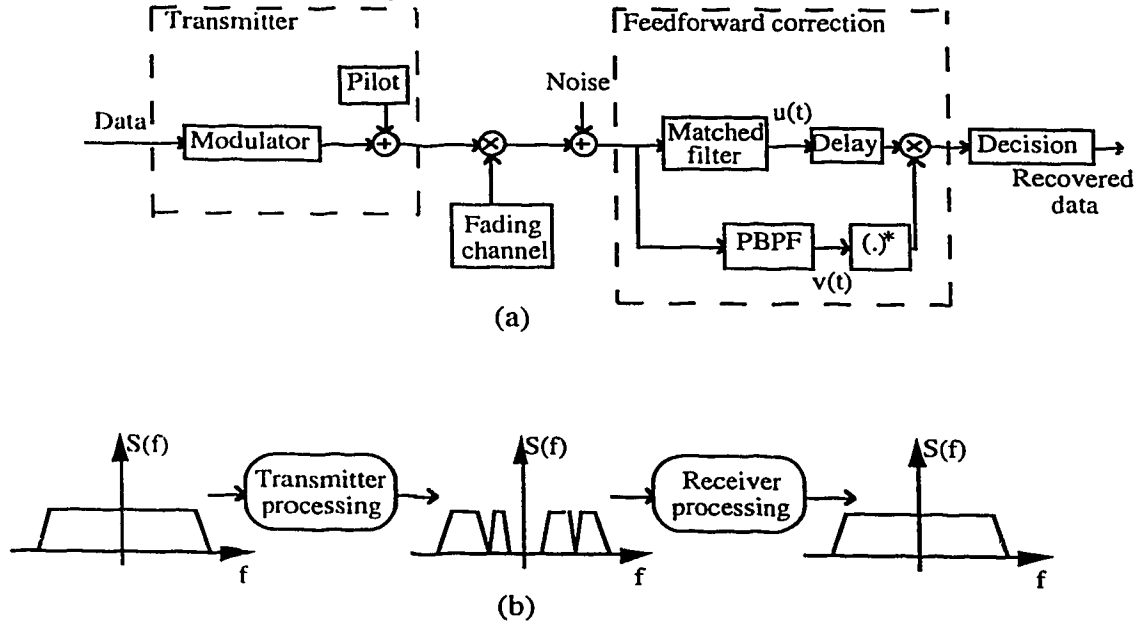


Fig. 2.11. (a) System based on pilot tone insertion.  
(b) Pilot tone insertion using spectral manipulation.

The receiver extracts the pilot with a *pilot bandpass filter (PBPF)* and uses the result as a phase reference to demodulate the data coherently. The two principal design tradeoffs are the fraction of the power devoted to the pilot tone, and the bandwidth of the PBPF. If the filter is too narrow-band, the frequency offset and Doppler spread will prevent the filter output from following the channel fluctuations, and if it is too wide it will admit too much noise. The matched filter output for a fading rate  $f_d \ll R_s$  is

$$u(kT) = c(kT)Am_k + n_u(kT) \quad (2-35)$$

where  $c(kT)$  represents the time varying complex gain of channel,  $m_k$  is the information signal and  $n_u$  is the noise component. Because the pilot tone is located in a spectral notch, there is no significant pilot tone energy in the matched filter output. The PBPF output  $v(t)$  and matched filter output  $u(t)$  are used to calculate the decision variable, as shown in Fig. 2.11a, on which the binary decision is made. Further details, analysis and results are given in the literature [25, 26].

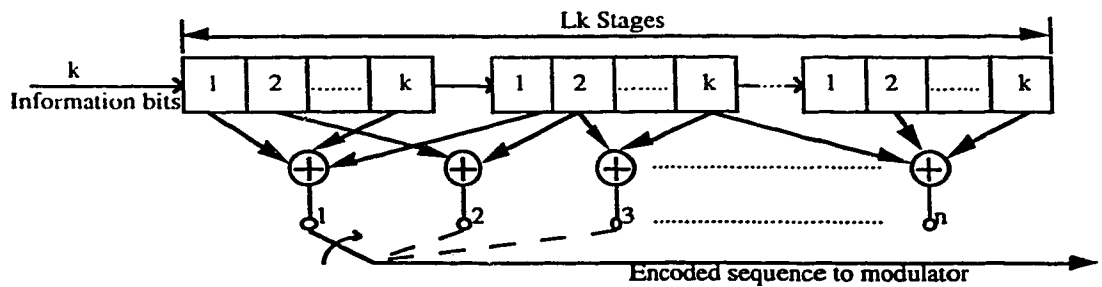
The principal virtue of tone calibrated transmission is that it suppresses the irreducible error rate. However, it requires complex signal processing at the receiver to create a spectral null at the carrier frequency or DC in baseband. Also, tone insertion results in inefficient bandwidth utilization since the pilot tone increases the required bandwidth, for the same data rate.

### 2.5.3 Coding and Interleaving

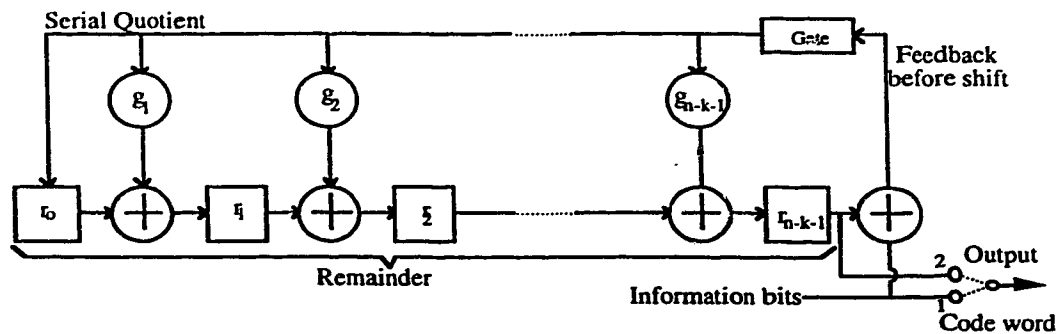
Coding and interleaving are quite successful approaches to combating channel fading effects. These methods are based on *Shannon's theorem* that a stationary channel can be made arbitrarily reliable, given that a fixed fraction of the channel is used for redundancy. The two major types of error control are *Automatic Request for Retransmission (ARQ)* and *Forward Error Control (FEC)* [27]. Both techniques add redundancy to the data prior to transmission in order to reduce the effect of errors that occur during transmission. ARQ utilizes redundancy to detect errors and, upon detection, it requests a repeat transmission. Two well-known techniques for retransmission are selective repeat and “Go-back N”. FEC utilizes the redundancy so that a decoder can extract the correct data

from the corrupted received signal. FEC codes have various forms and properties and are broadly classified as *block codes* and *convolutional codes*.

A convolutional encoder operates on the input bit stream such that each information bit can affect a finite number of consecutive symbols; i.e., coded message bits in the encoder output. The functional architecture of the encoder has multistage shift registers, modulo-2 adders, and interconnection between the two as per the constraint length, as shown in Fig. 2.12a. The decoder of these codes has to know the history of the decoded stream, that is, the values held in the shift registers, before it is able to decode a particular bit. Therefore, the decoder is more complex and an error may propagate if the decoder makes a mistake in the history of the stream.



(a)



(b)

Fig. 2.12. (a) Convolutional encoder. (b) Block encoder.



In block coding, the input data is split into discrete blocks and each block is independently processed by an encoding algorithm to add redundancy and produce a longer block, as shown in Fig. 2.12b. The decoder works on a similar basis; each block is individually processed. For block coding, synchronization is of major concern in the decoder because the block boundaries need to be known.

Efficient use of codes capable of correcting random errors requires the conversion of burst errors into random errors. This is achieved by spacing the individual bits of a each data block far apart in time so that they encounter independent fading. This technique is called interleaving. The simple *block interleaving* uses memory containing  $M$  rows and  $K$  columns, with a coded stream written into memory row by row, and read out column by column. Successive bits of the coded stream then appear as every  $K^{\text{th}}$  bit of the transmission stream. In reception, the coded stream is restored by using a corresponding  $M \times K$  memory as a deinterleaver.

Coding reduces the BER considerably; however the redundant bits used in a bandwidth constrained channel reduces the maximum throughput. Another consideration is that, to improve the performance at the receiver end, the data framing needs to be modified at the transmitter end. This is sometimes not practicable, because frame format is generally set by standards.

#### **2.5.4 Diversity**

The effect of fading can be combated by the use of diversity techniques either at the base station or the mobile station. Diversity reception works on the principle that if two or more independent samples of a random process are taken, then these samples will fade in an uncorrelated manner. These two uncorrelated fading signals, received via independently fading paths, are then combined to

reduce the effect of the fades. A *macroscopic diversity* scheme is used to reduce the effect of long term fading on the signals received from two or more different antennas at different base station sites. A *microscopic diversity* scheme, on the other hand, is used to reduce the effect of short term or multipath fading on signals received from two or more different antennas, but at only one receiving site.

There are six different types of microscopic diversity; *space, frequency, polarization, field component, angle and time* [28]. In space diversity, two antennas separated physically can provide two signals with low correlation among their fades. The separation required varies with antenna height. A separation of  $0.5\lambda$  can be used to obtain an almost uncorrelated signal at the mobile unit. As long as the correlation coefficient is less than 0.2, the two signals are considered to be uncorrelated. Frequency diversity is obtained by using two mobile-radio signals using two slightly different carrier frequencies. The frequency separation is chosen to be greater than the coherence bandwidth, so that the two signals fade independently. However, because of the congested frequency spectrum, this is not really a practicable solution. In polarization diversity, the transmitter power is fed to two differently polarized antennas, to transmit orthogonal electric field components. Two polarized antennas receive the two orthogonal signals with different fading effects. However, the splitting of the power at the transmitter results in a 3dB power reduction. Field component diversity is based on the electromagnetic theory concept that, when an E-field is propagating, an H-field is always associated with it and carries the same message information. Energy density antennas are used for field component diversity. Angle diversity makes use of two or more directional antennas pointed in different directions at the

receiving site, so as to receive uncorrelated fading signals. Time diversity means transmitting identical messages in different time slots to yield two uncorrelated fading signals at the receiver. The time separation needs to be greater than the coherence time of the channel.

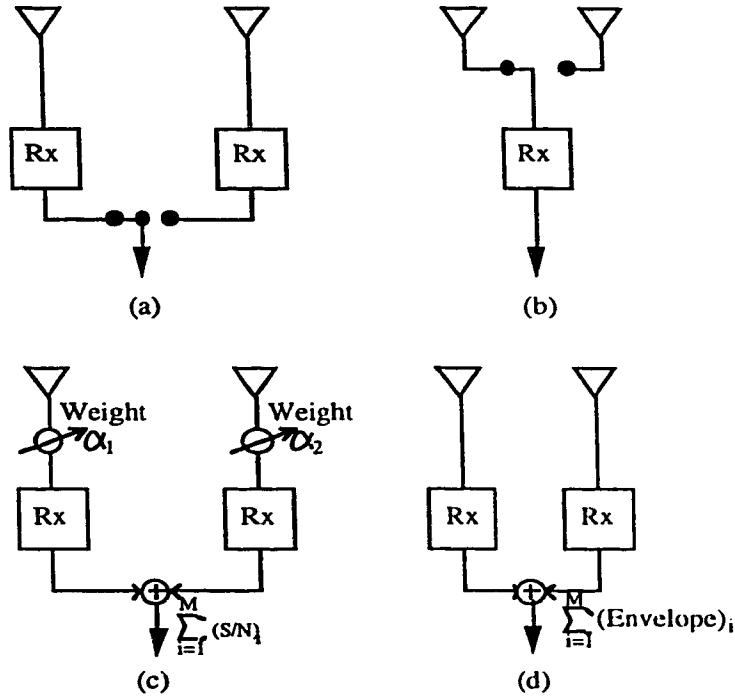


Fig. 2.13. Diversity combiners. (a) Selective combining. (b) Switched combining. (c) Maximal-ratio combining. (d) Equal-gain combining.

After the creation of diversity branches there are four major ways to combine them. These are the *selective, switched, maximal ratio and equal gain combining techniques*, as shown in Fig. 2.13. In selective combining, the strongest signal among all the branches is selected by monitoring each branch with a separate receiving front end. Switched diversity, uses the branch that has a signal level above the threshold value and switches the branch whenever the signal falls below the threshold. It needs only one receiver, but the performance is greatly affected by threshold level and switching noise. Maximal ratio is the best

combining technique, as each branch signal is combined with proper weights that depend on the individual signal strengths. When combining signals from all the different branches, the phase and time delay for each branch needs to be taken into account. Equal gain combines the signal of individual branches to get a sum of the instantaneous fading envelopes.

Diversity improves the transmission quality significantly against multipath fading and interference. However it is complex and expensive from an implementation view-point. Also, for a small-size portable unit, it may not be an attractive option, because of limitations due to size and hardware power consumption.

## **2.6 Summary**

This chapter has presented the basic structure of the transmitter, fading channel and receiver. The effect of a flat fading channel on the transmitted signal is discussed, followed by the various available schemes to improve the performance of the receiver. The limitations of each scheme are also presented in terms of bandwidth, power or complexity. This leads us to explore the decision-aided algorithm for detection and error correction, which has a minimum penalty in terms of the above parameters. This algorithm is discussed in the next chapter.

### 3. DECISION-AIDED CHANNEL ESTIMATION AND ERROR CORRECTION

This chapter proposes a method for reducing the error floor which is based on the data modulation alone, i.e. no additional information bits apart from data bits need to be transmitted. The aim is to achieve a practicable error reduction method, with no overhead and improved performance, that can be implemented using a digital signal processor (DSP) with a small amount of memory requirement and moderate computational complexity. A block diagram and its components are described in the following sections, giving the functional details. At the end of this chapter, a second approach for the detection and correction of errors is discussed.

#### 3.1 Decision-Aided Detection

The basic structure of a receiver with decision-aided detection is shown in Fig. 3.1. A traditional differential detector, as described in Chapter 2, is used to make the first decision. This is then followed by the decision-aided detector which extracts the channel information and makes a second decision on the transmitted data, using knowledge gained from the first decision and the received signal. It is for this reason that the scheme is called *decision-aided detection*. In a test situation, the second decision is compared with the transmitted data to determine the error performance.

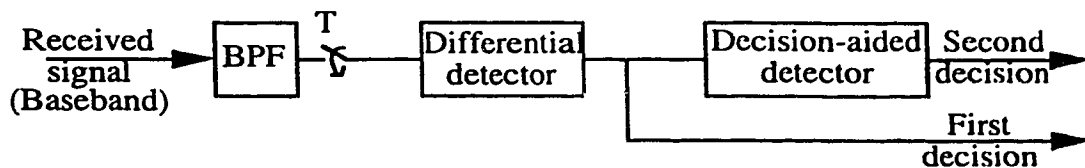


Fig. 3.1. Block diagram of receiver.

### 3.1.1 Block Diagram

The block diagram of a differential detector with decision-aided detection is shown in Fig. 3.2.

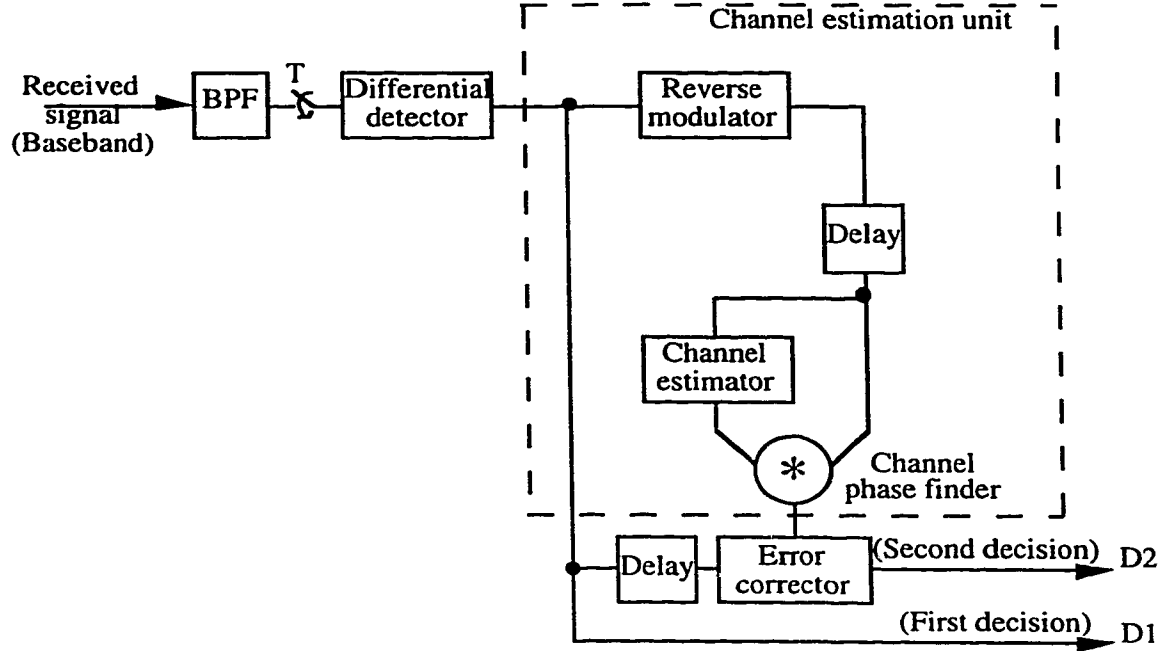


Fig. 3.2. Block diagram for decision-aided detector.

At the receiver input, the transmitted  $\pi/4$ DQPSK signal as affected by Rayleigh fading is down-converted from RF to complex baseband and sampled at  $f_s = 1/T_s$ .

This complex baseband input  $r$ , is given by

$$r(nT_s) = s(nT_s)\epsilon(nT_s) + \eta(nT_s) \quad (3-1)$$

where  $s$  is the transmitted signal,  $\epsilon$  is the fading process and  $\eta$  is the additive noise.

The signal passes through the receive filter in order to limit additive noise while minimizing the distortion of the desired signal. The output of the receive filter,  $r_z$ , which has been decimated to a rate of 1 sample per symbol, is given by

$$r_z(kT) = s(kT)\epsilon(kT) + \eta_z(kT) \quad (3-2)$$

The receive filter output is fed to a conventional differential detector, in order to make decisions about the transmitted information. The output signal of this correlator is given by

$$\begin{aligned} r_z([k+1]T)r_z(kT)^* &= \{s([k+1]T)\varepsilon([k+1]T) + \eta_1([k+1]T)\} \{s(kT)\varepsilon(kT) + \eta_1(kT)\}^* \\ &= U + jV \quad \text{where } U \text{ is the real part and } V \text{ is the imaginary part.} \end{aligned} \quad (3-3)$$

The ability to decode the transmitted information,  $s$ , is impaired by the additive noise,  $\eta_1$ , and the multiplicative fading,  $\varepsilon$ . The receiver could eliminate the effects of  $\eta_1$  and  $\varepsilon$  if it were able to estimate them. However, for practical purposes, the additive noise is unpredictable and its effect can only be reduced by increasing the transmitted signal power. In contrast, the fading process can be estimated because it is relatively narrow-band compared to the data signal; thus the receiver's performance can be significantly enhanced by estimating the effect of the channel.

The function of the decision-aided detector is to compute an estimate of  $\varepsilon$ . It consists of two basic units: a channel estimation unit and an error correction unit. The core of the decision-aided detector is the channel estimation unit, which comprises three parts: a reverse modulator, an estimation filter and a channel phase finder. The reverse modulator removes the modulation from the received signal based on the signal data as determined by the first decision **D1**. For the case of no ISI and no detection errors in **D1**, the phase of the resulting signal is a noisy estimate of the fading channel distortion.

$$Up + jVp = r(nT_s - D) \hat{s}^*(nT_s - D) \quad (3-4)$$

$$Up + jVp = \varepsilon(nT_s - D) + \eta_2(nT_s) \quad (3-5)$$

where  $D$  is the delay due to the receive filter.

In the practical situation, for a mobile radio channel, typically one out of hundred first decision errors are incorrect; therefore, the carrier recovery at the output of reverse modulator (**U<sub>p</sub>** and **V<sub>p</sub>**) is distorted. However, since the recovered carrier samples are 99% correct, a good estimate of the channel phase may be obtained by filtering the resulting channel samples. This is the function of the channel estimation filter. Once the fading estimate has been made, then the first decision is changed to accommodate the effect of the channel phase angle, resulting in a second decision **D2**. The following section will describe the functions and characteristics of the channel estimator and the error correction unit.

## **3.2 Channel Estimation**

### **3.2.1 Reverse Modulation**

The signal at the output of the differential detector (**U** and **V**) represents the in-phase and quadrature components of the phase change, as determined by the differential detector. Using this phase change, a first decision, **D1**, is made on the received symbol; if there is no error caused by the fading channel, then the detected symbol will be the same as the transmitted symbol. As described earlier in Chapter 2, the information symbols in  $\pi/4$ DQPSK modulation are transmitted as the difference between successive carrier phase angles. The possible values of these phase differences are  $\{\pm 45^\circ \text{ and } \pm 135^\circ\}$ . This means that, under ideal channel conditions (i.e. no noise or fading distortion), the received phase differences are limited to these four values. Thus, the **U** and **V** components of the detector output, if plotted on a vector diagram, must lie along axes that are at  $\pm 45^\circ$  or  $\pm 135^\circ$ , as shown in Fig. 3.3a. The labels '00', '01' ... on each of these axes indicate the corresponding demodulated symbols. However, due to the random phase modulation caused by the fading, the actual received **U** and **V** vectors do not lie exactly in these ideal directions. The deviation of the actual vector from the ideal



vector is represented by  $U_p$  and  $V_p$ , as shown in Fig. 3.3b.  $U_p$  and  $V_p$  are a measure of the phase deviation caused by the non-ideal channel, i.e. intersymbol interference, additive white Gaussian noise, and Rayleigh fading. It should be noted here that  $U_p$  and  $V_p$  are measured with respect to one of the four output ideal directions. The differential detector provides an output  $U$  and  $V$  and the decoder chooses the closest ideal vector direction in order to make a decision (Fig. 3.3a).

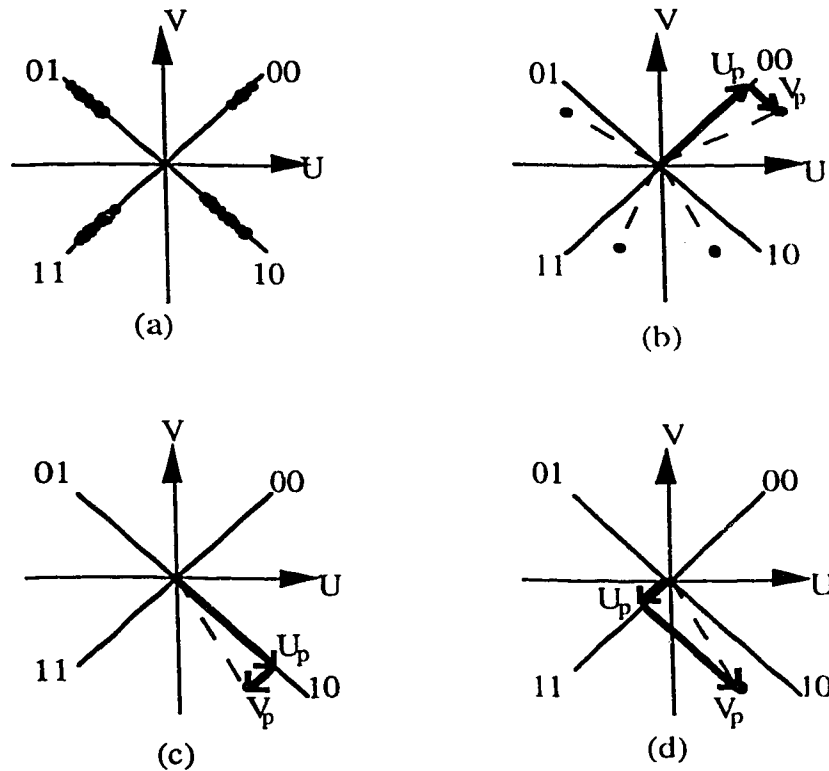


Fig. 3.3. Vector diagram for reverse modulation process.

When the effects of fading and noise are small, then  $U$  and  $V$  will lie very close to one of the ideal directions. Fig. 3.3b shows this situation. The received signal is relatively high, and  $U$ ,  $V$  lie close to  $+45^\circ$ .  $U_p$  is large and  $V_p$  is slightly negative. The decoded symbol corresponding to the received signal will be "00". During a fade the received signal will be smaller and the detector output will be

closer to the origin. This condition is shown in Fig. 3.3c. The vector  $U, V$  lies closest to the  $-45^\circ$  axis and the received symbol will be decoded as '10';  $U_p$  and  $V_p$  will be as shown. For this case however, noise and distortion may easily have caused a significant amplitude and phase error, moving  $U, V$  away from its correct direction and causing an error in the detected data. For example, the true data corresponding to Fig. 3.3c could be '11', but the channel has caused a phase error of almost  $90^\circ$ , placing  $U, V$  in the wrong quadrant. It is important to notice that any data errors will also cause the values of  $U_p$  and  $V_p$  to be incorrect. With reference to the direction '11',  $U_p$  and  $V_p$  should actually be taken as in Fig. 3.3d. It is this error in  $U_p$  and  $V_p$  that is used by the error detection and correction algorithm. Because the fading is a narrow-band process, the effect of the fading changes only slowly from one symbol to the next. Further, because typically 99 out of 100 symbol decisions are made correctly, only 1% of the  $U_p, V_p$  values are incorrect. By using a low-pass filter to smooth out the  $U_p$  and  $V_p$  values, the effect of the incorrect decisions can be made very small, and a good estimate of the fading channel characteristic can be made.

### 3.2.2 Estimation Filter

A good estimate of the phase change due to the fading channel ( $U_{pf}$  and  $V_{pf}$ ), for each decision point, is determined from the  $U_p$  and  $V_p$  values, using a filtering operation to remove, as far as possible, the effect of any incorrect  $U_p$  and  $V_p$  values. Here, to achieve the best possible performance both past and “future” values of  $U_p$  and  $V_p$  are used. Thus an interpolation method is used, rather than a simple prediction based on past values only. With respect to each first decision (D1), this requires storage of past and future values of the channel characteristics, in order to estimate the channel phase angle and then make a second decision. This is realized by storing successive values of  $U_p$  and  $V_p$  as determined by the first

decision D1, and making the corresponding second decisions several (20 to 30) symbol periods later.

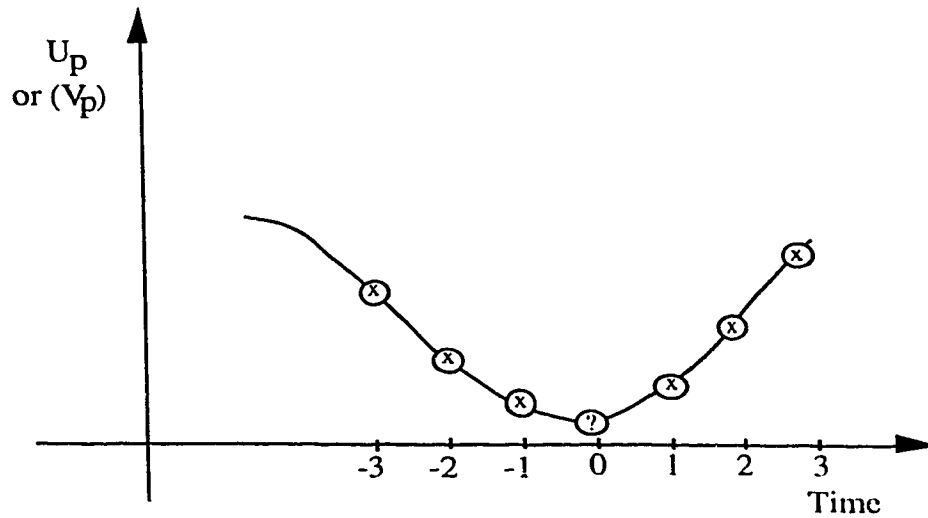


Fig. 3.4. Channel estimation.

The estimator is designed as a lowpass filter, since the fading channel characteristic is a narrow-band process having a two-sided bandwidth equal to 4 times the maximum Doppler frequency [15]. The fading bandwidth is doubled due to the multiplicative correlation process in the differential detector. A lowpass filter smooths out the channel estimates, thereby removing the errors caused by any wrong decisions, and also removing most of the noise. However the passband of the estimating filter has to be a tradeoff between a narrow and wide passband. A narrow passband is desired so as to reduce the effect of noise at low SNR, but at the same time, it has to be wide enough to pass the fading channel information without distortion.

The Rayleigh fading estimation filter determines the values of  $\mathbf{U}_{pf}$  and  $\mathbf{V}_{pf}$ . The  $\mathbf{U}_{pf}$  values corresponding to each decision point are obtained from the  $\mathbf{U}_p$  values using an FIR transversal filter. As shown in Fig. 3.4,  $\mathbf{U}_p$  values both

before and after the decision point are used, with the filter output corresponding to the tap at  $k=0$ . The  $V_{pf}$  values are obtained similarly. Mathematically

$$Upf(n) \equiv \sum_{k=-N}^N C_k Up(n-k) \quad (3-6)$$

where the  $C_k$  are the filter coefficients. The total length of the filter is  $2N+1$ , using  $N$  values on each side of the decision point. The channel estimation using this filter is not always perfect since, due to the data errors, erroneous samples of  $U_p$  or  $V_p$  will enter the filter at  $k=-N$  and will move through to  $k=0$  before they can be removed.

Various techniques can be used to determine a set of appropriate  $C_k$  values. These values must be chosen so that, when the channel samples are correct, the estimated values are exactly equal to the input values. This requires a flat spectral response over the bandwidth of the fading channel. The sampling theorem provides the basic approach to choosing a set of coefficients. This theorem states [29]:

*A signal bandlimited to  $B$  Hz ( i.e., a signal whose Fourier transform is zero for all  $|w| > 2\pi B$ ) is uniquely determined by its values at uniform intervals less than  $1/2B$  seconds apart,*

*or, alternatively,*

*If a continuous signal is multiplied by an ideal sampling function, then the signal can be recovered from the sampled version only if the original signal spectrum is entirely contained within a bandwidth of less than half the sampling rate.*

The original signal can be recovered from the samples by using an ideal lowpass filter that passes the signal spectrum centered on zero frequency and extending to within half the sampling frequency on either side. This filter also masks out all the undesired aliasing images. In the time domain, the inverse Fourier

transform of an ideal lowpass filter gives the sinc function. Thus, to recover the original time domain waveform, the sampled signal must be convolved with a unit sinc function. In other words, a lowpass waveform can be re-constructed from its samples by summing weighted sinc functions, where the weights are the discrete sample values. Mathematically,

$$g(t) = \text{sam}_{T_s}[g(t)] * \text{sinc}\left(\frac{t}{T_s}\right) \quad (3-7)$$

or, for discrete signals,

$$g(t) = \sum_{n=-\infty}^{\infty} g(nT_s) \text{sinc}(2B\tau n) \quad (3-8)$$

where  $g(nT_s)$  are the signal samples given, in our application by **Up** and **Vp**. The filter coefficients are given by the values of  $\text{sinc}(2B\tau n)$ . In principle, a filter designed in this way will give perfect reconstruction of the desired waveform. However, one important limitation for any practical implementation of this result is the infinite duration of the sinc function. Variation from the sinc function can be made by choosing different lowpass filter shapes, keeping a flat lowpass characteristic, but allowing variation in the roll-off and stopband characteristics.

Another approach for determining the best possible estimate is to use a least square error fit or a polynomial curve fit method for the coefficient calculation [30]. For either of these methods, a polynomial can be found from which **Upf** and **Vpf** can be calculated. Sample values of **Up** (or **Vp**) are considered on both sides of the decision point for which the estimate of **Upf** (or **Vpf**) is required. A polynomial of degree  $m$  can be represented as,

$$p(x) = a_0 + a_1x + a_2x^2 + \dots + a_mx^m = \sum_{k=0}^m a_k x^k. \quad (3-9)$$

With equally spaced sample times, however, the required estimated value reduces to a sum of weighted sample values, as given by Eq. (3-6). The least square method

aims at minimizing the discrepancy between the data points and the approximating polynomial, given by

$$Q(f, p) = \sum_{i=-n}^n [f_i - p(x_i)]^2 \quad (3-10)$$

where  $\{x_{-n}, \dots, x_{-2}, x_{-1}, x_0, x_1, x_2, \dots, x_n\}$  represent the domain point at the sampling instant and  $\{f_{-n}, \dots, f_{-2}, f_{-1}, 0, f_1, f_2, \dots, f_n\}$  are the corresponding sample values. The degree of the polynomial and the number of points used in the curve fitting procedure need to be varied in order to test the accuracy of estimation for the best possible estimate of the channel.

The two approaches are not totally independent. According to the first approach any function can be represented as a sum of sines and cosines, i.e. a Fourier series. For the second approach, polynomials can be used to represent any function. However, expanding sine and cosine functions in polynomial form shows the relation between the two approaches. Another technique available for designing the estimating filter is to use a signal processing based algorithm [31], such as the window method, Remez exchange algorithm, or the frequency sampling based design, etc. Since all these approaches can be represented in terms of Eq. (3-6), they all lead to an estimation filter design based on a lowpass FIR filter.

The estimate of the channel leads to two cases. In the first case, the estimated channel is almost the same as the original sample, indicating that no error has been made. If the two values are very different, then an error may have occurred. When the error is corrected, then, in order to improve future estimates, it may be required to replace the original values of  $U_p$  and  $V_p$  with the corrected values  $U_{pnew}$  and  $V_{pnew}$ . The decision criteria and values for replacement are further described in Section 3.3, the error correction section.

### 3.2.3 Channel Phase Finder

Once the fading process estimate is complete, the **Upf** and **Vpf** values so obtained are compared with the initially extracted channel information **Up** and **Vp**. This gives information about the phase change due to the channel, information which was not available while making the first decision about the transmitted data. When the first data decisions are all correct, then ideally **Upf** and **Vpf** will closely follow the **Up** and **Vp** values. However, when  $\Delta\theta_{\text{channel}}$  (channel phase change) plus the effect of noise, is  $>45^\circ$  then a data error will be made and the extracted **Up** and **Vp** will be placed in the wrong quadrant (as illustrated earlier in Fig. 3.3(c) and (d) ) as a result of which **Up** and **Vp** may be interchanged, or the signs may be reversed. However, since typically only 1 out of 100 channel samples is incorrect, and the estimation filter will smooth out the values that are in error, and **Upf** and **Vpf** will still give a good estimate of  $\Delta\theta_{\text{channel}}$ . By comparing these values with the original **Up** and **Vp**, a second decision **D2** may be made.

The error correction procedure is illustrated in Fig. 3.5. Fig. 3.5a shows a typical sequence of channel values  $I_{\text{CH}}$ ,  $Q_{\text{CH}}$  during a fade. This diagram also shows the **Up** and **Vp** values that should be extracted in order to correctly quantify the phase change due to the channel. However, this phase change will only be determined correctly if this incremental angle is less than  $\pm 45^\circ$ . Fig. 3.5b shows the values of **Up** and **Vp** that will actually be obtained. The values are all correct except for sample point #4 which corresponds to the channel phase of  $\approx 60^\circ$  that occurs from sample point 3 to 4 (in Fig. 3.5a). For this symbol, the data is decoded in the wrong quadrant ( $+90^\circ$  compared to the true data) due to the excessive channel phase change, and consequently the channel is extracted with an error of  $-90^\circ$ . This point #4 is extracted incorrectly. The dashed line in Fig. 3.5b shows the trajectory of the filtered **Upf**, **Vpf** values. Because most of the **Up**, **Vp** samples are correct,

the one point in error affects the  $U_{pf}$ ,  $V_{pf}$  values only slightly. By comparing  $U_p$ ,  $V_p$  with  $U_{pf}$ ,  $V_{pf}$  at each sample, a check is made on the first data decision and a correction made if required.

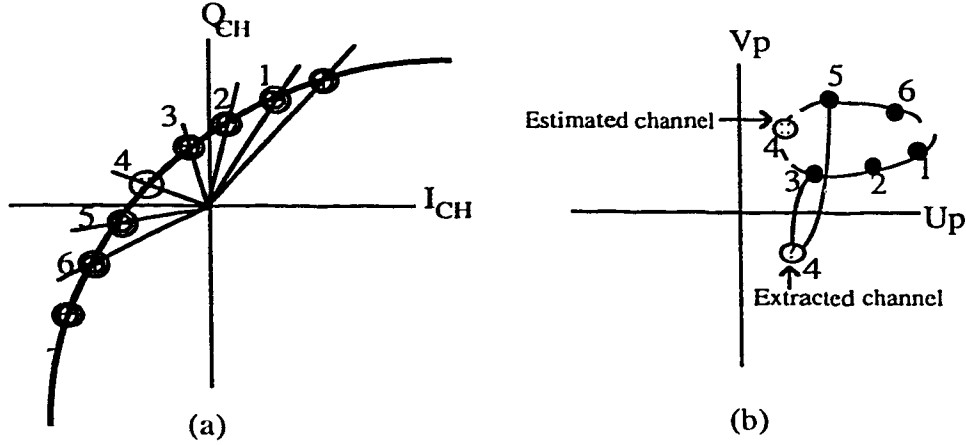


Fig. 3.5. (a) Typical channel. (b) Error correction.

The various angles are related by,

$$\Delta\theta_{\text{extracted\_channel}} = \Delta\theta_{\text{received}} - \Delta\theta_{\text{data,first\_decision}} \quad (3-11)$$

$$\Delta\theta_{\text{data,second\_decision}} = \Delta\theta_{\text{received}} - \Delta\theta_{\text{estimated\_channel}} . \quad (3-12)$$

Using phasor notation, the channel error may be defined in terms of quantities  $C$  and  $D$ , where

$$C + j D \equiv \Delta\theta_{\text{estimated\_channel}} - \Delta\theta_{\text{extracted\_channel}} . \quad (3-13)$$

The values of  $C$  and  $D$  are easily calculated from

$$C = U_p U_{pf} + V_p V_{pf} \quad (3-14a)$$

$$D = U_p V_{pf} - U_{pf} V_p . \quad (3-14b)$$

### 3.3 Error Correction

Finally, the receiver removes the effect of the additional channel phase ( $C$  and  $D$ ) from the first decision ( $D1$ ) thereby giving the second decision ( $D2$ ). There



are four possible cases for the second decision. These are: no change in **D1**, change **D1** by  $-90^\circ$ , change **D1** by  $+90^\circ$ , and lastly, change **D1** by  $180^\circ$ . The shift of angle refers to the Gray code quadrant used for transmission, and this corresponds to the detected data, as shown in Fig. 3.6.

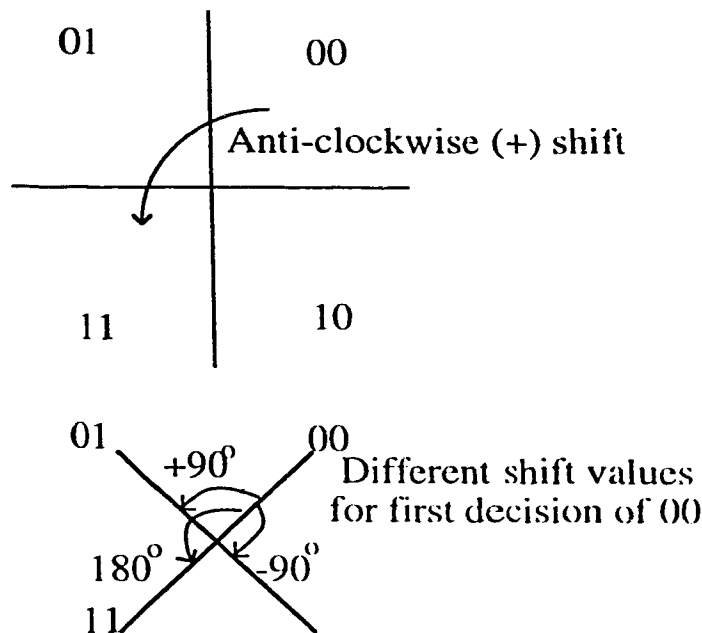


Fig. 3.6. Gray code to shift first decision.

$C+jD$  is a measure of how closely  $(U_p, V_p)$  agrees with  $(U_{pf}, V_{pf})$ . Since the data decisions are all based upon phase, then a correct decision should align  $(U_p, V_p)$  and  $(U_{pf}, V_{pf})$  as closely as possible, indicating that  $C+jD$  should represent a zero phase angle. From the value of  $C+jD$ , the phase is determined and a choice of **D2** as compared to **D1** is made as shown in Table 3.1.

TABLE 3.1  
RELATION BETWEEN  $\text{ang}(C+jD)$  AND DATA SHIFT.

Case number	Condition $\emptyset = \text{ang}(C+jD)$	Data shift
I	$-45 < \emptyset < 45$	No Shift
II	$45 < \emptyset < 135$	-90 Shift
III	$-135 < \emptyset < -45$	+90 Shift
IV	$135 < \emptyset < -135$	180 Shift

The same conditions are more clear from the vector diagram shown in Fig. 3.7. Since the channel estimate makes use of subsequent symbols, there is a delay between the second decision instant and the first decision instant. The amount of delay depends on the length of the estimation filter used. This delay has to be taken into account while shifting data **D1**, as per the Table 3.1, to obtain **D2**.

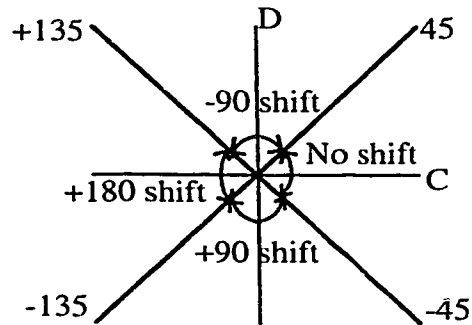


Fig. 3.7. Decision range for different shift values.

Referring to the example given in the previous subsection, shown in Fig. 3.5, the correction of the data is made so as to align the  $(U_p, V_p)$  values with the  $(U_{pf}, V_{pf})$  values. In the diagram, modulation point #4 gives better agreement if it is rotated through  $+90^\circ$ , indicating the original data decision **D1** should be corrected by  $-90^\circ$ .

As discussed in the previous section, errors in **D1** causes errors in (**Up**, **Vp**) which leads to errors in the filtered channel estimates (**Upf**, **Vpf**). When erroneous values enter the domain of the estimation filter, then the accuracy of the channel estimates (**Upf**, **Vpf**) will be impaired. However, the inaccuracy will be small because errors usually occur during fades, during which time the signal level is small. Once an erroneous value reaches the center of the filter, then, when the data is corrected, the (**Up**, **Vp**) value can also be changed. The experimental results (given in Chapter 4) show that, when this is done, the corrected error rate is somewhat improved. The corrected or new (**Up**, **Vp**) values are found from the initial values, as given in Table 3.2.

TABLE 3.2  
RELATION OF (**Up**, **Vp**) AND DATA SHIFT WITH (**Upnew**, **Vpnew**).

<b>Upnew</b>	<b>Vpnew</b>	<b>DATA SHIFT</b>
Up	Up	No Shift
-Vp	Up	-90 Shift
Vp	-Up	+90 Shift
-Up	-Vp	180 Shift

### 3.4 Scheme II for Decision-Aided Detection

This method is an extension of the method described in Sections 3.2 and 3.3. The only difference is that the reverse modulation is fed back to extract the channel phase angle from the received signal, unlike scheme I, where the output of the differential detector is used to obtain the channel information. In scheme I the channel phase change (for each symbol) is obtained, whereas in scheme II an attempt is made to track the true magnitude and phase angle of the channel characteristic (versus time). The motivation for trying to recover the channel, rather

than the “differential channel” is that during a fade the differential detector output becomes very small and can easily become lost in the noise. The incoming signal is less affected by noise, so the channel recovered from the signal should have a higher “channel-to-noise” ratio.

The principal disadvantage of trying to obtain the true channel angle is that, for a differentially encoded signal, the phase changes due to the detected data must be accumulated, and the overall total phase angle must be subtracted from the incoming signal (the complex baseband signal  $SI+jSQ$ ) in order to retrieve the channel. Whenever a data detection error occurs, the recovered channel suffers a phase discontinuity rather than having just a single point in error. While it is not difficult to detect that a phase discontinuity has occurred, it has been found difficult to locate the exact symbol point that is in error. For this method then, the error detection and correction algorithm must be considerably more mathematically sophisticated and computationally intensive than for the simple method of scheme I.

#### **3.4.1 Block Diagram**

The block diagram of the error detection and correction process is shown in Fig. 3.8. It consists of a differential detector, a re-modulation unit, a channel recovery unit, an error detection unit and an error correction algorithm. As in scheme I, the signal is first detected by a conventional differential detector. The past decisions  $D1_i$  are used for re-modulation, but in order to determine the data contribution to the received signal  $SI+jSQ$ , all the decision information must be accumulated. The cumulative phase angle for the data is subtracted from the incoming signal in order to recover the channel. If there is no decision error, then the channel magnitude and phase will be correctly recovered from the received signal.

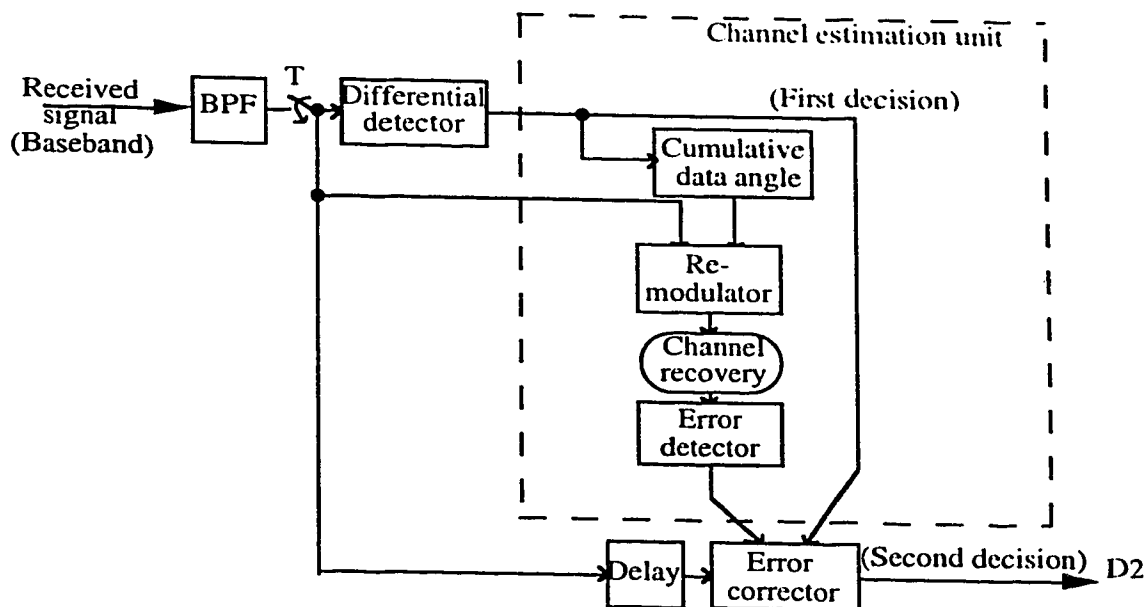


Fig. 3.8. Block diagram for scheme II (Decision-aided error detection).

For every error in the demodulated data, however, the accumulated channel angle will be incorrect by either  $90^\circ$ ,  $180^\circ$ , or  $270^\circ$ . This will affect not only the point in error, but will shift the phase of all later points as well. Because of this, the channel is recovered as a sequence of smooth segments with discontinuities at the points where the data (D1) errors occur, as shown in Fig. 3.9.

It is the function of the error detector to locate the discontinuities, and then determine how best to remove them. That is, a choice of data (or a change of phase angle) must be made that will give the smoothest possible channel characteristic. Simple filtering is not sufficient in this case. One method that can be used to locate the errors is to calculate the derivatives of the recovered channel characteristic. Since errors cause fairly sharp discontinuities, giving sudden changes of slope, etc., then the magnitude of derivative values is much larger in the vicinity of an error than elsewhere. This locates the error to within a few symbol locations, but it

does not however give the exact position. Using the derivatives thus enables various error zones to be identified.

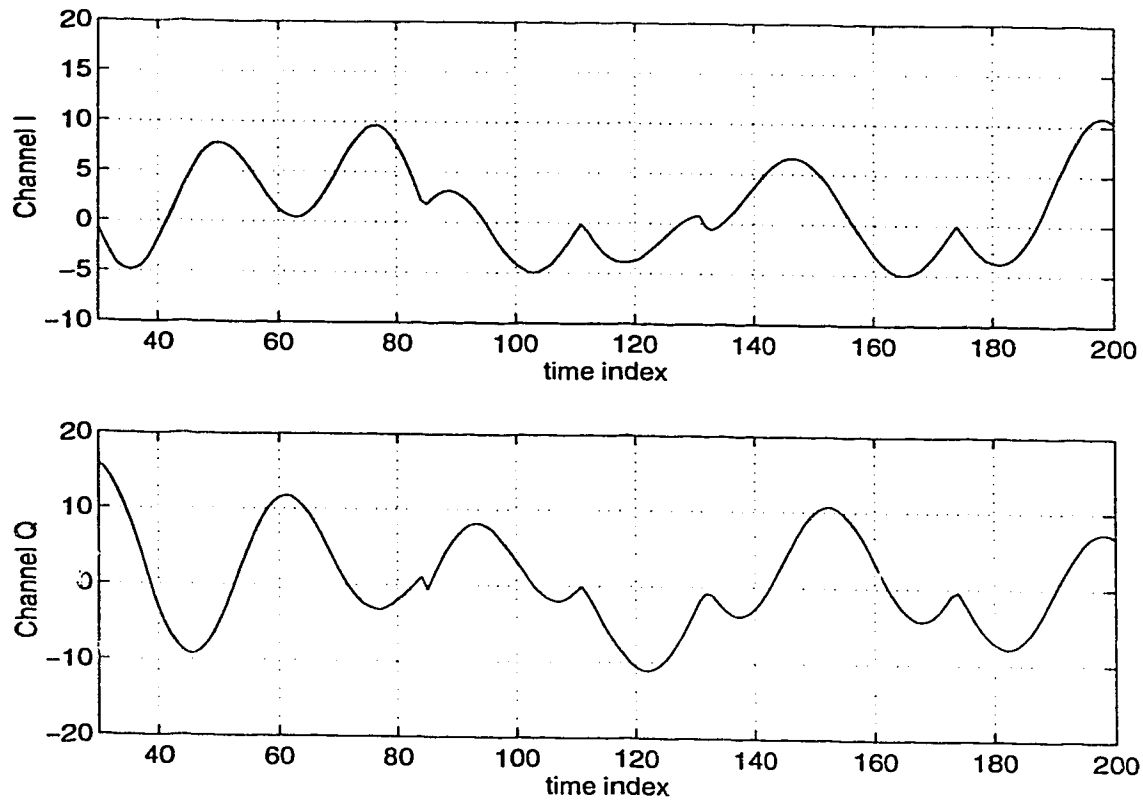


Fig. 3.9. Recovered channel.

### 3.4.2 Channel Estimation

Although the error zones appear quite distinct, it is difficult to determine exactly which symbol (or symbols) is in error. A number of techniques using the channel derivatives have been attempted with varying degree of success, but a completely satisfactory method has not yet been determined. This is an area where further work is required. Scheme II is further discussed in Chapter 5, together with some initial results.

### 3.5 Summary

In this chapter, decision-aided detection for  $\pi/4$ DQPSK signal is discussed and an algorithm capable for reducing the irreducible error floor is presented. The output of the differential detector is used to estimate the channel characteristic, and this information is then used to make a second decision about the transmitted data. The scheme is based on the transmitted symbol information only; i.e., no coding or overhead information is used. A second method which attempts to obtain the true channel characteristic from the incoming signal is also discussed. The DSP implementation and experimental results are presented in the following chapters.

## **4. DSP IMPLEMENTATION OF DECISION-AIDED DETECTOR**

Digital signal processors are presently very popular in digital communication system design as they provide potentially improved capability, performance, repeatability, flexibility, size and cost. The aim of this chapter is to present the real time digital signal processor implementation of the transceiver model described in the previous chapters. The hardware and software structure of the transmitter, channel and receiver, and the performance measurement module for scheme I are discussed in detail.

### **4.1 Transmitter**

The basic structure of the transmitter is implemented using the fixed point Texas Instruments DSP TMS320C50. The key features of this DSP are given in Table 4.1 [32, 33].

TABLE 4.1  
FEATURES OF DSP TMS320C50.

50ns instruction cycle (20MIPS)
9K $\times$ 16 bit on-chip program/data RAM
1056 $\times$ 16 bit dual-access on-chip data RAM
32 bit ALU, accumulator and accumulator buffer
8 auxiliary registers with dedicated arithmetic unit
2 indirectly addressed circular buffers
TDM serial port; Software controlled interval timer



The same DSP is programmed to simulate the channel as well, details of which are given in the next section. Because of the need to program the slowly varying channel as well as the transmitted signal in a single DSP, then in order to evaluate the performance of the scheme, the transmitted data is limited to a lower rate (2.4kb/s). The various components of the transmitter are discussed in the following sub-sections.

#### 4.1.1 Data Source

The data source in an actual system is either speech converted to digital form, or digital data from a fax machine, or a computer, etc.. This signal has no memory and can be considered to be completely random. The data stream is then compressed and placed into a specified standard frame structure [5]. However, to generate the data for testing, a maximal length pseudo random binary sequence generator is used.

The two commonly used methods to generate such random sequences are the multiplicative congruential method or mixed congruential method, and the M-sequence method [34]. The sequence generated by the mixed congruential method is based on a recurrence relation given by

$$Y_i = AY_{i-1} + C(\text{mod } R) \quad i = 1, 2, 3, \dots \quad (4-1)$$

where  $i$  is a discrete time interval,  $Y_i$  is the output pseudorandom sequence, and  $A$ ,  $C$  and  $R$  are constants; also,  $Y_0 > 0$ ,  $A > 0$ ,  $C \geq 0$ ,  $R > Y_0$ ,  $R > A$ ,  $R > C$ , and  $\text{mod}$  is the modulo operator. The mathematical definition of the M-sequence method is given by recurrence relation

$$X_i = \text{mod } 2 \sum_{k=1}^m \alpha_k X_{i-k} \quad i = 1, 2, 3, \dots \quad (4-2)$$

where  $i$  is a discrete time interval,  $X_i \in (0, 1)$  is the output pseudorandom sequence,  $m$  is the tap length,  $\alpha_k \in (0, 1)$  are the tap coefficients, and the summation sign

with mod2 represents modulo-2 addition. The multiplicative congruential method requires mathematical computations like multiplication, addition and the modulo-R operation as shown in Eq. (4-1). Thus the implementation based on this method requires a significant number of instruction cycles. By contrast, the M-sequence method requires only a modulo-2 summation or exclusive-OR operation, as shown in Eq. (4-2). The implementation simplicity of the M-sequence method, makes it a more suitable choice for realizing the pseudorandom binary sequence source.

The M-sequence generator that functions in accordance with expression (4-2) comprises an m-bit shift register and the set of modulo-2 adders for feedback. Since  $X_k$  is repeated every  $2^m-1$  outputs, it is required to set the value of m large enough so as to obtain independent and random  $X_k$  over the testing period. In this experiment, the length of shift register, m, is selected to be 31 so as to obtain a sequence length equal to  $2^{31}-1$ . Thus, for the data source of 1.2ks/sec, the output data sequence has a period of  $1.8 \times 10^6$  sec and gives  $2 \times 10^9$  symbols before repeating. The tap coefficients used in the feedback circuit, for a selected value of shift register length, is obtained from a standard M-sequence characteristic polynomial table [34]. In order to initialize the shift register for sequence generation, a non-zero value must be stored in at least one register.

The mathematical definition of the implemented data source is given by

$$\alpha_k = \begin{cases} 1 & k = 3, 31 \\ 0 & (1 \leq k \leq m) \cap (k \neq 3, 31) \end{cases}$$

$$X_i = X_{i-3} \oplus X_{i-31} \quad i = 0, 1, 2, \dots \quad (4-3)$$

where  $\oplus$  is the Exclusive-OR operator. Fig. 4.1 shows that the source consists of 31 clocked registers or memory locations and one modulo-2 addition operation.

These clocked memory locations form a 31 tap-delay line, and the contents of locations 3 and 31 are used as the inputs to the modulo-2 adder.

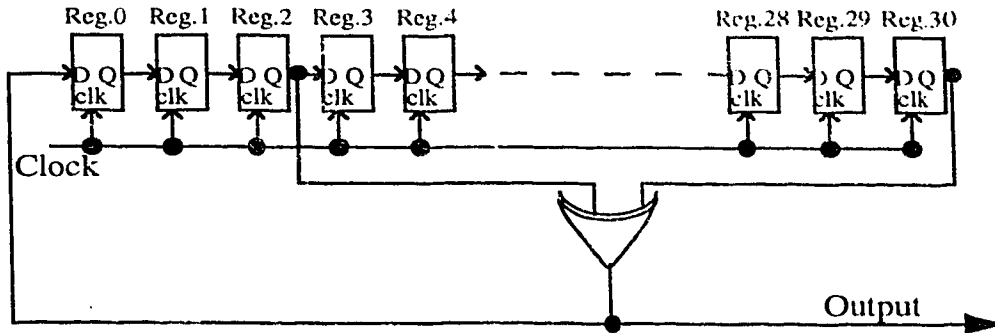


Fig. 4.1. M-sequence generator.

The software implementation of the same function is best done using a circular buffer. Since the circular buffer provided in the C50 has the limitation that it may be incremented or decremented by one step at a time, this could not be used directly. However, an address table was used to achieve the same action. Since the sequential bits of data are used by the encoder in pairs (refer Section 2.1.3), two independent generators are used to generate the data symbol, to avoid serial-to-parallel conversion. Also, since the channel implementation needs another two random sequence generators, a combined procedure that generates 16 uncorrelated random sequences is used. Further details of the implementation structure is given in Section 4.2.1, together with the channel implementation.

#### 4.1.2 Encoder and Modulator

Each pair of bits from the data source is encoded using a Gray code format, where each symbol corresponds to a particular differential phase angle ( $\Delta\phi$ ), as required by the  $\pi/4$ DQPSK modulation format. See Table 2.1 for the relation between the input pair of binary data and the phase change  $\Delta\phi$ . The

output of the phase encoder is fed to the modulator in order to obtain the in-phase (I) and quadrature phase (Q) signals. The modulation scheme is defined as

$$S_k = S_{k-1} e^{j\Delta\phi(b1_k, bo_k)} \quad (4-4)$$

where  $k$  is the output symbol index,  $S_k$  is the  $k^{\text{th}}$  complex output symbol from the modulator, and  $\Delta\phi(b1_k, bo_k)$  is the phase encoder function corresponding to  $bo_k$  and  $b1_k$  (the first and second data bits at the  $k^{\text{th}}$  index). This shows that,  $S_k$  is generated by rotating the phase of the previous symbol  $S_{k-1}$  by an angle  $\Delta\phi(b1_k, bo_k)$ , where  $\Delta\phi$  takes on one of  $\{\pm\pi/4, \pm3\pi/4\}$ . This produces a constellation diagram for the modulator signal output with eight possible states (see Fig. 2.3).

For software implementation simplicity, the above modulator equation is converted to a state equation given by

$$i_k = (i_{k-1} + \Delta\phi_s(b1_k, bo_k)) \bmod 8 \quad (4-5)$$

where  $k \in [0, 1, 2, 3, 4, 5, 6, 7]$  is the state number. Each state number represented by  $k$  corresponds to one of the 8 output symbols (i.e. State 0, 1 etc.) and  $\Delta\phi_s(b1_k, bo_k)$  is obtained by mapping  $\Delta\phi$  in  $\Delta\phi(b1_k, bo_k)$  to these states. Since state 0 is taken as the reference while mapping, the four possible differential angles provide the four state values  $\{1, 3, 5, 7\}$  to  $\Delta\phi_s(b1_k, bo_k)$ . Fig. 4.2a and b shows the constellation state diagram and the  $\Delta\phi_s(b1_k, bo_k)$  state diagram.

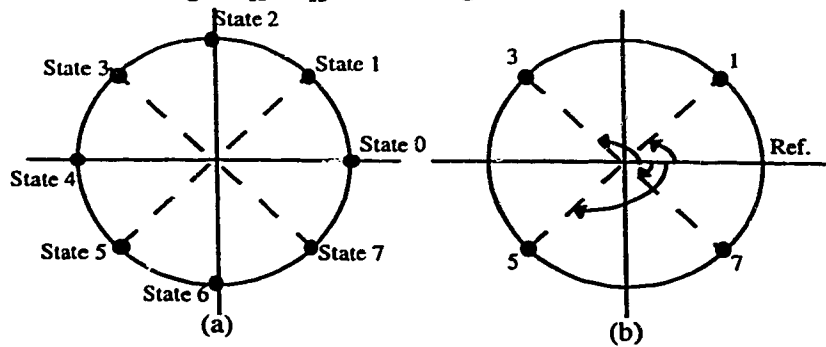


Fig. 4.2. (a) Constellation state diagram. (b) Phase change state diagram.

For the purpose of DSP implementation, the state equation is further simplified by replacing the modulo eight operation with an AND operation, using the binary constant “111”. Eq. (4-5) may then be re-written as

$$i_k = (i_{k-1} + \Delta\phi_s(b1_k, b0_k)) \text{AND } "00000111" \quad (4-6)$$

The complete software module to realize the encoder and modulator functions requires the phase encoder state generator function  $\Delta\phi_s(b1_k, b0_k)$  and the state equation of Eq. (4-6). Instead of using a table to generate  $\Delta\phi_s(b1_k, b0_k)$  from the data and then obtain  $i_k$  from  $\Delta\phi_s$ , digital logic is used to further simplify the implementation. The relationship between the input data bits and the corresponding state values of  $\Delta\phi_s(b1_k, b0_k)$  in binary form are as shown in Table 4.2.

TABLE 4.2  
RELATION BETWEEN DATA BITS AND STATE GENERATOR  
FUNCTION.

Input data (b <sub>1</sub> , b <sub>0</sub> )	$\Delta\phi_s(b1_k, b0_k)$ in decimal	$\Delta\phi_s(b1_k, b0_k)$ in binary (s <sub>2</sub> , s <sub>1</sub> , s <sub>0</sub> )
0,0	1	0,0,1
0,1	3	0,1,1
1,1	5	1,0,1
1,0	7	1,1,1

Representing  $i_k$  as  $s_2s_1s_0$ , then  $i_k$  can be easily obtained from each pair of data bits as

$$\begin{aligned} s_0 &= 1 \\ s_1 &= b_0 \oplus b_1 \\ s_2 &= b_1 \end{aligned} \quad (4-7)$$

Thus, the generation of  $\Delta\phi_s(b1_k, bo_k)$  utilizes one Exclusive-OR logic operation and some simple memory manipulation. The software implementation of the modulator, i.e. Eq. (4-6), consists of a look-up table, an addition, and an AND operation. The look-up table stores the complex values of the eight output symbol and is indexed by  $i$ . The index  $i$  is obtained by adding the new state value of the encoder to the previous state value and performing the AND “111” operation on the resulting value. The resulting index  $i$  is used to obtain the in-phase and quadrature components of the data modulator output from a look-up table, as listed in Table 4.3. At the same time this index value overwrites the previous state value for use in the next calculation.

TABLE 4.3  
LOOKUP TABLE FOR IN-PHASE AND QUADRATURE PART OF  
MODULATOR OUTPUT.

Index $i$	In-phase component	Quadrature component	Index $i$	In-phase component	Quadrature component
0	1	0	4	-1	0
1	0.707	0.707	5	-0.707	-0.707
2	0	1	6	0	-1
3	-0.707	0.707	7	0.707	-0.707

#### 4.1.3 Pulse Shaping Filter

The output of the modulator is passed through a pulse shaping filter. This filter serves two basic purposes: first, to modify the spectrum of the modulated signal to meet the regulatory constraints on the shape of the transmitted spectrum or on out-of-band power, etc.; second, to control the time domain characteristics of the impulse response, such as the pulse shape and zero crossings, so as to limit intersymbol interference (ISI). The two main design parameters for designing this filter are the spectral bandwidth and the zero crossings of the corresponding time

response. In order to have no ISI, the zero crossings in the time domain must be spaced at the symbol period. Nyquist has shown that a time domain pulse  $p(t)$  will have zero crossings once every  $T$  seconds (apart from  $t=0$ ) if its Fourier transform  $P(f)$  satisfies the following constraint [35]

$$\sum_{k=-\infty}^{\infty} P(f + kR_s) = T_s \quad \text{for } |f| < R_s/2 \quad (4-8)$$

One type of filter that gives this property is the raised cosine filter which has  $P(f)$  defined by

$$P(f) = \begin{cases} T_s & 0 \leq |f| \leq \frac{1-\alpha}{2T_s} \\ T_s \cos^2 \left\{ \frac{\pi}{4\alpha} [2|f|T_s - 1 + \alpha] \right\} & \frac{1-\alpha}{2T_s} \leq |f| \leq \frac{1+\alpha}{2T_s} \\ 0 & \text{otherwise} \end{cases} \quad (4-9)$$

The factor  $\alpha$  can be chosen to optimize the frequency response while maintaining the zero ISI condition. Plots of  $P(f)$  for several values of  $\alpha$  are shown in Fig. 4.3.

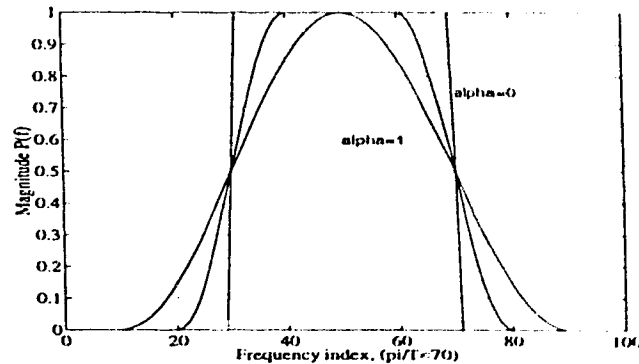


Fig. 4.3. Frequency domain response of the raised cosine filter.

Note that  $\alpha=0$  gives an ideal “brick wall” low pass filter response. The impulse response of a raised cosine filter  $p(t)$  has following properties:

$$\begin{aligned}
p(0) &= 1 \\
p(kT) &= 0 \quad k = \dots -2, -1, +1, +2, \dots \quad (4-10)
\end{aligned}$$

To provide the same filtering at both the transmitter and the receiver, the required  $P(f)$  can be split between two filters, chosen such that

$$P(f) = H_T(f)H_R(f) \quad (4-11)$$

where  $H_T(f)$  and  $H_R(f)$  are the filter transfer functions at transmitter and receiver respectively.

Based on the above conditions and criteria, the IS54 standard specifies the transmit filter to be a square root raised cosine (SRRC) filter with a roll off factor ( $\alpha$ ) of 0.35. The frequency domain definition of this filter is given in Eq. (2-1). The impulse response of this filter is given by Eq. (4.12) [14]; and the frequency characteristic and impulse response of this filter are given in Fig. 4.4.

$$h(t) = \begin{cases} 1 - \alpha + 4 \frac{\alpha}{\pi} & t = 0 \\ \frac{\alpha}{\sqrt{2}} \left[ \left( 1 + \frac{2}{\pi} \right) \sin\left(\frac{\pi}{4\alpha}\right) + \left( 1 - \frac{2}{\pi} \right) \cos\left(\frac{\pi}{4\alpha}\right) \right] & t = \pm \frac{T}{4\alpha} \\ \frac{\sin\left[\pi(1-\alpha)\frac{t}{T}\right] + 4\alpha \frac{t}{T} \cos\left[\pi(1+\alpha)\frac{t}{T}\right]}{\alpha \frac{t}{T} \left[ 1 - \left( 4\alpha \frac{t}{T} \right)^2 \right]} & \text{for all other } t \end{cases} \quad (4-12)$$

where  $T$  is the symbol period.

The pulse shaping filter is implemented in digital form in the C50 DSP. The two basic classes of filters are the *infinite impulse response* (IIR) and the *finite impulse response* (FIR). The FIR filter is selected for the pulse shaping filter because of its various advantages. A FIR filter has a linear phase response and is



always stable, with a finite and constant delay [36]. Fig. 4.5 shows the structure of a FIR filter using an N-tap discrete delay line and N tap coefficients. The most recent N data samples are stored in the delay line, and are multiplied by the corresponding tap coefficients. The products are then summed together to obtain the filter output at each sampling instant. The characteristics of the FIR filter depend on the tap coefficients ( $h_i$ ), and the length of the delay line (N). The tap coefficients are calculated by digitizing the impulse response  $h(t)$  of the pulse shaping filter at the sampling rate. For accurate implementation, the length N should be chosen large enough that all the significant values of the  $h(t)$  samples are included in the tap coefficients. For DSP implementation, N cannot be too large. For this filter, therefore, Matlab<sup>®</sup> (computer software) has been used to obtain an optimal design.

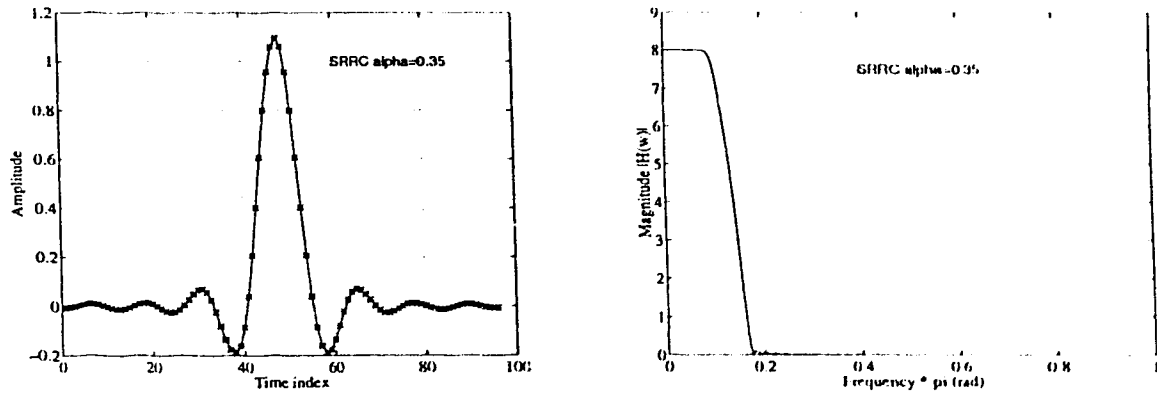


Fig. 4.4. Time domain and frequency domain response of SRRC filter.

Again, for accuracy of representation and signal processing, oversampling of the signal is required. In this work, an oversampling rate of 8 has been chosen, giving a sampling rate of 9600samples/second for a symbol rate of 1200symbols/sec. Since the symbols are generated at the lower rate, interpolation is required to bring the sampling rate up to 9600/second.

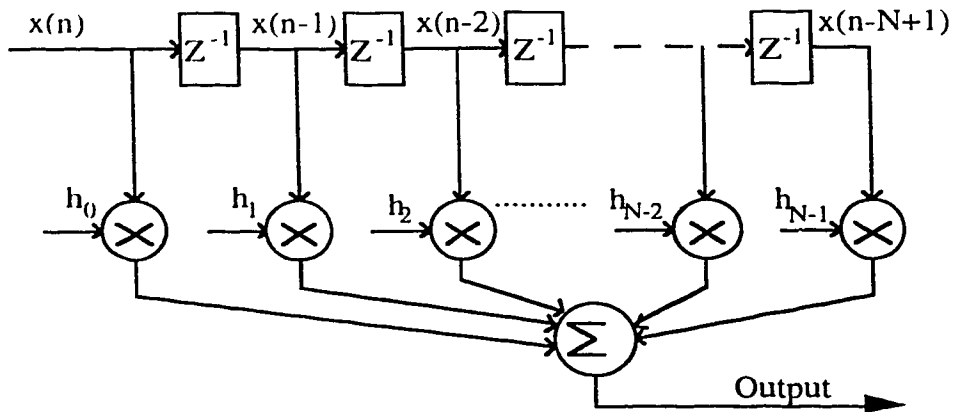
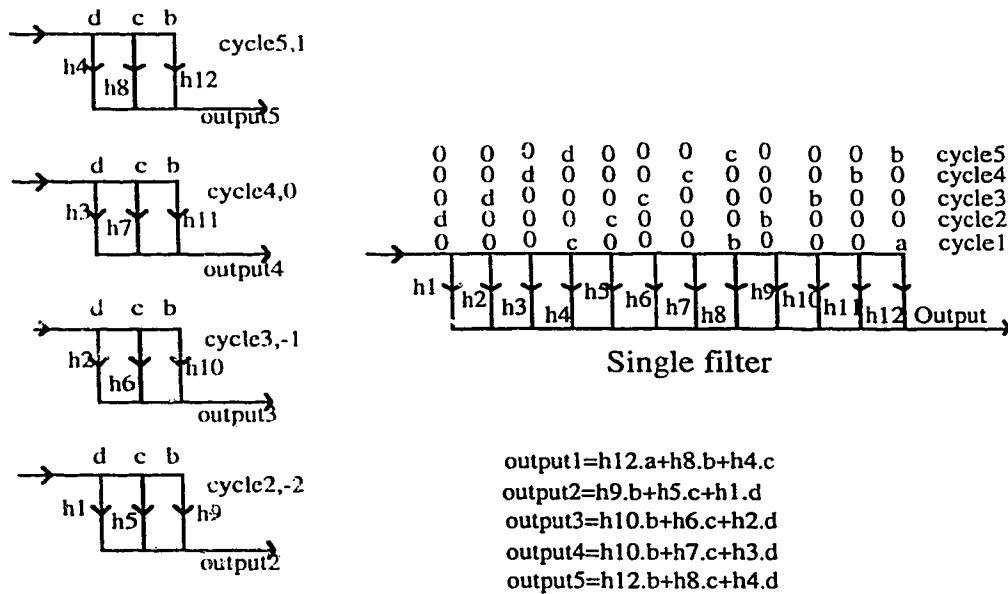


Fig. 4.5. FIR filter structure.



Filter banks

Fig. 4.6. Multirate interpolation filter structure (M=4).

As shown in Fig. 4.6 the interpolation can be performed by inserting zeroes in between the data symbol values, and then filtering this expanded data stream. However, if implemented as a simple N-tap FIR filter, each filtering operation would take N DSP clock cycles, and, as can be seen from Fig. 4.6, the majority of the multiplication results in zero. It is more time efficient to use a

multirate structure by dividing the filter into  $M$  sub-filters, where  $M$  is the oversampling ratio, and each sub-filter includes only those  $h(t)$  values that are multiplied by the actual data values [37]. Each sub-filter thus has only  $N/M$  coefficients; the filtering operation for each sample is also reduced to  $N/M$ . The grouping and operation of the sub-filters, for  $M=4$ , is shown in Fig. 4.6. The input counter directs the data input values to each sub-filter in turn. The  $h(t)$  coefficient values shown in each block correspond to the appropriate values in Fig 4.6. In the DSP the sequential use of each sub-filter is obtained using incremental addressing to access the coefficient blocks.

Matlab<sup>®</sup> is used to design the SRRC filter. A value of  $N=96$  was found to be sufficient to accurately obtain the desired response. With an oversampling factor ( $M$ ) of 8, this requires 8 filter blocks with 12 coefficients in each block. Since the output of the  $\pi/4$ DQPSK modulator is a complex signal ( $I$  and  $Q$  components), two of these filters are implemented in the TMS320C50 DSP. To facilitate the software development and to reduce the required number of instruction cycles, an object-oriented programming [38] technique is used in the filter implementation. The DSP program consists of 8 filter objects, with each object containing two 12-tap FIR filters, one for the  $I$  signal and the other for the  $Q$  signal. The timing of each object is controlled in a synchronous mode rather than burst mode, i.e. each filter object operates synchronously with the sampling clock and not  $1/8$ th of the sampling clock. The output of each object is the transmitter output, as shown in Fig. 4.7. For transmission to the receiver this output must be sequentially multiplied by the in-phase and quadrature components of the fading channel. The implementation of the fading channel is explained in the next section.

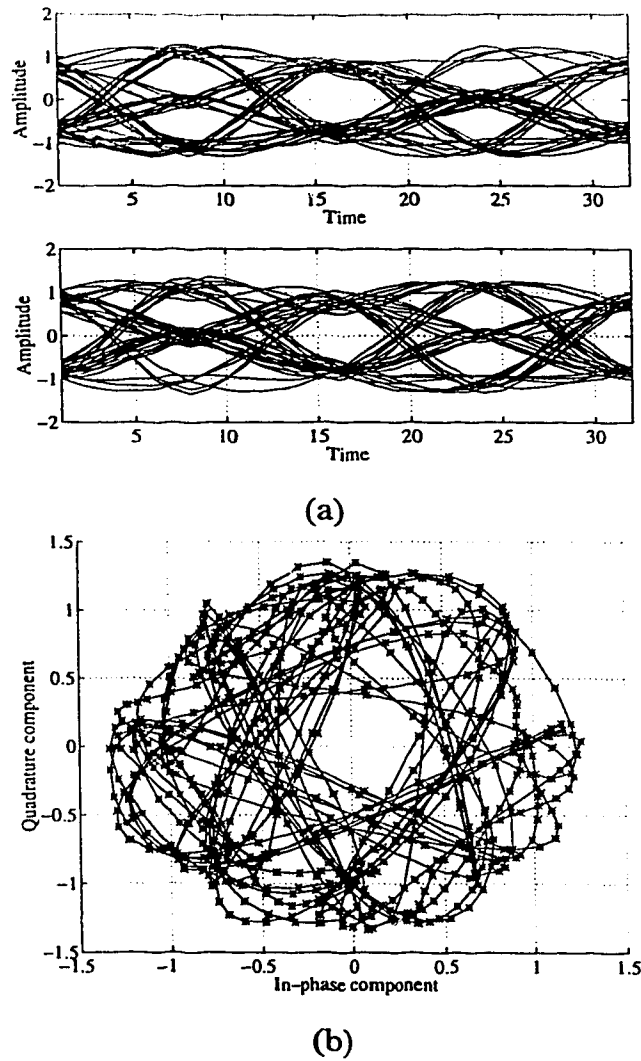


Fig. 4.7. Transmitted signal. (a) Eye-diagram. (b) Constellation diagram.

## 4.2 Flat Fading Channel

As described in Chapter 2, the transmitted signal propagates through the fading channel before reaching the receiver antenna mounted at the mobile unit. Different methods of simulating the baseband equivalent of the Rayleigh fading characteristics are described in Jakes [18]. The filter shaping method is preferred because of its simplicity of implementation in the DSP [39]. The block diagram of

the fading simulator is shown in Fig. 4.8; its implementation is explained in the following sub-sections.

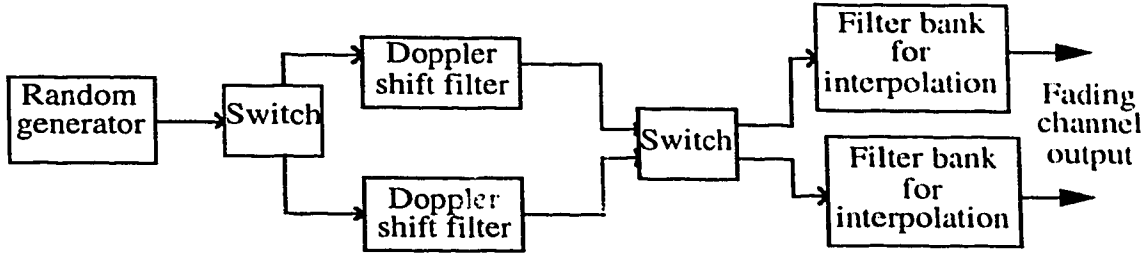


Fig. 4.8. Block diagram of fading channel model.

#### 4.2.1 Gaussian Sources

A complex base-band equivalent channel characteristic with a Rayleigh distributed envelope may be easily obtained using two Gaussian noise generators, one for the in-phase and the second for the quadrature component of the channel amplitude. These Gaussian signal (processes) are  $CI(t)$  and  $CQ(t)$  respectively of Eq. (2-6). In order to generate two independent Gaussian sources, the central limit theorem is invoked, which states that [19]

*The distribution of the sum of  $N$  statistically independent and identically distributed random variables with finite mean and variance approaches a Gaussian distribution as  $N$  approaches infinity.*

Since the channel characteristic must be spectrally shaped, the I and Q components are obtained as the output of two FIR filters. Uniformly distributed random numbers are used as input to these filters. Since each filter output consists of the sum of the input random numbers as modified by the filter coefficients, then, for a sufficiently long filter the central limit theorem will apply and the output will approach the Gaussian pdf. The uniformly distributed random sources are generated as a pseudo-random binary sequence (PRBS) using the M-sequence method, whose principle of operation is explained in Section 4.1.1. In order to

case the problem of implementing the four random generators (two used for data and two used for the fading channel), 16 parallel shift registers (PRBS sources) are used, instead of 4 independent shift registers. Each generator has a different seed so that the output of each generator is independent of the others. The number of parallel sources, 16 in this case, is limited by the word length of the DSP memory. The shift register length and tap values used in each of these generators must be identical for circular buffer implementation and parallel operation. As mentioned already, the sequence length is selected to be  $(2^{31}-1)$  since this gives a very long period of random generation, e.g. at a symbol rate of 1.2 ksymbols/sec, the sequence period is equal to 20.7 days. In order to further make sure that all the sources are independent, 16 equally spaced seed values are chosen from the 31 bit maximal length sequence; these seed values are then entered in the random generator block as 31 16-bit words, as shown in Fig. 4.9. Every cycle of the random generator produces a new random word, giving 16 independent binary bit sources. For each random 16 bit binary word, 7 bits are used for each of the **chI** (in-phase) and **chQ** (quadrature) random number inputs, and the remaining two bits are used to generate the data symbol as shown in Fig. 4.9. Care must be taken while extracting and storing each 7 bit segment from the 16 bit word, so as to maintain the appropriate sign bit in each source. After obtaining the uniformly distributed words, the filtering is done using a 121 point FIR filter. This is a large enough number of points that the output will approach a Gaussian noise source, as per the central limit theorem. Separate averaging must be done for **chI** and **chQ**, therefore two filters are required. The required tap weightings for shaping the power spectrum of these fading generators are obtained as described in the following sub-section, (4.2.2).

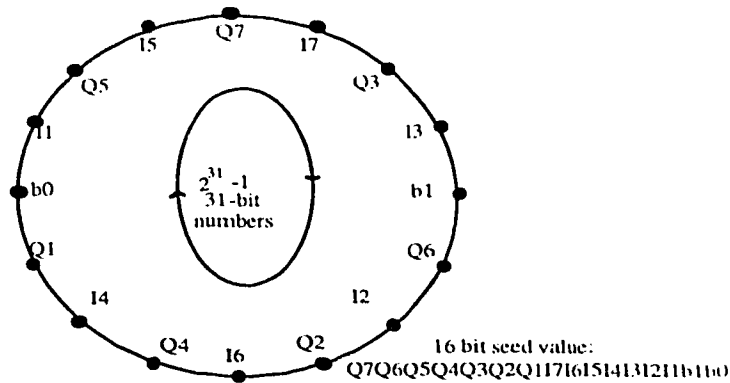


**Fig. 4.9.** Seed value generator for random generator.

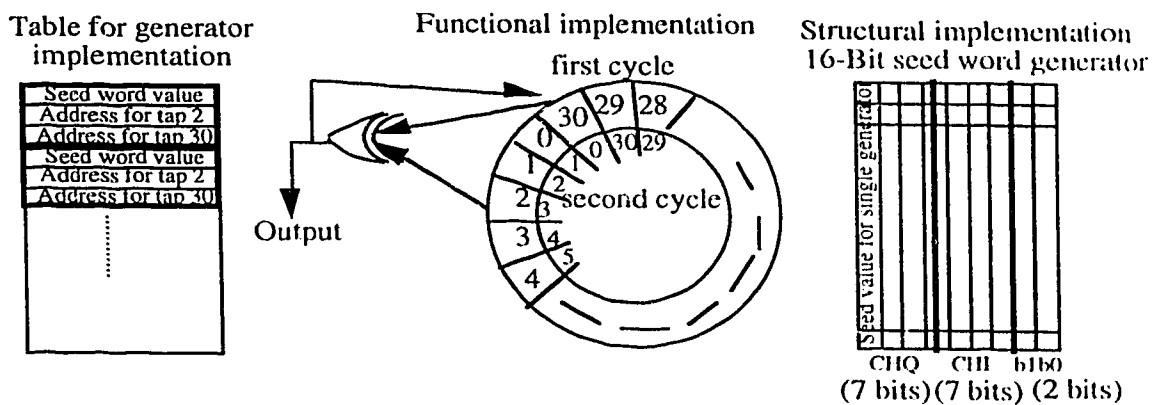


Fig. 4.10. Circular buffer implementation of random 16-bit word generator.

The actual software module for the 16-bit word generator is implemented using a “memory table” that simulates the action of a circular buffer. The circular buffer available in the C50 could not be used because of its limitation in increment count to  $\pm 1$ . The “memory table” uses 31 groups of 3 memory locations to implement a 31 length shift register. The first location in each group is a seed value (16 bit word) for the 16 bit generator. The second location in the group is the memory address containing the seed word (register) corresponding to tap 2, and the third location of the group has the address of the seed word (register) corresponding to tap 29. These taps are selected for maximal random sequence

length as described in Section 4.1.1. Unlike an independent shift register, the circular buffer implementation does not have fixed tap coefficient locations or registers. This is due to the dynamic change in register tap number; i.e., instead of shifting up the seed bits in the registers (locations), the register number is changed such that the overall effect is the same, as shown in Fig. 4.10. This implementation is not straight forward, but it requires less computation than other methods and is therefore preferred.

#### 4.2.2 Doppler Shift Filter

The Doppler shift filter serves two purposes: one is to produce a Gaussian distributed output and the second is to shape the output in order to obtain the required Doppler power spectrum. Two Doppler shift filters are used, one each for the in-phase (chI) and quadrature components (chQ) of the channel. These filters are designed to simulate the measured spectrum as it would be received in a practical mobile radio environment. It has been found experimentally that the received signal strength is very close to the analytical result, provided that an omnidirectional antenna is mounted at the receiver. It has been proved, as discussed in Section 2.2.2.1, that the spectrum can be formulated as [18]

$$S_s(f) = \begin{cases} \frac{C}{\sqrt{f_m^2 - f^2}} & -f_m \leq f \leq f_m \\ 0 & \text{otherwise} \end{cases} \quad (4-13)$$

where  $S_s(f)$  is the power spectrum of the fading signal,  $C$  is a constant depending on the antenna gain pattern and path attenuation factor, and  $f_m$  is the maximum Doppler frequency. The range of the Doppler frequency is between 0 and 83.3Hz, for a vehicle speed of up to 100km/hr when a carrier frequency of 900MHz is used. For a maximum Doppler shift frequency of 80Hz, the received signal



spectrum is as shown in Fig. 4.11. The Doppler shift filters are designed so that their transfer functions match this spectral shape as closely as possible.

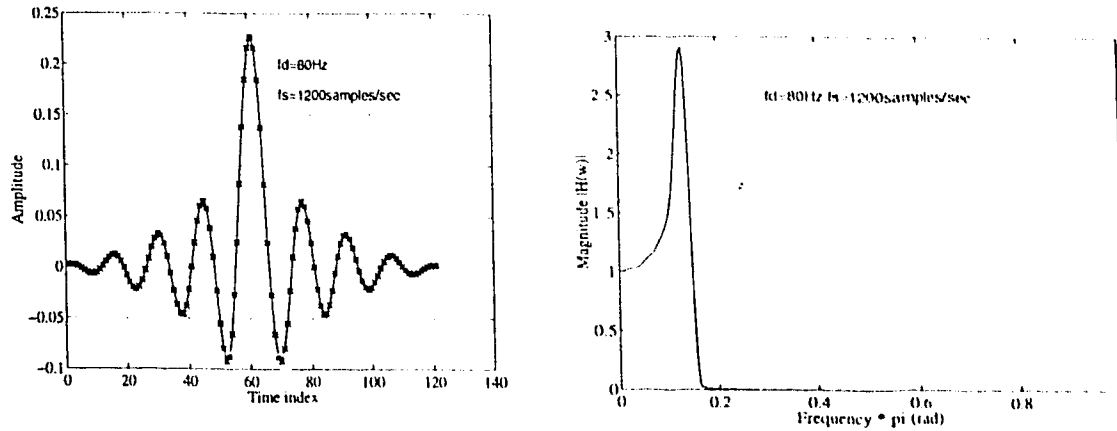


Fig. 4.11. Time domain and frequency response of Doppler shift filter.

The sampling rate of the channel needs to be the same as that of the data, namely 9600 samples/sec. Because it is difficult to design a filter with a high sampling rate to cut-off frequency ratio, the Doppler shift filter is initially designed with a sampling frequency of 1200samples/sec and a cutoff frequency of 80Hz. Interpolation is then used to increase the sampling rate, and if necessary, change the cut-off frequency at the same time; e.g., 16 times interpolation is used to produce an effective 9600 samples/sec with a 40Hz Doppler shift.

The Doppler shift filter is designed as an FIR (linear phase) filter, with a tap length of 121 coefficients. The *least square method* of filter design, from the Matlab<sup>®</sup> signal toolbox, is used to obtain the specified frequency and magnitude characteristics. An IIR filter with fewer taps could have been used but FIR is preferred over IIR because of its inherent stability and more pronounced peak at the maximum Doppler frequency. The power spectral density at the frequency  $f_m$  is about 10dB higher than that at  $f=0$ . The requirement of a variable bandwidth

filter (variable Doppler shift) is implemented using a variable sampling rate for both the filter and the Gaussian Noise generator. A programmable counter is used to provide the required sampling rate for each simulation case. The hardware and software control of the sampling rate and the Doppler shift frequency is further explained in the following sub-section.

### 4.2.3 Interpolating Filter

Two interpolation filters, one each for the in-phase and quadrature components of the channel are required. Interpolation increases the sampling rate of the Doppler shift filter output to a value equal to that of pulse shaping filter output for the data, thereby facilitating the digital superposition of the channel upon the transmitted signal. The multirate implementation, as discussed for the pulse shaping filter, is used so as to save instruction cycle time. The design of the filter depends on the interpolation factor and the required suppression of the undesired images.

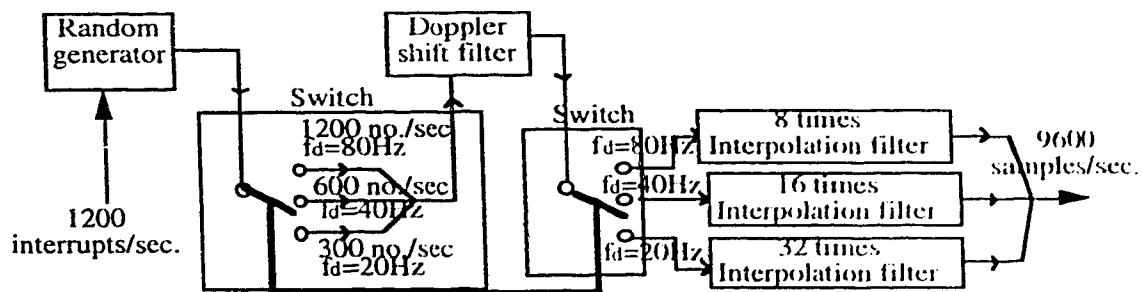


Fig. 4.12. Software architecture for fading channel.

The interpolation filter is designed as a FIR filter using the Matlab<sup>®</sup> signal processing toolbox. The tap length of the FIR filter depends on the sampling rate and the interpolation factor. The architecture of the algorithm for fading sample generation, for different Doppler frequencies, using a software switch, counter

and interrupts is shown in Fig. 4.12. For  $f_d = 40$  Hz, and a sampling rate of 600 samples/sec, the Doppler shift filter uses the same coefficients as were used for the Doppler shift filter with  $f_d=80$ Hz, at the sampling rate of 1200samples/sec. However a software counter is first used to lower the input rate to 600 samples/sec, and  $f_d=40$ Hz, then an interpolation filter with oversampling factor of 16 is used to interpolate between these samples, suppressing undesired images between  $(600-f_d)$  to  $(4800-f_d)$ . This effectively produces the same waveform as for the 80Hz Doppler shift filter, but slowed down in time by a factor of 2. For  $f_d = 20$ Hz, the software counter adjusts the Doppler shift filter input to 300 samples/sec; the interpolation filter is then designed to interpolate between these samples with oversampling factor of 32 suppressing undesired images between  $(300-f_d)$  to  $(4800-f_d)$ . The tap length of the designed interpolation filter is 96 for  $f_d$  equal to 40Hz, and 352 for  $f_d$  equal to 20Hz. Multirate implementation as discussed in Section 4.1.3, is used for these interpolation filters. The output of the fading simulator is shown in Fig. 4.13.

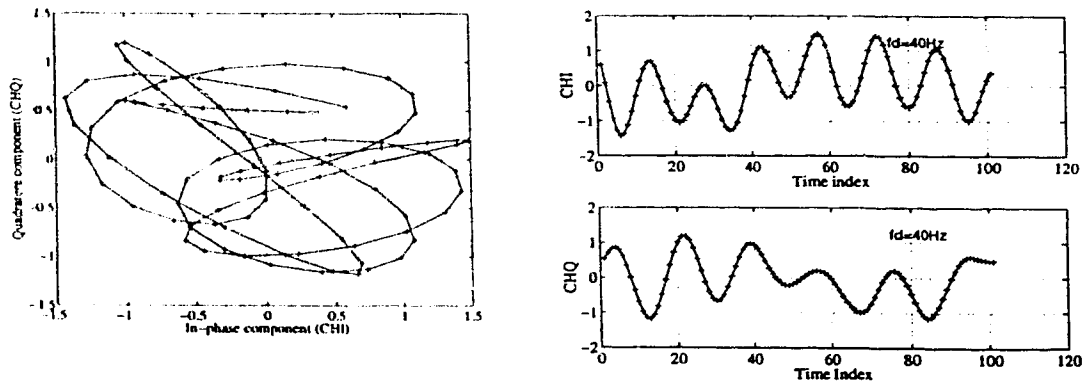


Fig. 4.13. Fading channel simulator output.

Although the filter structure is simple, it takes a large number of instruction cycles to generate the complete fading process, especially for the

lowest Doppler frequency value, because of the increase in tap length of the filters. It is for this reason that the data rate was limited to 1200symbols/second. Since both the transmitter and fading channel are sequentially implemented in one DSP, each generated data symbol has to wait for the fading sample generation process to be completed.

### 4.3 Channel Superposition on Transmitted Signal

#### 4.3.1 Complex Multiplication

Once the fading channel and transmitter output samples are calculated they are digitally combined using complex multiplication. The software module for this performs the following simple calculations,

$$rxI + jrxQ = (SI + jSQ)(chI + jchQ), \quad (4-14)$$

$$\text{so that } rxI = SI * chI - SQ * chQ \quad (4-15)$$

$$\text{and } rxQ = SI * chQ + SQ * chI \quad (4-16)$$

The output of the combiner is then fed sequentially to the DSP TMS320C30 using an external interface circuit, which is discussed in the following sub-section. This signal, representing the baseband equivalent of the signal received by the mobile unit receiver antenna, is shown in Fig. 4.14. By comparing Figs. 4.7, 4.13 and 4.14, the distortion of the transmitted signal due to the fading channel is clear.

#### 4.3.2 Interface

The interface circuit is required to buffer the output of the TMS320C50 and transfer it to TMS320C30. The design of the interfacing circuit depends on the operating mode used by the DSP program. Since the synchronous mode of operation is used, the circuit operates at the sampling frequency to buffer the data between two DSPs.

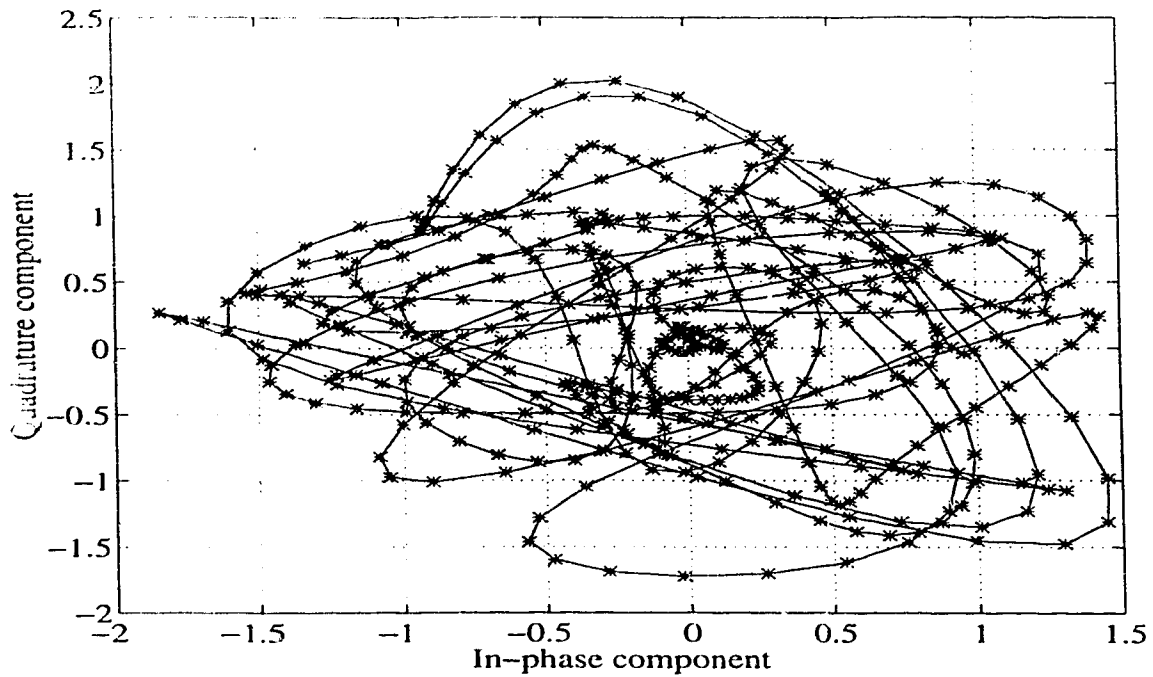


Fig. 4.14. Received signal waveform.

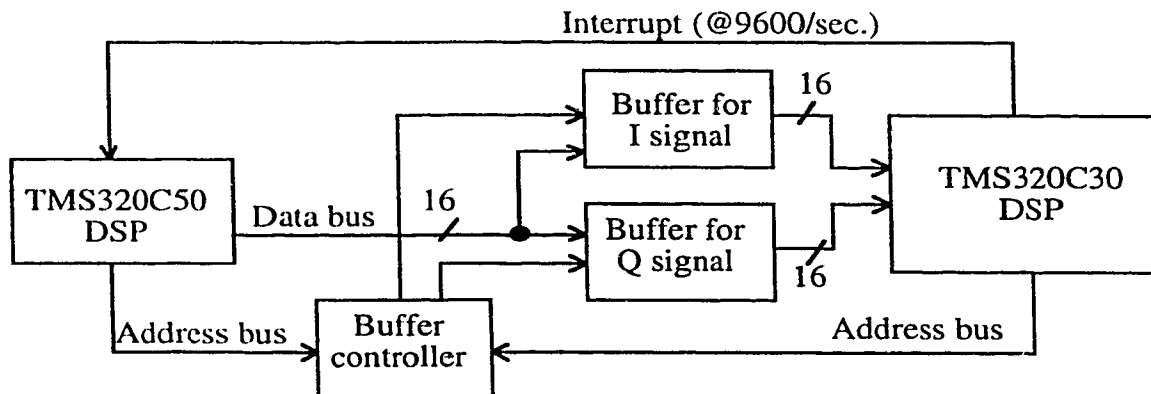


Fig. 4.15. Block diagram of interface circuit between DSP C50 and C30.

The block diagram of the interface circuit is shown in Fig. 4.15. It consists of two components: two 16-bit buffers for the in-phase and quadrature components of the received signal, and a buffer controller. The two 16-bit buffers provide a data access interface between the TMS320C50 DSP and the

TMS320C30 DSP. The buffer controller circuit monitors the TMS320C30 DSP address bus and the TMS320C50 address bus, and generates an appropriate control signal for the 16-bit buffers. These control circuits are used by the buffer for two functions: to latch a new set of samples from TMS320C50 (two operations, to write two 16 bit words into the buffer), or to enable the buffers for access by the TMS320C30 (a single read operation of all 32 bits of data). Initially the interface circuit was built using an SK-10 bread-board for prototype testing. Since the bread-board capacitance makes it unreliable at the clock rate of 20MHz, a printed circuit board (PCB) was built. The details of the PCB design process are shown in Appendix A.

#### **4.4 Receiver**

The receiver structure, as described in Chapters 2 and 3, is implemented using the Texas Instruments TMS320C30 DSP development platform [40, 41, 42] and an IBM PC486 compatible computer. The key features of this DSP are given in Table 4.4. A synchronization circuit is not designed in the receiver; instead, the sampling rate is controlled via a hardware interrupt on the C30 board. The basic building blocks of the receiver are described in the following sub-sections.

TABLE 4.4  
FEATURES OF DSP TMS320C30.

60ns instruction cycle (16.7MIPS and 33.3MFLOPS)
Two 1K × 32 bit dual-access on-chip RAM
32-bit instruction and data words, 24-bit addresses
40/32 bit floating point/integer ALU and multiplier
8 extended-precision registers
On-chip Direct Memory Access (DMA) controller
Two serial ports, two 32 bit timers

#### 4.4.1 Additive White Gaussian Noise Source

In nature, the ideal transmission of information is degraded by two types of phenomena: imperfect equipment (distortion), and the presence of "generalized noise", i.e., any signal other than the desired signal itself. The modeling of this noise as a Gaussian random process is well known. For simulation purposes we therefore need to be able to pseudorandomly generate such a process. Random samples generated independently at intervals of  $T_s$  correspond to a noise source with uniform power spectral density over a bandwidth equal to  $1/T_s$ . To simulate spectrally shaped Gaussian noise, "white" noise needs to be passed through a filter whose transfer function produces the desired shape. In the software implementation, the shift register method of PRBS generation is used to generate white noise. This is filtered by the SRRC filter at the receiver front end.

The noise generation program comprises modules to generate, add and measure the noise signal. A circular buffer of block length 28 is used as a shift

register, with feedback taps 3 and 28, to obtain a maximum sequence of length  $2^{28}-1$ . This length is chosen so as to make sure that the sequence is independent of all the other sequences previously obtained, which used a 31 length shift register. The complete 32-bit word length of the TMS320C30 is used to generate two components ( 16 bits each for the real and imaginary parts) of the complex noise process. 28 initial seed values are randomly selected so as to initiate the noise generation. Each 16-bit component is moved to the least significant part of the two noise output words using an arithmetic shift so as to retain the sign bit value. The integer values so stored are ~~changed~~ to floating point values so as to obtain good dynamic range for the noise power, and also so that they may be multiplied by a variable scaling factor. This scaling factor can be changed to obtain different levels of noise power, and thus different SNR values for the signal. The generated complex noise is added to complex received signal, i.e. the real and imaginary part of signal and noise are added separately, and the resulting output is fed to the receiver bandpass filter (a SRRC filter, identical to the transmitter filter). Power calculations use the sum of the square of the measured signal amplitude at the output of the bandpass filter, divided by the number of samples. To calculate the noise power and signal power so as to measure the SNR, an extra sub-module is added into the program. In this power measurement module, either the noise signal or the received signal is set to zero prior to the input bandpass filter, so that the other quantity may be measured, i.e. two runs of the program are used. It is essential to make both noise and signal power measurements because the transmitted signal power is not normalized to one. The ratio of the signal and noise powers is calculated manually, off-line, to find the SNR in dB.



#### 4.4.2 Receiver Bandpass Filter

The bandpass filter used at the front end of the receiver is exactly the same as the pulse shaping filter at the transmitter. As specified by the IS54 standard, the frequency response is the square root raised cosine shape with  $\alpha=0.35$ , as discussed previously in Section 4.1.3. This filter is implemented digitally in the C30, using an FIR structure. The only difference between the transmitter and receiver filters is in their implementation. Unlike the pulse shaping filter at the transmitter, the bandpass filter at the receiver is not used for interpolation or oversampling. Thus, the multirate form of implementation can not be used at the receiver end. Also, since the C30 is a floating point DSP, all the calculations for the receiver filtering operation are done in floating point format.

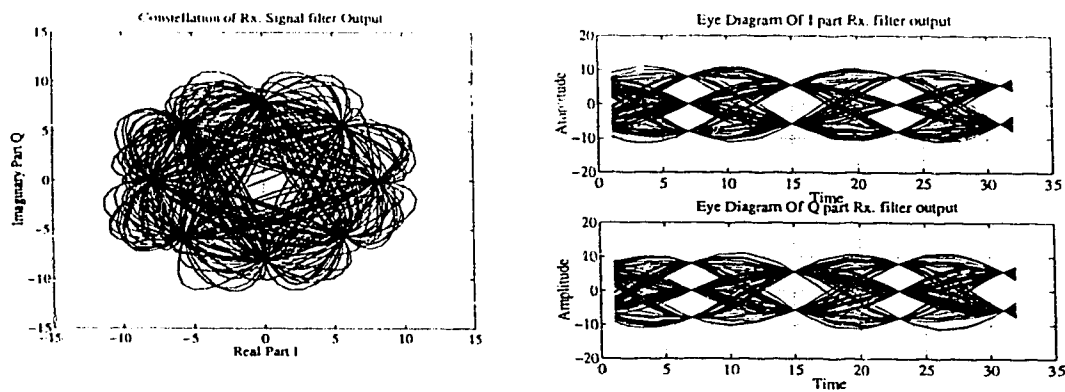


Fig. 4.16. Zero ISI waveform.

In order to observe the implementation correctness, the transmitter and receiver are connected back to back, with the noise and channel turned off (noise=0, channel=1). The constellation diagram and the eye diagram for this test are as shown in Fig. 4.16. The diagrams display a sharp pinch point at the sampling instants, indicating zero ISI, and the eye is wide open; this may be compared with the transmitter filter output shown earlier in Fig. 4.7. The overall

zero ISI is obtained because the combination of two square root raised cosine filters give a raised cosine filter, which meets the Nyquist criterion.

An important point to note here is that the zero intersymbol interference criterion is no longer valid once the effect of the fading channel and noise has been impressed on the transmitted signal. This is because the overall transfer function is the product of the transfer function of the two filters and the channel, which does not meet the Nyquist criterion. The received signal at the output of the bandpass filter (Fig. 4.17) does not exhibit sharp pinch points in either the eye-diagram or the constellation diagram, and the eye is no longer wide open at the sampling instant.

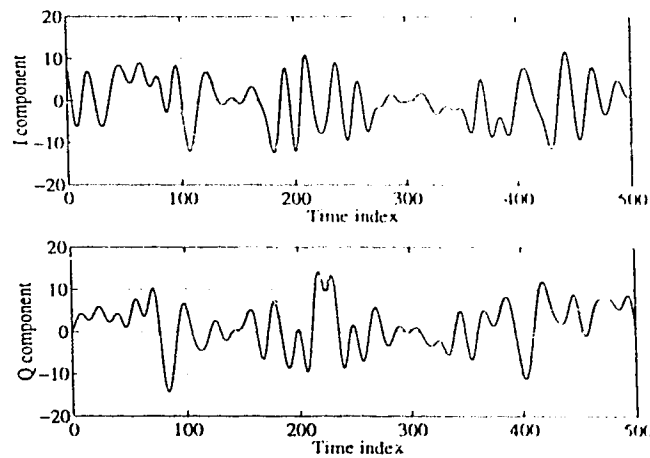


Fig. 4.17. Receiver bandpass filter output.

#### 4.4.3 Decision-Aided Detector

The bandpass filter output is sampled once per symbol period, in order to extract the sample corresponding to the instant when the eye is wide open. This is required by the detector so as to make its decision at the optimum time. In order to simplify the implementation, the sampling time is controlled by a C30 interrupt, rather than using a timing recovery algorithm. At the appropriate symbol instant, one sample is recovered from the received 8 samples per symbol

period. The appropriate symbol instant is the instant at which the pinch point is observed for the case of the back-to-back transmitter and receiver test. This is equivalent to the assumption that the transmitter and receiver are synchronized to the same clock. However, this assumption is not critical to the evaluation of the decision-aided error correction scheme because timing errors primarily affect D1, and the error improvement is measured as the ratio of D2 to D1.

#### **4.4.3.1 Differential Detector**

Differential detection, as discussed in Chapters 2 and 3, is used to make the first decision about the transmitted data, based on the information at the output of the receiver bandpass filter. This method of detection is preferred over coherent detection because it does not require complex processes for carrier synchronization, e.g. tracking, acquisition, lock detection, false lock prevention etc. Differential detection is accomplished by comparing the received signal phase in a given symbol interval (of duration  $T_S$  seconds ) with that in the previous symbol interval and making a decision on the difference between these two phases. In the absence of channel distortion and noise, the differential phase detected by the detector will be exactly equal to one of the 4 possible transmitted phase shifts  $\{\pm 45^\circ, \pm 135^\circ\}$ ; these are the differential phase shifts imposed by the  $\pi/4$ DQPSK modulation.

The DSP software implementation for the differential detector uses the rectangular co-ordinate system instead of the polar co-ordinate system, thereby avoiding any  $\tan^{-1}$  operations. The in-phase and quadrature phase components at the output of the bandpass filter are stored for both the  $k^{\text{th}}$  and  $(k-1)^{\text{th}}$  symbol instants, where  $k$  is an integer. The phase differential is obtained by simple

multiplication and addition/subtraction operations derived from the vector division of the signals at the times k and k-1. The signals are

$$r_k \angle \phi_k = I_k + jQ_k \quad \text{and} \quad r_{k-1} \angle \phi_{k-1} = I_{k-1} + jQ_{k-1}, \quad (4-17)$$

and the phase difference can be found from,

$$\frac{r_k \angle \phi_k}{r_{k-1} \angle \phi_{k-1}} = \frac{I_k + jQ_k}{I_{k-1} + jQ_{k-1}} = U + jV \quad (4-18)$$

Thus,  $U = b(I_k I_{k-1} + Q_k Q_{k-1})$  (4-19)

and  $V = b(Q_k I_{k-1} - I_k Q_{k-1})$  (4-20)

where b is scaling factor. For a typical signal, Fig. 4.18 shows the set of samples corresponding to the vector  $U+jV$ .

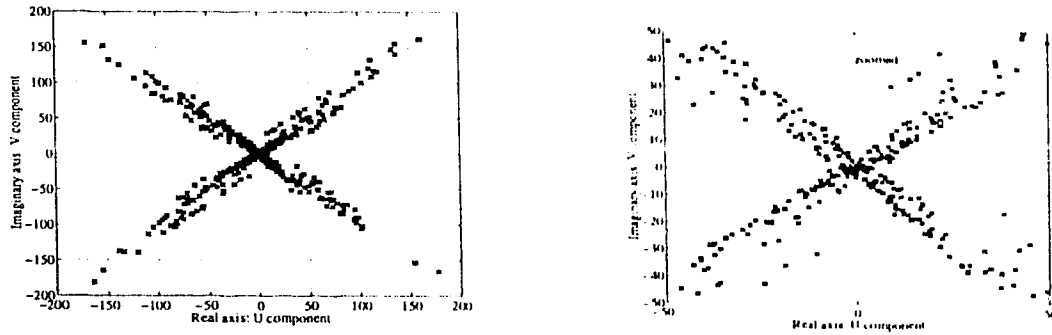


Fig. 4.18. Differential detector output ( $U+jV$ ).

The differential phase angle is  $\tan^{-1}(V/U)$ , but the decision about the transmitted data can be made based on the quadrant in which the vector corresponding to  $U+jV$  lies. For DSP software implementation, the decision is made using a small look-up table, the indices (i, j) of which are determined using the sign bit (positive or negative) of U and V. The indices calculation and look-up table entries for the first decision (D1) are shown in Table 4.5.

TABLE 4.5  
LOOK-UP TABLE FOR FIRST DECISION.

$U \geq 0$	$i=0$	for $i+j=0$	D1=00
$U < 0$	$i=2$	for $i+j=1$	D1=10
$V \geq 0$	$j=0$	for $i+j=2$	D1=01
$V < 0$	$j=1$	for $i+j=3$	D1=11

The first decision values are stored in circular buffers of length 31, i.e. the 31 most recent first decisions are stored and the older values are over-written by the new values in circular fashion, one by one. These stored values will be used while making the second decision using the decision-aided error correction algorithm. The first decision, in conjunction with the transmitted data, is used to calculate the primary symbol error rate, as explained in the error measurement section (Section 4.5).

#### 4.4.3.2 Reverse Modulator

Since the channel is a multipath fading channel with AWGN noise, the detected differential phase, as indicated by  $U$  and  $V$ , deviates from the ideal data phase change values of  $\{\pm 45^\circ, \pm 135^\circ\}$ . The deviation from the ideal phase angle, caused by the effect of the fading channel and noise, and called here the "extracted channel" is extracted by the reverse modulator. Note that the first decision (D1) is used by the reverse modulator to determine the transmitted phase change. A plot of the extracted channel phase, using a Matlab<sup>®</sup> simulation, is shown in Fig. 4.19. Since the fading is a narrowband process, the extracted channel should be band-limited to the  $2f_d$  ( $f_d$  is the maximum Doppler frequency). However, Fig. 4.19 shows some high frequency components; i.e., some points are out of place, which occurs mainly at the times when the

transmitted symbols are not detected correctly by the differential detector. This is expected because during deep fades the phase changes caused by the channel can be very large, leading to incorrect first decisions, and thus incorrect data phase information fed back to the reverse modulator. This directly results in errors in the extracted channel information.

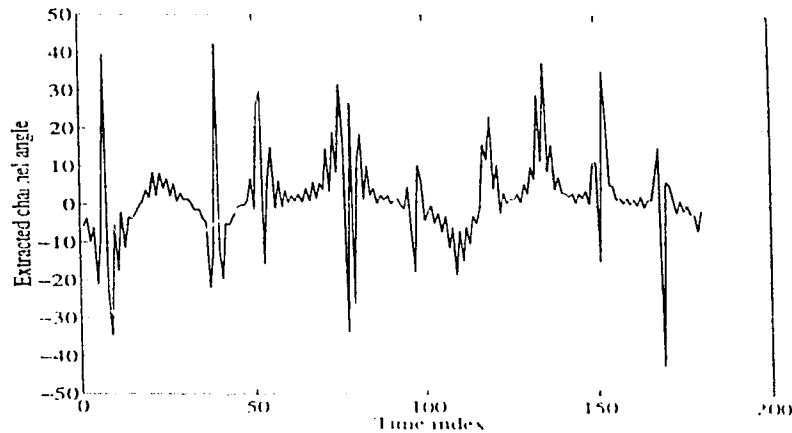


Fig. 4.19. Extracted channel using angles.

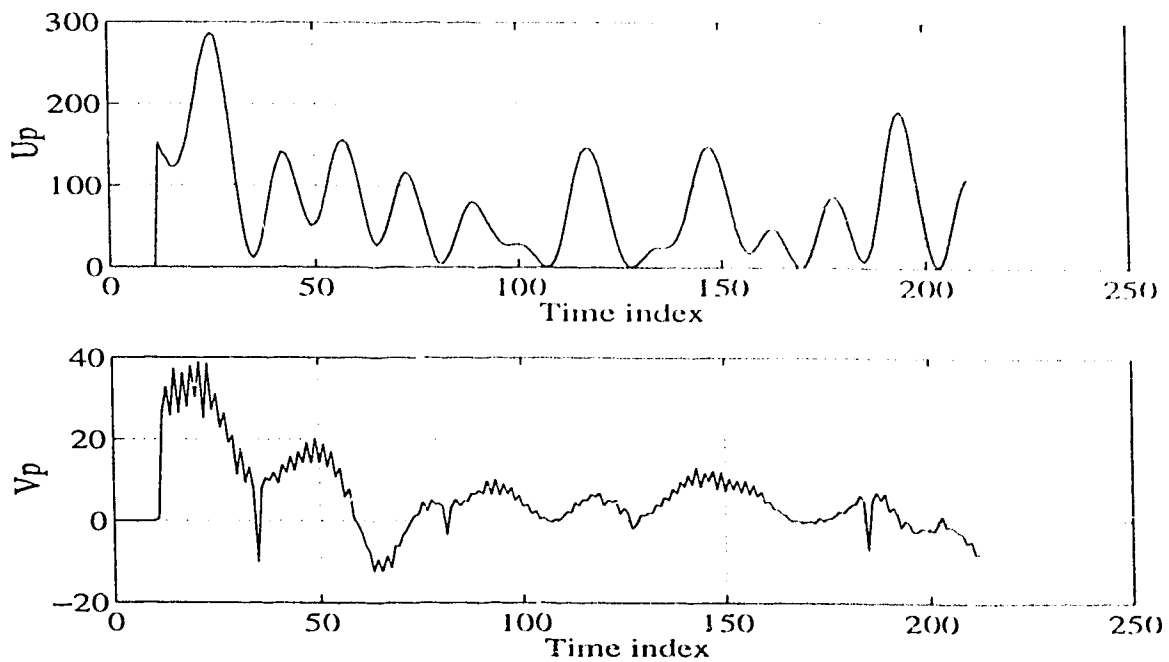


Fig. 4.20. Extracted channel using Up and Vp.

For DSP implementation, the use of  $\tan^{-1}$  is undesirable and therefore the reverse modulator finds the extracted channel phase information in terms of **Up** and **Vp**, as discussed in Chapter 3. Fig. 4.20 shows a typical **Up** and **Vp** graph. In the implementation, the phase deviation is always calculated with reference to the corresponding detected data phase change. This means that for each symbol, the reference corresponds to one of the four possible transmitted phase changes  $\{\pm 45^\circ, \pm 135^\circ\}$ , depending on the quadrant in which the received signal phase change corresponding to **U+jV** lies. Determination of **Up** and **Vp** for each of the four possible data phases is illustrated in Fig. 3.3b.

Mathematically,

$$\begin{aligned}
 \text{if } U + jV &= re^{j\Delta\phi_{rx}}, \\
 \text{then } U_p + jV_p &= re^{j(\Delta\phi_{rx} - 45^\circ)} \text{ for } D1=45^\circ, \text{ (first quadrant)} \\
 U_p + jV_p &= re^{j(\Delta\phi_{rx} - 135^\circ)} \text{ for } D1=135^\circ, \text{ (second quadrant)} \\
 U_p + jV_p &= re^{j(\Delta\phi_{rx} + 135^\circ)} \text{ for } D1=-135^\circ, \text{ (third quadrant)} \\
 U_p + jV_p &= re^{j(\Delta\phi_{rx} + 45^\circ)} \text{ for } D1=-45^\circ, \text{ (fourth quadrant)}. \quad (4-21)
 \end{aligned}$$

Calculating **Up** and **Vp** in terms of **U** and **V**, and using rectangular co-ordinates,

then

$$\begin{aligned}
 U_p + jV_p &= (U + jV)e^{-j45^\circ} & \text{for } D1=45^\circ, \\
 U_p + jV_p &= (U + jV)e^{-j135^\circ} & \text{for } D1=135^\circ, \\
 U_p + jV_p &= (U + jV)e^{+j135^\circ} & \text{for } D1=-135^\circ, \\
 U_p + jV_p &= (U + jV)e^{+j45^\circ} & \text{for } D1=-45^\circ. \quad (4-22)
 \end{aligned}$$

The resulting values of **Up** and **Vp** are given in Table 4.6.

TABLE 4.6  
REVERSE MODULATOR OUTPUT.

D1 values	Up (in terms of U and V)	Vp (in terms of U and V)
+45°	$(U+V)/\sqrt{2}$	$(V-U)/\sqrt{2}$
+135°	$(V-U)/\sqrt{2}$	$(-U-V)/\sqrt{2}$
-135°	$(-U-V)/\sqrt{2}$	$(U-V)/\sqrt{2}$
-45°	$(U-V)/\sqrt{2}$	$(U+V)/\sqrt{2}$

Thus the reverse modulation process is simplified to a conditional addition and/or subtraction operation. The conditions for the **Up** and **Vp** calculations are based on the first decision value, which depends on **U** and **V** (**U** and **V** in turn correspond to the differential received phase angle). Therefore, to implement this conditional logic, it is possible to use simple logic instead of a conditional branch instruction, which helps to reduce the instruction cycle time. Thus, the sign extraction of **U** and **V** is used by the implemented software module, as given in Table 4.7, for the reverse modulation.

TABLE 4.7  
LOGIC FOR REVERSE MODULATOR OUTPUT.

Condition	Intermediate variables for Up; where $U_p = j+1$	Intermediate variables for Vp; where $V_p = k+1$
$U \geq 0$	$j = U$	$k = V$
$U < 0$	$j = -U$	$k = -V$
$V \geq 0$	$l = V$	$m = -U$
$V < 0$	$l = -V$	$m = U$

These values of **Up** and **Vp** corresponds to the fading estimate as affected by the noise. Since the first detection is not always correct, this estimate includes the



effect of any incorrect first decisions as well. Therefore, the next step in the decision-aided detector is to minimize the effect of the incorrect first decisions on the fading estimate using the channel estimator.

#### **4.4.3.3 Channel Estimator and Error Corrector**

The channel estimator is the heart of the decision-aided detector and the performance of the algorithm depends largely on this part. The goal of the estimator, as discussed in detail in Chapter 3, is to obtain the best possible estimate of the phase changes due to the fading channel, using the extracted channel information at the output of the reverse modulator. Since, in a typical case, one out of one hundred first decisions are incorrect, the channel recovery at the output of the reverse modulator contains 1% incorrect estimates. The estimation filter is designed to remove this distortion as far as is possible, based on both past and future values of the recovered channel phase; i.e., an interpolation based method of estimation is used rather than a prediction based method. The design of the estimator is based on the fact that the fading is a narrow-band process having a bandwidth of twice the maximum Doppler shift.

As discussed in Chapter 3, in designing the channel estimation or reconstruction filter, a compromise must be made between the filter length and the accuracy of the spectral characteristics. Thus, the number of points ( $N$ ) that can be used for estimation, on each side of the decision point ( $k=-N$  to  $0$  to  $N$ ), is taken to be in the range of 2 to 30. Due to data errors, erroneous samples of  $U_p$  or  $V_p$  enter the estimation filter at  $k=-N$ . Any channel sample in error has its maximum effect as it reaches the middle of the filter, since the  $h(0)$  coefficient has the largest value. One improvement that may be made in the filter design is to modify the filter by setting the middle filter coefficient value to zero. Since the

gain of the filter must be kept at unity, the impulse response of the modified filter is then required to be

$$h(i) = \begin{cases} 0 & \text{for } i = 0 \\ \frac{h(i)}{1 - h(0)} & \text{elsewhere} \end{cases} \quad (4-23)$$

It should be noted however that any data errors will still have an effect on the channel estimate for  $k=-N$  to  $-1$ . If the error is corrected at  $k=0$ , then the channel data  $U_p$  and  $V_p$  will have no errors in the right hand part of the filter ( $k>0$ ). Some other practical considerations for designing the filter are: it is necessary that some of the filter coefficients be negative; and, also, the filter shape should be such that the coefficients away from the estimation point dies away towards zero, i.e. at the ends of the filter.

A number of "trial runs" with both the DSP and Matlab<sup>®</sup> were used to evaluate various possible filter designs. The coefficients of each filter tested were obtained using either the signal processing tool-box of Matlab, or a numerical analysis technique. In the various tests, the cut-off frequency, roll-off factor, and/or the degree of polynomial etc., and the length of the filter were changed, and tests were conducted in order to measure the error rate of the second decision as compared to the first decision. The Improvement Factor (IF) is thus defined as the ratio of the number of errors in the first decision to the number of errors in the second decision. Whatever filter design method is used, the filter should have a flat passband and a cutoff frequency of at least 2 times the maximum Doppler shift. Note that for these preliminary tests no noise is added at the receiver end.

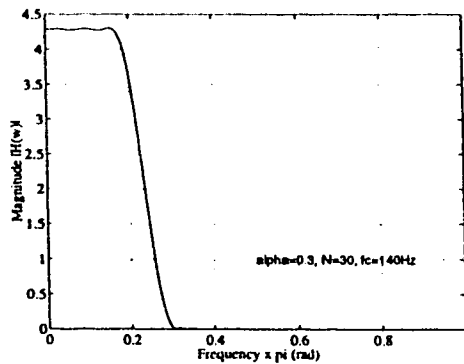
Initially, filter coefficients were calculated by sampling (1.2ks/s) the time domain response of a raised cosine filter, and changing the design parameters

such as roll-off factor, cut-off frequency, and the length of the filter. The results of these tests, together with the relevant parameters are given in Table 4.8.

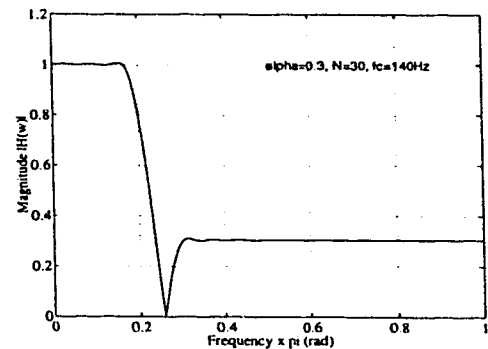
TABLE 4.8  
TEST RESULTS BASED ON RAISED COSINE ESTIMATION DESIGN.

Roll-off ( $\alpha$ )	Cut-off ( $f_c$ )	Points on each side (N)	Improvement factor (IF)	Doppler frequency ( $f_d$ )
0.30	140 Hz	30	7.2	20 Hz
0.50	140 Hz	20	14.03	20 Hz
0.30	80 Hz	20	1.7	20 Hz
0.30	190 Hz	20	11.72	20 Hz

For comparison purposes, Fig. 4.21a shows the frequency response of the first filter with both  $h(0) \neq 0$  and  $h(0) = 0$ . Fig. 4.21b shows the response for the other three filters with only  $h(0) = 0$ .



$h(0) \neq 0$



$h(0) = 0$

Fig. 4.21. Estimation filter design based on raised cosine filter.

(a) Filter response with  $h(0) \neq 0$  and  $h(0) = 0$ .

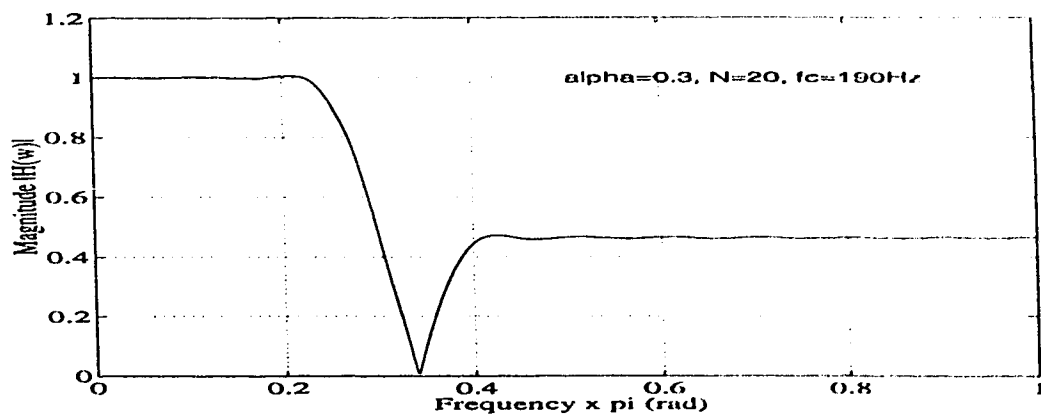
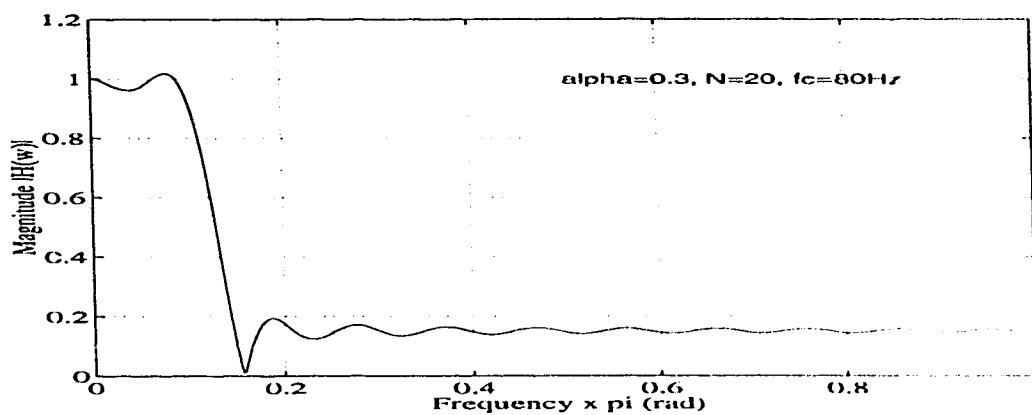
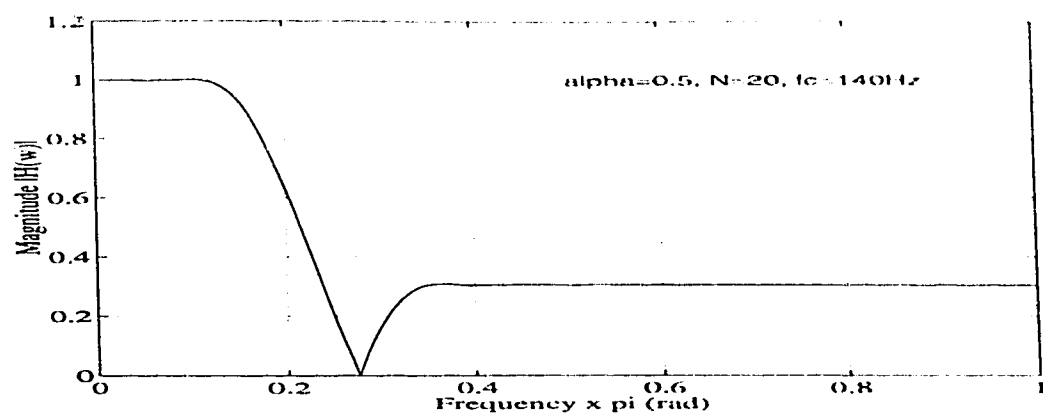


Fig. 4.21. (b) Filter response with  $h(0)=0$ .

Since the improvement factor was not significantly large, further tests were tried using least square error and curve fitting. Two sets of filter coefficients based on a least square fit were then used for estimation. The first test uses a cubic fit through three points on each side of the estimation point, while the second test uses four points on each side. The calculated values of the coefficients are:

Test I ::  $[-1/7 \ 3/14 \ 6/14 \ 0 \ 6/14 \ 3/14 \ -1/7]$

Test II ::  $[-21/172 \ 14/172 \ 39/172 \ 54/172 \ 0 \ 54/172 \ 39/172 \ 14/172 \ -21/172]$

The frequency responses of these filters are shown in Fig. 4.22a and b.

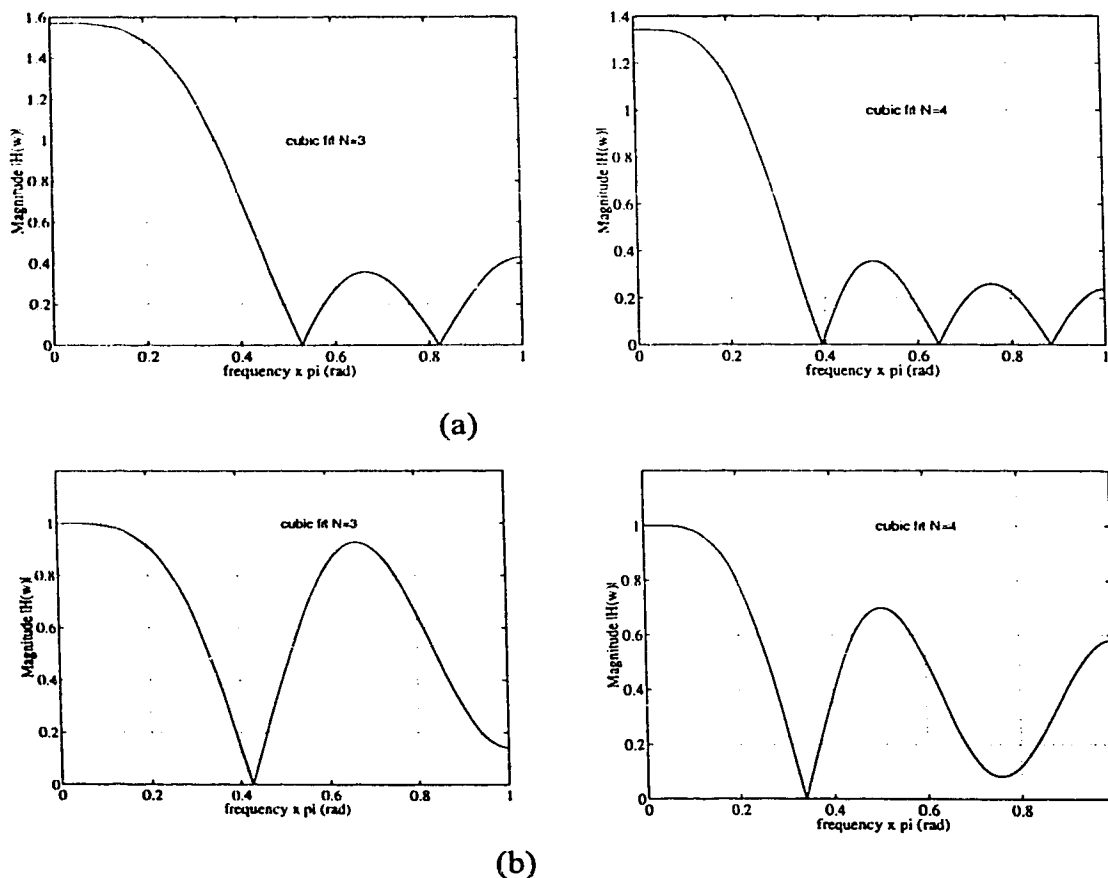


Fig. 4.22. Estimation filter design based on least square fit. (a) Filter response with  $h(0) \neq 0$ . (b) Filter response with  $h(0) = 0$ .

The improvement factor, IF, defined already is found to be about 11.8 for  $f_d = 20\text{Hz}$ , as shown in Table 4.9.

TABLE 4.9  
TEST RESULTS BASED ON LEAST SQUARE ERROR FIT.

Test	D1 errors	D2 errors	Run length	Improvement factor (IF)
I	320	27	60477	11.85
II	398	34	73441	11.705

The next experiment used coefficient values calculated using the polynomial fit approach. Again two different sets of coefficients were tested: the first set uses a cubic polynomial fit through two points on each side; the second, uses a fifth order polynomial through three points on each side. The values of the calculated coefficients are:

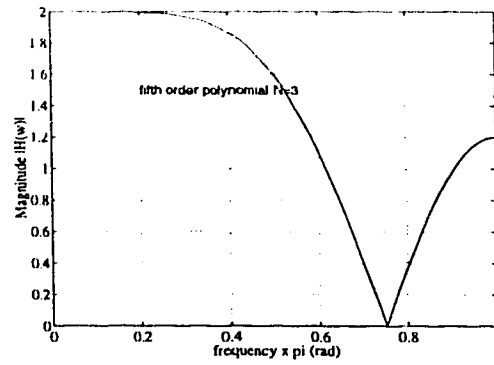
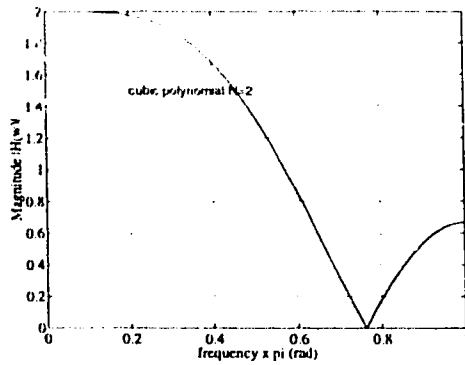
Test I :: [-1/6 2/3 0 2/3 -1/6]

Test II :: [0.05 -0.3 0.75 0 0.75 -0.3 0.05]

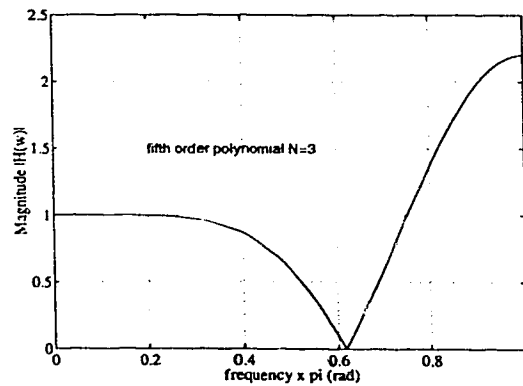
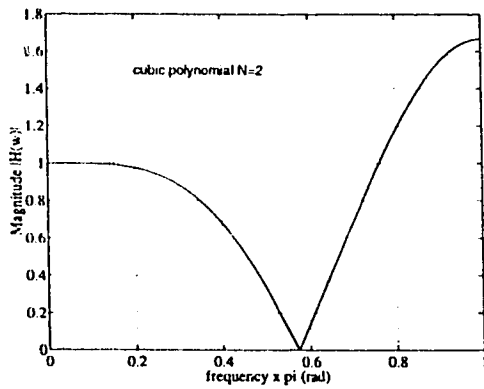
The frequency responses of these filters are shown in Fig. 4.23a and b. The improvement factor for this case is found to be only about 2.4 for  $f_d = 20\text{Hz}$ , as shown in Table 4.10.

TABLE 4.10  
TEST RESULTS BASED ON POLYNOMIAL FIT.

Test	D1 errors	D2 errors	Run length	Improvement factor (IF)
I	374	155	69478	2.419
II	321	145	61292	2.213



(a)



(b)

Fig. 4.23. Estimation filter design based on polynomial fit. (a) Filter response with  $h(0) \neq 0$ . (b) Filter response with  $h(0) = 0$ .

The spectrum of the various filters used in the above tests, together with the results can be used as a guide to improving the performance. The polynomial fit and least square fit have relatively high ( $>220\text{Hz}$ ) cut-off frequencies and high stop-band ripples. However the passband is very flat. For the least square fit both the cut-off frequency and the stopband ripple are reduced when the number of points ( $N$ ) is increased from 3 to 4. For the raised cosine filter (with  $h(0) = 0$ ), the

cut-off frequency depends on the design, but the passband has some noticeable ripple. Based on these tests, it is concluded that a filter with a very flat passband and low ripple in the stop band, with a tap length range of 20 to 30, and with an approximate cut-off of 4 times  $f_d$  may be an appropriate design.

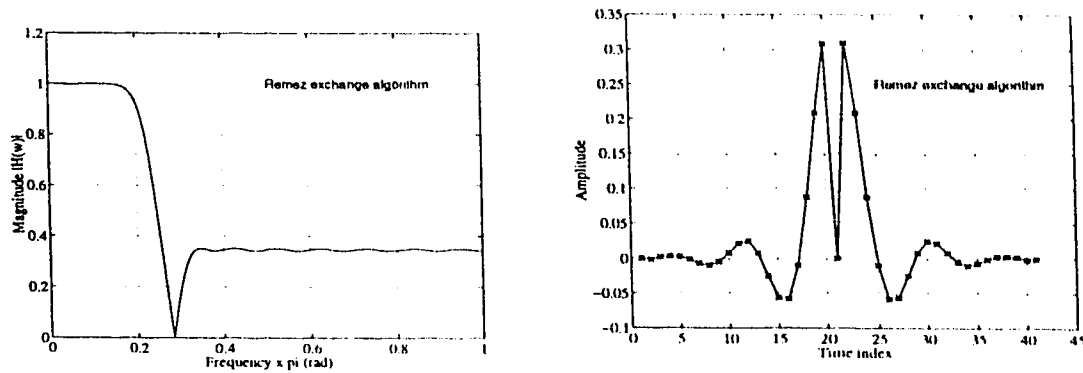


Fig. 4.24. Estimation filter design based on Remez exchange algorithm.

Therefore, a filter design based on the *Remez Exchange Algorithm* [31] is tested as an FIR filter structure with the flexibility that the passband can be made very flat by weighting the passband ripple by a large factor as compared to the stopband. The parameters chosen are:

$$fr=[0 \ 0.1333 \ 0.3333 \ 1],$$

$$mr=[1 \ 1 \ 0 \ 0],$$

$$wr=[500 \ 1],$$

$$br=remez(40,fr,mr,wr),$$

where  $fr$  defines the vector of desired frequency response with 1 corresponding to  $f_s/2$ ;  $mr$  is the vector containing the desired magnitude response at the frequencies specified in  $fr$ ;  $wr$  is the weighting factor on passband and stopband; and  $br$  is the



vector containing the tap coefficients returned by the Remez algorithm. The number "40" is the total number of taps, excluding the estimation point, (i.e.  $N=20$  in this case). The calculated coefficients were modified in order to set the middle point to zero, and to normalize the gain to unity. The magnitude response of this filter is shown in Fig. 4.24. The improvement factor is now found to be  $>250$ , as shown in Table 4.11.

TABLE 4.11  
TEST RESULTS BASED ON REMEZ EXCHANGE ALGORITHM.

$f_d$	D1 errors	D2 errors	Run length	Improvement factor (IF)
40 Hz	1508	6	61373	251.3
20 Hz	3767	10	602342	376.7

After making the error correction,  $U_p$  and  $V_p$  in the estimation filter was changed so as to remove the incorrect  $U_p$  and  $V_p$  from the right hand part of the filter, as discussed in Chapter 3. This software module when tested, shows the improvement factor increases from  $>250$  to  $>275$ , as shown in Table 4.12.

TABLE 4.12  
TEST RESULTS BASED ON REMEZ EXCHANGE ALGORITHM  
(WITH  $U_{pnew}$  AND  $V_{pnew}$ ).

$f_d$	D1 errors	D2 errors	Run length	Improvement factor (IF)
40 Hz	40904	127	6523048	322.078
20 Hz	60169	215	9652384	279.856

The estimated channel values,  $U_{pf}$  and  $V_{pf}$ , are shown in Fig. 4.25.

When the noise is added at the receiver, the estimation is expected to deteriorate because a smooth curve is difficult to fit through the sample points,

thereby degrading the improvement factor. The results for different values of SNR are presented in Chapter 5.

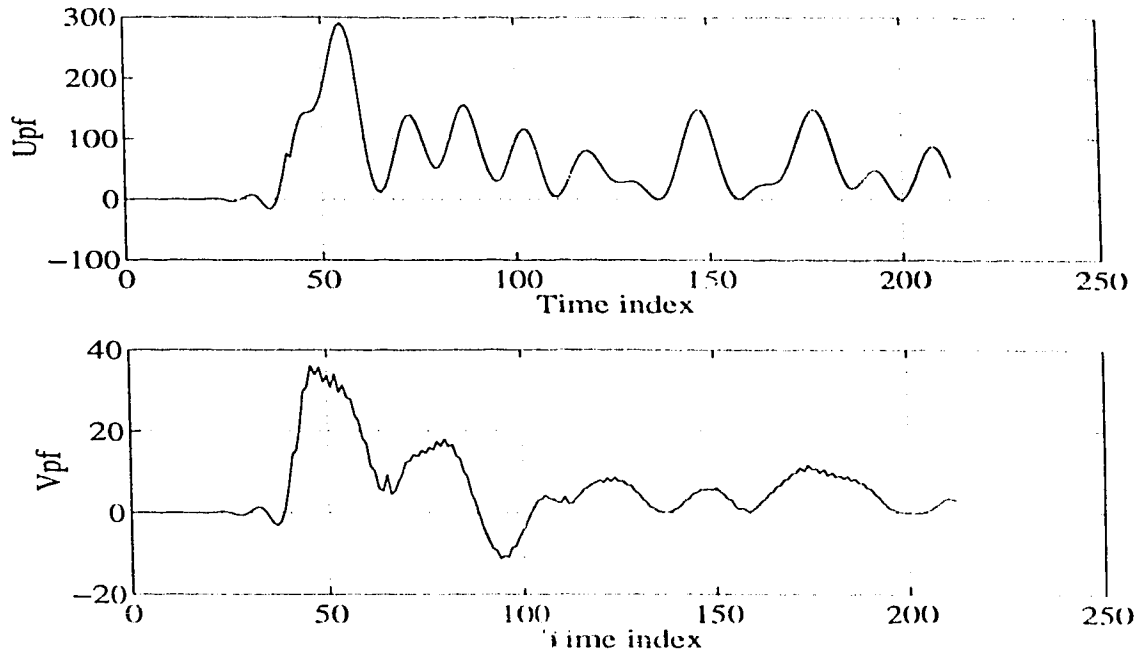


Fig. 4.25. Estimated channel (Upf and Vpf)

## 4.5 Error Measurement

The measurements of the symbol error rate (SER) and the signal to noise ratio (SNR) are used to find the performance of the error correction algorithm. The SNR measurement is discussed in Section 4.4.1. Two software SER testing modules are used, one for the differential detector output (first decision) and the other for the decision-aided detector output (second decision). The simulation is run long enough to obtain an accurate estimation of the error rate. Typically, at least 100 errors are counted to produce a 95% confidence interval, i.e. the error rate is measured within 25% of the actual BER 95% of the time [35]. The implementation of the SER tester requires two modules, as discussed in the following subsections.

#### **4.5.1 Duplicate Data Source with Delay and Storage**

To determine the SER, storage of the transmitted data information is required in order to compare it with the first and second decisions, because of the delay that exists between these decisions. The amount of delay between the transmitted data and the first decision depends on the lengths of the transmitting and receiving filters. Further, to make the second decision, additional delay exists due to the estimation filter. To store the data information, a circular buffer implementation is used. The length of this buffer depends on the delay; new data entering this buffer overwrites old data that has already been used by the comparator for the SER measurement. For implementation, since the transmitter is implemented in the C50 and the SER tester is in the C30, an additional duplicate data source was used in the C30.

#### **4.5.2 Comparators**

To measure the error rate, a simple comparison operation for equality is used between the detected data and the transmitted data. A software counter is incremented for each inequality. The total number of transmitted symbols is also counted. The overall SER for both D1 and D2 are determined using these two counter outputs.

### **4.6 Summary**

This chapter has presented the DSP implementation of the transmitter using  $\pi/4$ DQPSK modulation, the flat-fading channel, and the receiver with differential and decision-aided detection. The design and characterization of the filter responses, using Matlab<sup>®</sup> simulation, have also been presented. The performance of the implemented error correction algorithm will be discussed in the next chapter.

## 5. RESULTS

This chapter presents the test results for the performance of the decision-aided detector. First, the sampling rate, Doppler shift parameters, and fading channel spectrum etc., are described in Section 5.1. This is followed by the performance results for the decision-aided error correction algorithm for both an AWGN channel and a Rayleigh flat fading channel. The last section presents some preliminary results for the implementation and performance of Scheme II.

### 5.1 Sampling Rate, Doppler Shift and Related Parameters

The basic structure of the test setup for the detector, error correction algorithm, and BER measurement is shown in Fig. 5.1. Since the transmitter and the fading channel are both implemented in the same DSP, the rate at which data can be generated is affected by the instruction cycles required for the generation of the fading sample. The 150 instruction cycles for data and 350 instruction cycles for the fading sample requires 25 $\mu$ sec., limiting the maximum sample rate to 40 ksamples/sec for the C50, which has an instruction cycle time of 50ns. Since the exact length of the various filters and the software implementation structure were not known initially, and to enable a flexible software architecture, the sample generation rate for the testing was limited to 9.6ksamples/sec; with an oversampling factor of 8 the data symbol rate is thus chosen to be 1.2ks/sec.

The error rate due to fading depends on the ratio of the Doppler shift frequency and to the symbol rate. For a mobile unit moving at 100km/hr and for a 900 MHz carrier frequency, the Doppler frequency will be 83.3 Hz. Therefore, for simulation of the IS54 system, which has a symbol rate of 24.3ks/sec and carrier frequency of 900 MHz, the ratio of Doppler shift to symbol rate needs to be  $\cong 0.003$ .

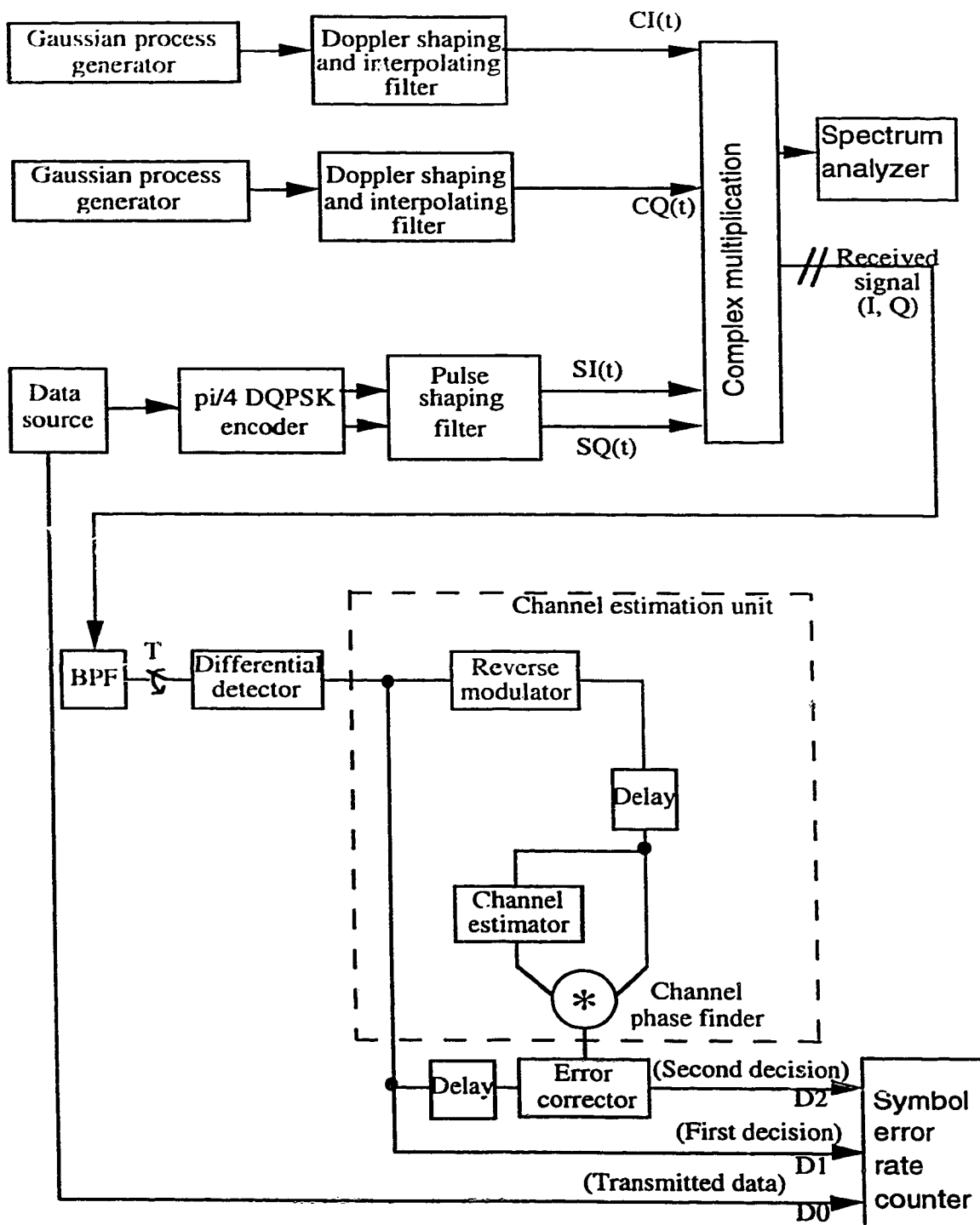


Fig. 5.1. Test setup for decision-aided detector.

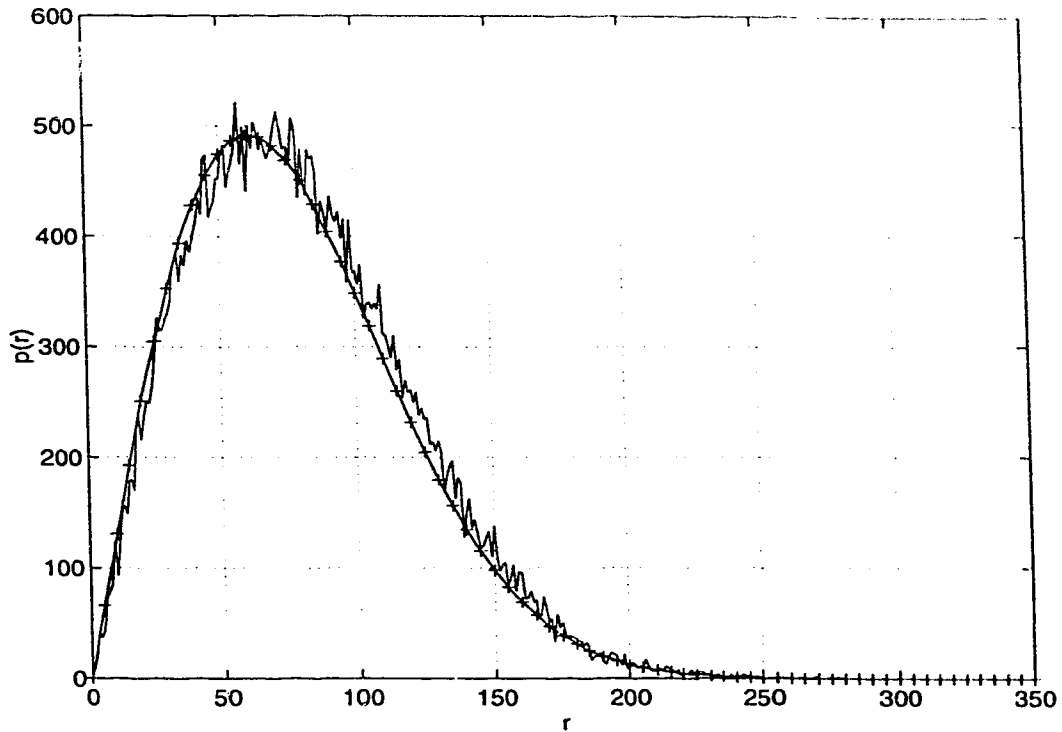


Fig. 5.2. PDF of envelope of the fading channel (from theory and simulation).

For a symbol rate of 1.2ks/s, this would require a Doppler frequency  $f_d \approx 4\text{Hz}$ . Generating a slowly fading sample (as compared to the data rate) is limited by the implemented test-setup, since simulation of slow fading requires very long FIR filters. Therefore, the algorithm is tested with relatively faster fading,  $f_d T = 0.016$  and  $0.033$ , corresponding to 20Hz and 40Hz Doppler shift values respectively; the filters for these Doppler shifts are not too long (up to 350 tap coefficients). These  $f_d$  rates are used to test the performance of the error correction algorithm; apart from their practicability they have the added advantage that the primary D1 error rate is higher, so that the test run-times do not have to be as long. The error correction process, in principle, does not depend on the fading rate and symbol period. The implementation of the error correction algorithm requires  $\approx 167$  instructions/symbol; thus for the TMS320C30 DSP at

60ns/instruction, only 10 $\mu$ s/symbol are needed. This would allow the error correction method to be implemented for symbol rates up to 100ks/sec.

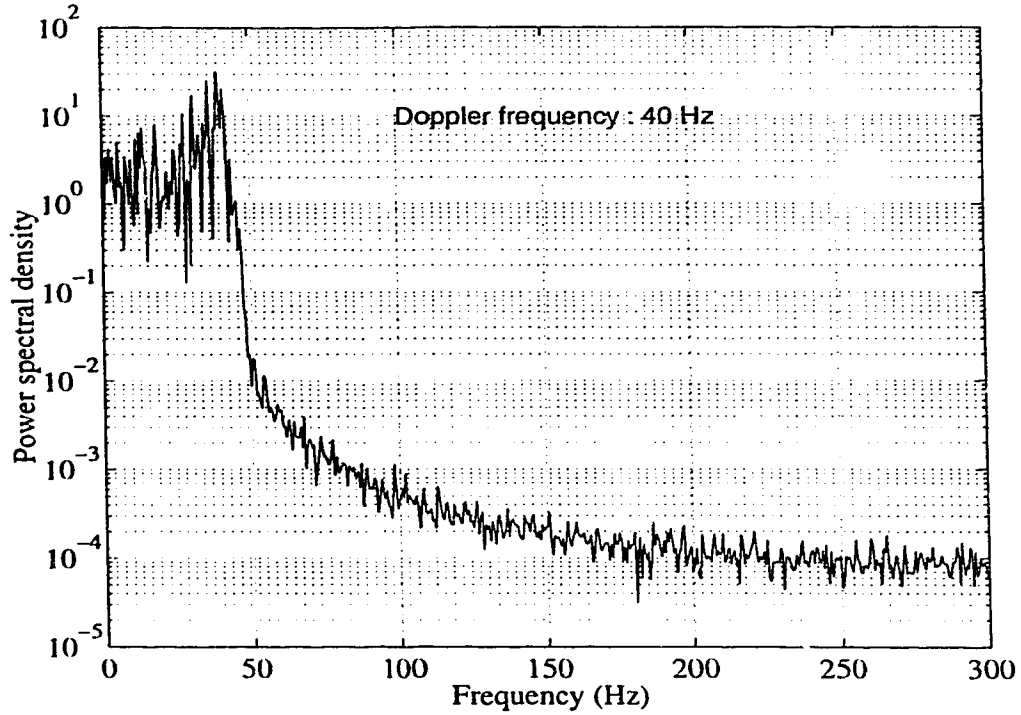


Fig. 5.3. Relative power spectrum of fading signal (Doppler frequency =40Hz).

Two important parameters for the simulation of the fading channel are the probability density function (pdf) and the frequency content. If the simulation results are to be valid, these two parameters should closely follow the theoretical and measured quantities. For the simulated channel in this work, the pdf is shown in Fig. 5.2 and the power spectrum for Doppler shift frequencies ( $f_d$ ) equal to 40Hz and 20Hz is shown in Fig. 5.3 and Fig. 5.4 respectively. The total time period of observation in the DSP is approximately 10min. (i.e. @600 symbols/sec number of symbols =360,000). The spectrum observed using the spectrum analyzer closely follows the expected Doppler spectrum obtained with an isotropic antenna, with a peak at  $f_d$  and with very little power at higher

frequencies (Refer Eq. (2-12) ). The waveforms shown in the figures are obtained using Matlab<sup>®</sup>, because of the difficulty of obtaining a printout from the spectrum analyzer.

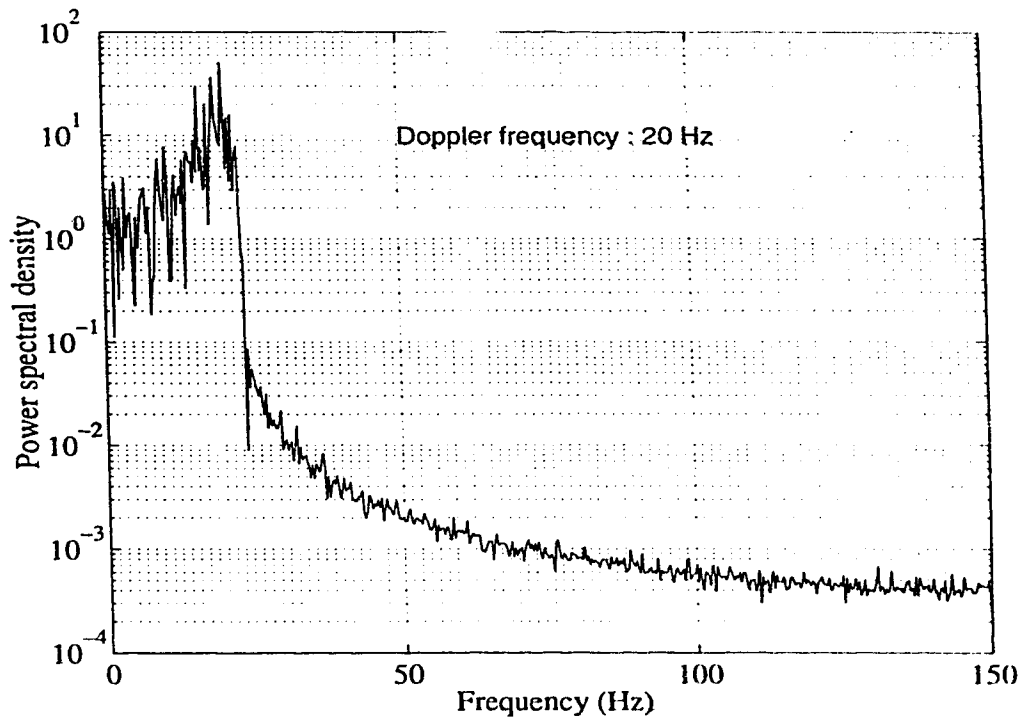


Fig. 5.4. Relative power spectrum of fading signal (Doppler frequency =20Hz).

## 5.2 Performance of Decision-aided Detector

The symbol error rate for both differential detection and decision-aided detection are obtained, and then compared to demonstrate the performance improvement quantitatively. As described earlier, the symbol error rate is measured for different signal to noise ratios.

### 5.2.1 AWGN Channel

Fig. 5.5 shows the system performance for both D1 and D2 in an AWGN channel. The performance for D1 (the differential detector) is good ( $BER < 10^{-5}$ ) for high values of SNR, but degrades at low SNR as the effect of the noise becomes significant; for this case there is no observable error floor. For a target



BER of  $10^{-3}$ , the SNR must be about 12dB or greater. As can be seen, the error rate for the decision-aided detector (D2) is no better than the differential detector output (D1); in fact, there is a 2dB degradation in performance. This is because, for an AWGN channel, when the channel estimation filter in the decision-aided detector tries to estimate the noisy channel, it fails because the noise is inherently random. In fact, the channel estimation filter smooths out the noise thus giving a very poor estimate for each individual point. Thus, for an AWGN channel, the first decision at the output of differential detector, is the better choice. However, the primary cause of error in cellular communication is the effect of the fading channel. Hence, the performance of the decision-aided error correction algorithm under Rayleigh fading conditions is more significant. This is presented next.

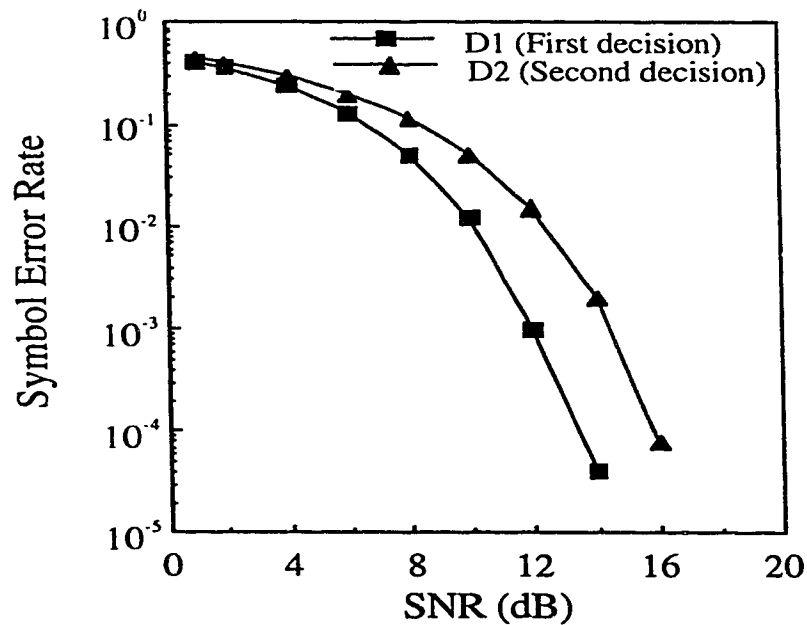


Fig. 5.5. SER performance for  $\pi/4$ DQPSK in an AWGN channel.

### 5.2.2 Fading Channel and AWGN, $f_d=40\text{Hz}$

Fig. 5.6 shows the error rates D1 and D2 for a channel with fast Rayleigh flat-fading and AWGN. The result at the output of the differential detector (D1) shows the significant degradation in system performance that occurs due to the phase shifts caused by fast fading. For all values of SNR, the system performance is considerably worse than the result for AWGN only. More importantly, the error performance shows an irreducible error floor; that is, the SER falls as the SNR is increased but then, above a certain SNR value, the SER becomes constant. The signal power can be increased, but there is no improvement in performance. This is due to the random FM effect of the fading channel. The actual error floor value depends on the value of the Doppler frequency. For  $f_dT=0.0333$ , ( $f_d=40\text{Hz}$ ) the error floor occurs at a SNR of 30dB, with a symbol error rate of  $2.4 \times 10^{-2}$ . Thus, due to random FM, the system can not meet a target BER of  $10^{-3}$ , no matter how high the signal power. These results show clearly that fading severely affects the performance of the  $\pi/4\text{DQPSK}$  modulation system. A similar result would be obtained for other phase shift modulation schemes.

The error rate (D2) at the output of the decision-aided detector, for the Rayleigh flat fading channel with  $f_dT=0.033$ , shows that the error rate falls to below  $10^{-4}$  before the onset of the error floor. Fig. 5.6 clearly shows the improvement in error rate that has been achieved by the error correction scheme, provided that the SNR is sufficiently high. The error floor is observed to be reduced from  $2.4 \times 10^{-2}$  to  $7.6 \times 10^{-5}$ , a reduction in error rate of about 300.

### 5.2.3 Fading Channel and AWGN, $f_d=20\text{Hz}$

Fig. 5.7 shows the system performance in a fast Rayleigh flat-fading channel, for  $f_d T=0.0166$  ( $f_d=20\text{Hz}$ ). The results are similar to those for  $f_d=40\text{Hz}$ . The error rate floor is reduced from  $5.4 \times 10^{-3}$  to  $1.5 \times 10^{-5}$ , which is again an improvement of about 300 in the SER, after execution of the error correction algorithm. As for the previous case ( $f_d=40\text{Hz}$ ), a SNR of 60 dB is required to obtain the greatest error improvement.

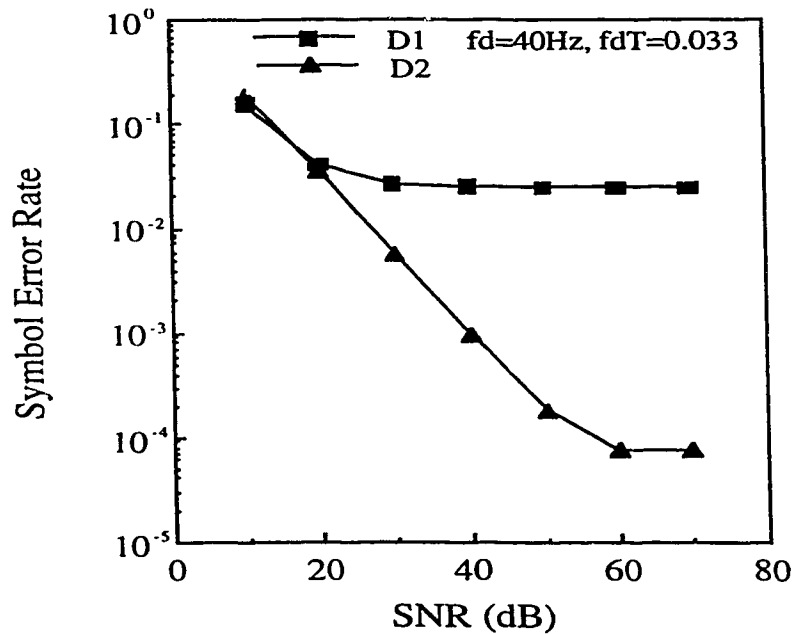


Fig. 5.6. SER performance of decision-aided detector for flat fading channel ( $f_d=40\text{Hz}$ ).

These performance curves (Fig. 5.6 and Fig. 5.7) also show that, at the lower SNR values, when the noise power dominates, the error correction algorithm fails to show any improvement. The main reason for this poor performance is the random characteristic of the noise, which cannot be estimated by the channel estimation filter (same behavior as for the case of a pure AWGN channel). An added factor is the noise multiplication in the differential detector,

which causes a fairly rapid deterioration in the quality of the recovered channel at low SNR values. Thus, the error correction works only when the D1 errors are due to the random slow channel phase modulation, not when the errors are due to Gaussian noise.

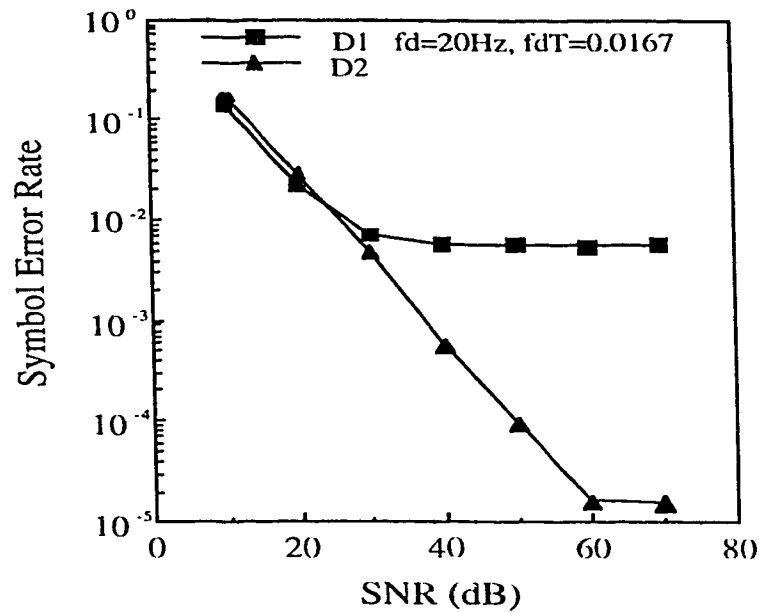


Fig. 5.7. SER performance of decision-aided detector for flat fading channel ( $f_d=20\text{Hz}$ ).

### 5.3 Scheme II

As discussed in Chapter 3, the extracted channel waveform shows clear discontinuities at the points where the first decisions are incorrect. One method of locating and removing these discontinuities, and hence also correcting the errors is to calculate the derivatives of the extracted channel waveforms (Ich and Qch). Fig. 5.8a shows a typical recovered channel waveform in the vicinity of an error. The channel is smooth on either side of the error and hence the derivatives do not change very quickly in these regions. There is an abrupt discontinuity however at the point of error. In Fig. 5.8a, the most obvious discontinuity is in the slope, but

the higher derivatives are also affected. Calculating the derivatives of the waveform (both I and Q) therefore provides one means of locating the error.

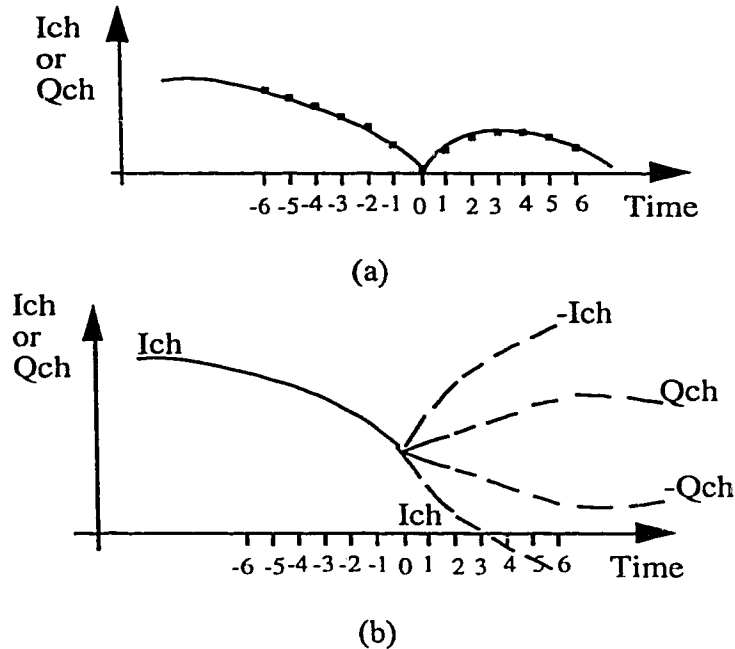


Fig. 5.8. Scheme II channel smoothing. (a) Recovered channel. (b) Actual channel possibilities.

It has been shown earlier that, whenever an error occurs, the channel waveform (Ich, Qch) suffers a phase shift that is a multiple of  $90^\circ$ . Thus, as the channel is reconstructed from the D1 decisions, there are, at each point, four possibilities; the channel may be recovered correctly, but there are three possibilities for making an error that involve the interchange of I and Q, and/or a change of sign. These four possibilities are illustrated in Fig. 5.8b. For correction of the errors the derivatives for the past channel values (the left side points in Fig. 5.8b) must be compared with the four possibilities for the derivatives based on the future (right side) values.

In this work, the derivatives have been calculated based on a least square cubic polynomial fit through 7 points. The derivatives at point 0 in Fig. 5.8 have

been calculated using a cubic polynomial fitted to the points -6 to 0, giving a “forward prediction” of the derivatives, and also the point 0 to +6 giving a “backward prediction”. The numerical values of the derivatives can be estimated using FIR filters with the coefficient values:

```
af_coeff = [1/36 -1/36 -1/36 0 1/36 1/36 -1/36]
bf_coeff = [-23/84 1/3 25/84 -4/84 -31/84 -1/3 33/84]
cf_coeff = [97/126 -269/252 -103/126 8/21 25/18 269/252 -31/18]
df_coeff = [-4/7 6/7 4/7 -3/7 -8/7 -4/7 16/7]
ar_coeff = [0 0 0 0 0 0 0 -1/36 1/36 1/36 0 -1/36 -1/36 1/36]
br_coeff = [0 0 0 0 0 0 0 33/84 -1/3 -31/84 -4/84 25/84 1/3 -23/84]
cr_coeff = [0 0 0 0 0 0 0 -31/18 269/252 25/18 8/21 -103/126 -269/252 97/126]
dr_coeff = [0 0 0 0 0 0 0 16/7 -4/7 -8/7 -3/7 4/7 6/7 -4/7]
```

where “af” gives the forward third derivative, “bf” gives the forward second derivative, etc., and “ar, br, cr, dr” are the reverse estimates.

For the recovered channel waveform of Fig. 3.9, the values of the forward and reverse third derivatives, “af” and “ar”, are shown in Fig. 5.9. To combine the derivative information into one parameter, the difference of these two values can be taken and squared. Thus for Ich

$$a_I = (af - ar)^2 \quad (5-1)$$

and for Qch,  $a_Q = (af - ar)^2$  . (5-2)

Using  $a_I$  and  $a_Q$ , the error zones show up very distinctly as shown in Fig. 5.10. To combine the I and Q channel results, these values may be added and squared. Thus, the final test parameter for location of the errors is

$$Err\_ch = (a_I + a_Q)^2 \quad (5-3)$$

This is plotted in Fig. 5.11. As can be seen, the value of “Err\_ch” is normally very small but has distinct peaks whenever the channel is in error.

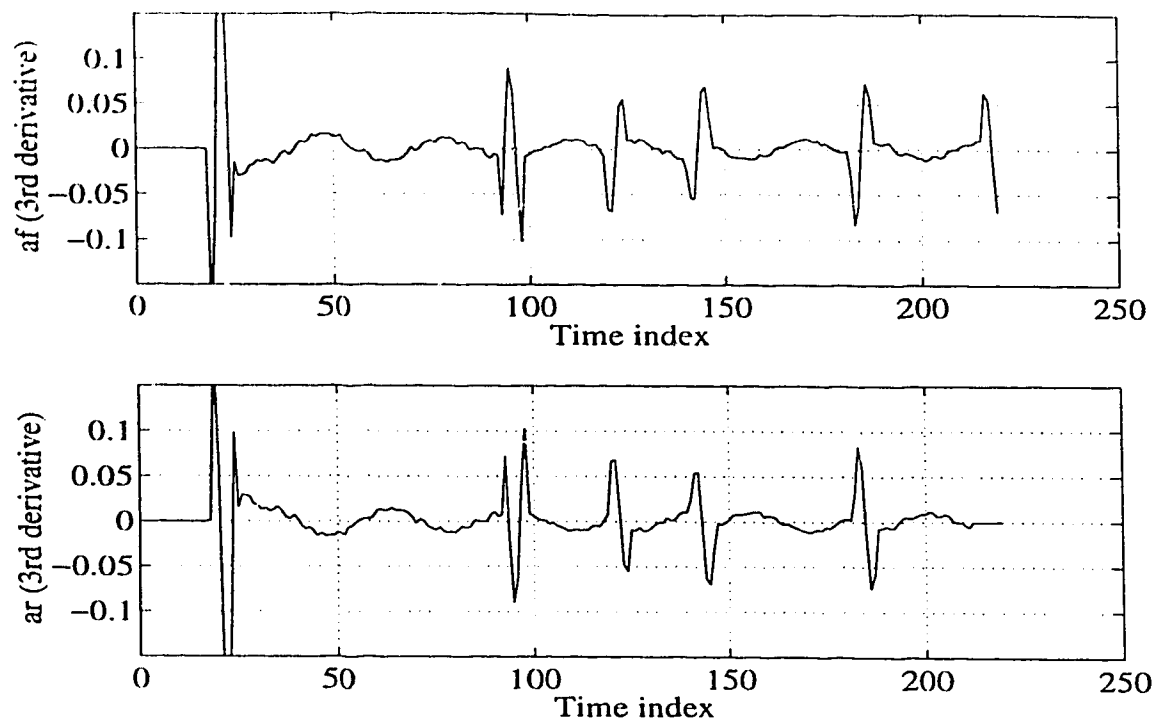


Fig. 5.9. Error zone detection using af, ar.

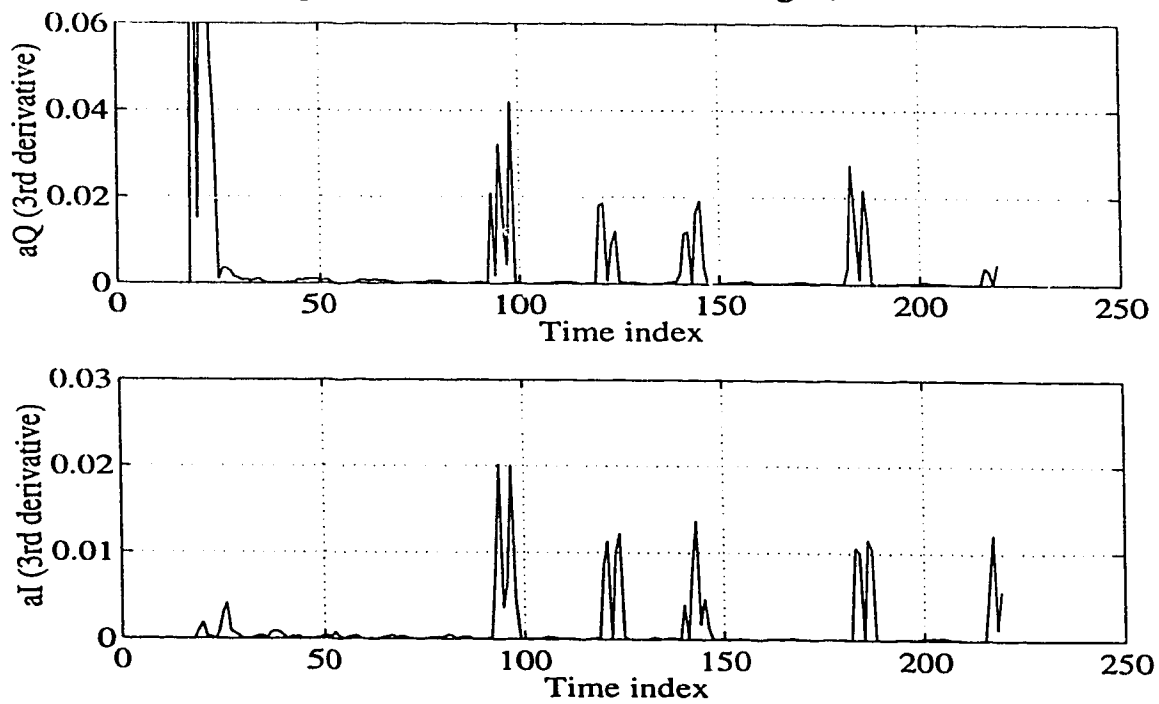


Fig. 5.10. Error zone detection using  $a_i$ ,  $a_Q$

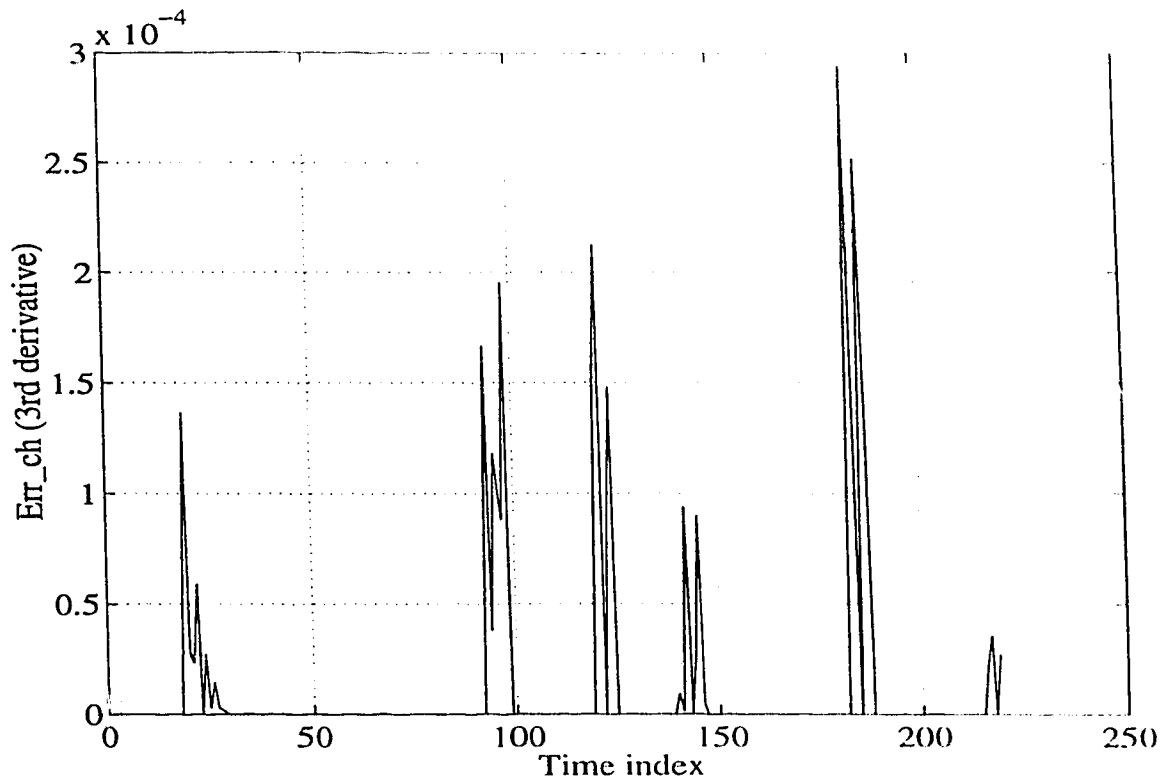


Fig. 5.11. Error zone detection using Err\_ch.

The errors for the test shown in Fig. 5.9 are located at symbol points [87, 113, 114, 134, 135, 176]. The detected error zones, using the third derivatives “af and ar”, appears as pronounced peaks. Comparing the value of “Err\_ch” with a fixed threshold value, the error zones are determined as [85 to 90, 112 to 116, 134 to 137, and 175 to 179]. Various tests show that although the error point is in the error zone, its exact position cannot be determined. Because of this every point within the error zone must be considered as a possible error location.

The simplest approach to smoothing the channel, and hence correcting the errors, is to consider the points within the error zone, sequentially one point at a time. The four possible channel (Ich, Qch) interchanges corresponding to no shift, 90°, 180° and 270° shift are tested at each candidate point. A choice is made,



based upon the derivatives, corresponding to the minimum discontinuity in the new channel. Based on this new channel, a corresponding new decision is made for the data. Fig. 5.12 and 5.13 shows the straightening of the channel and the consequent elimination of peaks from the smoothed channel.

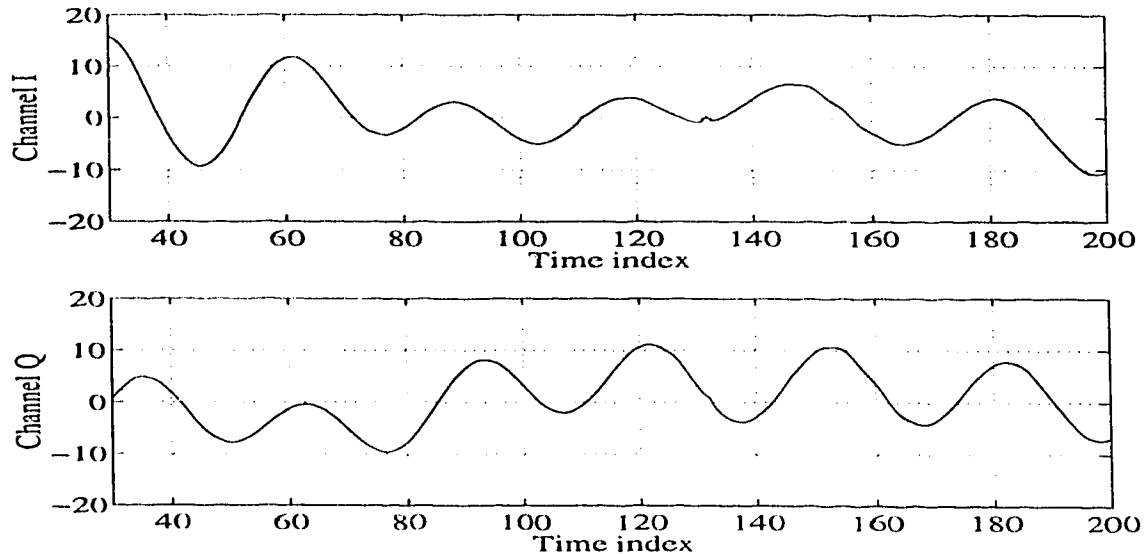


Fig. 5.12. Smooth channel using derivatives.

All the D1 errors have been removed except the double errors at 134, 135. Since some errors can be corrected, it appears that smoothing of the recovered channel may be a viable approach to the error correction problem. However, some problems encountered by this approach are:

- In testing the derivatives and choosing the minimum possible channel discontinuity, a change to the recovered channel may be indicated even though the actual discontinuity is at a neighbouring point. This results in the introduction of an additional error, rather than the removal of the actual error.
- Detection of the error peaks is sensitive to the range of points and to the chosen threshold value.

- Due to noise and ISI, the recovered channel is not always smooth, resulting in further deterioration as the choice of the new I and Q channel values becomes more prone to error.

Thus, it appears that a point-by-point approach may not be satisfactory. Other algorithms, more complex than that used in scheme I, may need to be investigated.

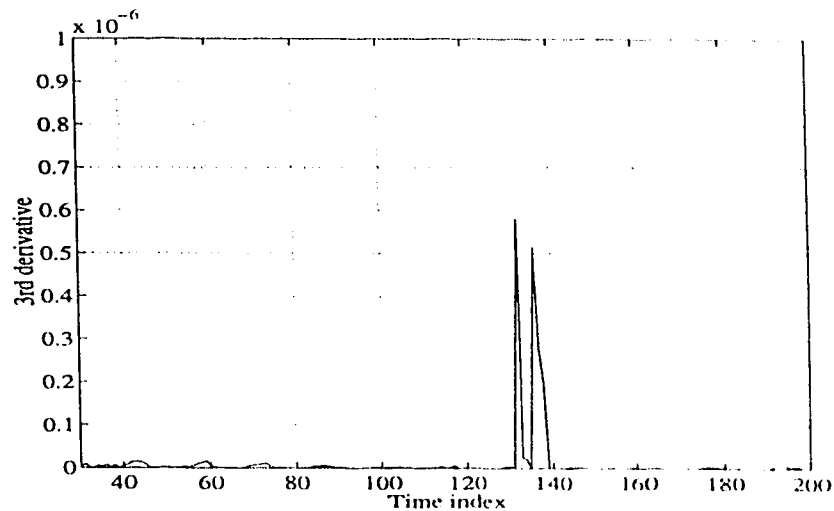


Fig. 5.13. Scheme II smooth channel peak detection.

## 5.4 Summary

The potential of a decision-aided error correction algorithm to improve the performance of cellular systems based on  $\pi/4$ DQPSK modulation is demonstrated by tests carried out in real time using digital signal processors. A simple method of error correction (Scheme I) works well when the SNR value is high. It lowers the error floor, obtained at the output of conventional differential detector, by a factor of more than 200. The proposed scheme II, which is intended to give better results for the lower range of SNR values, has been shown to be useful for detecting the presence of errors, but more investigation is needed to determine a suitable error correction algorithm.

## 6. SUMMARY AND CONCLUSIONS

A phase modulated signal, such as  $\pi/4$ DQPSK, is severely distorted by the short term fading arising from multipath propagation in the radio channel. The fading causes large variations in the amplitude of the received signal, but more importantly causes random phase modulation. These random phase variations appear as noise to the detector, resulting in a performance degradation for the conventional differential detector. The detection error can be reduced to a certain extent by increasing the signal power; however, beyond a certain level any further increase in the signal power fails to reduce the error rate, so that the BER versus SNR characteristic exhibits an irreducible error floor. This necessitates a method to mitigate the effect of the fading and random FM so as to reduce the error rate at the output of the detector.

Diversity reception, signal coding and pilot symbol insertion are known to be effective techniques for combating the undesired effect of fast random fades and the resulting random phase modulation. These methods, however, suffer from one or more drawbacks such as a bandwidth penalty, implementation complexity, and/or a power overhead. In this project, a decision-aided error correction algorithm for a  $\pi/4$ DQPSK modulated signal, based on the information data alone, has been investigated and implemented. This method achieves simple and practicable detection using a DSP, which requires only a small amount of memory, little computational power, and does not require any change in the signal format at the transmitting end. The latter is an attractive feature for systems with an already standardized transmitting format. The decision-aided detector consists of a reverse modulation unit, a channel estimation unit and an error correction unit, in addition to the normal differential detector. The complete error correction

algorithm has been implemented in a TMS320C30 DSP, using an IBM-compatible PC-based assembler and debugger.

In order to evaluate the performance of the decision-aided detector, a simplified structure for the transmitter and fading channel has been implemented using a TMS320C50 DSP. The complex baseband equivalent of the received signal is obtained digitally by multiplying the transmitted signal and the fading channel characteristic. A custom designed printed circuit board (PCB) with buffer and control circuitry is used to interface the two DSPs for parallel transfer of this signal. An additive white Gaussian noise (AWGN) source at the receiver input has been simulated in the C30, whose power output is software controlled .

The implemented transmitter has three building blocks: the data source, the  $\pi/4$ DQPSK encoder and the pulse shaping filter. The flat fading channel is also implemented with three components: the Gaussian noise source, the Doppler shift filter and the interpolation filter. A multirate filtering technique is used to have the flexibility to change the Doppler frequency. At the receiver, the bandpass filter and the decision-aided detector are the two major modules. A second data generator and the symbol error counter are also implemented in the C30, to obtain the algorithm performance results. The test results for the transmitter output show that the spectral content is as specified by the IS54 standard. Test results for the envelope of the fading channel signal show that the pdf closely follows the Rayleigh probability density function. The power spectrum characteristics of the fading channel for the Doppler frequencies of 40Hz and 20Hz were tested for accuracy using a spectrum analyzer.

The decision-aided error correction algorithm is tested for symbol error rate for different signal to noise ratios (SNR) and its performance is compared to

that of the conventional differential detector. The test results shows that the irreducible error floor at the output of decision-aided detector is reduced by a factor of more than 200 compared to that of the differential detector. The actual irreducible error rate depends on the product of Doppler frequency and symbol period ( $f_d T$ ). For  $f_d T = 0.033$ , the error floor is reduced from  $2.4 \times 10^{-3}$  to  $7.6 \times 10^{-5}$ . A second test using  $f_d T = 0.0166$ , gives a differential detector output symbol rate of  $5.4 \times 10^{-3}$ , which reduces to  $1.5 \times 10^{-5}$  after execution of the decision-aided algorithm.

The test results show that the decision-aided algorithm has good error correction performance; this is achieved without any significant overhead or complexity. The error correction performance depends significantly on the transfer function of the channel estimation filter. Conceptually the design of the filter is based on the fact that the fading is a narrowband process with a bandwidth of two times the maximum Doppler shift frequency. However, various tests using different estimation filters show that the performance is sensitive not only to the nominal cut-off frequency, but also to the filter length (number of taps) and the pass-band and stop-band ripple. The tests found that the major requirements of the filter for improved performance are a very flat passband, a narrow transition band, and an impulse response with tap coefficients that decrease smoothly to zero at the filter ends. The channel estimation process deteriorates, and consequently the error correction performance also deteriorates, at low signal-to-noise ratio values. The test results for the performance evaluation are limited to two  $f_d T$  values because both the fading channel and the transmitter model are implemented in a single DSP. Since the fading process is slow compared to transmitted signal rate, a large number of instruction cycles are required to generate one fading sample.

The slower the fading compared to the sampling rate, the longer is the filter length (or number of instruction cycles) required by the Doppler shift and interpolating filters. The implementation of the error correction algorithm requires  $\approx 167$  instruction cycles/symbol; i.e., for the TMS320C30 DSP with an instruction cycle time of  $\approx 60\text{ns}$ , it takes only  $10.02\mu\text{s/symbol}$ . Thus, the algorithm is easy to use, with a maximum possible symbol rate of  $\approx 100\text{ks/s}$ .

The final error tests also show that the error correction algorithm has good performance at high SNR values, but degrades as the noise becomes more dominant. This is a limitation of the algorithm. To improve the performance at low SNR values, Scheme II was investigated. The motivation here was to apply the decision-aided channel recovery directly to the received signal components rather than to the differential detector output, which suffers from the adverse effect of noise multiplication. Implementation of Scheme II has been only partially successful. It has been shown that the error zone can be detected within 4-6 symbols, but the exact position of an error is difficult to determine. For this reason the errors are hard to correct without a computationally intensive and sophisticated algorithm.

A number of ideas for further research to explore decision-aided detection are:

- ◆ Since the performance of the decision-aided error correction algorithm could be tested for only a few  $f_d T$  values in the present hardware setup, it would be interesting to change the hardware setup so as to use one separate DSP for the fading channel, in order to test the scheme for lower  $f_d T$  values. Although lowering the  $f_d T$  value from  $f_d = 40\text{Hz}$  to  $f_d = 20\text{Hz}$  produced a lowering of the error floor, smaller  $f_d T$  values may not give even better results because, with

very slow fading, burst errors may occur during the fades, which may be hard to correct.

- ◆ In this thesis, the decision-aided detector has been tested only for a flat fading channel. The performance of the detector should be investigated further for the case of a frequency selective fading channel.
- ✿ The second method (as discussed in Chapter 3 and 5) tested in this thesis locates the approximate position of an error, but an efficient error correction algorithm still needs to be determined. This needs to be explored as it may lead to improved performance under low SNR conditions.
- ◆ Decision-aided detection could also be tested in combination with other schemes such as diversity and equalization, since this may lead to a further improvement in the BER performance.
- ◆ In this work, the channel estimation filter is designed for  $f_d = 40\text{Hz}$ , and then the coefficients are kept constant. An adaptive algorithm should be investigated that will estimate a suitable set of tap coefficients in real time. This may be particularly suitable for systems where only slow fading is encountered.

## REFERENCES

- [1] D. M. Balston and R. C. V. Macario, *Cellular radio systems*. London: Artech House, 1993.
- [2] J. E. Padgett, C. G. Gunther, and T. Hattori, "Overview of wireless personal communications," *IEEE Commun. Mag.*, vol. 33, no. 1, pp. 28-41, Jan. 1995.
- [3] D. C. Cox, "Wireless personal communications: What is it?," *IEEE Personal Commun.*, vol. 2, no. 2, pp. 20-35, Apr. 1995.
- [4] V. Fung and T. S. Rappaport, "Bit-error simulation of  $\pi/4$ DQPSK in flat and frequency selective fading mobile radio channels with real time applications," *Proc. IEEE Int. Conf. on Commun.*, Denver, Co, pp. 553-557, June 1991.
- [5] EIA/TIA Interim Standard, "Cellular System Dual-Mode Station - Mobile Station-Base Station Compatibility Standard," IS-54, *Electronic Industries Association*, May 1990.
- [6] P. S. Mundra, T. L. Singal and R. Kapur, "The choice of a digital modulation scheme in a mobile radio system," *Proc. IEEE Veh. Technol. Conf.*, Secaucus, NJ, pp. 1-4, May 1993.
- [7] J. B. Andersen, T. S. Rappaport, and S. Yoshida, "Propagation measurements and models for wireless communications channels," *IEEE Commun. Mag.*, vol. COM-33, no. 1, pp. 42-49, Jan. 1995.
- [8] L. W. Couch II, *Digital and analog communication systems*. New York: Macmillan, Second edition, 1987.
- [9] S. Stein, "Fading channel issues in system engineering," *IEEE J. Select. Areas Commun.*, vol. SAC-5, no. 2, pp. 68-88, Feb. 1987.
- [10] H. Leib, "Data-aided noncoherent demodulation of DPSK," *IEEE Trans. Commun.*, vol. COM-43, no. 2/3/4, pp. 722-725, Feb./Mar./Apr. 1995.



- [11] A. Svensson, "Coherent detector based on linear prediction and decision feedback for DQPSK," *Electron. Lett.*, vol. 30, no. 20, pp. 1641-1642, Sep. 1994.
- [12] M. Li, A. Bateman, and J. P. McGeehan, "Decision feedback channel estimation - A precursor for adaptive data transmission management," *Proc. IEEE 41st Veh. Technol. Conf.*, pp. 730-734, St. Louis, Mo, May 1991.
- [13] Unpublished work by C G. Englefield at *Bristol University*, U.K., 1990
- [14] S. Chennakeshu and G. J. Saulnier, "Differential detection of  $\pi/4$ -shifted DQPSK for digital cellular radio," *Proc. IEEE 41st Veh. Technol. Conf.*, pp. 186-191, St. Louis, Mo, May 1991.
- [15] J. D. Parsons, *The mobile radio propagation channel*. New York: John Wiley, 1992.
- [16] T. Aulin, "A modified model for the fading signal at a mobile radio channel," *IEEE Trans.*, VT-28, no. 3, pp. 182-203, 1979.
- [17] E. A. Lee and D. G. Messerschmitt, *Digital communication*. London: Kluwer Academic, Second edition, 1994.
- [18] W. C. Jakes Jr., *Microwave mobile communications*. New York: John Wiley, 1974.
- [19] John G. Proakis, *Digital communications*. New York: McGraw-Hill, Third edition, 1995.
- [20] William C. Y. Lee, *Mobile communication engineering*. New York: McGraw-Hill, 1982.
- [21] K. Feher, "Modems for emerging digital cellular mobile radio system," *IEEE Trans. Veh. Technol.*, vol. VT-40, no. 2, pp. 355-365, May 1991.
- [22] C. L. Lui and K. Feher, "Noncoherent detection of  $\pi/4$ -QPSK systems in a CCI-AWGN combined interference environment," *IEEE Veh. Technol. Conf.*, San Francisco, CA, vol. VT-39, pp. 83-93, 1989.

- [23] S. Sampei and T. Sunaga, "Rayleigh fading compensation method for 16QAM in digital land mobile radio channels," *Proc. IEEE Veh. Technol. Conf.*, San Francisco, CA, vol. VT-39, pp. 640-646, May 1989.
- [24] J. K. Cavers, "An analysis of pilot symbol assisted modulation for Rayleigh fading channels," *IEEE Trans. Veh. Technol.*, vol. VT-40, no. 4, pp. 686-693, Nov. 1991.
- [25] J. K. Cavers, "Performance of tone calibration with frequency offset and imperfect filter," *IEEE Trans. Veh. Technol.*, vol. VT-40, no. 2, pp. 426-434, May 1991.
- [26] A. Bateman, "Feedforward transparent tone-in-band: its implementations and applications," *IEEE Trans. Veh. Technol.*, vol. VT-39, no. 3, pp. 235-243, Aug. 1990.
- [27] E. R. Berlekamp, R. E. Peile, and S. P. Pope, "The application of error control to communications," *IEEE Commun. Mag.*, vol. 25, no. 4, pp. 44-56, Apr., 1987.
- [28] J. D. Parsons, J. H. Henze, P. A. Ratliff, and M. J. Withers, "*Diversity techniques for mobile radio reception*," *IEEE Trans. Veh. Technol.*, vol. VT-25, no. 3, pp. 75-84, Aug. 1976.
- [29] A. Bateman and W. Yates, *Digital Signal Processing Design*. New York: Computer Science Press, 1989.
- [30] C. F. Gerald and P. O. Wheatley, *Applied numerical analysis*. New York: Addison-Wesley, Fourth edition, 1989.
- [31] A. V. Oppenheim and R. W. Schaffer, *Digital signal processing*. New Jersey: Prentice-Hall, 1975.
- [32] *TMS320C5x user's guide*, Texas Instruments, 1994.
- [33] *TMS320C5x DSP starter kit user's guide*, Texas Instruments, 1994.
- [34] V. N. Yarmolik and S. N. Demidenko, *Generation and application of pseudorandom sequences for random testing*. New York: John Wiley, 1988.

- [35] M. C. Jeruchim, P. Balaban and K. S. Shanmugan, *Simulation of communication systems*. New York: Plenum Press, 1992.
- [36] L. B. Jackson, *Digital filters and signal processing*. London: Kluwer Academic, 1989.
- [37] J. A. Mitchell, "Multirate filters alter sampling rates even after you've captured the data," EDN, Aug. 1992.
- [38] B. Stroustrup, *The C++ programming language*. New York: Addison Wesley, Second edition, 1993.
- [39] R. A. Goubran, H. M. Hafez, and A. U. H. Sheikh, "Implementation of a real-time mobile channel simulator using a DSP chip," *IEEE Trans. Ins. Measure.*, vol. IM-40, no. 4, pp. 709-714, Aug. 1991.
- [40] *TMS320 floating point DSP assembly language tools user's guide*, Texas Instruments, 1993.
- [41] *TMS320C3x user's guide*, Texas Instruments, 1990.
- [42] *Theory, algorithms, and implementation*, vol. 2, Texas Instruments, 1990.

## APPENDIX A.

PCB FOR INTERFACE BETWEEN TEXAS INSTRUMENTS TMS320C50 AND  
TMS320C30 DSPs.

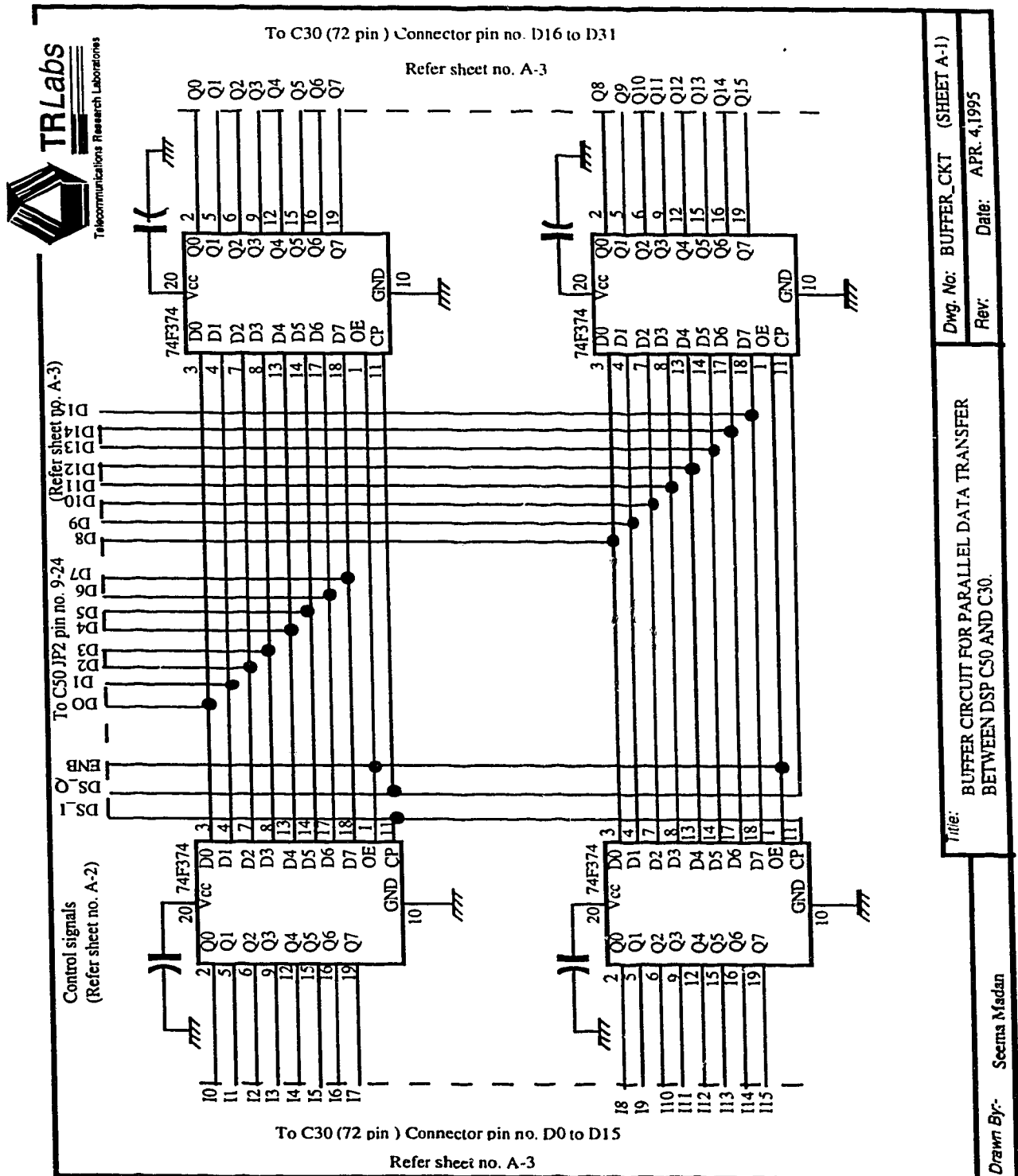


Fig. A.1. Circuit diagram of buffer circuit.

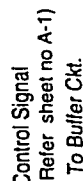
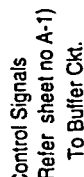
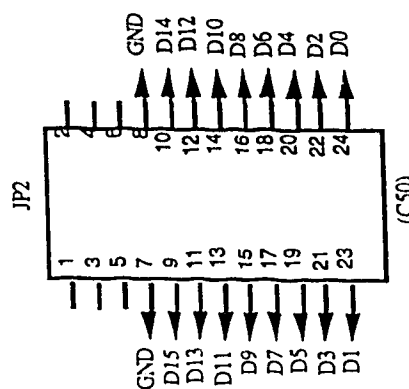
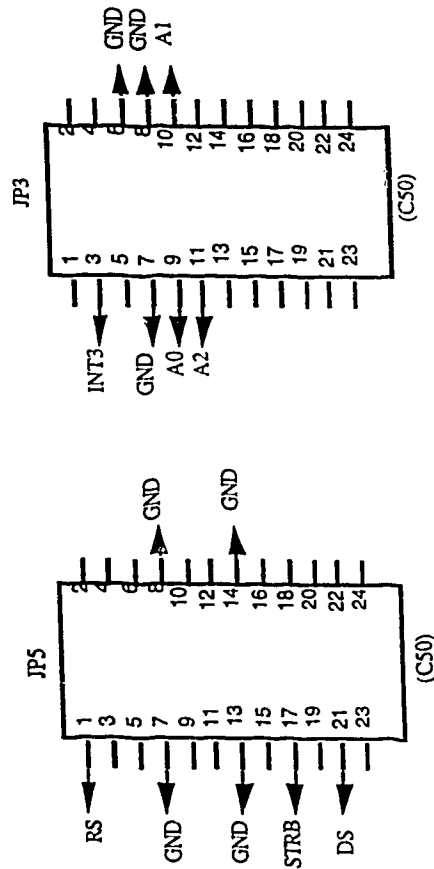


Fig. A.2. Circuit diagram of control circuit.

A	B	C
Vcc	Vcc	1
GND	xxx	2
D0	xxx	3
D1	xxx	4
D2	GND	5
D3	GND	6
D4	RS	7
D5	STRB	8
D6	xxx	9
D7	xxx	10
D8	xxx	11
D9	xxx	12
D10	xxx	13
D11	GND	14
D12	TMR1	15
D13	GND	16
D14	xxx	17
D15	xxx	18
GND	xxx	19
xxx	xxx	20
xxx	xxx	21
xxx	xxx	22
xxx	xxx	23
xxx	xxx	24
xxx	xxx	25
xxx	xxx	26
xxx	xxx	27
xxx	xxx	28
xxx	GND	29
xxx	GND	30
A1	xxx	31
A0	xxx	32
Vcc	Vcc	

Memory Expansion Connector  
72 pin (C30)



Dwg. No: DSP\_CKT (SHEET A-3)

Rev: Date: Apr. 4, 1995

Title: JUMPER CONNECTIONS OF DSP C50 AND C30

Drawn By:- Seema Madan

Fig. A.3. Jumper pin connections for C50 and C30 DSP.

	6 - Pad Master.	4 - Annotation.	2 - PCB Outline.
	5 - Common Features.	3 - Component Layout.	1 - Drawing Master.

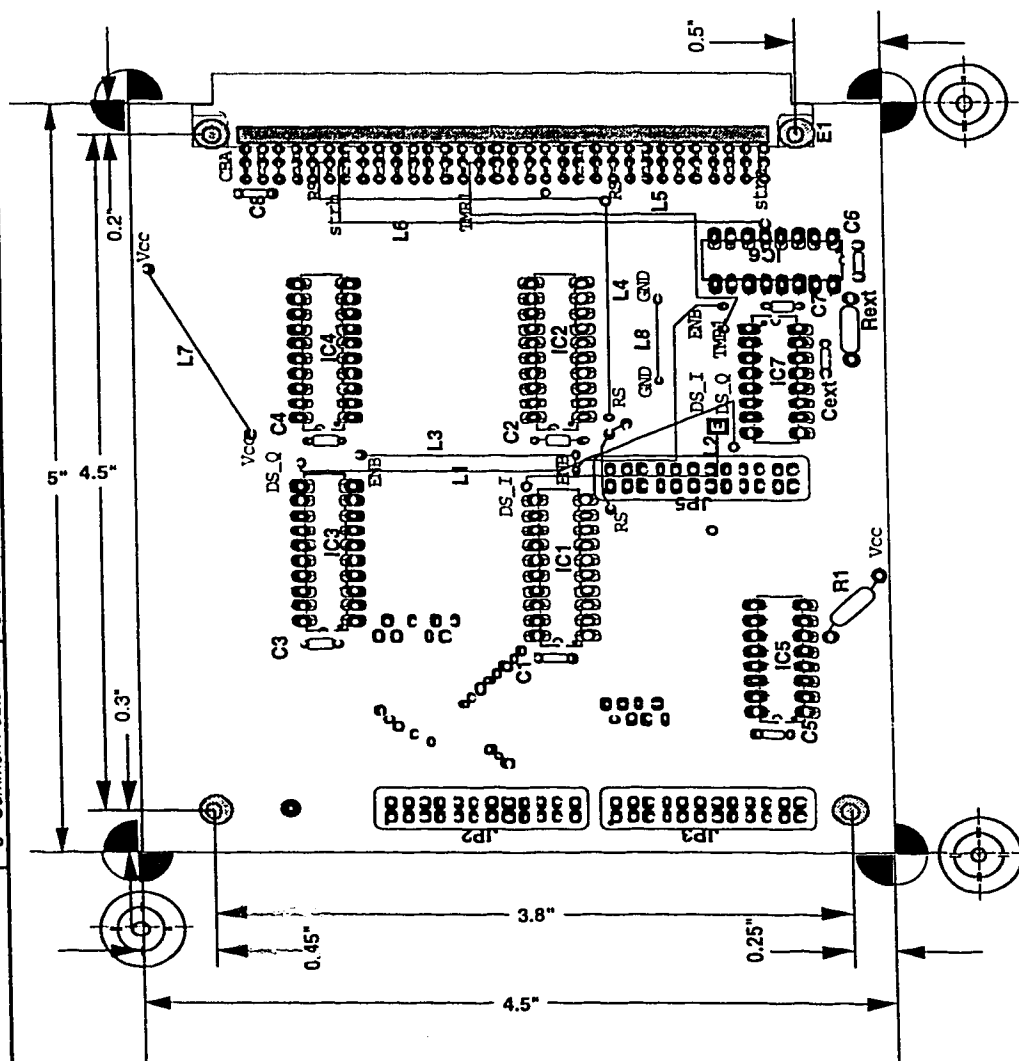
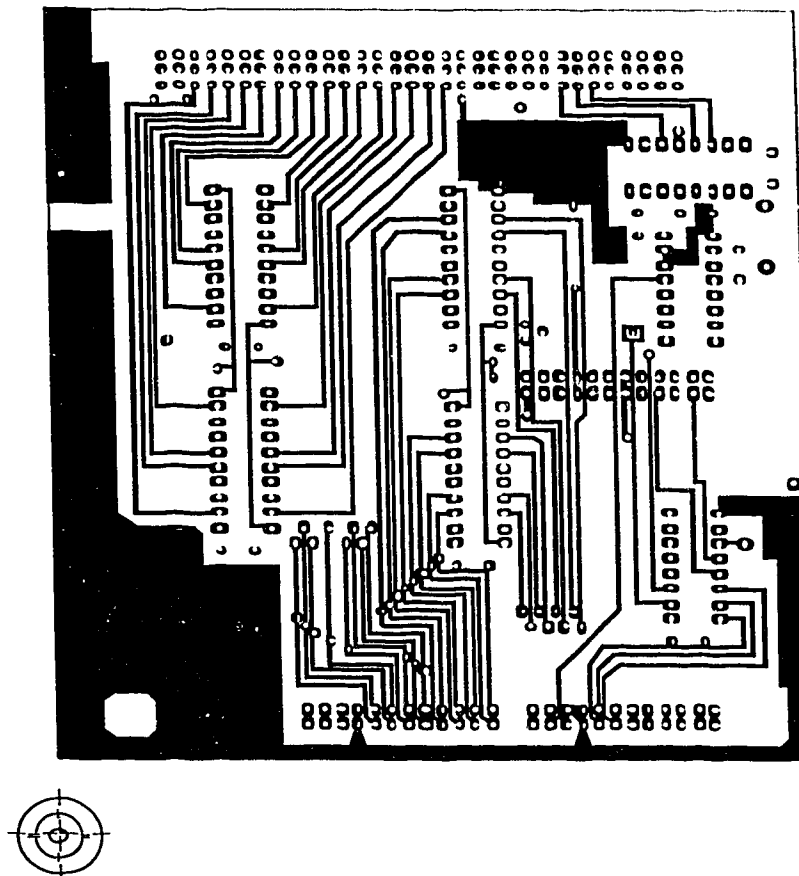


**Fig. A.4. Component layout and common features for PCB.**

LAYERS:	8 - Component Side	6 - Pad Master.	2 - PCB Outline.
			1 - Drawing Master.



Dwg. No: DSP BUFFER PCB-01 SHEET A-5  
Rev: Date: Apr. 13, 1995

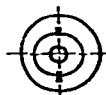
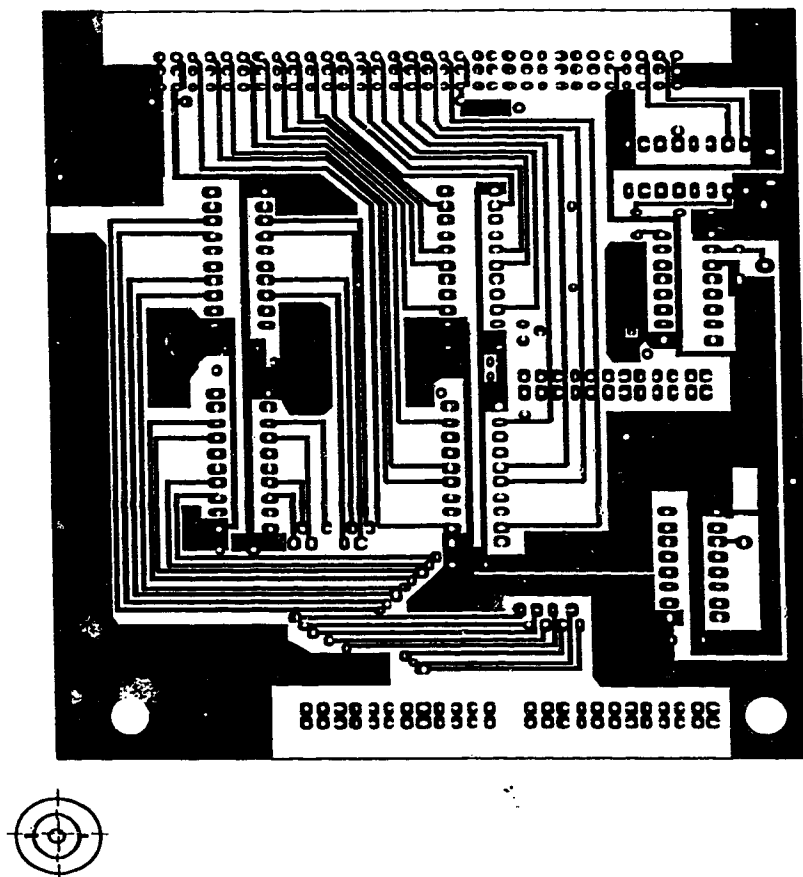
Title: DATA INTERFACE BETWEEN DSP TMS320C30 AND TMS320C30

Drawn By: Seema Madan

Fig. A.5. Component side for PCB.



<b>LAYERS:</b>	7 - Wiring Side.	6 - Pad Master.	2 - PCB Outline. 1 - Drawing Master.



Dwg. No: DSP BUFFER PCB-01 (SHEET A-6)  
Rev: Date: Apr. 13, 1995

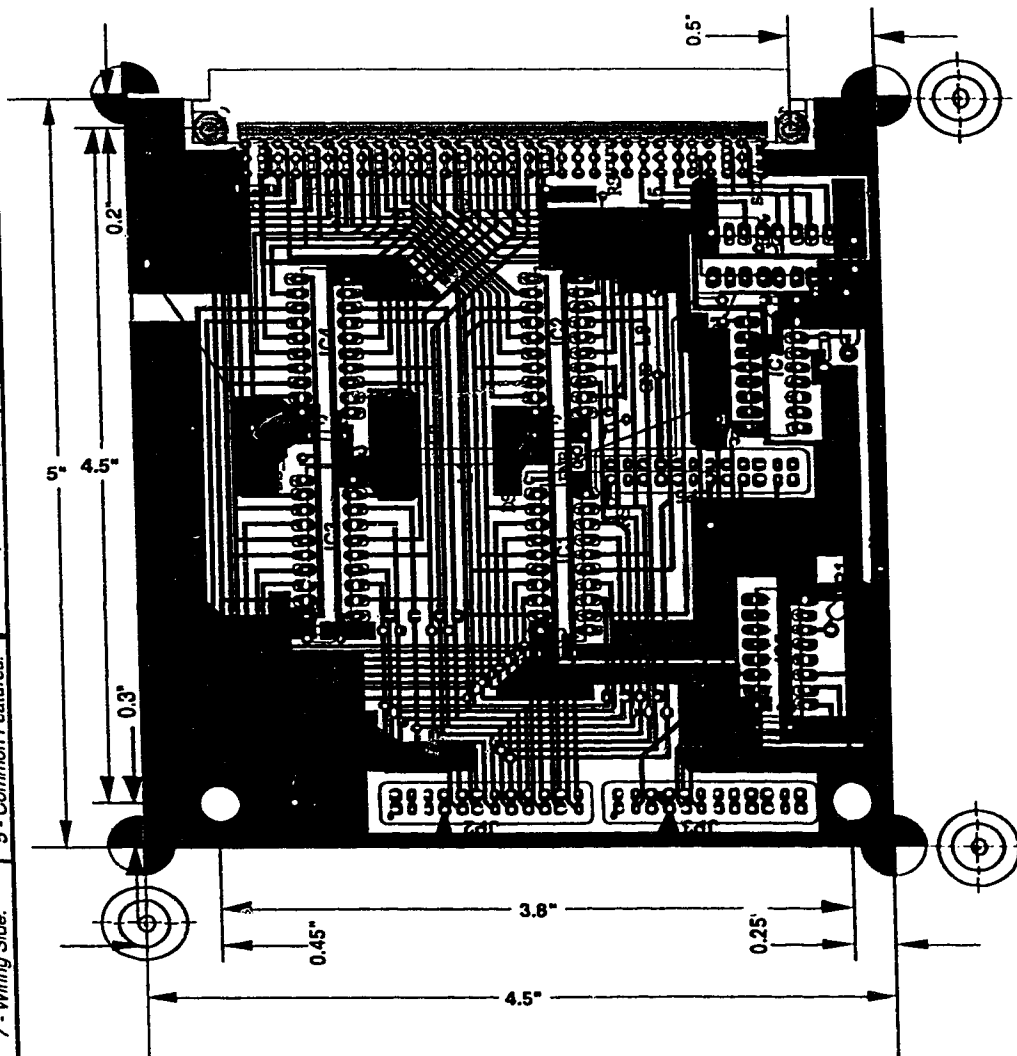
Title: DATA INTERFACE BETWEEN DSP TMS320C50 AND TMS320C30

Drawn By:- Seema Madan

Fig. A.6. Wiring side for PCB.

**LAYERS:**

8 - Component Side	6 - Pad Master.	4 - Annotation.	2 - PCB Outline.
7 - Wiring Side.	5 - Common Features.	3 - Component Layout.	1 - Drawing Master.



Dwg. No: DSP BUFFER PCB-01 (SHEET A-7)

Rev: Date: Apr. 13, 1995

Title: DATA INTERFACE BETWEEN DSP TMS320C50 AND TMS320C30

Drawn By: Seema Madan

Fig. A.7. Double layer PCB.

## APPENDIX B.

### DSP PROGRAM LISTS FOR REAL TIME TRANSCEIVER IMPLEMENTATION

- \*PROGRAM : SHIFT7.ASM
- \*TABLE FOR SHIFT REGISTER SIMULATION
- \*USED FOR RANDOM GENERATOR FOR PRWS
- \*Total group = 31 = tap length
- \*Each group has three words
- \*First word of group is seed value/random no.
- \*Second word is address for 30th seed value
- \*Third word is updated address for 2nd seed value
- \*Groupings as per:
- \* bit 0 >> DATA I
- \* bit 1 >> DATA Q
- \* bit 2 to bit 8 >> CHANNEL I
- \* bit 9 to bit 15 >> CHANNEL Q

300h	.word	58129	;sec
301h	.word	354h	
302h	.word	306h	
303h	.word	49340	;seed2
304h	.word	357h	
305h	.word	309h	
306h	.word	2807	;seed3
307h	.word	35ah	
308h	.word	30ch	
309h	.word	44744	;seed4
310h	.word	300h	
311h	.word	30fh	
312h	.word	12312	;seed5
313h	.word	303h	
314h	.word	312h	
315h	.word	49261	;seed6
316h	.word	306h	
317h	.word	315h	
318h	.word	27436	;seed7
319h	.word	309h	
320h	.word	318h	
321h	.word	61712	;seed8
322h	.word	30ch	
323h	.word	31bh	
324h	.word	537	;seed9
325h	.word	30fh	
326h	.word	31ch	
327h	.word	45869	;seed10
328h	.word	312h	
329h	.word	321h	
330h	.word	29397	;seed11
331h	.word	315h	
332h	.word	324h	
333h	.word	29938	;seed12
334h	.word	318h	
335h	.word	327h	
336h	.word	43613	;seed13
337h	.word	31bh	
338h	.word	32ah	
339h	.word	35111	;seed14
340h	.word	31ch	
341h	.word	32dh	
342h	.word	12935	;seed15
343h	.word	321h	
344h	.word	330h	
345h	.word	17692	;seed16
346h	.word	324h	

347h	.word	333h	
348h	.word	43955	;seed17
349h	.word	327h	
350h	.word	336h	
351h	.word	12509	;seed18
352h	.word	32ah	
353h	.word	339h	
354h	.word	4038	;seed19
355h	.word	32dh	
356h	.word	33ch	
357h	.word	53693	;seed20
358h	.word	330h	
359h	.word	33fh	
360h	.word	23906	;seed21
361h	.word	333h	
362h	.word	342h	
363h	.word	14497	;seed22
364h	.word	336h	
365h	.word	345h	
366h	.word	38290	;seed23
367h	.word	339h	
368h	.word	348h	
369h	.word	26323	;seed24
370h	.word	33ch	
371h	.word	34bh	
372h	.word	30551	;seed25
373h	.word	33fh	
374h	.word	34ch	
375h	.word	41830	;seed26
376h	.word	342h	
377h	.word	351h	
378h	.word	51741	;seed27
379h	.word	345h	
380h	.word	354h	
381h	.word	23023	;seed28
382h	.word	348h	
383h	.word	357h	
384h	.word	42080	;seed29
385h	.word	34bh	
386h	.word	35ah	
387h	.word	56061	;seed30
388h	.word	34ch	
389h	.word	300h	
390h	.word	29151	;seed31
391h	.word	351h	
392h	.word	303h	

\*PROGRAM : DSC2.ASM  
 \*FILTER COEFF FOR DOPPLER SHIFT FIR 121 LENGTH FILTER  
 \*This is calculated using freq. response graph in matlab  
 \*Q15 notation is used here.

```

    .ps      0990h
coeffp      .int      75,82,62,23,-33,-102,-164,-203,-210,-167
              .int      -82,39,174,298,383,400,334,190,-20,-259
              .int      -485,-646,-705,-632,-426,-108,269,639,927,1072
              .int      1022,773,347,-187,-741,-1206,-1484,-1504,-1239,-708
              .int      7,786,1491,1976,2127,1884,1262,334,-750,-1806
              .int      -2621,-3024,-2884,-2156,-881,800,2684,4519,6052,7071
              .int      7429
              .int      7071,6052,4519,2684,800,-881,-2156,-2884,-3024,-2621
              .int      -1806,-750,334,1262,1884,2127,1976,1491,786,7
              .int      -708,-1239,-1504,-1484,-1206,-741,-187,347,773,1022
              .int      1072,927,639,269,-108,-426,-632,-705,-646,-485
              .int      -259,-20,190,334,400,383,298,174,39,-82
              .int      -167,-210,-203,-164,-102,-33,23,62,82,75
  
```

\*PROGRAM : IPC96.ASM  
 \*INTERPOLATING FILTER COEFF. FOR fd = 40Hz  
 \*Tap length = 96  
 \*This is calculated using Matlab  
 \*Scaleup by 15 , Q15 notation  
 \*16x6 interpolating filter bank coeff

```

    .ps      2080h
    .int      1742,7455,11505,7858,1987,1518,7045,11469,8253,2251,174
    .int      1314,6632,11399,8636,2535,202
    .int      1130,6218,11294,9005,2839,238
    .int      965,5806,11155,9357,3160,283
    .int      819,5398,10984,9689,3499,338
    .int      691,4997,10781,10000,3854,405
    .int      580,4605,10548,10287,4223,485
    .int      485,4223,10287,10548,4605,580
    .int      405,3854,10000,10781,4997,691
    .int      338,3499,9689,10984,5398,819
    .int      283,3160,9357,11155,5806,965
    .int      238,2839,9005,11294,6218,1130
    .int      202,2535,8636,11399,6632,1314
    .int      174,2251,8253,11469,7045,1518
    .int      151,1987,7858,11505,7455,1742
  
```

\*PROGRAM : IPC352\_1.ASM  
 \*INTERPOLATING FILTER COEFF. FOR fd = 20Hz  
 \*Tap length = 352  
 \*This is calculated using Matlab  
 \*32x11 interpolating filter bank coeff

```

    .ps      2080h
    .int      -132,-19,897,2675,4224,4252,2735,942,-5,-134,-70
    .int      -130,-32,852,2615,4194,4279,2794,988,9,-136,-71
    .int      -128,-43,809,2555,4162,4304,2854,1036,24,-138,-72
    .int      -125,-54,766,2495,4129,4327,2913,1084,40,-139,-73
    .int      -123,-65,725,2434,4094,4349,2971,1133,57,-140,-74
    .int      -121,-74,684,2374,4058,4369,3029,1183,75,-141,-75
    .int      -118,-83,645,2314,4021,4387,3087,1233,94,-142,-77
    .int      -116,-91,606,2253,3982,4404,3144,1285,114,-143,-78
    .int      -113,-98,569,2193,3942,4418,3200,1337,134,-143,-80
    .int      -111,-105,533,2133,3900,4431,3256,1390,156,-143,-82
    .int      -108,-111,497,2074,3857,4442,3311,1444,179,-143,-83
  
```

```

.int      -106,-117,463,2014,3813,4451,3365,1499,203,-142,-85
.int      -103,-121,430,1955,3767,4459,3419,1554,227,-141,-87
.int      -101,-126,398,1896,3721,4464,3472,1610,253,-140,-89
.int      -98,-130,367,1838,3673,4468,3523,1666,280,-138,-91
.int      -96,-133,337,1780,3624,4470,3574,1723,308,-136,-94
.int      -94,-136,308,1723,3574,4470,3624,1780,337,-133,-96
.int      -91,-138,280,1666,3523,4468,3673,1838,367,-130,-98
.int      -89,-140,253,1610,3472,4464,3721,1896,398,-126,-101
.int      -87,-141,227,1554,3419,4459,3767,1955,430,-121,-103
.int      -85,-142,203,1499,3365,4451,3813,2014,463,-117,-106
.int      -83,-143,179,1444,3311,4442,3857,2074,497,-111,-108
.int      -82,-143,156,1390,3256,4431,3900,2133,533,-105,-111
.int      -80,-143,134,1337,3200,4418,3942,2193,569,-98,-113
.int      -78,-143,114,1285,3144,4404,3982,2253,606,-91,-116
.int      -77,-142,94,1233,3087,4387,4021,2314,645,-83,-118
.int      -75,-141,75,1183,3029,4369,4058,2374,684,-74,-121
.int      -74,-140,57,1133,2971,4349,4094,2434,725,-65,-123
.int      -73,-139,40,1084,2913,4327,4129,2495,766,-54,-125
.int      -72,138,24,1036,2854,4304,4162,2555,809,-43,-128
.int      -71,-136,9,988,2794,4279,4194,2615,852,-32,-130
.int      -70,-134,-5,942,2735,4252,4224,2675,897,-19,-132

```

**\*PROGRAM : PSC2.ASM**  
**\*FILTER COEFF. FOR PULSE SHAPING FIR 96 LENGTH FILTER**  
**\*This is calculated using freq. response graph in Matlab**  
**\*Q14 notation is used here.**  
**\*Reverse the order of coeff. so as for MAC inst. to work correctly**

```

.ps      2020h
obj1     .int      157,-81,-319,1143,-2631,17365,654,421,-399,145,52,-100
obj2     .int      150,-168,-156,1070,-3091,15681,3389,-362,-242,218,-39,-74
obj3     .int      108,-207,19,795,-2887,13109,6596,-1299,47,226,-128,-21
obj4     .int      45,-191,157,419,-2214,9958,9958,-2214,419,157,-191,45
obj5     .int      -21,-128,226,47,-1299,6596,13109,-2887,795,19,-207,108
obj6     .int      -74,-39,218,-242,-362,3389,15681,-3091,1070,-156,-168,150
obj7     .int      -100,52,145,-399,421,654,17365,-2631,1143,-319,-81,157
obj8     .int      -96,123,33,-417,936,-1388,17951,-1388,936,-417,33,123

```

**\*PROGRAM : IF3.ASM**  
**\*RECEIVED SIGNAL SAMPLE GENERATING PROGRAM**  
**\*Doppler frequency=40Hz.**  
**\*Additional Files Req'd.: SHIFT7.ASM+DSC2.ASM+IPC96.ASM**  
**\*DSP TMS320C50**

```

.mmregs
*Table for prws generation simulating circular buffer (CB)
.ds      0300h          ;Start address for shift reg table
.include "shift7.asm"    ;Table of length (31*3)=93 words
I_mask   .word      508    ;Mask for I Channel
Q_mask   .word      65024  ;Mask for Q Channel
ipfact   .word      0      ;initial status for interpolation

* 121 Coeff. for doppler shift FIR filter
.ps      0990h
.include "dsc2.asm"      ;Table of Coeff for Doppler Shift filter

*Address value for ipfact used for fading interpolation
aipfact  .set      35fh    ;if ipfact=0 interpolation is over

*Address values for Iprws,Qprws in Data mem.
I_ch     .set      360h    ;I channel in upper seven bits
Q_ch     .set      3dbh    ;Q channel in upper seven bits

*Address for first Coeff of DS filter in Prog. mem.

```

```
coeffp    set    0990h                ;Program memory address for DS filter coeff.
```

\* Ichannel data page for filtering by DS filter

```
ds Ich    set    3dah                ;DS filter output for I channel
lst Ich    set    361h                ;First delay element for I channel
Lst Ich    set    3d8h                ;361h+dec(120) Last delay element for I channel
           .ds    361h
           .space  780h                ;Initialize delay elements with zeros
                                           ;780h = no. of bits = (120 * 16)hex
```

\* Qchannel data page for filtering by DS filter

```
ds Qch    set    455h                ;DS filter output for I channel
lst Qch    set    3dch                ;First delay element for I channel
Lst Qch    set    453h                ;362h+dec(120) Last delay element for I channel
           .ds    3dch
           .space  780h                ;Initialize delay elements with zeros
                                           ;780h = no. of bits = (120 * 16)hex
```

\*96 point for fd=40Hz

```
.ps        2080h
.include "ipc96.asm" ;Table of coeff. for channel interpolating filter
```

\* Q channel data page for interpolating filter delay line

```
lst_dsQ    set    456h
Lst_dsQ    set    45ah                ;6 taps    ;458h >4 taps for MP ::for 11 taps 45fh
RF_Q       set    461h
           .ds    456h
           .space  0b0h
```

\* I channel data page for interpolating filter delay line

```
ds Ichl    set    465h
lst_dsl    set    466h
Lst_dsl    set    46ah                ;6 taps    ;468h >4 taps for MP:: for 11 taps46fh
RF_I       set    471h
           .ds    466h
           .space  0b0h
           .ds    47ah
```

```
ip_count .word    16                ;16=40Hz;32=20Hz;64=10Hz
```

```
ip_index .word    16
```

```
ini_adr .word    8320 ;2080h        ;initial address for filter coeff
```

```
sub_fl .word    8320 ;2080h        ;subfilter coeff. address
```

\* Data page 9 for Transmit Signal generation

\* from address 4a0 to 4fh only.

```
D_mask    set    4a0h
Data      set    4a1h
E_tbl     set    4a2h
E_data    set    4a3h
prv_ph    set    4a4h
M_tbl     set    4a5h
```

```
M_DI      set    4a6h
lst_DI    set    4a7h
Lst_DI    set    4b1h
MOD_I     set    4b3h
```

```
M_DQ      set    4b6h
lst_DQ    set    4b7h
Lst_DQ    set    4c1h
MOD_Q     set    4c3h
```

```
RX_I      set    4c4h
RX_Q      set    4c5h
```

```
adshift   set    4c6h
adfreq    set    4c7h
```

```
.ds        4a0h
```

```

.word    3                ;Data Mask =3
.word    0                ;Data value
.word    8192             ;dma:4a2>E_tbl(2000h)
.word    0000h           ;dma:4a3h>E_data
.word    0000h           ;dma:4a4h>prv_ph
.word    8208             ;dma:4a5h>M_tbl(2010h)

.ds      4a7h            ;Delay line for data I
.space   0c0h            ;Initialize to zero

.ds      4b7h            ;Delay line for data Q
.space   0c0h            ;Initialize to zero

```

**\*Initial setting for Doppler Shift Value**

```

.ds      4c6h
dshift   .word    2        ;= dfreq ;To set initial value of doppler shift/freq.
dfreq    .word    2        ;= dshift ;80Hz=1; 40Hz=2; 20Hz=4; 10Hz=8.

```

**\*Look-up Table for encoder in program memory**

```

.ps      2000h
.word    0001,0003,0007,0005

```

**\*Look up table for Modulator in Q14 notation**

```

.ps      2010h
.word    16384,0
.word    11585,11585
.word    0,16384
.word    -11585,11585
.word    -16384,0
.word    -11585,-11585
.word    0,-16384
.word    11585,-11585

.ps      2020h
.include "psc2.asm" ;Table of Coeff for Pulse Shaping filter

```

**\*Set up the address for interrupt service routine vector**

```

.ps      00806h
rete

.ps      00b00h
.entry
SETC     INTM                ; Disable interrupts
LDP      #0                  ; Set data page pointer
OPL      #0834h,PMST
LACC     #0
SAMB     CWSR                ; Set software wait state to 0
SAMB     PDWSR
CLRC     OVM                  ; OVM = 0
SPM      0
SETC     SXM
LDP      DXR
SPLK     #0h,DBMR            ;Used for comparison for fd change
SPLK     #06h,IMR
SPLK     #20h,TCR            ; To generate 10 MHz from Tout
SPLK     #01h,PRD            ; for AIC master clock
LACC     #00c0h              ; Reset tx/rx port
SACL     SPC
CLRC     INTM                ; enable

```

**\*PRWS generation**

```

lar      ar6,#0300h

```

**S\_no1**

```

loop     idle
         ldp      #9h
         lacc     RX_I

```



```

*      lacc      MOD 1
*      ldp      #8h
*      lacc      RF 1
      ldp      #58h
      sac1     0
      ldp      #9h
      lacc      RX Q
*      lacc      MOD Q
*      ldp      #8h
*      lacc      RF Q
      ldp      #58h
      sac1     1

```

#### \*\*\*\*\*PRWS GENERATION\*\*\*\*\*

```

      mar      *,ar6
      lacc     *+                ;load acc. with TAP:2
      lar      ar6,*            ;Get address for TAP:30
      xor      *                ;XOR for M-sequence PRWS method
      sacb                    ;Pseudo Random Word Seq.
      mar      *,ar6
      sac1     *+                ;Store result in TAP:30
      mar      *+ar6            ;Update address for New TAP:2
      lar      ar6,*

```

#### \*\*\*\*\*END of PRWS generation\*\*\*\*\*

\*Check if new value for fading to be generated or to continue

\*with interpolation

```

      ldp      #6h
      cpl      aipfact          ;chk if ipfact=0(DBMR) set TC=1 else TC=0
      bend     ip_cont,NTC      ;If TC=0 Branch to interpolation else new sample

```

```

      ldp      #6h
      lacc     1 mask
      andb                    ;Store Channel I value
      sac1     1 ch,7           ;scaling Channel I value
      lacc     1 ch
      sfr

```

```

*      sfr
      sac1     1 ch
      lacc     Q_mask
      andb
      ldp      #7h
      sac1     Q_ch             ;Store Channel Q value

```

\*As the DS filter is overflowing reduce the mag. of

\*its input. One SFR command is OK but two SFR reduces any

\*remote chance of overflow.

\*We have used setc SXM mode so as to maintain the sign

```

      lacc     Q_ch
      sfr

```

```

*      sfr
      sac1     Q_ch

```

#### \*-----I Channel FIR DOPPLER SHIFT FILTER-----

\*Doppler shift Filter 120 length FIR filter

```

      lacc     #0h              ;Zero Accumulator
      zpr
      mar      *,ar3
      lar      ar3,#Lst_1ch
      DSF_1    rpt      #120    ;FIR filter for Doppler Shift
      macd     coeffp,*-
      apac
      ldp      #7h
      sach     ds_1ch,1        ;not really reqd. to save here. CHK.??
      ldp      #8h
      sach     ds_1ch1,1       ;store on two locations

```

#### \*-----END of I channel Doppler shift filter-----

#### \*-----Q Channel FIR DOPPLER SHIFT FILTER-----

```

* Doppler shift Filter 120 length FIR filter
    ldp    #8h                ;data page no.
    lacc   #0h                ;Zero Accumulator
    zpr
    *
    mar    *,ar3
    lar    ar3,#Lst_Qch
DSF_Q     rpt    #120          ;FIR filter for Doppler Shift
    macd   coeffp,*-
    apac
    ldp    #8h
    sach   ds_Qch,l

```

\*-----END of Q channel Doppler shift filter-----

```

* Data generation
ip_cont  ldp    #9h
        lacc   D_mask
        andb
        sac1   Data            ;Store Data value

```

```

* Data encoding
    lacc   E_tbl
    add    Data
    tblr   E_data

```

```

* Previous phase (state) reference
    lacc   E_data
    add    prv_ph
    and    #0007h
    sac1   prv_ph

```

```

* Data modulating
    sfl
    add    M_tbl
    tblr   M_DI
    add    #1
    tblr   M_DQ

```

\*----- Pulse shaping + Interpolating for Data Q -----

```

    lacc   #0h
    zpr
    mar    *,ar5
    lar    ar5,#Lst_DQ
PS_QI     rpt    #11
    mac    obj1,*-
    apac
    sach   MOD_Q,2            ,store as Q14 output

```

\*----- Pulse shaping + Interpolating for Data I -----

```

    lacc   #0h
    zpr
    lar    ar5,#Lst_DI
PS_I1     rpt    #11
    mac    obj1,*-
    apac
    sach   MOD_I,2            ,store as Q14 output

```

\*-----END of Pulse shaping-----

```

CALL     CH_IP

```

\*Multiply (complex) transmitted signal and flat fading

```

    lacc   #0h
    ldp    #8h
    lt     RF_I
    ldp    #9h
    mpy    MOD_I              ;Preg=RF_I*MOD_I
    ldp    #8h
    lt     RF_Q

```

```

ldp      #9h
mpya     MOD_Q      ;Preg=RF_Q*MOD_Q ; Acc=RF_I*MOD_I
mpys     MOD_I      ;Preg=RF_Q*MOD_I ; Acc=RF_I*MOD_I-RF_Q*MOD_Q
sach     RX_I,1      ;store as Q14
lace     #0h
ldp      #8h
lt       RF_I
ldp      #9h
mpya     MOD_Q      ;Preg=RF_I*MOD_Q ; Acc=RF_Q*MOD_I
apac     RF_Q*MOD_I+RF_I*MOD_Q
sach     RX_Q,1

S no2    idle
ldp      #9h
lace     RX_I
*        lace     MOD_I
*        ldp      #8h
*        lace     RF_I
ldp      #58h
sac1     0
ldp      #9h
lace     RX_Q
*        lace     MOD_Q
*        ldp      #8h
*        lace     RF_Q
ldp      #58h
sac1     1

*----- Pulse shaping + Interpolating for Data Q -----
ldp      #9h
lace     #0h
zpr
mar      *,ar5
lar      ar5,#Lst_DQ
PS_Q2    rpt      #11
mac      obj2,*-
apac
sach     MOD_Q,2      ,store as Q14 output

*----- Pulse shaping + Interpolating for Data I -----
lace     #0h
zpr
lar      ar5,#Lst_DI
PS_I2    rpt      #11
mac      obj2,*-
apac
sach     MOD_I,2      ,store as Q14 output

*-----END of Pulse shaping-----

CALL     CH_IP
*Multiply (complex) transmitted signal and flat fading

lace     #0h
ldp      #8h
lt       RF_I
ldp      #9h
mpy      MOD_I      ;Preg=RF_I*MOD_I
ldp      #8h
lt       RF_Q
ldp      #9h
mpya     MOD_Q      ;Preg=RF_Q*MOD_Q ; Acc=RF_I*MOD_I
mpys     MOD_I      ;Preg=RF_Q*MOD_I ; Acc=RF_I*MOD_I-RF_Q*MOD_Q
sach     RX_I,1      ;store as Q14
lace     #0h
ldp      #8h
lt       RF_I
ldp      #9h
mpya     MOD_Q      ;Preg=RF_I*MOD_Q ; Acc=RF_Q*MOD_I

```

```

                                ;Acc=RF_Q*MOD_I+RF_I*MOD_Q
                                apac
                                sach      RX_Q,I

S_no3  idle
        ldp      #9h
        lacc      RX_I
        *        lacc      MOD_I
        *        ldp      #8h
        *        lacc      RF_I
        ldp      #58h
        saci      0
        ldp      #9h
        lacc      RX_Q
        *        lacc      MOD_Q
        *        ldp      #8h
        *        lacc      RF_Q
        ldp      #58h
        saci      1

*----- Pulse shaping + Interpolating for Data Q -----
        ldp      #9h
        lacc      #0h
        zpr
        mar      *,ar5
        lar      ar5,#1,st_DQ
PS_Q3   rpt      #11
        mac      obj3,*-
        apac
        sach      MOD_Q,2      ,store as Q14 output
*----- Pulse shaping + Interpolating for Data I -----
        lacc      #0h
        zpr
        lar      ar5,#1,st_DI
PS_I3   rpt      #11
        mac      obj3,*-
        apac
        sach      MOD_I,2      ,store as Q14 output
*-----END of Pulse shaping-----

        CALL     CH_IP

*Multiply (complex) transmitted signal and flat fading

        lacc      #0h
        ldp      #8h
        lt        RF_I
        ldp      #9h
        mpy       MOD_I      ;Preg=RF_I*MOD_I
        ldp      #8h
        lt        RF_Q
        ldp      #9h
        mpya      MOD_Q      ;Preg=RF_Q*MOD_Q ; Acc=RF_I*MOD_I
        mpys      MOD_I      ;Preg=RF_Q*MOD_I ; Acc=RF_I*MOD_I-RF_Q*MOD_Q
        sach      RX_I,I      ;store as Q14
        lacc      #0h
        ldp      #8h
        lt        RF_I
        ldp      #9h
        mpya      MOD_Q      ;Preg=RF_I*MOD_Q ; Acc=RF_Q*MOD_I
        apac      ;Acc=RF_Q*MOD_I+RF_I*MOD_Q
        sach      RX_Q,I

S_no4   idle
        ldp      #9h
        lacc      RX_I
        *        lacc      MOD_I

```

```

*      ldp      #8h
*      lacc     RF_I
      ldp      #58h
      sac1     0
      ldp      #9h
      lacc     RX_Q
*      lacc     MOD_Q
*      ldp      #8h
*      lacc     RF_Q
      ldp      #58h
      sac1     1

```

\*----- Pulse shaping + Interpolating for Data Q -----

```

      ldp      #9h
      lacc     #0h
      zpr
      mar      *,ar5
      lar      ar5,#Lst_DQ
PS_Q4    rpt     #11
      mac      obj4,*-
      apac
      sach     MOD_Q,2           ,store as Q14 output

```

\*----- Pulse shaping + Interpolating for Data I -----

```

      lacc     #0h
      zpr
      lar      ar5,#Lst_DI
PS_I4    rpt     #11
      mac      obj4,*-
      apac
      sach     MOD_I,2           ,store as Q14 output

```

\*-----END of Pulse shaping-----

CALL CH\_IP

\*Multiply (complex) transmitted signal and flat fading

```

      lacc     #0h
      ldp      #8h
      lt       RF_I
      ldp      #9h
      mpy      MOD_I           ;Preg=RF_I*MOD_I
      ldp      #8h
      lt       RF_Q
      ldp      #9h
      mpya     MOD_Q           ;Preg=RF_Q*MOD_Q ; Acc=RF_I*MOD_I
      mpys     MOD_I           ;Preg=RF_Q*MOD_I ; Acc=RF_I*MOD_I-RF_Q*MOD_Q
      sach     RX_I,1          ;store as Q14
      lacc     #0h
      ldp      #8h
      lt       RF_I
      ldp      #9h
      mpya     MOD_Q           ;Preg=RF_I*MOD_Q ; Acc=RF_Q*MOD_I
      apac
      sach     RX_Q,1          ;Acc=RF_Q*MOD_I+RF_I*MOD_Q

```

```

S_no5    idle
      ldp      #9h
      lacc     RX_I
*      lacc     MOD_I
*      ldp      #8h
*      lacc     RF_I
      ldp      #58h
      sac1     0
      ldp      #9h
      lacc     RX_Q
*      lacc     MOD_Q
*      ldp      #8h
*      lacc     RF_Q
      ldp      #58h

```

```

sac1      1

*----- Pulse shaping + Interpolating for Data Q -----
ldp      #9h
lacc     #0h
zpr
mar      *,ar5
lar      ar5,#Lst_DQ
PS_Q5    rpt      #11
mac      obj5,*-
apac
sach     MOD_Q,2      ,store as Q14 output
*----- Pulse shaping + Interpolating for Data I -----
lacc     #0h
zpr
lar      ar5,#Lst_DI
PS_I5    rpt      #11
mac      obj5,*-
apac
sach     MOD_I,2      ,store as Q14 output

*-----END of Pulse shaping-----

CALL     CH_IP

*Multiply (complex) transmitted signal and flat fading

lacc     #0h
ldp      #8h
lt       RF_I
ldp      #9h
mpy      MOD_I      ;Preg=RF_I*MOD_I
ldp      #8h
lt       RF_Q
ldp      #9h
mpya     MOD_Q      ;Preg=RF_Q*MOD_Q ; Acc=RF_I*MOD_I
mpys     MOD_I      ;Preg=RF_Q*MOD_I ; Acc=RF_I*MOD_I-RF_Q*MOD_Q
sach     RX_I,1      ;store as Q14
lacc     #0h
ldp      #8h
lt       RF_I
ldp      #9h
mpya     MOD_Q      ;Preg=RF_I*MOD_Q ; Acc=RF_Q*MOD_I
apac     ;Acc=RF_Q*MOD_I+RF_I*MOD_Q
sach     RX_Q,1

S_no6    idle
ldp      #9h
lacc     RX_I
*        lacc     MOD_I
*        ldp      #8h
*        lacc     RF_I
ldp      #58h
sac1     0
ldp      #9h
lacc     RX_Q
*        lacc     MOD_Q
*        ldp      #8h
*        lacc     RF_Q
ldp      #58h
sac1     1

*----- Pulse shaping + Interpolating for Data Q -----
ldp      #9h
lacc     #0h
zpr
mar      *,ar5

```

```

        lar      ar5,#Lst_DQ
PS_Q6   rpt      #11
        mac      obj6,*-
        apac
        sach     MOD_Q,2          ,store as Q14 output

```

```

*----- Pulse shaping + Interpolating for Data I -----
        lacc     #0h

```

```

        zpr
        lar      ar5,#Lst_DI
PS_I6    rpt      #11
        mac      obj6,*-
        apac
        sach     MOD_I,2          ,store as Q14 output

```

```

*-----END of Pulse shaping-----

```

```

        CALL     CH_IP

```

```

*Multiply (complex) transmitted signal and flat fading

```

```

        lacc     #0h
        ldp      #8h
        lt       RF_I
        ldp      #9h
        mpy      MOD_I          ;Preg=RF_I*MOD_I
        ldp      #8h
        lt       RF_Q
        ldp      #9h
        mpya     MOD_Q          ;Preg=RF_Q*MOD_Q ; Acc=RF_I*MOD_I
        mpys     MOD_I          ;Preg=RF_Q*MOD_I ; Acc=RF_I*MOD_I-RF_Q*MOD_Q
        sach     RX_I,1          ;store as Q14
        lacc     #0h
        ldp      #8h
        lt       RF_I
        ldp      #9h
        mpya     MOD_Q          ;Preg=RF_I*MOD_Q ; Acc=RF_Q*MOD_I
        apac
        sach     RX_Q,1          ;Acc=RF_Q*MOD_I+RF_I*MOD_Q

```

```

S_no7    idle
        ldp      #9h
        lacc     RX_I
        *        lacc     MOD_I
        *        ldp      #8h
        *        lacc     RF_I
        ldp      #58h
        sac1     0
        ldp      #9h
        lacc     RX_Q
        *        lacc     MOD_Q
        *        ldp      #8h
        *        lacc     RF_Q
        ldp      #58h
        sac1     1

```

```

*----- Pulse shaping + Interpolating for Data Q -----

```

```

        ldp      #9h
        lacc     #0h

```

```

        zpr
        mar      *,ar5
        lar      ar5,#Lst_DQ

```

```

PS_Q7    rpt      #11
        mac      obj7,*-
        apac
        sach     MOD_Q,2          ,store as Q14 output

```

```

*----- Pulse shaping + Interpolating for Data I -----
        lacc     #0h

```

```

zpr
lar      ar5,#Lst_DI
PS_17   rpt      #11
macd     obj7,*-
apac
sach     MOD_I,2          ,store as Q14 output

```

\*-----END of Pulse shaping-----

```
CALL     CH_IP
```

\*Multiply (complex) transmitted signal and flat fading

```

lacc     #0h
ldp      #8h
lt       RF_I
ldp      #9h
mpy      MOD_I          ;Preg=RF_I*MOD_I
ldp      #8h
lt       RF_Q
ldp      #9h
mpya     MOD_Q          ;Preg=RF_Q*MOD_Q ; Acc=RF_I*MOD_I
mpys     MOD_I          ;Preg=RF_Q*MOD_I ; Acc=RF_I*MOD_I-RF_Q*MOD_Q
sach     RX_I,1          ;store as Q14
lacc     #0h
ldp      #8h
lt       RF_I
ldp      #9h
mpya     MOD_Q          ;Preg=RF_I*MOD_Q ; Acc=RF_Q*MOD_I
apac     MOD_I          ;Acc=RF_Q*MOD_I+RF_I*MOD_Q
sach     RX_Q,1

```

```

S_no8   idle
ldp      #9h
lacc     RX_I
*       lacc     MOD_I
*       ldp      #8h
*       lacc     RF_I
ldp      #58h
sac      0
ldp      #9h
lacc     RX_Q
*       lacc     MOD_Q
*       ldp      #8h
*       lacc     RF_Q
ldp      #58h
sac      1

```

\*----- Pulse shaping + Interpolating for Data Q -----

```

ldp      #9h
lacc     #0h
zpr
mar      *,ar5
lar      ar5,#Lst_DQ
PS_Q8   rpt      #11
macd     obj8,*-
apac
sach     MOD_Q,2          ,store as Q14 output

```

\*----- Pulse shaping + Interpolating for Data I -----

```

lacc     #0h
zpr
lar      ar5,#Lst_DI
PS_I8   rpt      #11
macd     obj8,*-
apac
sach     MOD_I,2          ,store as Q14 output

```

\*-----END of Pulse shaping-----



# CALL CH\_IP

\*Multiply (complex) transmitted signal and flat fading

```

lacc    #0h
ldp     #8h
lt      RF_I
ldp     #9h
mpy     MOD_I      ;Preg=RF_I*MOD_I
ldp     #8h
lt      RF_Q
ldp     #9h
mpya    MOD_Q      ;Preg=RF_Q*MOD_Q ; Acc=RF_I*MOD_I
mpys    MOD_I      ;Preg=RF_Q*MOD_I ; Acc=RF_I*MOD_I-RF_Q*MOD_Q
sach    RX_I,1      ;store as Q14
lacc    #0h
ldp     #8h
lt      RF_I
ldp     #9h
mpya    MOD_Q      ;Preg=RF_I*MOD_Q ; Acc=RF_Q*MOD_I
apac     ;Acc=RF_Q*MOD_I+RF_I*MOD_Q
sach    RX_Q,1

*
ldp     #9h
lacc    adshift
sub     #1h
sac1    adshift      ;dshift=dshift-1
bend    ip_over,cq    ;if dshift=0 branch to ip_over
lacc    #1h          ;else set ipfact=1 i.e. continue
ldp     #6h
sac1    aipfact      ;interpolation for fading
b       loop         ;and generate new data symbol
ip_over lacc    adfreq      ;set dshift to initial value
sac1    adshift      ;to continue the cycle
lacc    #0h          ;set ipfact=0 to generate new fading
ldp     #6h
sac1    aipfact      ;point as well
b       loop

```

\*Subroutine for multiphase interpolation filtering for Channel I and Q

```

CH_IP   ldp     #8h
lacc    sub_fil
samm    bmar
lacc    #0h

*-----Interpolating for Channel Q -----
zpr
mar     *,ar4
lar     ar4,#Lst_dsQ
rpt     #5
mads    *.
apac
sach    RF_Q,1      ,store as Q15 output

*-----Interpolating for Channel I -----
lacc    sub_fil
samm    bmar
lacc    #0h
zpr
lar     ar4,#Lst_dsl
rpt     #5
mads    *.
apac
sach    RF_I,1      ,store as Q15 output

*-----Channel Interpolation-----
lacc    ip_index      ;previous subfilter count
sub     #1h          ;decrement by one
sac1    ip_index      ;new subfilter number
bend    ip_last,cq    ;when filtering is complete branch to last

```

```

        lacc      sub_fil      ;previous address of subfilter coeff
        add      #6           ;add 4
        sac1     sub_fil      ;new subfilter address
        ret

ip_last  lar      ar4,#Lst_dsQ      ;After last subfilter
        rpt      #6
        dmov     *-           ;move data up the delay line
        lar      ar4,#Lst_dsl
        rpt      #6
        dmov     *-
        lacc     ini_adr      ;re-initialize the first subfilter address
        sac1     sub_fil
        lacc     ip_count     ;re-initialize the subfilter count
        sac1     ip_index
        ret

        .end

```

**\* PROGRAM : IF4\_20.ASM**  
**\* RECEIVED SIGNAL SAMPLE GENERATING PROGRAM**  
**\* Doppler shift fd=20Hz**  
**\* Change channel interpolating to 32\*11 taps**  
**\* Additional Files Req'd.: SHIFT7.ASM+DSC2.ASM+IPC352\_1.ASM**

```

        .mmregs

*Table for prws generation simulating circular buffer (CB)
        .ds      0300h      ;Start address for shift reg table
        .include "shift7.asm" ;Table of length (31*3)=93 words
I_mask  .word     508       ;Mask for I Channel
Q_mask  .word     65024     ;Mask for Q Channel
ipfact   .word     0        ;initial status for interpolation

* 121 coeff. for doppler shift FIR filter
        .ps      0990h
        .include "dsc2.asm" ;Table of Coeff for Doppler Shift filter

*Address value for ipfact used for fading interpolation
aipfact  .set 200h          ;if ipfact=0 interpolation is over

*Address values for Iprws,Qprws in Data mem.
I_ch     .set     360h      ;I channel in upper seven bits
Q_ch     .set     3dbh      ;Q channel in upper seven bits

*Address for first Coeff of DS filter in Prog. mem.
coeffp   .set     0990h     ;Program memory address for DS filter coeff.

* Ichannel data page for filtering by DS filter
ds_Ich   .set     3dah      ;DS filter output for I channel
lst_Ich   .set     361h      ;First delay element for I channel
Lst_Ich   .set     3d8h      ;361h+dec(120) Last delay element for I channel
        .ds      361h
        .space    780h      ;Initialize delay elements with zeros
                        ;780h = no. of bits = (120 * 16)hex

* Qchannel data page for filtering by DS filter
ds_Qch   .set     455h      ;DS filter output for I channel
lst_Qch   .set     3dch      ;First delay element for I channel
Lst_Qch   .set     453h      ;362h+dec(120) Last delay element for I channel
        .ds      3dch
        .space    780h      ;Initialize delay elements with zeros
                        ;780h = no. of bits = (120 * 16)hex

*32*11 point for fd=20Hz
        .ps      2080h
        .include "ipc352_1.asm" ;Table of coeff. for channel interpolating filter

```

\* Q channel data page for interpolating filter delay line

```

lst_dsQ .set 456h
lst_dsQ .set 45fh ;45ah 6 taps;458h >4 taps for MP::for 11 taps 45fh
RF_Q .set 461h
      .ds 456h
      .space 0b0h

```

\* I channel data page for interpolating filter delay line

```

ds_1chl .set 465h
lst_dsl .set 466h
lst_dsl .set 46fh ;46ah 6 taps;468h >4 taps for MP:: for 11 taps46fh
RF_I .set 471h
      .ds 466h
      .space 0b0h
      .ds 47ah
ip_count .word 32 ;16=40Hz;32=20Hz;64=10Hz
ip_index .word 32
ini_adr .word 8320 ;2080h ;initial address for filter coeff
sub_fil .word 8320 ;2080h ;subfilter coeff. address

```

\* Data page 9 for Transmit Signal generation

\* from address 4a0 to 4ffh only.

```

D_mask .set 4a0h
Data .set 4a1h
E_tbl .set 4a2h
E_data .set 4a3h
prv_ph .set 4a4h
M_tbl .set 4a5h

M_DI .set 4a6h
lst_DI .set 4a7h
lst_DI .set 4b1h
MOD_I .set 4b3h

M_DQ .set 4b6h
lst_DQ .set 4b7h
lst_DQ .set 4c1h
MOD_Q .set 4c3h

RX_I .set 4c4h
RX_Q .set 4c5h

adshift .set 4c6h
adfreq .set 4c7h

      .ds 4a0h
      .word 3 ;Data Mask =3
      .word 0 ;Data value
      .word 8192 ;dma:4a2>E_tbl(2000h)
      .word 0000h ;dma:4a3>E_data
      .word 0000h ;dma:4a4>prv_ph
      .word 8208 ;dma:4a5>M_tbl(2010h)

      .ds 4a7h ;Delay line for data I
      .space 0c0h ;Initialize to zero

      .ds 4b7h ;Delay line for data Q
      .space 0c0h ;Initialize to zero

```

\*Initial setting for Doppler Shift Value

```

      .ds 4c6h
dshift .word 4 ;= dfreq ;To set initial value of doppler shift/freq.
dfreq .word 4 ;= dshift ;80Hz=1; 40Hz=2; 20Hz=4; 10Hz=8.

```

\*Look-up Table for encoder in program memory

```

.ps 2000h
.word 0001,0003,0007,0005

```

\*Look up table for Modulator in Q14 notation

```
.ps      2010h
.word    16384,0
.word    11585,11585
.word    0,16384
.word    -11585,11585
.word    -16384,0
.word    -11585,-11585
.word    0,-16384
.word    11585,-11585
```

```
.ps      2020h
.include "psc2.asm"           ;Table of Coeff for Pulse Shaping filter
```

\*Set up the address for interrupt service routine vector

```
.ps      00806h
rete

.ps      00b00h
.entry
SETC     INTM                 ; Disable interrupts
LDP      #0                   ; Set data page pointer
OPL      #0834h,PMST
LACC     #0
SAMB     CWSR                 ; Set software wait state to 0
SAMB     PDWSR
CLRC     OVM                   ; OVM = 0
SPM      0
SETC     SXM
LDP      DXR
SPLK     #0h,DBMR             ;Used for comparison for fd change
SPLK     #06h,IMR
SPLK     #20h,TCR             ; To generate 10 MHz from Tout
SPLK     #01h,PRD             ; for AIC master clock
LACC     #00c0h               ; Reset tx/rx port
SACL     SPC
CLRC     INTM                 ; enable
```

\*PRWS generation

```
lar      ar6,#0300h
```

```
S_no1
loop      idle
          ldp      #9h
          lacc     RX_I
*         lacc     MOD_I
*         ldp      #8h
*         lacc     RF_I
          ldp      #58h
          sacb     0
          ldp      #9h
          lacc     RX_Q
*         lacc     MOD_Q
*         ldp      #8h
*         lacc     RF_Q
          ldp      #58h
          sacb     1
```

\*\*\*\*\*PRWS GENERATION\*\*\*\*\*

```
mar      *,ar6
lacc     *+                   ;load acc. with TAP:2
lar      ar6,*                 ;Get address for TAP:30
xor      *                     ;XOR for M-sequence PRWS method
sacb     *,ar6                 ;Pseudo Random Word Seq.
mar      *,ar6
sacb     *+                   ;Store result in TAP:30
```

```

mar      *,ar6          ;Update address for New TAP.2
lar      ar6,*
*****END of PRWS generation*****
*Check if new value for fading to be generated or to continue
*with interpolation
ldp      #6h
cpl      aipfact          ;chk if ipfact=0(DBMR) set TC=1 else TC=0
bend     ip_cont,NTC      ;If TC=0 Branch to interpolation else new sample

ldp      #6h
lacc     I_mask
andb
sac1     I_ch,7          ;Store Channel I value
lacc     I_ch            ;scaling Channel I value
sfr
*
sfr
sac1     I_ch
lacc     Q_mask
andb
ldp      #7h
sac1     Q_ch            ;Store Channel Q value

*As the DS filter is overflowing reduce the mag. of
*its input. One SFR command is OK but two SFR reduces any
*remote chance of overflow.
*We have used setc SXM mode so as to maintain the sign
lacc     Q_ch
sfr
sfr
sac1     Q_ch

*-----I Channel FIR DOPPLER SHIFT FILTER-----
*Doppler shift Filter 120 length FIR filter
lacc     #0h            ;Zero Accumulator
zpr
mar      *,ar3
lar      ar3,#1.st_Ich
DSF_I    rpt            #120          ;FIR filter for Doppler Shift
macd     coeffp,*-
apac
ldp      #7h
sach     ds_Ich,1        ;not really reqd. to save here.
ldp      #8h
sach     ds_Ich1,1        ;store on two locations
*-----END of I channel Doppler shift filter-----

*-----Q Channel FIR DOPPLER SHIFT FILTER-----
*Doppler shift Filter 120 length FIR filter
ldp      #8h            ;data page no.
lacc     #0h            ;Zero Accumulator
zpr
*
mar      *,ar3
lar      ar3,#Lst_Qch
DSF_Q    rpt            #120          ;FIR filter for Doppler Shift
macd     coeffp,*-
apac
ldp      #8h
sach     ds_Qch,1

*-----END of Q channel Doppler shift filter-----

*Data generation
ip_cont  ldp      #9h
lacc     D_mask
andb
sac1     Data            ;Store Data value

*Data encoding

```

```

        lacc    E_tbl
        add     Data
        tblr    E_data

*Previous phase (state) reference
        lacc    E_data
        add     prv_ph
        and     #0007h
        sac1    prv_ph

*Data modulating
        sfl
        add     M_tbl
        tblr    M_DI
        add     #1
        tblr    M_DQ

*----- Pulse shaping + Interpolating for Data Q -----
        lacc    #0h
        zpr
        mar     *,ar5
        lar     ar5,#Lst_DQ
PS_Q1    rpt     #11
        mac     obj1,*-
        apac
        sach    MOD_Q,2           ,store as Q14 output

*----- Pulse shaping + Interpolating for Data I -----
        lacc    #0h
        zpr
        lar     ar5,#Lst_DI
PS_I1    rpt     #11
        mac     obj1,*-
        apac
        sach    MOD_I,2           ,store as Q14 output

*-----END of Pulse shaping-----

        CALL    CH_IP

*Multiply (complex) transmitted signal and flat fading

        lacc    #0h
        ldp     #8h
        lt      RF_I
        ldp     #9h
        mpy     MOD_I           ;Preg=RF_I*MOD_I
        ldp     #8h
        lt      RF_Q
        ldp     #9h
        mpya    MOD_Q           ;Preg=RF_Q*MOD_Q ; Acc=RF_I*MOD_I
        mpys    MOD_I           ;Preg=RF_Q*MOD_I ; Acc=RF_I*MOD_I-RF_Q*MOD_Q
        sach    RX_I,1           ;store as Q14
        lacc    #0h
        ldp     #8h
        lt      RF_I
        ldp     #9h
        mpya    MOD_Q           ;Preg=RF_I*MOD_Q ; Acc=RF_Q*MOD_I
        apac    ;Acc=RF_Q*MOD_I+RF_I*MOD_Q
        sach    RX_Q,1

S_no2    idle
        ldp     #9h
        lacc    RX_I
        *       lacc    MOD_I
        *       ldp     #8h
        *       lacc    RF_I
        ldp     #58h
        sac1    0

```

```

        ldp        #9h
        lacc      RX_Q
    *        lacc      MOD_Q
    *        ldp        #8h
    *        lacc      RF_Q
        ldp        #58h
        sac1      1

*----- Pulse shaping + Interpolating for Data Q -----
        ldp        #9h
        lacc      #0h
        zpr
        mar      *,ar5
        lar      ar5,#1st_DQ
PS_Q2    rpt      #11
        mac      obj2,*-
        apac
        sach      MOD_Q,2          ,store as Q14 output

*----- Pulse shaping + Interpolating for Data I -----
        lacc      #0h
        zpr
        lar      ar5,#Lst_DI
PS_I2    rpt      #11
        mac      obj2,*-
        apac
        sach      MOD_I,2          ,store as Q14 output

*-----END of Pulse shaping-----

        CALL      CH_IP
*Multiply (complex) transmitted signal and flat fading

        lacc      #0h
        ldp        #8h
        lt        RF_I
        ldp        #9h
        mpy      MOD_I          ;Preg=RF_I*MOD_I
        ldp        #8h
        lt        RF_Q
        ldp        #9h
        mpya     MOD_Q          ;Preg=RF_Q*MOD_Q ; Acc=RF_I*MOD_I
        mpys     MOD_I          ;Preg=RF_Q*MOD_I ; Acc=RF_I*MOD_I-RF_Q*MOD_Q
        sach     RX_I,1          ;store as Q14
        lacc      #0h
        ldp        #8h
        lt        RF_I
        ldp        #9h
        mpya     MOD_Q          ;Preg=RF_I*MOD_Q ; Acc=RF_Q*MOD_I
        apac     MOD_I          ;Acc=RF_Q*MOD_I+RF_I*MOD_Q
        sach     RX_Q,1

S_no3    idle
        ldp        #9h
        lacc      RX_I
    *        lacc      MOD_I
    *        ldp        #8h
    *        lacc      RF_I
        ldp        #58h
        sac1      0
        ldp        #9h
        lacc      RX_Q
    *        lacc      MOD_Q
    *        ldp        #8h
    *        lacc      RF_Q
        ldp        #58h
        sac1      1

```

```

*----- Pulse shaping + Interpolating for Data Q -----
        ldp        #9h
        lacc        #0h
        zpr
        mar        *,ar5
        lar        ar5,#Lst_DQ
PS_Q3    rpt        #11
        mac        obj3,*-
        apac
        sach        MOD_Q,2          ,store as Q14 output
*----- Pulse shaping + Interpolating for Data I -----
        lacc        #0h
        zpr
        lar        ar5,#Lst_DI
PS_I3    rpt        #11
        mac        obj3,*-
        apac
        sach        MOD_I,2          ,store as Q14 output
*-----END of Pulse shaping-----

        CALL      CH_IP

*Multiply (complex) transmitted signal and flat fading

        lacc        #0h
        ldp        #8h
        lt         RF_I
        ldp        #9h
        mpy        MOD_I          ;Preg=RF_I*MOD_I
        ldp        #8h
        lt         RF_Q
        ldp        #9h
        mpya       MOD_Q          ;Preg=RF_Q*MOD_Q ; Acc=RF_I*MOD_I
        mpys       MOD_I          ;Preg=RF_Q*MOD_I ; Acc=RF_I*MOD_I-RF_Q*MOD_Q
        sach       RX_I,1          ;store as Q14
        lacc        #0h
        ldp        #8h
        lt         RF_I
        ldp        #9h
        mpya       MOD_Q          ;Preg=RF_I*MOD_Q ; Acc=RF_Q*MOD_I
        apac       ;Acc=RF_Q*MOD_I+RF_I*MOD_Q
        sach       RX_Q,1

S_no4    idle
        ldp        #9h
        lacc       RX_I
*        lacc       MOD_I
*        ldp        #8h
*        lacc       RF_I
        ldp        #58h
        sac1       0
        ldp        #9h
        lacc       RX_Q
*        lacc       MOD_Q
*        ldp        #8h
*        lacc       RF_Q
        ldp        #58h
        sac1       1

*----- Pulse shaping + Interpolating for Data Q -----
        ldp        #9h
        lacc        #0h
        zpr
        mar        *,ar5
        lar        ar5,#Lst_DQ
PS_Q4    rpt        #11
        mac        obj4,*-
        apac

```



```

sach      MOD_Q,2          ,store as Q14 output
*----- Pulse shaping + Interpolating for Data I -----
lace      #0h
zpr
lar      ar5,#Lst_DI
PS_I4     rpt      #11
mac      obj4,*-
apac
sach      MOD_I,2          ,store as Q14 output
*-----END of Pulse shaping-----

CALL      CH_IP
*Multiply (complex) transmitted signal and flat fading

lace      #0h
ldp      #8h
lt      RF_I
ldp      #9h
mpy      MOD_I          ;Preg=RF_I*MOD_I
ldp      #8h
lt      RF_Q
ldp      #9h
mpya     MOD_Q          ;Preg=RF_Q*MOD_Q ; Acc=RF_I*MOD_I
mpys     MOD_I          ;Preg=RF_Q*MOD_I ; Acc=RF_I*MOD_I-RF_Q*MOD_Q
sach     RX_I,1          ;store as Q14
lace      #0h
ldp      #8h
lt      RF_I
ldp      #9h
mpya     MOD_Q          ;Preg=RF_I*MOD_Q ; Acc=RF_Q*MOD_I
apac     RX_Q,1          ;Acc=RF_Q*MOD_I+RF_I*MOD_Q
sach

S_no5     idle
ldp      #9h
lace     RX_I
*      lace     MOD_I
*      ldp      #8h
*      lace     RF_I
ldp      #58h
sac1     0
ldp      #9h
lace     RX_Q
*      lace     MOD_Q
*      ldp      #8h
*      lace     RF_Q
ldp      #58h
sac1     1

*----- Pulse shaping + Interpolating for Data Q -----
ldp      #9h
lace     #0h
zpr
mar      *,ar5
lar      ar5,#Lst_DQ
PS_Q5     rpt      #11
mac      obj5,*-
apac
sach      MOD_Q,2          ,store as Q14 output
*----- Pulse shaping + Interpolating for Data I -----
lace      #0h
zpr
lar      ar5,#Lst_DI
PS_I5     rpt      #11
mac      obj5,*-
apac
sach      MOD_I,2          ,store as Q14 output

```

\*-----END of Pulse shaping-----

CALL CH\_IP

\*Multiply (complex) transmitted signal and flat fading

```

lacc    #0h
ldp     #8h
lt      RF_I
ldp     #9h
mpy     MOD_I          ;Preg=RF_I*MOD_I
ldp     #8h
lt      RF_Q
ldp     #9h
mpya    MOD_Q          ;Preg=RF_Q*MOD_Q ; Acc=RF_I*MOD_I
mpys    MOD_I          ;Preg=RF_Q*MOD_I ; Acc=RF_I*MOD_I-RF_Q*MOD_Q
sach    RX_I,1         ;store as Q14
lacc    #0h
ldp     #8h
lt      RF_I
ldp     #9h
mpya    MOD_Q          ;Preg=RF_I*MOD_Q ; Acc=RF_Q*MOD_I
apac    ;Acc=RF_Q*MOD_I+RF_I*MOD_Q
sach    RX_Q,1

```

```

S_no6   idle
ldp     #9h
lacc    RX_I
*       lacc    MOD_I
*       ldp     #8h
*       lacc    RF_I
ldp     #58h
sac1    0
ldp     #9h
lacc    RX_Q
*       lacc    MOD_Q
*       ldp     #8h
*       lacc    RF_Q
ldp     #58h
sac1    1

```

\*----- Pulse shaping + Interpolating for Data Q -----

```

ldp     #9h
lacc    #0h
zpr
mar     *,ar5
lar     ar5,#Lst_DQ
PS_Q6   rpt     #11
mac     obj6,*-
apac
sach    MOD_Q,2        ,store as Q14 output

```

\*----- Pulse shaping + Interpolating for Data I -----

```

lacc    #0h
zpr
lar     ar5,#Lst_DI
PS_I6   rpt     #11
mac     obj6,*-
apac
sach    MOD_I,2        ,store as Q14 output

```

\*-----END of Pulse shaping-----

CALL CH\_IP

\*Multiply (complex) transmitted signal and flat fading

```

lacc    #0h

```

```

ldp      #8h
lt       RF_I
ldp      #9h
mpy      MOD_I      ;Preg=RF_I*MOD_I
ldp      #8h
lt       RF_Q
ldp      #9h
mpya     MOD_Q      ;Preg=RF_Q*MOD_Q ; Acc=RF_I*MOD_I
mpys     MOD_I      ;Preg=RF_Q*MOD_I ; Acc=RF_I*MOD_I-RF_Q*MOD_Q
sach     RX_I,1      ;store as Q14
lacc     #0h
ldp      #8h
lt       RF_I
ldp      #9h
mpya     MOD_Q      ;Preg=RF_I*MOD_Q ; Acc=RF_Q*MOD_I
apac     ;Acc=RF_Q*MOD_I+RF_I*MOD_Q
sach     RX_Q,1

S_no7    idle
ldp      #9h
lacc     RX_I
*        lacc     MOD_I
*        ldp      #8h
*        lacc     RF_I
ldp      #58h
saci     0
ldp      #9h
lacc     RX_Q
*        lacc     MOD_Q
*        ldp      #8h
*        lacc     RF_Q
ldp      #58h
saci     1

*----- Pulse shaping + Interpolating for Data Q -----
ldp      #9h
lacc     #0h
zpr
mar      *,ar5
lar      ar5,#Lst_DQ
PS_Q7    rpt      #11
mac      obj7,*-
apac
sach     MOD_Q,2      ,store as Q14 output
*----- Pulse shaping + Interpolating for Data I -----
lacc     #0h
zpr
lar      ar5,#Lst_DI
PS_I7    rpt      #11
mac      obj7,*-
apac
sach     MOD_I,2      ,store as Q14 output

*-----END of Pulse shaping-----

CALL     CH_IP

*Multiply (complex) transmitted signal and flat fading

lacc     #0h
ldp      #8h
lt       RF_I
ldp      #9h
mpy      MOD_I      ;Preg=RF_I*MOD_I
ldp      #8h
lt       RF_Q
ldp      #9h

```

```

        mpya    MOD_Q          ;Preg=RF_Q*MOD_Q ; Acc=RF_I*MOD_I
        mpys    MOD_I          ;Preg=RF_Q*MOD_I ; Acc=RF_I*MOD_I-RF_Q*MOD_Q
        sach    RX_I,1         ;store as Q14
        lacc    #0h
        ldp     #8h
        lt      RF_I
        ldp     #9h
        mpya    MOD_Q          ;Preg=RF_I*MOD_Q ; Acc=RF_Q*MOD_I
        apac    MOD_I          ;Acc=RF_Q*MOD_I+RF_I*MOD_Q
        sach    RX_Q,1

S_no8      idle
        ldp     #9h
        lacc    RX_I
        *      lacc    MOD_I
        *      ldp     #8h
        *      lacc    RF_I
        ldp     #58h
        sacd    0
        ldp     #9h
        lacc    RX_Q
        *      lacc    MOD_Q
        *      ldp     #8h
        *      lacc    RF_Q
        ldp     #58h
        sacd    1

*----- Pulse shaping + Interpolating for Data Q -----
        ldp     #9h
        lacc    #0h
        zpr
        mar     *,ar5
        lar     ar5,#Lst_DQ
        PS_Q8   rpt           #11
        macd    obj8,*-
        apac
        sach    MOD_Q,2        ,store as Q14 output
*----- Pulse shaping + Interpolating for Data I -----
        lacc    #0h
        zpr
        lar     ar5,#Lst_DI
        PS_I8   rpt           #11
        macd    obj8,*-
        apac
        sach    MOD_I,2        ,store as Q14 output
*-----END of Pulse shaping-----

        CALL    CH_IP

*Multiply (complex) transmitted signal and flat fading

        lacc    #0h
        ldp     #8h
        lt      RF_I
        ldp     #9h
        mpy     MOD_I          ;Preg=RF_I*MOD_I
        ldp     #8h
        lt      RF_Q
        ldp     #9h
        mpya    MOD_Q          ;Preg=RF_Q*MOD_Q ; Acc=RF_I*MOD_I
        mpys    MOD_I          ;Preg=RF_Q*MOD_I ; Acc=RF_I*MOD_I-RF_Q*MOD_Q
        sach    RX_I,1         ;store as Q14
        lacc    #0h
        ldp     #8h
        lt      RF_I
        ldp     #9h
        mpya    MOD_Q          ;Preg=RF_I*MOD_Q ; Acc=RF_Q*MOD_I
        apac    MOD_I          ;Acc=RF_Q*MOD_I+RF_I*MOD_Q

```

```

sach      RX_Q,1
*
ldp      #9h
lacc     adshift
sub      #1h
sac1     adshift      ;dshift=dshift-1
bend     ip_over,eq    ;if dshift=0 branch to ip_over
lacc     #1h          ;else set ipfact=1 i.e. continue
ldp      #6h
sac1     aipfact      ;interpolation for fading
b        loop         ;and generate new data symbol
ip_over  lacc     adfreq ;set dshift to initial value
sac1     adshift      ;to continue the cycle
lacc     #0h          ;set ipfact=0 to generate new fading
ldp      #6h
sac1     aipfact      ;point as well
b        loop

```

\*Subroutine for multiphase interpolation filtering for Channel I and Q

```

CH_IP    ldp      #8h
lacc     sub_fil
samm     bmar
lacc     #0h
*-----Interpolating for Channel Q -----
zpr
mar      *,ar4
lar      ar4,#Lst_dsQ
rpt      #10
mads     *-
apac
sach     RF_Q,1      ;store as Q15 output
*-----Interpolating for Channel I -----
lacc     sub_fil
samm     bmar
lacc     #0h
zpr
lar      ar4,#Lst_dsl
rpt      #10
mads     *-
apac
sach     RF_I,1      ;store as Q15 output
*-----END of Channel Interpolation-----
lacc     ip_index    ;previous subfilter count
sub      #1h         ;decrement by one
sac1     ip_index    ;new subfilter number
bend     ip_last,eq  ;when filtering is complete branch to last
lacc     sub_fil     ;previous address of subfilter coeff
add      #11         ;add 11
sac1     sub_fil     ;new subfilter address
ret
ip_last  lar      ar4,#Lst_dsQ ;After last subfilter
rpt      #10
dmov     *-         ;move data up the delay line
lar      ar4,#Lst_dsl
rpt      #10
dmov     *-
lacc     ini_adr     ;re-initialize the first subfilter address
sac1     sub_fil
lacc     ip_count    ;re-initialize the subfilter count
sac1     ip_index
ret
.end

```

\*PROGRAM : map.cmd  
 \*C30 Linker Command File containing Memory Map

/\* All Memory is RAM \*/

MEMORY /\* This describes the hardware \*/

{  
 /\* External SRAM on the Main Board \*/

VECTS:	origin=000000h	length=000C0h	/* Part of Bank0 */	
EPROG:	origin=0000d0h	length=00380h	/* Zero-wait */	
EDTBLK:	origin=000450h	length=00330h	/* Zero-wait */	
MAP:	origin=000780h	length=00080h	/* Zero-wait */	
/*	PROG:	origin=000160h	length=00300h	Zero-wait */
/*	MAP:	origin=000460h	length=00200h	Zero-wait */
/*	DTBLK:	origin=000660h	length=001A0h	Zero-wait */

/\* The gap in between PROG DTBLK is used for buffering  
 since this region of memory will be transferred to  
 809800h, this gap is reserved for the buffer \*/

BANK0:	origin=000800h	length=0F800h	/* Zero-wait */
BANK1:	origin=010000h	length=10000h	/* SRAM upgrade option */
BANK2:	origin=020000h	length=10000h	/* SRAM upgrade option */
BANK3:	origin=030000h	length=0F400h	/* One-wait */

/\* Bank 3 is dual-ported between the 'C30 and the PC.  
 The length shown is for the default 64Kx4 devices, but 16Kx4 can be used.  
 In both cases the top C00h locations are reserved for monitor use.  
 If the monitor is not used, you can have this area. \*/

/\* Cached DRAM Memory Expansion on Daughter Board \*/

EXPAND:	origin=400000h	length=400000h	/* One of various options */
---------	----------------	----------------	------------------------------

/\* On-chip \*/

BLK0_P:	origin=809800h	length=300h
BLK0_M:	origin=809B00h	length=300h
BLK1_D:	origin=809E00h	length=200h

}

SECTIONS /\* Allocates uses to the hardware \*/

```
{
    .init:    {}      load=VECTS
    .c.text:  {}      load=EPROG
    .edata:   {}      load=EDTBLK
    .map:     {}      load=MAP
    /*      .text:    {}      load=PROG
    .data:    {}      load=DTBLK
    .dual:    {}      load=BANK3      */
}
```

\*PROGRAM : b1.asm

\*CHANNEL ESTIMATION FILTER (AVERAGING FILTER) COEFFICIENT

\*Design using Remez exchange algorithm in Matlab

.float	0,0,0,0,0,0,0,0
.float	-3.926372438188776e-004
.float	-1.813169595538090e-003
.float	2.030365302177151e-003

```

.float      3.246944093698858e-003
.float      2.866728976386388e-003
.float      -1.195512611524607e-003
.float      -7.147002615347359e-003
.float      -1.017372560841225e-002
.float      -5.340408466161841e-003
.float      7.628598999227749e-003
.float      2.159887944285561e-002
.float      2.461030015014358e-002
.float      7.854643868360649e-003
.float      -2.536674816506901e-002
.float      -5.641569517189035e-002
.float      -5.812463639649386e-002
.float      -9.718022814264368e-003
.float      8.828031503043306e-002
.float      2.089504950612768e-001
.float      3.085997315447801e-001
.float      0
.float      3.085997315447801e-001
.float      2.089504950612768e-001
.float      8.828031503043306e-002
.float      -9.718022814264368e-003
.float      -5.812463639649386e-002
.float      -5.641569517189035e-002
.float      -2.536674816506901e-002
.float      7.854643868360649e-003
.float      2.461030015014358e-002
.float      2.159887944285561e-002
.float      7.628598999227749e-003
.float      -5.340408466161841e-003
.float      -1.017372560841225e-002
.float      -7.147002615347359e-003
.float      -1.195512611524607e-003
.float      2.866728976386388e-003
.float      3.246944093698858e-003
.float      2.030365302177151e-003
.float      -1.813169595538090e-003
.float      -3.926372438188776e-004
.float      0,0,0,0,0,0,0,0

```

\*PROGRAM : h1.asm

\*Header used in ADDN1.ASM

```

primwd      .set      0800h
expwd       .set      0000h
primary     .set      4
expanse     .set      0
BPF_TL      .set      96
z_isi1      .set      576h
z_isi2      .set      577h
SEED_LEN    .set      31
AVF_TL      .set      61
DIBUF_LEN   .set      31
NSDLEN      .set      28
NSCALE1     .set      1.0e-06

```

```

;length of noise seed generator
;Factor K to change S/N (K<1)

```

```

      .sect      ".init"
RESET    .word    start
INT0      .word    start
INT1      .word    TXDATA
INT2      .word    start
INT3      .word    start
XINT0     .word    start
RINT0     .word    start
XINT1     .word    start
RINT1     .word    start
TINT0     .word    start

```

```

TINT1 .word start
DINT .word start
*To store output in memory if debugging is reqd.
.sect ".map"
.space 128
.data ".edata"
BUS_CTL .word 00808060h ;450h Primary and Expansion Bus Address
* .data
BUFFER .word 00040000h ;451h
ADCADR .word 00804000h ;452h Address Channel A Analog interface
TIMECTL .word 00808030h ;453h TIMER 1 CONTROL REGISTER
PERIOD .word 00808038h ;454h TIMER 1 PERIOD REGISTER
RSTCTRL .word 601h ;455h TIMER 1 CONTROL REG. TO STOP TIMER
SETCTRL .word 6c1h ;456h TIMER 1 CONTROL REG. TO START TIMER
COUNT .word 868 ;457h for 9600 samples/sec
; 6944 for 1200 samples/sec ;TIMER 1 PERIOD
INC .word 1h ;458h SW wait for DSP C50
VALUE .word 9000000 ;459h SW wait for DSP C50
VALUE2 .word 500 ;45ah Debugging Loop
VALUE3 .word 0 ;45bh RAMP GENERATE
INC3 .word 1000000h ;45ch RAMP GENERATE
zero .word 0000h ;45dh
one .word 1 ;45eh
SEED2 .word 460h ;45fh seed2 address
SEED .int 1,0,3,0,0,1,0,0,2,1,1,2,1,3,3
.int 0,3,1,2,1,2,1,2,3,3,2,1,3,0,1,3
;460h to 47eh seed values
.space 1 ;47fh
;BP FILTER COEFF. from 480h to 4dth
* BPF filter coeff
.float -100,-74,-21,45,108,150,157,123
.float 52,-39,-128,-191,-207,-168,-81,33
.float 145,218,226,157,19,-156,-319,-417
.float -399,-242,47,419,795,1070,1143,936
.float 421,-362,-1299,-2214,-2887,-3091,-2631,-1388
.float 654,3389,6596,9958,13109,15681,17365,17951
.float 17365,15681,13109,9958,6596,3389,654,-1388
.float -2631,-3091,-2887,-2214,-1299,-362,421,936
.float 1143,1070,795,419,47,-242,-399,-417
.float -319,-156,19,157,226,218,145,33
.float -81,-168,-207,-191,-128,-39,52,123
.float 157,150,108,45,-21,-74,-100,-96
.space 29 ;4e0h to 4fch
BPF_COF .word 480h ;4fdh Received Filter (BPF) Coeff. start address
BPI_DLS .word 500h ;4feh BPF Delay line start for I signal
BPI_DLE .word 55fh ;4fth BPF Delay line end for I signal
DL_I .space 96 ;500h to 55fh Delay line = 96 for I signal
I1 .float 0.0 ;560h (560hto563h)>BPF filter output array for Ik,Ikm1,Qk,Qkm1
Q1 .float 0.0 ;561h
I2 .float 0.0 ;562h
Q2 .float 0.0 ;563h
SIGN_U .word 0080000000h ;564h To extract sign of U for first decision
SIGN_V .word 0040000000h ;565h To extract sign of V for first decision
.space 10 ;566h to 56fh
DATA0 .word 0h ;570h First Decision Data 00
DATA2 .word 2h ;571h First Decision Data 10
DATA1 .word 1h ;572h First Decision Data 01
DATA3 .word 3h ;573h First Decision Data 11
D1 .word 0h ;574h First Decision for Data
.space 1 ;575h
Lz_isi1 .word 0h ;576h Store zero isi point(obj 8) for scope output
Lz_isi2 .word 0h ;577h Store zero isi point(obj16) for scope output
CONST2 .word 562h ;578h
D1_TBL .word 570h ;579h Decision first look-up table address
STORE .word 0780h ;57ah Store in .map for debugging
D1_DATA .word 0 ;57bh Store data (delay=11) to compare with D1
D1_ERR .word 0 ;57ch Number of errors after first decision
D1_DLY .word 261 ;57dh Delay of 11 before BPR calculation for D1

```



DATA_PT	word	0		;57ch Number of Data points used for D1 error calculation
	space	1		;57fh
DL_Q	space	96		;580h to 5dfh Delay line = 96 for Q signal
BPO_DLS	word	580h		;5e0h
BPO_DLE	word	5dfh		;5e1h
CONSTEL	word	560h		;5e2h
Up_dly	word	0h		;5e3h
Vp_dly	word	0h		;5e4h
D1_0	word	0		;5e5h to 5ebh Constellation points for shift...
D1_1	word	1		;5e6h ...as per index Q
D1_3	word	3		;5e7h
D1_2	word	2		;5e8h
RPT_0	word	0		;5e9h
RPT_1	word	1		;5eah
RPT_3	word	3		;5ebh
D2	word	0		;5ech Second decision value
	space	3		;5edh to 5efh
D10_5f0	word	5e5h		;5f0h Base address + first decision of 0
D11_5f0	word	5e6h		;5f1h
D12_5f0	word	5e8h		;5f2h
D13_5f0	word	5e7h		;5f3h
BASE_ADR	word	5f0h		;5f4h Base address for d1 addition
D2_DATA	word	0		;5f5h Store data (delay=41) to compare with D2
D2_ERR	word	0		;5f6h Number of errors after second decision
D2_DLY	word	291	;fading built up delay of 250pts ;41;	5f7h Delay of 41 before BER calculation for D2
SYMB_PT	word	0		;5f8h Number of Symbol points used for D2 error calculation
	space	6		;5f9h to 5feh
DATA_BUF	word	600h		;5ffh
DATA_ST	space	31		;600h to 61ch for data storage
D1_BUF	word	620h		;61fh First element of 30 word long buffer for first decision storage
D1_ST	space	31		;620h to 63ch for first decision storage
D1_DLY	word	0		;63fh Prev. 30th D1 so as to shift as per D2 (delay = av. filter length)
*Averaging Filter Coeff. ;640h to 67ch				
.include "b1.asm"				
AVF_COF	word	640h		;67dh Averaging Filter (AVF) Coeff. start address
AVU_DLS	word	680h		;67eh AVF Delay line start for Up signal
AVU_DLE	word	6bch		;67fh AVF Delay line end for Up signal
DL_Up	space	61		;680h to 6bch Delay line = 61 for Up signal
	space	1		;6bdh
AVV_DLS	word	6c0h		;6bch AVF Delay line start for Vp signal
AVV_DLE	word	6fch		;6bfh AVF Delay line end for Vp signal
DL_Vp	space	61		;6c0h to 6fch Delay line = 61 for Vp signal
	space	2		;6fdh & 6feh
D_BUF	word	700h		;6ffh pointer for data storage location
D_ST	space	42		;700h to 729h data storage for D2 BERT
*To add noise I and Q part				
	space	2		;72ah,72bh
NI	float	0		;72ch noise I part value after scaling
NQ	float	0		;72dh noise Q part value after scaling
POWI	float	0	;72ch	
POWQ	float	0	;72fh	
POWSP	int	0	;730h	
NSCALE	float	0.1		;731h Factor K to change S/N (K<1)
	space	13		;732h to 73ch
NSDLOC	word	740h		;73fh location for noise gen. seed
*seed value for noise I and Q ; 740h to 75bh				
NSEED	int	0c31171dfh,0c0bcdafdh,00af7a460h,0aec859efh		
	int	03018ca1dh,0c06da366h,077576b2ch,066d3f110h		
	int	09592d096h,038a1b32dh,05d6272d5h,0d1bd74f2h		
	int	00fc6aa5dh,030dd8927h,0abb33287h,0451ca49eh		
	int	05924ceadh,02d768b06h,0302a2020h,05e932b43h		
	int	072f618f5h,0bd32b343h,066b7d4e8h,0567fd695h		
	int	0a24af876h,08ddb5499h,01f25d897h,0c84d36bah		
RSP	word	STACK		;75ch Define Stack Location
STACK	word	0		;75dh Beginning of the stack

```

*PROGRAM : N1.ASM
*TO GENERATE, ADD, AND MEASURE NOISE

NGEN    PUSH    BK
        PUSH    AR2
        PUSH    IR0
        PUSHF   R6
        PUSHF   R7
        LDI     NSDLEN,BK                ;28 length long prbs generator
*GENERATE NOISE
        LDI     @NSDLOC,AR2              ;pointer to seed 2 (tap)
*        STI     AR2,*AR0++(1)            ;chk
        LDI     25,IR0
        LDI     0,R0
        XOR     *AR2++(IR0)%,R0,R0        ;seed 2 xor seed 27 => seed 27
        XOR     *AR2%,R0,R0
        STI     R0,*AR2++(2)%             ;store result over old seed 30
*        STI     R0,*AR0++(1)            ;chk
        STI     AR2,@NSDLOC              ;store new seed 2 address
*Separate NI and NQ
        LDI     R0,R1
*        STI     R0,*AR0++(1)            ;chk
        LSH     16,R0
        ASH     -16,R0
        ASH     -16,R1
*        STI     R0,*AR0++(1)            ;chk
*        STI     R1,*AR0++(1)            ;chk
        FLOAT   R0,R7
        FLOAT   R1,R6
*        STF     R7,*AR0++(1)            ;chk
*        STF     R6,*AR0++(1)            ;chk
*Scaling so as to change SNR by changing noise level
        LDF     @NSCALE,R4
        MPYF3   R7,R4,R0
        MPYF3   R6,R4,R1
*        STF     R0,*AR0++(1)            ;chk
*        STF     R1,*AR0++(1)            ;chk
        STF     R0,@NI                    ;store noise I in memory
        STF     R1,@NQ                    ;store noise Q in memory
        POPF    R7
        POPF    R6
        POP     IR0
        POP     AR2
        POP     BK
        RETS

*Add noise to the signal at the input of receiver
ADDN    LDF     @NI,R5                    ;R5=ni and R7=rxI
        LDF     @NQ,R4                    ;R4=nQ and R6=rxQ
*        STF     R5,*AR0++(1)            ;chk
*        STF     R4,*AR0++(1)            ;chk
*To make noise = zero
        LDF     @zero,R5
        LDF     @zcro,R4
*To make signal= zero
*        LDF     @zcro,R7
*        LDF     @zcro,R6
*Chk if pop and push are making R6,R7 work fine
*        STF     R7,*AR0++(1)            ;chk
*        STF     R6,*AR0++(1)            ;chk
*Add signal I and Q with noise I and Q
        ADDF3   R7,R5,R0                  ;Rxsni
        ADDF3   R6,R4,R1                  ;RxsnQ
*        STF     R0,*AR0++(1)            ;chk
*        STF     R1,*AR0++(1)            ;chk

```

```

        STF      R0,*AR5++%           ;store signal in BPF delay line
        STF      R1,*AR3++%           ;store signal in BPF delay line
        RETS

*To calculate Noise Power and Signal Power so as to find SNR
CSNR    MPYF3    R2,R2,R0
        MPYF3    R3,R3,R1
*        STF      R2,*AR0++(1)         ;chk
*        STF      R0,*AR0++(1)         ;chk
*        STF      R3,*AR0++(1)         ;chk
*        STF      R1,*AR0++(1)         ;chk
        LDF      @POWI,R4
        ADDEF3   R0,R4,R4
*        STF      R4,*AR0++(1)         ;chk
        STF      R4,@POWI
        LDF      @POWQ,R4
        ADDEF3   R1,R4,R4
*        STF      R4,*AR0++(1)         ;chk
        STF      R4,@POWQ
*Count the length of span to calculate power ratio
        LDI      @POWSP,R4
        ADDI     @one,R4
*        STI      R4,*AR0++(1)         ;chk
        STI      R4,@POWSP
        RETS

* PROGRAM : ADDN1.ASM
* RECEIVER ALGORITHM
        .include "hcs12em"
* External Program : C50, C30 address 0D0h
        .sect
* SET UP PRIMARY C50 EXPANSION BUS WAIT STATE
start    LDP      BUS_CTL
        LDI      @BUS_CTL,ar0
        LDI      primwd,r5
        LDI      expwd,r6
        STI      r5,*+ar0(primary)
        STI      r6,*+ar0(expanse)

* Set up Stack Pointer
        LDI      @RSP,SP
*SET UP DAC CHANNEL A,B
        LDI      @ADCA_DR,AR0
        LDI      0,R7
        STI      R7,*+AR0(0)
||       STI      R7,*+AR0(1)
* Set up BPF filter parameters
LOOP     LDI      BPF_TL,BK
        LDI      @BPQ_DLE,AR3           ;Load pointer for Q signal delay line
        LDI      @BPI_DLE,AR5           ;Load pointer for I signal delay line
        LDI      @BPF_COEF,AR4          ;Load pointer for Band-pass filter Coeff.
        LDI      @STORE,AR0

*Wait for C50 to stabilize
*Load C30 software; before starting C30 software
*load C50 software and run C30 software
*Use this time to Reset C50 and start C50 software
        LDI      @VALUE,AR6
        SUBI     @INC,AR6
        STI      AR6,@VALUE
        CMPI     0,AR6
        BZ       okstart
        BR       LOOP

okstart
*To start c50 at the same point always
* SET UP TIMER 1 to set sampling rate
        LDI      @TIMECTL,AR2
        LDI      @RSTCTRL,R2

```

```

        STI      R2,*AR2          ;RESET TIMER CONTROL REGISTER
        LDI      @PERIOD,AR6
        LDI      @COUNT,R2
        STI      R2,*AR6          ;SET TIMER 1 PERIOD REGISTER (PERIOD)
        LDI      @SETCTRL,R2
        STI      R2,*AR2          ;SET TIMER 1 CONTROL REGISTER (START)
* SET UP INTERRUPTS
        LDI      0H,IF
        LDI      2H,IE
        OR       2000H,ST
* WAIT FOR INTERRUPTS
* Use very first interrupt, so as to neglect the first buffer read
* of arbitrary data
        idle
* Continue with receiver logic
WAIT
obj1     idle
        LDI      @BUFFER,AR1      ;Read the C50 Buffer Output
        LDI      *AR1,R4
        *        STI      R4,*AR0++(1)      ;chk
        LDIU     R4,AR7
        LDIU     R4,AR6
        LSH      16,AR7
        ASH      -16,AR7           ;Store I signal separately
        ASH      -16,AR6           ;Store Q signal separately
        FLOAT    AR7,R7
        FLOAT    AR6,R6
        *        STF      R7,*AR0++(1)      ;chk
        *        STF      R6,*AR0++(1)      ;chk
        CALL     NGEN
        CALL     ADDN
        *        STF      R7,*AR3++%        ;Load I signal to C1 delay line
        *        STF      R6,*AR3++%        ;Load Q signal to C1 delay line
*B.P. Rx. Filter for I signal
        LDF      @zero,R0          ;Initialize intermediate storage registers
        LDF      @zero,R2
*FIR Filter for square root raised cosine received band-pass filter
*for I signal
        RPTS     BPF_TL-1
        MPYF3    *AR5++%,*AR4++%,R0
        ADDF3    R0,R2,R2
        ADDF      R0,R2            ;R2 has BP I filter output
*B.P. Rx. Filter for Q signal
        LDF      @zero,R1          ;Initialize intermediate storage registers
        LDF      @zero,R3
*FIR Filter for square root raised cosine received band-pass filter
*for Q signal
        RPTS     BPF_TL-1
        MPYF3    *AR3++%,*AR4++%,R1
        ADDF3    R1,R3,R3
        ADDF      R1,R3            ;R3 has BP Q filter output
        CALL     CSNR
        CALL     DATA

obj2     idle
        LDI      @BUFFER,AR1      ;Read the C50 Buffer Output
        LDI      *AR1,R4
        *        STI      R4,*AR0++(1)      ;chk
        LDIU     R4,AR7
        LDIU     R4,AR6
        LSH      16,AR7
        ASH      -16,AR7           ;Store I signal separately
        ASH      -16,AR6           ;Store Q signal separately
        FLOAT    AR7,R7
        FLOAT    AR6,R6
        *        STF      R7,*AR0++(1)      ;chk
        *        STF      R6,*AR0++(1)      ;chk
        CALL     NGEN

```

```

CALL    ADDN
*      STF    R7,*AR5++%           ;Load I signal to CB delay line
*      STF    R6,*AR3++%           ;Load Q signal to CB delay line
                                           ;B.P. Rx. Filter for I signal

      LDF    @zero,R0           ;Initialize intermediate storage registers
      LDF    @zero,R2
*FIR Filter for square root raised cosine received band-pass filter
      RPTS    BPF_TL-1
      MPYF3    *AR5++%,*AR4++%,R0
||      ADDF3    R0,R2,R2
      ADDF    R0,R2           ;R2 has BP I filter output
*B.P. Rx. Filter for Q signal
      LDF    @zero,R1           ;Initialize intermediate storage registers
      LDF    @zero,R3
*FIR Filter for square root raised cosine received band-pass filter
*for Q signal
      RPTS    BPF_TL-1
      MPYF3    *AR3++%,*AR4++%,R1
||      ADDF3    R1,R3,R3
      ADDF    R1,R3           ;R3 has BP Q filter output
      CALL    CSNR

obj3    idle
      LDI    @BUFFER,AR1           ;Read the C50 Buffer Output
      LDI    *AR1,R4
*      STI    R4,*AR0++(1)         ;chk
      LDIU    R4,AR7
      LDIU    R4,AR6
      LSH    16,AR7
      ASH    -16,AR7           ;Store I signal separately
      ASH    -16,AR6           ;Store Q signal separately
      FLOAT    AR7,R7
      FLOAT    AR6,R6
*      STF    R7,*AR0++(1)         ;chk
*      STF    R6,*AR0++(1)         ;chk
      CALL    NGEN
      CALL    ADDN
*      STF    R7,*AR5++%           ;Load I signal to CB delay line
*      STF    R6,*AR3++%           ;Load Q signal to CB delay line
                                           ;B.P. Rx. Filter for I signal
      LDF    @zero,R0           ;Initialize intermediate storage registers
      LDF    @zero,R2
*FIR Filter for square root raised cosine received band-pass filter
      RPTS    BPF_TL-1
      MPYF3    *AR5++%,*AR4++%,R0
||      ADDF3    R0,R2,R2
      ADDF    R0,R2           ;R2 has BP I filter output
*B.P. Rx. Filter for Q signal
      LDFU    @zero,R1           ;Initialize intermediate storage registers
      LDFU    @zero,R3
*FIR Filter for square root raised cosine received band-pass filter
*for Q signal
      RPTS    BPF_TL-1
      MPYF3    *AR3++%,*AR4++%,R1
||      ADDF3    R1,R3,R3
      ADDF    R1,R3           ;R3 has BP Q filter output
      CALL    CSNR

obj4    idle
      LDI    @BUFFER,AR1           ;Read the C50 Buffer Output
      LDI    *AR1,R4
*      STI    R4,*AR0++(1)         ;chk
      LDIU    R4,AR7
      LDIU    R4,AR6
      LSH    16,AR7
      ASH    -16,AR7           ;Store I signal separately
      ASH    -16,AR6           ;Store Q signal separately
      FLOAT    AR7,R7

```

```

*      FLOAT   AR6,R6
*      STF     R7,*AR0++(1)      ;chk
*      STF     R6,*AR0++(1)      ;chk
      CALL     NGEN
      CALL     ADDN
*      STF     R7,*AR5++%         ;Load I signal to CB delay line
*      STF     R6,*AR3++%         ;Load Q signal to CB delay line
                                   ;B.P. Rx. Filter for I signal
      LDF      @zero,R0           ;Initialize intermediate storage registers
      LDF      @zero,R2
*FIR Filter for square root raised cosine received band-pass filter
      RPTS     BPF_TL-1
      MPYF3    *AR5++%,*AR4++%,R0
||      ADDF3   R0,R2,R2
      ADDF     R0,R2              ;R2 has BP I filter output
*B.P. Rx. Filter for Q signal
      LDF      @zero,R1           ;Initialize intermediate storage registers
      LDF      @zero,R3
*FIR Filter for square root raised cosine received band-pass filter
*for Q signal
      RPTS     BPF_TL-1
      MPYF3    *AR3++%,*AR4++%,R1
||      ADDF3   R1,R3,R3
      ADDF     R1,R3              ;R3 has BP Q filter output
      CALL     CSNR

obj5    idle
      LDI      @BUFFER,AR1        ;Read the C50 Buffer Output
      LDI      *AR1,R4
*      STI      R4,*AR0++(1)      ;chk
      LDIU     R4,AR7
      LDIU     R4,AR6
      LSH      16,AR7
      ASH      -16,AR7             ;Store I signal separately
      ASH      -16,AR6             ;Store Q signal separately
      FLOAT    AR7,R7
      FLOAT    AR6,R6
*      STF     R7,*AR0++(1)      ;chk
*      STF     R6,*AR0++(1)      ;chk
      CALL     NGEN
      CALL     ADDN
*      STF     R7,*AR5++%         ;Load I signal to CB delay line
*      STF     R6,*AR3++%         ;Load Q signal to CB delay line
                                   ;B.P. Rx. Filter for I signal
      LDF      @zero,R0           ;Initialize intermediate storage registers
      LDF      @zero,R2
*FIR Filter for square root raised cosine received band-pass filter
      RPTS     BPF_TL-1
      MPYF3    *AR5++%,*AR4++%,R0
||      ADDF3   R0,R2,R2
      ADDF     R0,R2              ;R2 has BP I filter output
*B.P. Rx. Filter for Q signal
      LDF      @zero,R1           ;Initialize intermediate storage registers
      LDF      @zero,R3
*FIR Filter for square root raised cosine received band-pass filter
*for Q signal
      RPTS     BPF_TL-1
      MPYF3    *AR3++%,*AR4++%,R1
||      ADDF3   R1,R3,R3
      ADDF     R1,R3              ;R3 has BP Q filter output
      CALL     CSNR

obj6    idle
      LDI      @BUFFER,AR1        ;Read the C50 Buffer Output
      LDI      *AR1,R4
      LDIU     R4,AR7
      LDIU     R4,AR6
      LSH      16,AR7

```

```

        ASH      -16,AR7                      ;Store I signal separately
        ASH      -16,AR6                      ;Store Q signal separately
        FLOAT    AR7,R7
        FLOAT    AR6,R6
*       STF      R7,*AR0++(1)                ;chk
*       STF      R6,*AR0++(1)                ;chk
        CALL     NGEN
        CALL     ADDN
*       STF      R7,*AR5++%                  ;Load I signal to CB delay line
*       STF      R6,*AR3++%                  ;Load Q signal to CB delay line
                                           ;B.P. Rx. Filter for I signal

        LDF      @zero,R0                    ;Initialize intermediate storage registers
        LDF      @zero,R2
*FIR Filter for square root raised cosine received band-pass filter
        RPTS     BPF_TL-1
        MPYF3    *AR5++%,*AR4++%,R0
||      ADDF3    R0,R2,R2
        ADDF     R0,R2                      ;R2 has BP I filter output
*B.P. Rx. Filter for Q signal
        LDF      @zero,R1                    ;Initialize intermediate storage registers
        LDF      @zero,R3
*FIR Filter for square root raised cosine received band-pass filter
*for Q signal
        RPTS     BPF_TL-1
        MPYF3    *AR3++%,*AR4++%,R1
||      ADDF3    R1,R3,R3
        ADDF     R1,R3                      ;R3 has BP Q filter output
        CALL     CSNR

obj7     idle
        LDI      @BUFFER,AR1                ;Read the C50 Buffer Output
        LDI      *AR1,R4
        LDIU     R4,AR7
        LDIU     R4,AR6
        LSH      16,AR7
        ASH      -16,AR7                      ;Store I signal separately
        ASH      -16,AR6                      ;Store Q signal separately
        FLOAT    AR7,R7
        FLOAT    AR6,R6
*       STF      R7,*AR0++(1)                ;chk
*       STF      R6,*AR0++(1)                ;chk
        CALL     NGEN
        CALL     ADDN
*       STF      R7,*AR5++%                  ;Load I signal to CB delay line
*       STF      R6,*AR3++%                  ;Load Q signal to CB delay line
                                           ;B.P. Rx. Filter for I signal

        LDF      @zero,R0                    ;Initialize intermediate storage registers
        LDF      @zero,R2
*FIR Filter for square root raised cosine received band-pass filter
        RPTS     BPF_TL-1
        MPYF3    *AR5++%,*AR4++%,R0
||      ADDF3    R0,R2,R2
        ADDF     R0,R2                      ;R2 has BP I filter output
*B.P. Rx. Filter for Q signal
        LDF      @zero,R1                    ;Initialize intermediate storage registers
        LDF      @zero,R3
*FIR Filter for square root raised cosine received band-pass filter
*for Q signal
        RPTS     BPF_TL-1
        MPYF3    *AR3++%,*AR4++%,R1
||      ADDF3    R1,R3,R3
        ADDF     R1,R3                      ;R3 has BP Q filter output
        CALL     CSNR

obj8     idle
        LDI      @CONSTEL,AR2                ;Pointer to store Q1,I1
        LDI      @BUFFER,AR1                ;Read the C50 Buffer Output
        LDI      *AR1,R4

```

```

        LDIU    R4,AR7
        LDIU    R4,AR6
        LSH     16,AR7
        ASH     -16,AR7
        ASH     -16,AR6
        FLOAT   AR7,R7
        FLOAT   AR6,R6
*       STF     R7,*AR0++(1)    ;chk
*       STF     R6,*AR0++(1)    ;chk
        CALL    NGEN
        CALL    ADDN
*       STF     R7,*AR5++%      ;Load I signal to CB delay line
*       STF     R6,*AR3++%      ;Load Q signal to CB delay line
                                   ;B.P. Rx. Filter for I signal
        LDF     @zero,R0        ;Initialize intermediate storage registers
        LDF     @zero,R2
*FIR Filter for square root raised cosine received band-pass filter
        RPTS    BPF_TL-1
        MPYF3   *AR5++%,*AR4++%,R0
||      ADDF3   R0,R2,R2
        ADDF    R0,R2           ;R2 has BP I filter output
        STF     R2,@z_isi1      ;store zero isi pt. in memory for scope output
*       FLOAT   R2,R6
*       STF     R6,*AR2++(1)    ;Store I1 for U and V calculation in memory
*       STF     R2,*AR0++(1)    ;chk
        STF     R2,*AR2++(1)    ;Store I1 for U and V calculation in memory

*B.P. Rx. Filter for Q signal
        LDF     @zero,R1        ;Initialize intermediate storage registers
        LDF     @zero,R3
*FIR Filter for square root raised cosine received band-pass filter
*for Q signal
        RPTS    BPF_TL-1
        MPYF3   *AR3++%,*AR4++%,R1
||      ADDF3   R1,R3,R3
        ADDF    R1,R3           ;R3 has BP Q filter output
        STF     R3,@z_isi2      ;store zero isi pt. in memory for scope output
*       FLOAT   R3,R7
*       STF     R7,*AR2++(1)    ;Store Q1 for U and V calculation
*       STF     R3,*AR0++(1)    ;chk
        STF     R3,*AR2++(1)    ;Store Q1 for U and V calculation
        CALL    CSNR

*Calculate U and V for first Decision
        LDI     2,IR0
        MPYF3   *AR2,*-AR2(IR0),R5
        MPYF3   *+AR2(1),*-AR2(1),R4
        ADDF3   R4,R5,R6        ;U = Q1*Q2+I1*I2
*       STF     R6,*AR0++(1)    ;chk
        LDIN    2,R0            ;extract sign of U and store
        LDINN    0,R0           ;value to calculate index for D1
        MPYF3   *+AR2(1),*-AR2(IR0),R5
        MPYF3   *-AR2(1),*AR2,R4
        SUBF3   R5,R4,R7        ;V = I2*Q1-I1*Q2
*       STF     R7,*AR0++(1)    ;chk
        LDIN    1,R1            ;extract sign of V and store
        LDINN    0,R1           ;value to calculate index for D1
*First Decision based on U and V
        ADDI3   R0,R1,IR1        ;Index for look-up table for first decision
        LDI     @D1_TBL,AR2      ;based on sign of U and V
        LDI     *+AR2(IR1),R5     ;D1 = First Decision
        STI     R5,@D1           ;store D1 in memory
*       STI     R5,*AR0++(1)    ;chk
        CALL    BER
        CALL    STORE_D1
*Extract Channel Characteristics i.e. Up and Vp
        NEGF    R6,R4            ;R6=-U and R4=-U
        NEGF    R7,R5            ;R7=-V and R5=-V

```



```

LDF      R6,R6                ;extract sign of U for Up and Vp
LDFNN    R6,R0                ;for +ive U, Up1=R0=U
LDFNN    R7,R1                ;for +ive U, Vp1=R1=V
LDFN     R4,R0                ;for -ive U, Up1=R0=-U
LDFN     R5,R1                ;for -ive U, Vp1=R1=-V
LDF      R7,R7                ;extract sign of V for Up and Vp
LDFNN    R7,R2                ;for +ive V, Up2=R2=V
LDFNN    R4,R3                ;for +ive V, Vp2=R3=-U
LDFN     R5,R2                ;for -ive V, Up2=R2=-V
LDFN     R6,R3                ;for -ive V, Vp2=R3=U
ADDF3    R0,R2,R4              ;Up=Up1+Up2=R0+R2 based on sign of U and V or D1
ADDF3    R1,R3,R5              ;Vp=Vp1+Vp2=R1+R3 based on sign of U and V or D1
*        STF      R4,*AR0++(1) ;chk
*        STF      R5,*AR0++(1) ;chk
*Averaging filter for Up and Vp
CALL      AVF                  ;Call Averaging Filter Subroutine
obj9      idle
LDI       @BUFFER,AR1          ;Read the C50 Buffer Output
LDI       *AR1,R4
LDIU      R4,AR7
LDIU      R4,AR6
LSH       16,AR7
ASH       -16,AR7              ;Store I signal separately
ASH       -16,AR6              ;Store Q signal separately
FLOAT     AR7,R7
FLOAT     AR6,R6
*        STF      R7,*AR0++(1) ;chk
*        STF      R6,*AR0++(1) ;chk
CALL      NGEN
CALL      ADDN
*        STF      R7,*AR5++%    ;Load I signal to CB delay line
*        STF      R6,*AR3++%    ;Load Q signal to CB delay line
                                   ;B.P. Rx. Filter for I signal
LDF       @zero,R0            ;Initialize intermediate storage registers
LDF       @zero,R2
*FIR Filter for square root raised cosine received band-pass filter
RPTS      BPF_TL-1
MPYF3     *AR5++%,*AR4++%,R0
||        ADDF3    R0,R2,R2
ADDF      R0,R2                ;R2 has BP I filter output
*B.P. Rx. Filter for Q signal
LDF       @zero,R1            ;Initialize intermediate storage registers
LDF       @zero,R3
*FIR Filter for square root raised cosine received band-pass filter
*for Q signal
RPTS      BPF_TL-1
MPYF3     *AR3++%,*AR4++%,R1
||        ADDF3    R1,R3,R3
ADDF      R1,R3                ;R3 has BP Q filter output
CALL      CSNR
CALL      DATA
obj10     idle
LDI       @BUFFER,AR1          ;Read the C50 Buffer Output
LDI       *AR1,R4
LDIU      R4,AR7
LDIU      R4,AR6
LSH       16,AR7
ASH       -16,AR7              ;Store I signal separately
ASH       -16,AR6              ;Store Q signal separately
FLOAT     AR7,R7
FLOAT     AR6,R6
*        STF      R7,*AR0++(1) ;chk
*        STF      R6,*AR0++(1) ;chk
CALL      NGEN
CALL      ADDN
*        STF      R7,*AR5++%    ;Load I signal to CB delay line
*        STF      R6,*AR3++%    ;Load Q signal to CB delay line

```

```

                                ;B.P. Rx. Filter for I signal
                                ;Initialize intermediate storage registers
                                LDF    @zero,R0
                                LDF    @zero,R2
*FIR Filter for square root raised cosine received band-pass filter
RPTS    BPF_TL-1
MPYF3    *AR5++,*AR4++,R0
||
ADDF3    R0,R2,R2
ADDF      R0,R2                                ;R2 has BP I filter output
*B.P. Rx. Filter for Q signal
                                LDF    @zero,R1                                ;Initialize intermediate storage registers
                                LDF    @zero,R3
*FIR Filter for square root raised cosine received band-pass filter
*for Q signal
RPTS    BPF_TL-1
MPYF3    *AR3++,*AR4++,R1
||
ADDF3    R1,R3,R3
ADDF      R1,R3                                ;R3 has BP Q filter output
CALL      CSNR

obj11    idle
LDI      @BUFFER,AR1                                ;Read the C50 Buffer Output
LDI      *AR1,R4
LDIU     R4,AR7
LDIU     R4,AR6
LSH      16,AR7
ASH      -16,AR7                                ;Store I signal separately
ASH      -16,AR6                                ;Store Q signal separately
FLOAT    AR7,R7
FLOAT    AR6,R6
*      STF    R7,*AR0++(1)                                ;chk
*      STF    R6,*AR0++(1)                                ;chk
CALL      NGEN
CALL      ADDN
*      STF    R7,*AR5++%                                ;Load I signal to CB delay line
*      STF    R6,*AR3++%                                ;Load Q signal to CB delay line
                                ;B.P. Rx. Filter for I signal
                                ;Initialize intermediate storage registers
                                LDF    @zero,R0
                                LDF    @zero,R2
*FIR Filter for square root raised cosine received band-pass filter
RPTS    BPF_TL-1
MPYF3    *AR5++,*AR4++,R0
||
ADDF3    R0,R2,R2
ADDF      R0,R2                                ;R2 has BP I filter output
*B.P. Rx. Filter for Q signal
                                LDF    @zero,R1                                ;Initialize intermediate storage registers
                                LDF    @zero,R3
*FIR Filter for square root raised cosine received band-pass filter
*for Q signal
RPTS    BPF_TL-1
MPYF3    *AR3++,*AR4++,R1
||
ADDF3    R1,R3,R3
ADDF      R1,R3                                ;R3 has BP Q filter output
CALL      CSNR

obj12    idle
LDI      @BUFFER,AR1                                ;Read the C50 Buffer Output
LDI      *AR1,R4
LDIU     R4,AR7
LDIU     R4,AR6
LSH      16,AR7
ASH      -16,AR7                                ;Store I signal separately
ASH      -16,AR6                                ;Store Q signal separately
FLOAT    AR7,R7
FLOAT    AR6,R6
*      STF    R7,*AR0++(1)                                ;chk
*      STF    R6,*AR0++(1)                                ;chk
CALL      NGEN
CALL      ADDN

```

```

*      STF      R7,*AR5++%      ;Load I signal to CB delay line
*      STF      R6,*AR3++%      ;Load Q signal to CB delay line
                                   ;B.P. Rx. Filter for I signal
      LDF      @zero,R0      ;Initialize intermediate storage registers
      LDF      @zero,R2
*FIR Filter for square root raised cosine received band-pass filter
      RPTS      BPF_TL-1
      MPYF3     *AR5++%,*AR4++%,R0
||      ADDF3     R0,R2,R2
      ADDF      R0,R2      ;R2 has BP I filter output
*B.P. Rx. Filter for Q signal
      LDF      @zero,R1      ;Initialize intermediate storage registers
      LDF      @zero,R3
*FIR Filter for square root raised cosine received band-pass filter
*for Q signal
      RPTS      BPF_TL-1
      MPYF3     *AR3++%,*AR4++%,R1
||      ADDF3     R1,R3,R3
      ADDF      R1,R3      ;R3 has BP Q filter output
      CALL      CSNR

obj13  idle
      LDI      @BUFFER,AR1      ;Read the C50 Buffer Output
      LDI      *AR1,R4
      LDIU     R4,AR7
      LDIU     R4,AR6
      LSH      16,AR7
      ASH      -16,AR7      ;Store I signal separately
      ASH      -16,AR6      ;Store Q signal separately
      FLOAT    AR7,R7
      FLOAT    AR6,R6
*      STF      R7,*AR0++(1)      ;chk
*      STF      R6,*AR0++(1)      ;chk
      CALL     NGEN
      CALL     ADDN
*      STF      R7,*AR5++%      ;Load I signal to CB delay line
*      STF      R6,*AR3++%      ;Load Q signal to CB delay line
                                   ;B.P. Rx. Filter for I signal
      LDF      @zero,R0      ;Initialize intermediate storage registers
      LDF      @zero,R2
*FIR Filter for square root raised cosine received band-pass filter
      RPTS      BPF_TL-1
      MPYF3     *AR5++%,*AR4++%,R0
||      ADDF3     R0,R2,R2
      ADDF      R0,R2      ;R2 has BP I filter output
*B.P. Rx. Filter for Q signal
      LDF      @zero,R1      ;Initialize intermediate storage registers
      LDF      @zero,R3
*FIR Filter for square root raised cosine received band-pass filter
*for Q signal
      RPTS      BPF_TL-1
      MPYF3     *AR3++%,*AR4++%,R1
||      ADDF3     R1,R3,R3
      ADDF      R1,R3      ;R3 has BP Q filter output
      CALL      CSNR

obj14  idle
      LDI      @BUFFER,AR1      ;Read the C50 Buffer Output
      LDI      *AR1,R4
      LDIU     R4,AR7
      LDIU     R4,AR6
      LSH      16,AR7
      ASH      -16,AR7      ;Store I signal separately
      ASH      -16,AR6      ;Store Q signal separately
      FLOAT    AR7,R7
      FLOAT    AR6,R6
*      STF      R7,*AR0++(1)      ;chk
*      STF      R6,*AR0++(1)      ;chk

```

```

CALL    NGEN
CALL    ADDN
*      STF    R7,*AR5++,%           ;Load I signal to CB delay line
*      STF    R6,*AR3++,%           ;Load Q signal to CB delay line
                                           ;B.P. Rx. Filter for I signal

LDF     @zcro,R0                     ;Initialize intermediate storage registers
LDF     @zcro,R2

*FIR Filter for square root raised cosine received band-pass filter
RPTS    BPF_TL-1
MPYF3   *AR5++%,*AR4++%,R0
||      ADDF3  R0,R2,R2
      ADDF    R0,R2                     ;R2 has BP I filter output

*B.P. Rx. Filter for Q signal
*without array storage for now
LDF     @zcro,R1                     ;Initialize intermediate storage registers
LDF     @zcro,R3

*FIR Filter for square root raised cosine received band-pass filter
*for Q signal
RPTS    BPF_TL-1
MPYF3   *AR3++%,*AR4++%,R1
||      ADDF3  R1,R3,R3
      ADDF    R1,R3                     ;R3 has BP Q filter output
CALL    CSNR

obj15   idle
LDI     @BUFFER,AR1                 ;Read the C50 Buffer Output
LDI     *AR1,R4
LDIU    R4,AR7
LDIU    R4,AR6
LSH     16,AR7
ASH     -16,AR7                     ;Store I signal separately
ASH     -16,AR6                     ;Store Q signal separately
FLOAT   AR7,R7
FLOAT   AR6,R6
*      STF    R7,*AR0++(1)          ;chk
*      STF    R6,*AR0++(1)          ;chk
CALL    NGEN
CALL    ADDN
*      STF    R7,*AR5++%             ;Load I signal to CB delay line
*      STF    R6,*AR3++%             ;Load Q signal to CB delay line
                                           ;B.P. Rx. Filter for I signal

LDF     @zcro,R0                     ;Initialize intermediate storage registers
LDF     @zcro,R2

*FIR Filter for square root raised cosine received band-pass filter
RPTS    BPF_TL-1
MPYF3   *AR5++%,*AR4++%,R0
||      ADDF3  R0,R2,R2
      ADDF    R0,R2                     ;R2 has BP I filter output

*B.P. Rx. Filter for Q signal
LDF     @zcro,R1                     ;Initialize intermediate storage registers
LDF     @zcro,R3

*FIR Filter for square root raised cosine received band-pass filter
*for Q signal
RPTS    BPF_TL-1
MPYF3   *AR3++%,*AR4++%,R1
||      ADDF3  R1,R3,R3
      ADDF    R1,R3                     ;R3 has BP Q filter output
CALL    CSNR

obj16   idle
LDI     @CONST2,AR2                 ;Pointer to store Q2,12
LDI     @BUFFER,AR1                 ;Read the C50 Buffer Output
LDI     *AR1,R4
LDIU    R4,AR7
LDIU    R4,AR6
LSH     16,AR7
ASH     -16,AR7                     ;Store I signal separately
ASH     -16,AR6                     ;Store Q signal separately

```

```

        FLOAT   AR7,R7
        FLOAT   AR6,R6
*       STF     R7,*AR0++(1)      ;chk
*       STF     R6,*AR0++(1)      ;chk
        CALL    NGEN
        CALL    ADDN
*       STF     R7,*AR5++%         ;Load I signal to CB delay line
*       STF     R6,*AR3++%         ;Load Q signal to CB delay line
                                     ;B.P. Rx. Filter for I signal
        LDF     @zero,R0          ;Initialize intermediate storage registers
        LDF     @zero,R2
*FIR Filter for square root raised cosine received band-pass filter
        RPTS    BPF_TL-1
        MPYF3   *AR5++%,*AR4++%,R0
||      ADDF3    R0,R2,R2
        ADDF     R0,R2            ;R2 has BP I filter output
        STF     R2,@z_isi1        ;store zero isi pt. in memory for scope output
*       FLOAT   R2,R6
*       STF     R6,*AR2            ;Store I2 for U and V calculation in memory
*       STF     R2,*AR0++(1)      ;chk
        STF     R2,*AR2            ;Store I2 for U and V calculation in memory

*B.P. Rx. Filter for Q signal
        LDF     @zero,R1          ;Initialize intermediate storage registers
        LDF     @zero,R3
*FIR Filter for square root raised cosine received band-pass filter
*for Q signal
        RPTS    BPF_TL-1
        MPYF3   *AR3++%,*AR4++%,R1
||      ADDF3    R1,R3,R3
        ADDF     R1,R3            ;R3 has BP Q filter output
        STF     R3,@z_isi2        ;store zero isi pt. in memory for scope output
*       FLOAT   R3,R7
*       STF     R7,*AR2(1)        ;Store Q2 for U and V calculation in memory
*       STF     R3,*AR0++(1)      ;chk
        STF     R3,*AR2(1)        ;Store Q2 for U and V calculation in memory
        CALL    CSNR

*Calculate U and V for first decision
        LDI     2,IR0
        MPYF3   *AR2,*-AR2(IR0),R5
        MPYF3   *+AR2(1),*-AR2(1),R4
        ADDF3    R4,R5,R6         ;U = Q1*Q2+I1*I2
*       STF     R6,*AR0++(1)      ;chk
        LDIN    2,R0              ;extract sign of U and store
        LDINN    0,R0             ;value to calculate index
        MPYF3   *+AR2(1),*-AR2(IR0),R5
        MPYF3   *-AR2(1),*AR2,R4
        SUBF3    R4,R5,R7         ;V = I2*Q1-I1*Q2
*       STF     R7,*AR0++(1)      ;chk
        LDIN    1,R1              ;extract sign of V and store
        LDINN    0,R1             ;value to calculate index

*First Decision based on U and V
        ADDI3    R0,R1,IR1        ;Index for look-up table for first decision
        LDI     @D1_TBL,AR2       ;based on sign of U and V
        LDI     *+AR2(IR1),R5     ;D1 = First Decision
        STI     R5,@D1            ;store D1 in memory
*       STI     R5,*AR0++(1)      ;chk
        CALL    BER               ;calculate error rate
        CALL    STORE_D1          ;store 30 D1 values in an array

*Extract Channel Characteristics i.e. Up and Vp
        NEGF     R6,R4            ;R6=U and R4=-U
        NEGF     R7,R5            ;R7=V and R5=-V
        LDF     R6,R6             ;extract sign of U for Up and Vp
        LDFNN    R6,R0            ;for +ive U, Up1=R0=U
        LDFNN    R7,R1            ;for +ive U, Vp1=R1=V
        LDFN     R4,R0            ;for -ive U, Up1=R0=-U

```

```

        LDFN    R5,R1                ;for -ive U, Vp1=R1=-V
        LDF     R7,R7                ;extract sign of V for U and Vp
        LDFN    R7,R2                ;for +ive V, Up2=R2=V
        LDFN    R4,R3                ;for +ive V, Vp2=R3=-U
        LDFN    R5,R2                ;for -ive V, Up2=R2=-V
        LDFN    R6,R3                ;for -ive V, Vp2=R3=U
        ADDF3   R0,R2,R4            ;Up=Up1+Up2=R1+R2 based on sign of U and V or D1
        ADDF3   R1,R3,R5            ;Vp=Vp1+Vp2=R1+R3 based on sign of U and V or D1
*      STF     R4,*AR0++(1)          ;chk
*      STF     R5,*AR0++(1)          ;chk
* Averaging filter for Up and Vp
        CALL    AVF                 ;Call Averaging Filter Subroutine

*CONTROL LOOP NUMBER BY VALUE COUNT
*      LDI     @VALUE2,R6
*      SUBI    @INC,R6
*      STI     R6,@VALUE2
*      CMPI    0,R6
*      BZ      LWAIT
*LWAIT BR      LWAIT

        BR      WAIT
*INTERRUPT SERVICE ROUTINE
*Output Received data on channel A and B
*      .align      ;Cache ??setting

TXDATA PUSH    ST
        PUSH    AR0
        LDI     @ADCADR,AR0
*Output zero isi constellation pts.
*      LDI     @z_isi1,R2
*      LDI     @z_isi2,R3
*      STI     R2,*AR0
*      STI     R3,*+AR0(1)

*Prog. to generate RAMP OUTPUT
*      LDI     @VALUE3,AR6
*      ADDI    @INC3,AR6
*      STI     AR6,@VALUE3
*      STI     AR6,*AR0
*      STI     AR6,*+AR0(1)
        POP     AR0
        POP     ST
        RETI

*Data Symbol generator and storage buffer
*Subroutine to generate same data as in C50 for BER calculations
DATA    PUSH    BK                ;length of generator and storage buffer
        PUSH    AR2                ;seed no. pointer for generator
        PUSH    IR0                ;disp= 28 as seed2 + 28 = seed 30
        PUSH    R0                ;intermediate for data generation
        PUSH    AR3                ;Pointer for storage location
        PUSH    R1
        LDI     SEED_LEN,BK        ;31 length long prbs generator + storage buffer
*Generator
        LDI     @SEED2,AR2        ;point to seed 2
        LDI     28,IR0
        LDI     0,R0
        XOR     *AR2++(IR0)%,R0,R0 ;seed 2 xor seed 30 => seed 30
        XOR     *AR2%,R0,R0
        STI     R0,*AR2++(2)%      ;store result in old seed 30
*      STI     R0,*AR0++(1)        ;chk the data
        STI     AR2,@SEED2        ;store new seed 2 address

*Storage for D1 BERT
        LDI     @DATA_BUF,AR3     ;point to first storage
        STI     R0,*AR3++(1)%     ;store data in buffer

```

```

STI    AR3,@DATA_BUF ;store new address for storage
LDI    *AR3--(12)%,R1 ;Dummy storage so as to point to
LDI    *AR3,R1        ;last 11th input
STI    R1,@D1_DATA    ;Store in memory for D1 comparison
CALL   ST_DATA
POP    R1
POP    AR3
POP    R0
POP    R0
POP    AR2
POP    BK
RETS

```

\*Storage for D2 BERT

\*R1 has data

```

ST_DATA PUSH    BK
        PUSH    AR3
        LDI     42,BK ;42 length long CB for storage of data
        LDI     @D_BUF,AR3 ;point to first storage of
*       STI     AR3,*AR0++(1) ;chk
*       STI     R0,*AR0++(1)% ;store data and point to last 41st element
        STI     R0,*AR0++(1) ;chk
        STI     AR3,@D_BUF ;store new address for storage
        LDI     *AR3,R1 ;store last 41st input
*       STI     R1,*AR0++(1) ;chk
        STI     R1,@D2_DATA ;store in memory for D2 comparison
        POP     AR3
        POP     BK
RETS

```

\*BER Calculations for D1

\*Ignore first 11 pts. and then compare D1 with D1 Data

\*increase error count by one if not matching, zero otherwise.

```

BER     PUSH    R1
        PUSH    R2
        PUSH    R0
*Ignore first 11 points because of delay due to BP filter
        LDI     @D1_DLY,R0 ;delay count =11
        SUBI    @one,R0 ;decrement
        STI     R0,@D1_DLY ;new delay count
        BNN     DLY
        NEGI    R0,R1
        STI     R1,@DATA_PT ;Total number of Data Symbols for error calculation
*Find number of errors in first decision
        LDI     @D1_ERR,R0 ;initial symbol error count
        LDI     @D1,R1 ;first decision value
*       STI     R1,*AR0++(1)
        LDI     @D1_DATA,R2 ;transmitted data value
        CMPI    R1,R2 ;compare for symbol error
        BZ      NO_ERR ;no increment if same
        ADDI    @one,R0 ;increment error count
        LDI     @DATA_PT,R1 ;Data point in error
*       STI     R1,*AR0++(1) ;stored in buffer for analysis
        NO_ERR STI     R0,@D1_ERR ;store new symbol error count
        DLY     POP    R0
        POP     R2
        POP     R1
RETS

```

\*Averaging filter subroutine for Up and Vp filtering and get

\*Upf and Vpf at the output.

```

AVF     PUSH    BK
        PUSH    AR3
        PUSH    AR4
        PUSH    AR5
        PUSH    R1
        LDI     AVF_TL,BK ;Length = 6i for averaging filter CB
        LDI     @AVU_DLE,AR5 ;Up delay line end address

```

```

LDI @AVF_COEF,AR4 ;Averaging filter coeff. start address
LDI @AVV_DLE,AR3 ;Vp delay line end address
LDI 30,IR1 ;Index to point to middle of delay line
* STI AR5,*AR0++(1) ;chk
LDF *AR5--(IR1)%,R6 ;Dummy storage to change pointer using index
* STI AR5,*AR0++(1) ;chk
LDF *AR3--(IR1)%,R7 ;Dummy storage to change pointer using index
LDF *AR5++(IR1)%,R6 ;Change pointer back to end of delay line
LDF *AR3++(IR1)%,R7 ;after storing middle point i.e. Up(-31),Vp(-31)
STF R6,@Up_dly
STF R7,@Vp_dly
* STF R6,*AR0++(1) ;chk
* STF R7,*AR0++(1) ;chk
STF R4,*AR5++% ;Store new Up to buffer end, pt. to start for filter
STF R5,*AR3++% ;Store new Vp to buffer end, pt. to start for filter
LDFU 0,R0
LDFU 0,R2
RPTS AVF_TL-1 ;FIR filter for Up
MPYF3 *AR5++%,*AR4++%,R0
|| ADDF3 R0,R2,R2
ADDF R0,R2 ;Upf = filter output
* STF R2,*AR0++(1) ;chk
LDFU 0,R1
LDFU 0,R3
RPTS AVF_TL-1 ;FIR filter for Vp
MPYF3 *AR3++%,*AR4++%,R1
|| ADDF3 R1,R3,R3
ADDF R1,R3 ;Vpf = filter output
* STF R3,*AR0++(1) ;chk
STI AR3,@AVV_DLE ;Store new Vp storage address for next initial pt.
STI AR5,@AVU_DLE ;Store new Up storage address for next initial pt.
* STI AR3,*AR0++(1) ;chk
* STI AR5,*AR0++(1) ;chk
*Calculate C and D to find phase change because of channel
*Note R2=Upf, R3=Vpf, R6=Up_dly, R7=Vp_dly
* C = Upf*Up_dly + Vpf*Vp_dly
* D = Vpf*Up_dly - Upf*Vp_dly
* STF R2,*AR0++(1) ;chk
* STF R6,*AR0++(1) ;chk
* STF R3,*AR0++(1) ;chk
* STF R7,*AR0++(1) ;chk

MPYF3 R2,R6,R0 ;Upf*Up_dly
MPYF3 R3,R7,R1 ;Vpf*Vp_dly
ADDF3 R0,R1,R4 ;>> C = Upf*Up_dly + Vpf*Vp_dly

* STF R4,*AR0++(1) ;chk
MPYF3 R3,R6,R0 ;Vpf*Up_dly
MPYF3 R2,R7,R1 ;Upf*Vp_dly
SUBF3 R1,R0,R5 ;>> D = Vpf*Up_dly - Upf*Vp_dly
* STF R5,*AR0++(1) ;chk

```

\*Extract sign of C and D to calculate index Q

\*C=R4 and D=R5

\*Look-up Table for index calculation (Q)

* K=C>0	L= C > D	M=D>0	Q	Shift of D1
* True	True	don't care	00	No shift
* False	True	don't care	10	180 degree shift(2 Quad a.c.)
* don't care	False	True	11	-90 degree shift(3 Quad a.c.)
* don't care	False	False	01	+90 degree shift(1 Quad a.c.)
	LDF R4,R4			;extract sign of C
	LDIN 2,R0			;C<0 R0=2
	LDINN 0,R0			;C>=0 R0=0
	LDF R5,R5			;extract sign of D
	LDIN 0,R1			;D<0 R1=0
	LDINN 2,R1			;D>=0 R1=2
	ABSF R4,R4			;magnitude of C



```

        ABSF      R5,R5                ;magnitude of D
        CMPF      R5,R4                ;see |C|-|D| for relative mag
        LDIN      1,R3                ;|C|-|D|
        LDIN      R1,R0                ;replace R0 by R1 (old R0 is don't care)
        LDINN     0,R3                ;|C|>|D| R3=0
        ADDI3     R0,R3,R3            ;Index Q for second Decision
                                      ;R0+R3=Index Q
*      STI        R3,*AR0++(1)        ;chk
*      STI        R3,*AR0++(1)        ;chk
* Refer back to averaging filter delay line pointer, extract location of
* Up_dly and Vp_dly and change their value based on index Q.

        LDF       @Up_dly,R4          ;R4=Up(old) Old value of Up (extracted channel info.)
        LDF       @Vp_dly,R5          ;R5=Vp(old) Old value of Vp
*      STF        R4,*AR0++(1)        ;chk
*      STF        R5,*AR0++(1)        ;chk
        NEGF      R4,R6                ;R6=-Up(old)
        NEGF      R5,R7                ;R7=-Vp(old)
        CMPI      0,R3                ;for Q=0 i.e. no shift
        LDFZ      R4,R0                ;Up(new)=Up(old)
        LDFZ      R5,R1                ;Vp(new)=Vp(old)
        CMPI      2,R3                ;for Q=2 i.e. 180deg data shift
        LDFZ      R6,R0                ;Up(new)=-Up(old)
        LDFZ      R7,R1                ;Vp(new)=-Vp(old)
        CMPI      1,R3                ;for Q=1 i.e. +90deg data shift
        LDFZ      R5,R0                ;Up(new)=Vp(old)
        LDFZ      R6,R1                ;Vp(new)=-Up(old)
        CMPI      3,R3                ;for Q=3 i.e. -90deg data shift
        LDFZ      R7,R0                ;Up(new)=-Vp(old)
        LDFZ      R4,R1                ;Vp(new)=Up(old)
        LDI       31,IR1              ;Index to point to store new Up_dly
        LDF       *AR5--(IR1)%,R6     ;Dummy storage to adjust pointer to old Up_dly
        LDF       *AR3--(IR1)%,R7     ;Dummy storage to adjust pointer to old Vp_dly
*      STF        R6,*AR0++(1)        ;CHK
*      STF        R7,*AR0++(1)        ;CHK
        STF       R0,*AR5              ;Store new Up_dly to replace old Up_dly
        STF       R1,*AR3              ;Store new Vp_dly to replace old Vp_dly
*      STF        R0,*AR0++(1)        ;CHK
*      STF        R1,*AR0++(1)        ;CHK
*      STI        AR5,*AR0++(1)        ;CHK
*      STI        AR3,*AR0++(1)        ;CHK
        CALL      CORRECT
        CALL      DII_BER
        POP       IR1
        POP       AR5
        POP       AR4
        POP       AR3
        POP       BK
        RETS

```

\* Store first decision previous 31 values so as to use later during  
\* correction

```

STORE_D1
        PUSH      BK
        PUSH      AR3
        LDI       DIBUF_LEN,BK        ;30 length long D1 value storage buffer
        LDI       @DI_BUF,AR3         ;point to first storage
*      STI        AR3,*AR0++(1)        ;chk
        LDI       @D1,R0
*      STI        R0,*AR0++(1)        ;chk
        STI       R0,*AR3++(1)%       ;store data in buffer
        STI       AR3,@DI_BUF         ;store new address for storage
        LDI       *AR3,R1              ;last 30th input
        STI       R1,@DI_DLY          ;Store in memory for D1 comparison

```

```

*      STI      R1,*AR0++(1)      ;chk
      POP      AR3
      POP      BK
      RETS

*Correct first decision based on index Q so as to have second decision
*Note R3 has index Q value
CORRECT PUSH      AR2
      PUSH     AR3
      PUSH     IR1
      LDI      R3,IR1              ;In'x Q for quadrant shift
*      STI      R3,*AR0++(1)      ;chk
      LDI      @D1_DLY,R4
*      STI      R4,*AR0++(1)      ;chk
      LDI      @BASE_ADR,R5
      ADDI     R4,R5,AR2           ;first decision to be shifted
*      STI      AR2,*AR0++(1)      ;chk
      LDI      *AR2,AR3           ;Address pointer i.e. DI+Base adr. => Adr. pointer
*      STI      AR3,*AR0++(1)      ;chk
      LDI      *AR3++(IR1),R1     ;Dummy storage to change address pointer as per Q
*      STI      AR3,*AR0++(1)      ;chk
      LDI      *AR3,R1            ;Second decision i.e. shifted first decision
*      STI      R1,*AR0++(1)      ;chk
      STI      R1,@D2             ;Store second decision value
      POP      IR1
      POP      AR3
      POP      AR2
      RETS

```

\*BER Calculations for D2

\*Ignore first 41 pts. and then compare D2 with D2 Data

\*increase error count by one if not matching, zero otherwise.

```

D2 BER PUSH      R1
      PUSH     R2
      PUSH     R6

*Ignore first 41 points because of delay due to BP filter
      LDI      @D2_DLY,R0          ;delay count =41
*      STI      *0,*AR0++(1)      ;chk
      SUBI     @onc,R0             ;decrement
      STI      R0,@D2_DLY         ;new delay count
      BNN     DLY_ON
      NEGI     R0,R1
*      STI      R1,@SYMB_PT        ;Total number of Data Symbols for error calculation
      STI      R1,*AR0++(1)      ;chk

*Find number of errors in second decision
      LDI      @D2_ERR,R0          ;initial symbol error count
      LDI      @D2,R1             ;second decision value
*      STI      R1,*AR0++(1)      ;chk
      LDI      @D2_DATA,R2        ;transmitted data value
*      STI      R2,*AR0++(1)      ;chk
      CMPI     R1,R2              ;compare for symbol error
      BZ      ERR_FRE             ;no increment if same
      ADDI     @onc,R0            ;increment error count
      LDI      @SYMB_PT,R1        ;Data point in error
*      STI      R1,*AR0++(1)      ;stored in buffer for analysis
ERR_FRE STI      R0,@D2_ERR        ;store new symbol error count
*      STI      R0,*AR0++(1)      ;chk
DLY_ON POP      R0
      POP      R2
      POP      R1
      RETS

```

\*Module to generate,add,measure noise to signal at receiver antenna

.include "N1.ASM"

.end

\*TABLE FOR NOISE FACTOR (NSCALE) USED FOR VARIOUS SNR

SNR(dB)	NSCALE for fd=40Hz	NSCALE for fd=20Hz
70	1.199802e-4	0.585050e-4
60	0.379411e-3	0.185009e-3
50	1.199802e-3	0.585050e-3
40	0.379411e-2	0.185009e-2
30	1.199802e-2	0.585050e-2
20	0.379411e-1	0.185009e-1
10	1.199802e-1	0.585050e-1